**Mineral and Energy
Economy Research
Institute**
Polish Academy of Sciences

2nd International Conference

**Strategies toward
Green Deal Implementation**

Water, Raw Materials & Energy

MONOGRAPH

PART I

HONORARY PATRONAGE

Ministry of Climate
and Environment

Minister
Edukacji i Nauki

Izba Gospodarcza
WODOCIĄGI POLSKIE

MEERI PAS

8–10 December 2021

SCIENTIFIC EDITOR

Prof. Marzena SMOL
Mineral and Energy Economy Research Institute Polish Academy of Sciences
Division of Biogenic Raw Materials

COVER & COMPOSITION

Paulina MARCINEK & Dominika SZOŁDROWSKA
Mineral and Energy Economy Research Institute Polish Academy of Sciences
Division of Biogenic Raw Materials

SCIENTIFIC COMMITTEE

Prof. **Marzena Smol**, *Mineral and Energy Economy Research Institute, Polish Academy of Sciences, Poland, Chairwoman*

Dr-Ing. **Christian Adam**, *Federal Institute for Materials Research and Testing (BAM), Germany*

Dr. **Anna Avdiushchenko**, *Jagiellonian University, Poland*

Prof. **Tomasz Bajda**, *AGH University of Science and Technology, Poland*

Prof. **Miriam Balaban**, *University Campus Bio-Medico of Rome, Italy*

Dr. **Anna Berbesz**, *Wroclaw University of Science and Technology, Poland*

Prof. **Augusto Bianchini**, *Universita di Bologna, Italy*

Prof. **Michał Bodzek**, *Institute of Environmental Engineering of the Polish Academy of Sciences in Zabrze, Poland*

Prof. **Idiano D'Adamo**, *Spienza University of Rome, Italy*

Prof. **Joanna Duda**, *AGH University of Science and Technology, Poland*

Prof. **Krzysztof Galos**, *Mineral and Energy Economy Research Institute, Polish Academy of Sciences, Poland*

Prof. **Krzysztof Gaska**, *Silesia University of Technology, Poland*

Prof. **Lidia Gawlik**, *Mineral and Energy Economy Research Institute, Polish Academy of Sciences, Poland*

Prof. **Agnieszka Generowicz**, *Cracow University of Technology, Poland*

Prof. **Ludwig Halicz**, *Geological Survey of Israel, Israel*

Mr. **Ludwig Hermann**, *President of the European Sustainable Phosphorus Platform (ESPP), Proman Management GmbH, Austria*

Prof. **Mika Horttanainen**, *Lappeenranta-Lahti University of Technology, Finland*

Prof. **Māris Kļaviņš**, *University of Latvia, Latvia*

Prof. **Jiří Jaromír Klemeš**, *Brno University of Technology, Czech Republic*

Prof. **Eugeniusz Koda**, *Warsaw University of Life Sciences – SGGW, Poland*

Prof. **Viktor Koval**, *Southern Scientific Center of National Academy of Sciences of Ukraine and Ministry of Education and Science of Ukraine, Ukraine*

Prof. **Jolita Kruopienė**, *Kaunas University of Technology, Lithuania*

Dr. **Marcin Kuczera**, *CreativeTime, Poland*

Dr. **Edyta Kudlek**, *Silesia University of Technology, Poland*

Dr. **Katalin Kurucz**, *Bay Zoltán Nonprofit Ltd. Applied Research, Hungary*

Dr**. Bartłomiej Macherzyński**, *Cardinal Stefan Wyszynski University in Warsaw, Poland*

Prof. **Izabela Majchrzak-Kucęba**, *Czestochowa University of Technology, Poland*

Prof. **Jacek Mąkinia**, Gdańsk University of Technology, Poland

Prof. **Alfonso Mejia**, Pennsylvania State University, United States

Prof. **Eugeniusz Mokrzycki**, Mineral and Energy Economy Research Institute, Polish Academy of Sciences, Poland

Prof. **Majeti Narasimha Vara Prasad**, *University of Hyderabad, India*

Dr. **Konstantinos Moustakas**, *National Technical University of Athens, Greece*

Prof. **Zenon Pilecki**, *Mineral and Energy Economy Research Institute, Polish Academy of Sciences, Poland*

Prof. **Eric Pirard**, *University of Liège, Belgium*

Prof. **Arkadiusz Piwowar**, *Wroclaw University of Economics and Business, Poland*

Prof. **Alexandra Ribeiro**, *NOVA University Lisbon, Portugal*

Prof. **Czesława Rosik-Dulewska**, *Actual Member of the Polish Academy of Sciences,*
Institute of Environmental Engineering of the Polish Academy of Sciences in Zabrze, Poland

Dr. **Monika Sady**, *Cracow University of Economics, Poland*

Prof. **Agnieszka Sobczak-Kupiec**, *Cracow University of Technology, Poland*

Prof. **Alexandros Stefanakis**, *School of Environmental Engineering, Technical University of Crete, Greece*

Prof. **Krzysztof Szamałek**, *University of Warsaw, Poland*

Dr. **Beata Szatkowska**, *Aquateam COWI, Norway – Poland*

Dr. **Renata Tomczak-Wandzel**, *Aquateam COWI, Norway – Poland*

Prof. **Konstantinos Tsagarakis**, *Democritus University of Thrace, Greece*

Prof. **Magdalena Wdowin**, *Mineral and Energy Economy Research Institute, Polish Academy of Sciences, Poland*

Prof. **Sebastian Werle**, *Silesian University of Technology, Poland*

Prof. **Maria Włodarczyk – Makuła**, *Czestochowa University of Technology, Poland*

Dr. **Dariusz Włóka**, *GreenBack, Poland*

Dr. **Kari Ylivainio**, *Natural Resources Institute (Luke), Finland*

Contents

Reviewers

Prof. **Augusto Bianchini***, University of Bologna, Italy*

Prof. **Idiano D'Adamo***, Sapienza University of Rome, Italy*

Prof. **Marta Gmurek***, Lodz University of Technology, Poland*

Prof. **Mika Horttanainen***, Lappeenranta-Lahti University of Technology, Finland*

Ph.D. Eng. **Waldemar Kępys***, AGH University of Science and Technology, Poland*

Ph.D. **Agnieszka Kiersnowska***, Warsaw University of Life Sciences – SGGW, Poland*

Dr. **Jolita Kruopienė***, Kaunas University of Technology, Lithuania*

Prof. **Izabela Majchrzak-Kucęba***. Czestochowa University of Technology, Poland*

Ph.D. Eng. **Bartłomiej Macherzyński***, Cardinal Stefan Wyszyński University in Warsaw, Poland*

Prof. **Eugeniusz Mokrzycki***, Mineral and Energy Economy Research Institute, Polish Academy of Sciences, Poland*

Prof. **Majeti Narasimha Vara Prasad***, Emeritus Professor (Honorary)*

Prof. **Justyna Starzyk***, Poznań University of Life Sciences, Poland*

Ph.D. Eng. **Magdalena Staszewska***, AGH University of Science and Technology, Poland*

Ph.D. Eng. **Renata Tomczak-Wandzel***, Aquateam COWI Norway-Poland*

Prof. **Blanka Tundys***, University of Szczecin, Poland*

Ph.D. Eng. **Katarzyna Witt***, Bydgoszcz University of Science and Technology, Poland*

Prof. **Magdalena Wojnarowska***, Cracow University of Economics, Poland*

Preface

The 2nd International Conference on Strategies toward Green Deal Implementation – Water, Raw Materials & Energy (ICGreenDeal2021) was organised by the Division of Biogenic Raw Materials of the Mineral and Energy Economy Research Institute, Polish Academy of Sciences, on December 8–10 2021. Due to the COVID-19 pandemic the conference was organised as the virtual event (online).

The purpose of the conference was to discuss issues related to climate change and methods of preventing it, e.g. through innovative solutions – technological, environmental, social – that can be implemented under the Green Deal.

During the Conference, 16 thematic sessions were held, including both oral and poster presentations. The scientific nature of the Conference meant that its main participants were representatives of the academic community who deal with research for the development of innovative pro-environmental solutions. The conference was also attended by scientists and entrepreneurs supporting the development of "green innovations", and the total number of participants was 1032 people. There were 208 speakers among the above-mentioned participants, who presented works on various areas related to the topic of climate change.

The following thematic sessions were the most popular among the participants:
- green deal strategies,
- cooperation for climate,
- sustainable management of water and raw materials,
- sustainable developments of regions,
- water and sewage in circular economy,
- bioeconomy,
- raw materials and waste,
- innovative materials for sustainable future,
- green strategies for waste and energy,
- actions for climate and circular economy,
- water – waste – energy in green deal.

The conference made it possible to create a platform presenting knowledge of great practical and scientific importance, where Participants from various spheres of the environment could exchange their experiences. The initiated project has also con-

tributed to establishing new contacts between the scientific community and industry, which may result in joint research and industrial projects in the future.

The Monograph "Strategies toward Green Deal Implementation – Water, Raw Materials & Energy" includes the selected papers that have been presented during the 2nd edition of International Conference on Strategies toward Green Deal Implementation – Water, Raw Materials & Energy.

I would like to thank all Authors and Reviewers for their valuable work in the preparation of papers and their reviews.

Prof. Marzena Smol

Michał Bodzek

Institute of Environmental Engineering Polish Academy of Science; e-mail: michal.bodzek@ipispan.edu.pl

The use of nanoparticles in water and wastewater treatment

ABSTRACT: The supply of clean and affordable water to meet human needs is the most important challenge of the 21st century. Problems with increasing scarcity of water for drinking, domestic and industrial purposes are exacerbated by rapid population growth, global climate change, deteriorating quality of natural waters and wastewater discharged to the environment. Solving this problem requires implementation of new, innovative water and wastewater treatment technologies. In this context, introduction of nanotechnology into traditional processes, offers new opportunities in the development of advanced processes of water and wastewater technology. Considering the functions of nanotechnology in unit processes of water and wastewater treatment, nanomaterials are used as adsorbents and photocatalysts and in the production of semi-permeable membranes.

KEYWORDS: nanotechnology, adsorption process, nanocomposite membranes

Introduction

The world of the science of environmental engineering and nanotechnology are moving at a rapid pace today. Depletion of fossil fuel resources, environmental degradation and loss of ecological biodiversity are urging the global scientific domain to take visionary steps towards green and environmental sustainability. The vision and the sagacity of nanotechnology applications in environmental engineering and energy engineering are the forerunners towards a new dawn in the field of sustainable development today (Palit 2021).

Nanotechnology is a field of applied science, focused on the design, synthesis, characterization and application of materials and devices on the nanoscale (Mansoori et al. 2008). Nanomaterials (NMs) are commonly defined as materials that at least one dimension is smaller than 100 nm (Tesh and Scott 2014). NMs often exhibit novel and

significantly changing physical, chemical and biological properties due to their size and structure (Mansoori et al. 2008). Also, a unique aspect of nanotechnology is the "vastly increased ratio of surface area to volume", present in many nanoscale materials, which opens new possibilities in surface-based sciences (Mansoori et al. 2008). Similar to nanotechnology's success in consumer products and other sectors, nanoscale materials have the potential to improve the environment, both through direct applications of those materials to detect, prevent, and remove pollutants, as well as indirectly by using nanotechnology to design cleaner industrial processes and create environmentally responsible products (Mansoori 2008).

One of the main environmental applications of nanotechnology is in the water sector. As freshwater sources become increasingly scarce due to overconsumption and contamination, scientists have begun to consider another source for drinking water, e.g. seawater, water reused and so on. Water contamination caused by numerous inorganic/organic pollutants can significantly threaten the human's well-being and viability of all. Pesticides, plasticizers, phenols and drug residues are known as the most important types of organic pollutants while, arsenic, cadmium, mercury, chromium are considered as the prominent sorts of inorganic contaminants (Pishnamazi et al. 2020; Buruga et al. 2019). Therefore, development of promising technologies for water purification is of great interest. Many traditional water and wastewater treatment methods do not effectively remove these emerging contaminants, and/or are not capable of removing enough to meet increasingly stringent water quality standards. Contamination of surface waters also constitutes a risk to water supplies because pollutants may penetrate into aquifers, where they can be transported to drinking water sources (Adeleye et al. 2016). These challenges, among others, bring into focus the need for alternative water treatment and pollutant remediation methods to complement or replace existing technologies. Thanks of nanoparticles (NPs) size-dependent effects, the current water and wastewater treatment process could be greatly improved by introducing NMs into the system (Zhang et al. 2016). The use of NMs for water treatment is currently limited to exploring their potential to act as effective adsorbents (Sarma et al. 2019; Bodzek et al. 2020a), membranes (Bodzek et al. 2020b), disinfectants (Collivignarelli et al. 2018; Bodzek 2022), and reactive agents (Bodzek et al. 2021a), although they show promise for full scale water treatment and environmental remediation (Qu et al. 2013; Ren et al. 2013). While some pilot and full scale field studies applying nanoscale zerovalent iron (nZVI)-based remediation methods have been reported in the literature (Mueller et al. 2012; Kuiken 2010), the majority of other remediation and water purification studies with ENMs remain at a bench scale proof of concept stage (Qu et al. 2013).

Since the cost for nanomaterials are decreasing, they have become more competitive for water and wastewater treatment. However, there are still inherent disadvantages for use of unbounded NPs in water and wastewater treatment processes. Firstly, NPs tend to aggregate in fluidized system or in fixed bed, resulting in severe activity loss and pressure drop (Lofrano et al. 2016). Secondly, it is still a difficult to separate most of the used NPs (except for magnetic NPs) from the treated water for reuse,

which would be undesirable in terms of the economical consideration (Al-Hamadani et al. 2015, Qu et al. 2013). Thirdly, proper clarification and understanding of the role and mechanism of interaction of the nano-material with the living organisms during water and wastewater treatment process should be fully understood, and the impact of nanomaterials on the aquatic environment and human health is a major issue that could hinder the application of nanotechnology (Ganguly et al. 2018). To avoid or mitigate the potentially negative effect, it is desirable to develop a material or a device that could minimize the release or mobilization of the nanomaterials while maintaining their high reactivity. Nanocomposite materials is proved to be an effective and promising solutions and their fabrication is simple by loading desired nanoparticles onto various supporting materials, such as polymers or membranes (Petronella et al. 2016). It could be defined as a multiphase material which at least one dimension of the constituent phases is <100 nm (Tesh and Scott 2014). Some of the reported nanocomposites were highly efficient in water decontamination, recyclable, cost-effective and compatible with existing infrastructure (Lofrano et al. 2016; Yin and Deng 2015).

The article provides an overview of recent advances in nanotechnologies for water and wastewater treatment. The major applications of NMs are critically reviewed based on their functions in unit operation processes. This review focuses on various nanomaterials used for adsorption, separation and catalytic degradation from water or wastewater using both free NPs and nanocomposites. The barriers for their full-scale application and the research needs for overcoming these barriers are also discussed. The potential impact of nanomaterials on human health and ecosystem as well as any potential interference with treatment processes are beyond the scope of this review and thus will not be detailed addressed here.

1. Adsorption

Adsorption is a widely used unit process for the removal of organic and inorganic contaminants from water and wastewater both organic and inorganic (Mohan et al. 2008; Kuppusamy et al. 2016, Sharma and Bhattacharya 2017; Crini and Lichtfouse 2019). Two types of forces are distinguished in adsorption processes, i.e. physical and chemical interactions.

In adsorption first of all carbonaceous materials are used to trap pollutants inside its pore structure, first of all high quality activated carbon (AC) (Mohan et al. 2008). In the last three decades, numerous approaches using non-conventional adsorbents have been studied for the development of cheaper and more effective adsorbents to eliminate pollutants at trace levels (Crini et al. 2019). Nanomaterials based adsorbents, i.e. nanometals and metal oxides, carbon nanotubes (CNTs), graphene and nanocomposites, possess large specific surface and corresponding number of active sites suitable to sorption, high reactivity, short diffusion path inside particles, fast kinetic

and specific affinity to various contaminants and their adsorption efficiencies against many contaminants are several times higher than those of traditional adsorbents (Ali 2012; Khajeh et al. 2013; Tosco et al. 2014; Sharma et al. 2009).

1.1. Metal/metal oxide based nano-adsorbents

Due to unique sorption properties of metal and metal oxides nanoparticles (NPM, NPMO) they are widely used to removal of contaminants from wastewater (Sharma et al. 2009). The most popular NPMs and NPMOs are zero-valent iron (Ali 2012; Khajeh et al. 2013) and silver (Fabrega et al. 2011) as well as magnetic iron oxides (Feng et al. 2012), manganese oxides (Gupta et al. 2011b), titanium oxide (Luo et al. 2010), etc. (Hua et al. 2013). Many research confirm that NPMs and NPMOs nanoparticles reveal highly efficient and selective sorption of contaminants like heavy metals (Lakshmipathiraj et al. 2006; Engates and Shipley 2011; Yu et al. 2014), typical anionic contaminants, e.g. phosphates (Wen et al. 2014) and organic contaminants (Fan et al. 2009).

Metal oxides nano-adsorbents, mainly iron oxide, titanium dioxide, aluminum oxide and other, are efficient and cheap adsorbent for heavy metals like arsenic, lead, copper, cadmium, nickel and reveal much higher potential in comparison with AC (Sharma et al. 2009). Sorption is mainly controlled by complexation of dissolved metal ions with oxygen from metal oxides, which is the two stage process. In the first stage fast sorption on external sorbent surface occurs, while next slower diffusion to a particle interior along micropores wall takes place (Trivedi and Axe 2000). Nanoscale metal oxides possess higher adsorption ability and faster kinetics due to larger specific surface, shorter diffusion pathway to particle interior and higher number of active sites (i.e. corners, edges and other). For example, when the size of nano-magnetite particle is decreased from 300 to 11 nm, its arsenic adsorption capacities increases more than 100 times (Yean et al. 2005). Moreover, when particles size is decreased to below 20 nm, the specific surface increases and the ability of arsenic sorption by nano-magnetite of 11 nm diameter increases three times. This nanoscale effect is related with magnetite surface structure change and new active adsorption sites are formed (Yean et al. 2005).

The most commonly used iron oxides based nano-sorbents are: nonmagnetic **goethite** (α-FeOOH), **hematite** (α-Fe$_2$O$_3$), magnetic **magnetite** (Fe$_3$O$_4$) and **maghemite** (γ-Fe$_2$O$_3$) as well as **hydrated iron oxides** (HIO) (Madhura et al. 2018; Zhang et al. 2016a; Lu and Astruc 2018; Sarma et al. 2019; Runowski 2014). Getite and hematite possess a range of geochemical and ecological, important oxyanions and cations in their complex matrices, thus they are found as effective and cheap sorbents to removal of various contaminants (Gehrke et al. 2015). Due to their small size, however, their separation and recovery after wastewater treatment can be troublesome. On the other hand, iron oxide based nanoparticles like nano-maghemite (γ-Fe$_2$O$_3$) and nano-magnetite, despite their high adsorption ability possess superparamagnetic prop-

erties. If the size of a magnetic particle is smaller than the critical value (ca. 40 nm), its separation and recovery in low gradient magnetic field is easy (Gehrke et al. 2015; Runowski 2014). Magnetic NPMOs are composed of a magnetic core and a coating/shell (Gehrke et al. 2015) and a core can be cobalt, iron, nickel and their oxides or alloys of ferromagnetic or superparamagnetic properties, whereas coatings can be formed from inorganic components like silica (Mashhadizadeh and Amoli-Diva 2013) and aluminum oxide (Karimi et al. 2012) or from organic components like polymers (Li et al. 2010a) or surface active agents (Fig. 1). In regard to stability and recycling of NPMs and NPMOs coats play very important role (Pandey et al. 2017), especially small organic particles, organic polymers (polystyrene, polyaniline or biopolymers like cellulose or chitosan) or inorganic supports. NPMs can be used as adsorptive filters media and in suspended bed reactors (Madhura et al. 2018; Runowski 2014).
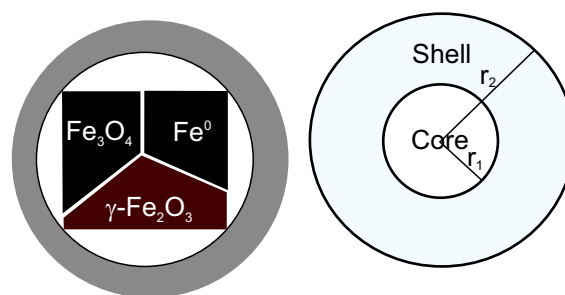

Figure 1.
The scheme of a nanoparticle composed of a magnetic core and a coat

The adsorption of metal ions (Pb(II) and Cd(II), Cu(II), Zn(II)) on nano-hematite was studied as a function of sorbent concentration, pH and temperature (Shipley et al. 2013). The results showed that 100% Pb, 94% Cd, 89% Cu and 100% Zn were adsorbed at an adsorbent dose of 0.5 g/L (Shipley et al. 2013; Hu et al. 2006). The effect of temperature on adsorption showed the endothermic nature of the reaction for Pb(II), Cu(II) and Cd(II), while exothermic for Zn(II). The kinetics and mechanism of adsorption of Cu(II) ions on nano-goethite indicate that Cu(II)/goethite complexes are formed on the adsorbent surface (Shipley et al. 2013). In the case of hematite, which is also highly reactive, the maximum Cu(II) adsorption capacity is 84.46 mg/g. This result is lower compared to the adsorption efficiency of nano- goethite (149.25 mg/g Cu(II)), although both oxides show similar adsorption kinetics and mechanism (Bodzek et al. 2020a). Nano-hematite was found to be also a good adsorbent for the elimination arsenic(V) and chromium(VI) ions from water (Bodzek et al. 2020a; Shipley et al. 2013). In oversaturated solutions, iron compounds hydrolyse, precipitate and aggregate as amorphous structures of high porosity forming so called hydrated iron oxides (HIO) (Mercer and Tobiason 2008), which possess better possibility of metal ions sorption than crystalline oxides like goethite. HIO possess active sites for sorption of vario-

us dissolved substances, mainly due to surface complexation and ligands exchange. It has been found, that adsorption of Cu(II) or Pb(II) ions on amorphous HIO is independent of ionic strength, while it increases with pH increase (Zhang et al. 2016a). Nano-iron hydroxide [α-FeO(OH)] is stable, mechanically resistant adsorbent of large specific surface, which enables adsorption of arsenic from waste and potable water (Klein and Pawlik 2012). ArsenXnp (SolmeteX Inc., Philadelphia, PA, US) is available on the market as a hybrid medium to ion exchange containing nanoparticles of iron oxide and polymers and is very efficient to arsenic removal (Gehrke et al. 2015). Due to its small size, recovery and separation of non-magnetic NTMs after wastewater treatment can be difficult to carry out.

There are numerous research on the use of nano-maghemite and magnetite to heavy metals sorption, including arsenic, chromium, selenium, lead and nickel from synthetic (model) and natural aqueous systems (Hu et al. 2006). Maghemite nanoparticles (10 nm) of surface 178 m^2/g reveal selective adsorption on ions and fast process kinetics, what is confirm by negligible effect of co-ions, e.g. Na$^+$, Ca^{2+}, Mg^{2+}, Cu^{2+}, Ni^{2+}, NO^{3-}, and Cl$^-$ (Hu et al. 2006). The adsorption mechanism is related with electrostatic attraction and ion exchange. Akhbarizadeh et al. (2014) have investigated maghemite (γ-Fe$_2$O$_3$) nanoparticles as an adsorbent for removal of Cu(II), Ni(II), Mn(II), Cd(II) and Cr(VI) from solutions. pH of a solution plays very important role in adsorption of Ni(II), Mn(II) and Cd(II), for which alkaline conditions are preferable (pH range of 8.5–10), while in case of Cu(II) and Cr(VI) acidic pH is required (pH 6.5 and 2.6). Nano-magnetite is also used to remove contaminants like Cr(VI), Cu(II), Zn(II) and As(III/V), Se(IV) (Hu et al. 2004), as well as methylene blue and dichlorophenol from aqueous solutions (Mak and Chen 2004). The process mechanism of metals corresponds to monolayer adsorption according to Langmuir isotherm with maximum capacity equal 20–24 mg/g depending on metal type. Adsorption efficiency is in following order: Cu (II) > Cr (VI) > Mn(II) > Ni(II) > Cd(II). The author have found that ionic radius and electronegativity play an important role in adsorption process. As it was already mentioned, the separation of magnetic adsorbent saturated with a metal from treated water could be easily obtained by the simple application of magnetic field (Hu et al. 2006).

Titanium dioxide TiO$_2$ nanoparticles are biologically and chemically inert and have high oxidative potential and are usually used to photochemical degradation of organic contaminants (Anandan et al. 2009) and as the adsorbent for removal of heavy metals from water (George et al. 2016). For example nano-TiO$_2$ modified with thioglycolic acid and immobilized on silica gel ad well as TiO$_2$ nanotubes have been used as adsorbents to remove ions like Ni^{2+}, Cd^{2+} and Pb^{2+} from water (George et al. 2016), whereas TiO$_2$ nanoparticles (Anatase) with activated carbon have been applied to remove Cr(VI) (Mani et al. 2015). As conventional semiconductor, TiO$_2$ is most commonly used as a photocatalyst with high oxidation potential, often used at activation with sun light. Photocatalysis with TiO$_2$ results in formation of highly reactive hydroxyl radicals (*OH), superoxide anions (O$_2^-$) and superoxides (O$_2^{2-}$), which can decompose organic compounds at UV, visible or sun light radiation (Zhang et al.

2016b). Morphological structure, crystalline phase, structure damage, energy gap and hydrophilicity can be adjusted by change of TiO_2 type, chain length or introduction of surface active agent to production process (Zhang et al. 2016b). Photocatalysis with nano-TiO_2 is widely used in wastewater treatment to decompose and mineralize various contaminants and micropollutants like endocrine disruptors, cyanotoxins, antibiotics, pesticides, dyes, polymers, phenolic contaminants, aldrin, polychlorinated bisphenols and other (Fagan et al. 2016) as well as in the deactivation of bacteria: *Escherichia coli, Pseudomonas aeruginosa, Salmonella typhimurium* and *Enterobacter cloaca* (Fagan et al. 2016).

Porous nano **zinc oxide** (n-ZnO) plates of pores diameter 5-20 nm and large specific surface (147 m^2/g) have revealed strong and selective adsorption of cations of toxic metals (Wang et al. 2010), including Cu(II) with efficient >1600 mg/g. Such the high adsorption capacity results from the high number of polar active sites of nano-plates with bond hydrated Cu(II) ions by formation of Cu-O-Cu bonds on pores walls (Wang et al. 2010). n-ZnO can also effectively remove Cd(II) and Hg(II) ions with maximum capacity equal 387 and 714 mg/g, respectively (Sheela et al. 2012). Hydroxyl groups on n-ZnO surface have been found to play an important role in adsorption of various heavy metals. ZnO nanoparticles, next to TiO_2, have been accepted as an efficient and promising photocatalysis to wastewater treatment. Photocatalytic features of nano-ZnO are comparable to TiO_2 due to the fact, that its energy band is practically identical, while it is cheaper and adsorbs sun light in wider spectrum in comparison with other semiconductors made of metal oxides (Gomez-Solís et al. 2015).

For the removal od heavy metals other nano-metal oxides are used, mainly **aluminum oxide** (Zhang et al. 2008), **manganese oxide** (Madhura et al. 2018) and **magnesium oxide** (Tyagi et al. 2017).

Nanoadsorbents formed from metal oxide can be easily regenerated by solution pH change (Sharma et al. 2009). In many case adsorption capacity of metal oxides nanosorbents can be recovered even after several regeneration and reuse cycles (Hu et al. 2006). Relatively low costs of production of metal oxides based nanosorbents are also important. High adsorption ability, low cost, easy separation and regeneration make metal oxide based nanosorbents technologically and economically advantageous. Thus, metal oxide nanoparticles are efficient and promising nano-adsorbents to removal of a wide range of toxic contaminants from wastewater (Madhura et al. 2018; Zhang et al. 2016b; Lu and Astruc 2018; Sarma et al. 2019; Runowski 2014).

Table 1 presents some example of performance of metal oxides nanoadsorbents (Zhang et al. 2016b; Adeleye et al. 2016).

Recently, information on the use of various **metals nanoparticles**, mainly iron, silver, gold, nickel, aluminum and zinc, to wastewater treatment (Madhura et al. 2018) can be found in literature.

Zero valent iron (ZVI) is efficient substance to water treatment, especially zero valent nano-iron (nZVI). nZVI characterizes with high reactivity with a wide range of contaminants due to large specific surface and number of active sites as well as small particles size (Tosco et al. 2014) in comparison with regular ZVI. The research have

Table 1.

Metal oxides for contaminant removal from water

Nano-adsorbent	Nano-adsorbent properties	Pollutant	Removal efficiency
Goethite (α-FeOOH)	Needlelike particles, length 200 nm, with <50 nm, 50 m^2/g	Cu(II) F	100% Capacity 59mg/g
Hematite (α-Fe$_2$O$_3$)	Particle – 37 nm, 31.7 m^2/g, Dose 0.5g/L	Pb(II), Cd(II), Cu(II), Zn(II)	100% Pb(II) and Zn(II) 94% Cd(II), 89% Cu(II)
Maghemite (γ-Fe$_2$O$_3$)	Particle – 10 nm, 198 m^2/g Particle – 10 nm, 178 m^2/g	Cr(VI), Cu(II), Ni(II), Cr(VI)	
Magnetite (Fe$_3$O$_4$)	Particle – 10–20 nm	Se(IV)	Reduction to <5 µg/L
Hydrous ferric oxide (HFO)	148 m^2/g	F	Maximum capacity 6.71 mg F/g at pH 6.5; Capacity in column experiments 3.26 mg/g HFO
Al$_2$O$_3$	Particle – 62–87 nm, 178 m^2/g	Pb(II), Cd(II), Cr(III), Co(II), Ni(II), Mn(II)	Maximum capacity of Cr(III), Cd(II) and Pb(II) in a mixture of six ion – 100.0, 83.33 and 100.0 mg/g, respectively
TiO$_2$	Particle – 8.3 nm, 185.5 m^2/g	Pb(II), Cd(II), Cu(II), Ni(II), Zn(II), dye, micro-pollutants	Pb: 2.0 µmol/L(99.9%), Cd: 3.9 µmol/L (96.2%), Zn: 6.3 µmol/L (98.2%) i
ZnO	Particle – 26 nm	Zn(II), Cd(II), Hg(II)	Maximum capacity 357, 387, 714 mg/g for Zn(II), Cd(II), Hg(II);
ZrO$_2$	–	Cd(II)	215 mg/g
Fe$_3$O$_4$/SiO$_2$ Fe$_3$O$_4$/SiO$_2$/NH/Cs$_2$Na	– –	Hg(II)	17 mg/g, 50%; 25 mg/g, 74%
TiO$_2$-In$_2$O$_3$ TiO$_2$ (P25) TiO$_2$	– – –	2-chlorophenol	17 mg/g, 26%/1.5 h; 58 mg/g, 68%/2 h; 248 mg/g, 99%/1.5 h;
Pt/TiO$_2$ SiO$_2$/ TiO$_2$ fibers	– –	Rhodamine B	6.0 mg/g, 95%/5 h; 300 mg/g, 100%/2.7 h;
TiO$_2$ TiO$_2$ nanotubes	– –	Methylene blue	50 mg/g, 100%/0.75 h; 174 mg/g, 87%/0.67 h;
TiO$_2$/SnO$_2$ Ag/TiO$_2$	– –	Methyl orange	38 mg/g, 95%/12 min; 135 mg/g, 90%/0.8 h;
TiO$_2$	–	Chlorhexidine	3200 mg/g, 64%/1 h

shown, that by the decrease of size of ZVI from microscale to nanoscale, the rate of removal of As(V) can be increased by three times (Xu et al. 2012). Additionally, nZVI surface can be easily modified, possesses excellent magnetic properties and high bio-compatibility (Xu et al. 2012). nZVI nanoparticles possess core-coat structure with external layer of iron oxides and internal Fe^0 core (Fig. 2). The iron hydroxide layer around Fe^0 core has be found to be the strong adsorbent. Fe^0 core can be oxidized to iron oxides in reaction with water, and next it can be transformed to as number of corrosion products, including goethite (α-FeOOH), akageneite (β-FeOOH), lepidocrocite (γ-FeOOH), magnetite (Fe_3O_4), maghemite (γ-Fe_2O_3) or green siderite ($FeCO_3$). These corrosion products also reveal significant adsorption affinity to large amounts of contaminants (Fig. 2) (Xu et al. 2012).
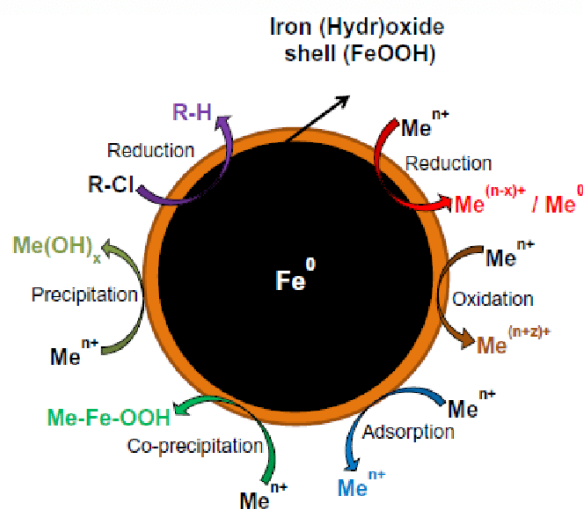

Figure 2.
Core–shell structure of nZVI depicting various mechanisms for the removal
of metals and chlorinated compounds (Li et al. 2010a)

nZVI are widely used as an adsorbent to contaminants removal. Hua et al. (2012) have shown complete removal of As(V) using adsorbent doses equal to 0.1, 0.2 and 0.4 g/L of nZVI added to three different types of real wastewater. The research have also shown that As(V) adsorption occurs due to complexation at internal nZVI layer (Hua et al. 2012). It has also been found that many metals like Cd, Cr, etc. are also adsorbed by nZVI due to formation of complexes with internal part of nZVI (Yu et al. 2014). Some contaminants like As(III/V), U(VI), Se(VI) can decrease their oxidation state by adsorption on nZVI surface. Crane et al. (2011) state, that U(VI) can be removed due to nZVI adsorption to concentration below 10 µg/L (>98% removal) within 2 hours, and it can be partially reduced to U(IV) at simultaneous oxidation of Fe. Li et al. (2014) have shown, that average adsorption capacity of Cu(II) on nZVI

equals 343 mg/g due to reduction to metallic copper or cuprite (Cu_2O). Ramos et al. (2009) have found, that As(V) or As(III) are partially reduced to As(0) after reaction with nZVI. Additionally, As(III) forms As(0), As(III) and As(V) on nZVI surface, what means that during the reaction both, reduction and oxidation of As(III) occurs. Double redox function of nZVI is possible due to core-coat structure, as the core is the metallic iron of strong reduction tendency, while the external layer containing thin, amorphous iron hydroxide promotes coordination and oxidation. Despite above mentioned ions, nZVI can also remove phosphates (Wen et al. 2014), nitrates (Ryu et al. 2011), dyes (Fan et al. 2009) and antibiotics (Fang et al. 2011) due to mechanisms of physical adsorption, oxidation, reduction and co-precipitation.

Silver nanoparticles (NPs) are highly toxic to microorganisms, thus it is able to destruct fungi (Krishnaraj et al. 2012), bacteria (Kalhapure et al. 2015) and viruses (Borrego et al. 2016). Due to this feature Ag NPs are widely used to water disinfection also in point-of-use disinfection. Ag NPs sheets reveal efficient antibacterial effects to Enterococcus faecalis, Escherichia coli, deactivating bacteria cells during filtration. It has been found that Ag NPs interact with bacteria cell walls, next reach the cell interior and deform cell's wall structure increasing its permeability (Sondi et al. 2004). During Ag NPs interaction with a cell free radicals can also be formed, thus bacteria cell wall is damaged and the cell dies (Sondi et al. 2004). Ag NPs have been efficiently applied to wastewater treatment. The main disadvantage of this material is the formation of clusters in water by non-modified Ag NPs, what affects their antibacterial properties during long-term use (Li et al. 2011). On the other hand, systems integrating Ag NPs with membranes or filters are used to water disinfection due to the efficient antibacterial effect and low costs (Quang et al. 2013).

Zinc nanoparticles are found to be an alternative solution for Ag and Fe NPs (Bokare et al. 2013). With their highly negative standard reduction potential, Zn NPs are much stronger reducer than Fe NPs. Hence, the ability of contaminants degradation by Zn NPs is faster and more efficient. The use of Zn NPs is related with wastewater dechlorination, degradation of carbon tetrachloride and octachlorodibenzo-p-dioxin (Tratnyek et al. 2010). The degradation of the latter in wastewater have been investigated using four different metals nanoparticles, i.e. nickel, aluminum, iron and zinc. At optimum reaction condition the highest efficiency of octachlorodibenzo-p-dioxin have been reached with the use of zinc nanoparticles.

1.2. Carbon based nanoadsorbents

Carbon based nano-adsorbents include carbon nanotubes (CNT), graphene and graphene oxide, fullerenes and carbon nitride. They characterize with large specific surface area, high thermal stability and ability to adsorb inorganic and organic contaminants (Ren and Smith 2013; Wang et al. 2012a). They usability to remove contaminants from water usually requires proper surface modification due to relatively poor interaction of ions (metals) and other substances with an adsorbent surface.

Graphene is a layer of tightly packed carbon atoms, which are bond together in a honeycomb shape matrix (Fig. 3a), while as it is of a single atom thickness of ca. 0.3 nm, it structure is simplified to 2D. It is an allotrope of carbon, built of planar atoms bond with strong sigma bonds of sp^2 hybridization and of very short length (0,142 nm) (Cohen-Tanugi et al. 2014; Bodzek et al. 2020c). Graphene characterizes with large specific surface, which may be simply modified. **Graphene oxide** (GO) is a single-layer oxidized graphene with oxygen-containing functional groups, mainly hydroxyl, carboxyl, carbonyl and epoxy ones (Fig. 3b) (Bodzek et al. 2020c). Reduced graphene oxide (RGO) possesses more defects and smaller conductivity than graphene, but its modification with various functional groups is easier (Bodzek et al. 2020c). Thus, it characterizes with excellent hydrophilicity and better reactivity with a number of contaminants (Santhosh et al. 2016). The characteristic feature of GO/RGO, due to the presence of oxygen atoms in functional groups, are easy electrostatic interactions with organic and inorganic contaminants. Adsorption at graphene-based nanomaterials may also run due to hydrophobic interactions and π-π, hydrogen or covalent bonds formation (Sarma et al. 2019).
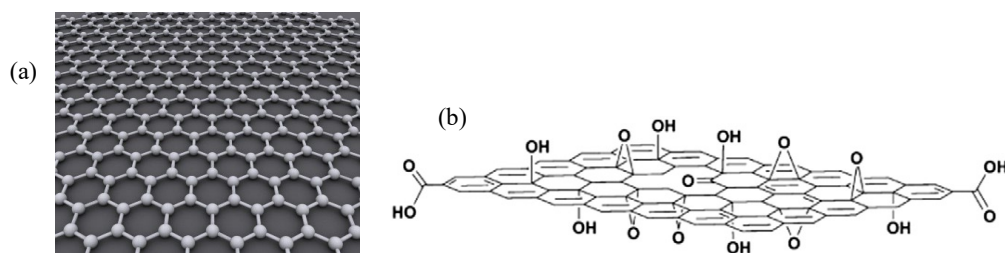

Figure 3.
Two-dimensional model of graphene structure(a), graphene oxide (GO) model (b)

Graphene and its modified forms (GO/RGO) have been widely used to removal of such heavy metals like Pb(II), Zn(II), Cu(II), Cd(II), Hg(II) and As(III/V) (Sitko et al. 2013). Wang et al. (2013a) have investigated the impact of pH, GO dose, presence of other ions and contact time on the efficiency of Zn(II) adsorption. The results have shown that optimum pH for Zn(II) removal equals 7.0 at relatively fast reaching of equilibrium with maximum adsorption capacity amounted to 246 mg/g. Madadrang et al. (2012) have found, that GO modification with EDTA allows for efficient adsorption of Pb(II) due to its chelating properties. It has been shown, that adsorption capacity can obtain ca. 480 mg/g at pH 6.8, while the equilibrium is reached within 20 minutes. Huang et al. (2011) have also discussed Pb (II) adsorption using oxidized and pure graphene sheets. In the design of composite adsorption materials, graphene and graphene oxides nanosheets can be combined with metal oxides to form adsorbents suitable to remove various contaminants from wastewater. Kumar et al. (2014) have used magnetic nanocomposite of GO with iron(II) manganite to efficient removal of Pb(II) and As(III/V) from contaminated water. The maximum sorption capacity

has been established at 673 mg/g for Pb(II), 146 mg/g for As(III) and 207 mg/g for As(V). The advantage of the adsorbent, except for its high capacity, is its simple separation in magnetic field. Ions of toxic metals like lead(II), zinc(II) and cadmium(II) have been removed from aquatic environment by means of adsorption with composite material composed of graphene oxide/TiO_2 (Lee et al. 2012). The efficiency of adsorption of lead(II), zinc(II) and cadmium(II has reached 65.6 mg/g, 88.9 mg/g and 72.8 mg/g, respectively, at pH 5.6. The adsorption capacity of the composite material has been higher than in case of graphene oxide or titanium dioxide themselves. The results of the removal efficiency of various metals using GO based adsorbents are presented in Table 2 (Madadrang et al. 2012; Kumar et al. 2014; Lee et al. 2012; Hur et al. 2015; Nandi et al. 2013; Ozmen et al. 2010; Wang et al. 2013b; Hao et al. 2012; Sreeprasad et al. 2011).

Table 2.

Graphene nanocomposites used in removal of metal ions

Metal	Graphene nanocomposite	Adsorption efficiency (mg/g)
Cu(II)	Graphene oxide (GO)/Fe_3O_4	18.3
	GO/Fe_3O_4/sulfanilic acid	50.7–56.8
	GO/Fe_3O_4	23.1
	GO/Mn-doped Fe(III)oxide	129.7
Pb(II)	GO/silica/Fe_3O_4	333.3
	GO-$MnFe_2O_4$	673
	GO/Fe_3O_4	299.4
	TiO_2/GO	65.6
	GO-EDTA	479
Cd(II)	GO/silica/Fe_3O_4	166.7
	GO/Mn-doped Fe(III)oxide	87.2
Hg(II)	GO/Fe_3O_4	4.4
	MnO_2/GNs	10.8

Except for metal ions removal, graphene-based adsorbents have also been investigated in regard to adsorption of anionic contaminants (e.g. fluorides, phosphates, perchlorates) (Sarma et al. 2019). Graphene was found to be a good adsorbent of fluoride with an adsorption capacity of up to 36.5 mg/g at pH 7.02 and 25°C (Li et al. 2011). The mechanism of adsorption relies on the exchange of fluorides present in solution to hydroxyl ions present in adsorbent structure. Vasudevan and Lakshmi (2012) have performed systematic research on phosphates adsorption on graphene. The experimental results have shown that graphene adsorption capacity reaches 89.37 mg/g. Zhang et al. (2011) have developed a hybrid composite of graphene-poly-

pyrrole (Ppy) to remove perchlorates (ClO_4^-). The composite has characterized with higher perchlorates sorption capacity than single Ppy films, while the adsorption mechanism has relied only on ion exchange.

The adsorption of humic acids (HA) on GO, at maximum adsorption capacity amounted to 190 mg/g, what is much higher than the one of activated carbon (Hartono et al. 2009). The adsorption of some dyes (Liu et al. 2012) and antibiotics (tetracycline, oxytetracycline and doxycycline) on GO were also studied and their efficiencies were also much higher than those of activated carbon (Yu et al. 2015). Their removal results are shown in Table 3 (Wang et al. 2012a; Gao et al. 2012; Liu et al. 2012; Zhang et al. 2013a; Xie et al. 2012; Fan et al. 2012; Bai et al. 2012; Bradder et al. 2010; Shi et al. 2017; Pastrana-Martinez et al. 2012; Ma et al. 2015; Yu et al. 2015; Chen et al. 2015; Zhao et al. 2015; Ghadim et al. 2013; Lin et al. 2013). The adsorption mechanism of ionic dyes mainly involves electrostatic interaction and covalent bonding.

Carbon nanotubes (CNTs) are an allotropic variety of carbon whose walls are made of graphene (a one-atom layer of graphite) coiled into a tubular structure

Table 3.

Adsorption of organic contaminants using graphene based materials

Contaminant	Graphene based nanocomposite	Sorption capacity (mg/g)
Methylene blue	Polyethersulphone/GO Fe_3O_4/GO Sponge GO RGO/CdS RGO–$MnFe_2O_4$ GO GNs	62.5 167.2 397.0 94 (%) 92 (%) 351.0 154–204
Rhodamine B	RGO–$MnFe_2O_4$ RGO/ZnO	92 (%) –
Methylene violet	GO sponge	467.0
Methylene orange	Reduced GO–TiO_2	–
Ciprofloxacin	Porous graphene hydrogel KOH-activated graphene Single layer GO	235.6 194.6 379.0
Tetracycline	TiO_2-graphene sponge GO F–GO and MNPs	1,805.0 381.8 39.1
Doxycycline	F–GO and MNPs GO	35.5 398.4
Oxytetracycline	GO F–GO and MNPs	212.3 45.0
Chlortetracycline	F–GO and MNPs	42.6

(Ahmad et al. 2012). Carbon nanotubes (CNT) are one of the most important material, which has promoted research and development of nanotechnology. There are three types of CNTs: single-walled CNT (SWCNTs), multi-walled CNT (MWCNT) and composite CNT (CCNT, including functionalized FCNT) (Fig. 4) (Wang et al. 2012a). SWCNTs consist of a coiled single graphene layer (Fig. 4b), while MWCNTs have multiple coaxially aligned graphene sheets (Fig. 4a). The diameter of SWCNTs ranges from a fraction to a few nanometers (0.3–2 nm), while MWCNTs range from a few to tens of nanometers (2–100 nm) (Bodzek et al. 2021b; Ahmad et al. 2012). The length of both types of nanotubes can reach micro- or even millimeter values, so the ratio of their length to diameter is remarkably high and is within 10^3–10^5, which allows them to be classified as one-dimensional objects. SWCNTs consist of two separate regions with different physical and chemical properties. The first is the sidewall of the nanotube and the second is the end cap (tip) of the tube (Ahmad et al. 2012). High adsorption efficiency of CNT results mainly from large specific surface area and interactions with contaminants. In comparison with conventional granular or powdered activated carbon, CNT possess controlled pore size distribution and high ration of active surface to volume, what results in unique sorption efficiency. Functionalized CNTs are of great importance in adsorption (Fig. 4c). Functionalization of CNTs with HNO_3, H_2SO_4, HCl, H_2O_2, $KMnO_4$, and/or NaOCl results in the introduction of oxygen functional groups attached to the sidewalls, cores, and ends of CNTs (Ren et al. 2011). The functionalization also aims to eliminate the dispersion of CNTs and facilitate the adsorption efficiency in the elimination of anaerobes from water or wastewater.
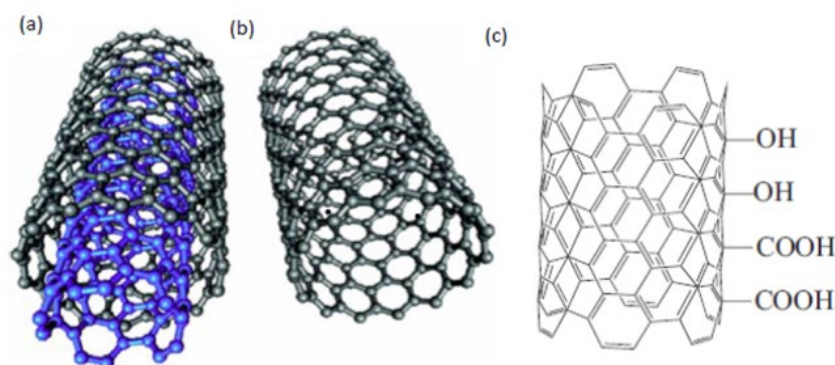
Figure 4.
Structures of multi-walled (a), single-walled (b) and functionalized (c) carbon nanotubes
(Lu and Astruc 2018; Das et al. 2014a)

In CNT sorption takes place mainly due to physical interactions of non-polar compounds and chemical bonding of polar substances. The ability of sorption of CNT mainly depends on the type of an adsorbate and type of functional groups on the adsorbent surface, such as carboxylic, hydroxyl, phenolic and amine functional

groups (Wang et al. 2008). On the other hand, the sorption ability is also observed for CNT, which are not functionalized, for example in removal of nonpolar polyaromatic hydrocarbons (Stafiej and Pyrzynska 2007). Strong sorption of many polar organic compounds results from various interactions of CNT with contaminants, including hydrophobic effect, π-π interactions, hydrogen and covalent bonding and electrostatic interactions (Yang and Xing 2010). π-electrons rich CNT surface allows for π-π bonds interactions with organic compounds containing C=C bonds or benzene rings, such as in case of polyaromatic hydrocarbons (PAHs) and polar aromatic compounds (Lin and Xing 2008). Organic compounds, which possess functional groups like -COOH, -OH, -NH$_2$ may form hydrogen bonds with graphite CNT surface, which becomes an electron donor (Yao et al. 2011). Electrostatic attraction enables adsorption of organic compounds, which at suitable pH are positively charged, e.g. some antibiotics (Ji et al. 2009). Sorption effect of CNT is the highest at high pH in the range of 7 to 10.

CNT has been investigated in regard to removal of dyes from water and wastewater. For example multi-walled CNT impregnated with chitosan hydrogel have been used in research on the efficiency of removal of Congo red from aqueous solutions (Chatterjee et al. 2010) with adsorption efficiency of 423.1 mg/g at pH 4.0. Adsorption fit to Langmuir model and pseudo second order equation. Single-walled CNT has also been used to remove reactive Red 120 dye from textile wastewater in dependence on pH. At optimal pH = 5.0, adsorption capacity was equal to 426.5 mg/g. It has been also found that the dye adsorption efficiency increases with the adsorbent dose increase and reaches 882.84 mg/g at equilibrium contact time 180 min (Bazrafshan et al. 2013). The adsorption capacity of Procion MX-5B red dye during treatment of different types of industrial wastewater with multi-walled CNT has been investigated by Wu et al. (2007). The obtained results have shown that adsorption efficiency increase with temperature increase as mobility of dye particles increases, what confirms, that adsorption process is endothermic. At pH 6.5, the maximum adsorption equal to 20.93, 22.87, 27.20 and 30.53 mg/g has been reached at temperatures 281, 291, 301 and 321 K, respectively. It has also been found, that Langmuir isotherm and pseudo second order kinetic model are suitable to describe this dye adsorption.

Promising results has been obtained in removal of natural organic matter (NOM) from aqueous solutions using multi-walled CNT due to adsorbent's hydrophobicity (Hyung and Kim 2008). NOM in surface and groundwater undergoes ionization at pH range 3.0–9.0 and strong adsorption (2.5–50 mgC/L) at CNT surface is observed.

Adsorption of trihalomethanes, i.e. chloroform, dichlorobromomethane, dibromochlomethane and bromoform has also been investigated in different water types using multi-walled CNT (Lu et al. 2005). It has been found that chloroform adsorption equilibrium has been reached fasted than ones of dichlorobromomethane, dibromochloromethane and bromoform due to smaller size and easier permeation of pores interior. Additionally, it has been shown that the increase of temperature from 5 to 35°C decreases the adsorption efficiency. At 5°C maximum adsorption capacity of chloroform, dichlorobromomethane, dibromochloromethane and bromoform has reached 3,158; 2,016; 2,008 and 1,976 mg/g, respectively.

Functionalized CNT reveal high adsorption capacity toward metal ions. Surface functional groups of CNT (carboxylic, hydroxyl and phenolic ones) are main adsorption sited for metal ions, mainly due to electrostatic attraction and chemical bonding (Rao et al. 2007). Resulting surface oxidation may significantly increase adsorption ability of CNT. A number of research show that CNT are much better adsorbent than activated carbons in regard to heavy metals (Cu^{2+}, Pb^{2+}, Cd^{2+} and Zn^{2+}) (Table 4) (Li et al. 2002 2003; Anitha et al. 2015; Lu and Liu 2006; Lu and Chiu 2006), and adsorption kinetic is higher for CNT due to easily accessible adsorption sites and short diffusion path to particle interior. Gupta et al. (2011a) has investigated removal of chromium(III) using multi-walled CNT, also containing ferric oxide nanoparticles, functionalized with carbonyl and hydroxy group.

Table 4.

Adsorption of heavy metal ions at different types of carbon nanotubes (CNT)

Metal ion	Nanoadsorbent	Adsorption efficiency
Pb(II)	$CNTs(HNO_3)$ CNT-OH $CNT-CONH_2$ CNT-COO- $MWCNTs (HNO_3)$	49.95 mg/g at pH: 7.0 2.07 mmol/g 1.907 mmol/g 4 mmol/g 97.08 mg/g at pH: 5.0
Cd(II)	CNTs-COO- CNT-OH $CNT-CONH_2$	3.325 mmol/g 1.513 mmol/g 1.563 mmol/g
Ni(II)	MWCNTs SWCNTs	7.53 mg/g at pH: 7.0 9.22 mg/g at pH: 7.0
Zn(II)	MWCNTs SWCNTs	43.66 and 32.68 mg/g
Cu(II)	CNTs CNT-OH $CNT-CONH_2$ CNT-COO-	1.219 mmol/g 1.342 mmol/g 1.755 mmol/g 3.565 mmol/g

Regeneration is a very important feature, which determines the usability of adsorbents. Adsorption of metal ions at CNT is reversible process enabled by solution pH decrease. The recovery rate of a metal is usually above 90%, while at pH<2 it often reaches 100% (Li et al. 2005). Additionally, the sorption capacity is stable, even after regeneration. For example, adsorption capacity of Zn^{2+} ions indicated for SWCNT and MWCNT has decrease by 25% after 10 regeneration cycles and reuse of adsor-

bent, while for activated carbon it has decreased by 50% already after first regeneration cycle (Lu et al. 2007).

Fullerene is an allotrope of carbon whose molecule consists of carbon atoms connected by single and double bonds so as to form a closed or partially closed mesh, with fused rings of five to seven atoms (Yannoni et al. 1991; Kroto et al. 1985; Tycko et al. 1991). Fullerenes with a closed mesh topology are informally denoted by their empirical formula Cn, where n is the number of carbon atoms. Among several forms of fullerenes, fullerene C60 is the most common and best studied fullerene. C60 is a spherical molecule with the carbon atoms arranged at the vertices of a truncated icosahedron structure (Fig. 5) (Yannoni et al. 1991; Kroto et al. 1985; Tycko et al. 1991). There are other less stable forms such as C70, C76, C78, and C80 used in a multitude of biological and medical applications. 60 carbon atoms make up 20 six membered rings and 12 five-membered rings, composed of 60 vertices, all carbon atoms are equivalent (Yannoni et al. 1991; Kroto et al. 1985). Fullerene C60 is spherical, and the σ bond of C60 is different from sp^2 hybrid σ bond in graphite and diamond sp^3 hybrid bond. Fullerene C60 has strong antioxidant and antiviral activity and rich redox properties (Pan et al. 2020). C60 has a large surface area, are inexpensive, and has been used as an adsorbent for environmental remediation (Yang et al. 2006; Cheng et al. 2005; Gupta and Saleh 2013). The π electrons present in the inner and outer spheres of fullerene interact with pollutants by π-π bonds. However, fullerenes have many advantages, the dispersion and solubility of fullerenes in solution are not very good. Therefore, the modification of fullerenes to obtain their derivatives for photocatalytic reaction received great attention (Pan et al. 2020).
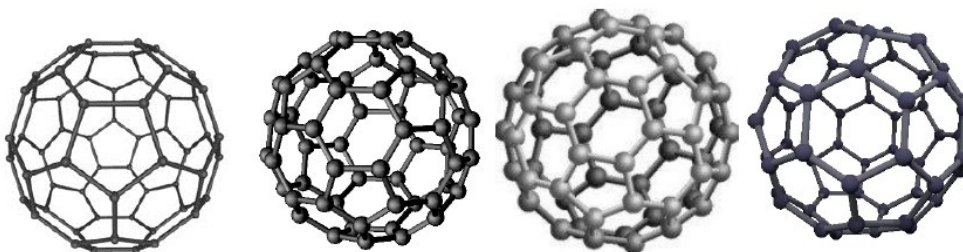
Figure 5.
Scheme presenting fullerene C60, C70, C78, C80

Many types of contaminants in water, such as organic dyes and other organic pollutants and heavy metal ions, have been widely studied by photocatalysis, with the application of fullerene-based photocatalysts and their derivatives (Pan et al. 2020). It has been found that the adsorption efficiency of organics by fullerenes is much higher than that of activated carbon or carbon black.

Bai et al. (2014) modified the fullerene with a hydroxyl group to obtain a polyhydroxy fullerene, and then combined with TiO_2 to prepare a photocatalyst for removing the organic dye. For the conditions used, about 17% of 2-chlorophenol and 28% of

"rose Bengal" were removed after 30 min of irradiation (Chae et al. 2014). Adsorption studies of polyaromatic compounds (pyrene, naphthalene, and phenanthrene) on C60 were also carried out (Yang et al. 2006). It was also found that C60 adsorbs phenols (phenol 10%, 3,4-dimethylphenol 48%, 2-tert-butylphenol 54%, 2-isopropoxyphenol 62% and 4-chlorophenol 45%) successfully, polyaromatic compounds (naphthalene 22%, phenanthrene 37%, anthracene 42% and perylene 62%), and amines (methyl-lethylenediamine 10%, aniline 14% and 1,2-phenylenediamine 28%) (Ballesteros et al. 2000). Cheng et al. (2005) investigated the absorption potential of naphthalene and 1,2-dichlorobenzene (1,2-DCB) with nano-sized C60 fullerene aggregates. Pan et al. (2020) have found that adsorption of toulene was 99%, benzene 27–87% and nitro-benzene 10%.

Composites of fullerene with other photocatalysts or polymers show higher adsorption efficiency. Bai et al (2014) used a composite nanomaterial of fullerene C60 and carbon nitride to degrade dye methylene blue and phenolic pollutants. Compared with pure carbon nitride, the activity of the composite photocatalyst was dramatically improved after C60 modification. Long et al. (2009) studied C60-doped TiO_2 nano-rods and found that this photocatalyst had a high degradation efficiency (99%) for rhodamine B after 1.5 h of reaction. Ding et al. (2017) and Qi et al. (2016) also found that $C60/TiO_2$ and C60-modified SnO_2 composites have good degradation effect on organic dyes. Xu et. al. (2016a) found that $C60/Ag_3PO_4$ composites degraded acid red 18 (AR18) almost 3.5 times faster compared to the degradation rate of C60 without modification, and the removal efficiency was 90%. Park et al. (2009) used water-soluble fullerol (C60(OH)x) to activation of titanium dioxide under visible light to prepare a composite catalyst, which had a good effect on reducing toxic Cr(VI) in water to less toxic Cr(III). Examples of photocatalytic applications of fullerenes in the degradation of organic pollutants are shown in Table 5.

Carbon nitride (C_3N_4) is a layered, stable, and polymeric metal-free material that has been discovered as a visible-light-response photocatalyst. With a suitable "forbidden band" energy value and high chemical and thermal stability, non-metallic polymeric graphitic carbon nitride with 2D structure (g-C_3N_4) is an important photocatalytic material for environmental and energy applications (Murugesan et al. 2019; Liu et al. 2020). Various strategies have been adopted to enhance the disinfection efficiency of pure g-C_3N_4. Due to its large adsorption surface area, graphitic carbon nitride g-C_3N_4 is a new class of photo-catalysts, which exhibits enhanced activity in water and wastewater treatment for a wide variety of synthetic toxic contaminants, including microorganisms (Hao et al. 2016; Belver et al. 2019).

The electron-rich surface of g-C_3N_4 selectively adsorbs cationic dyes (methylene dyes) because g-C_3N_4 behaves as a negatively charged surface in aqueous media (Liu et al. 2015). Zhang et al. (2016b) synthesized a g-C_3N_4 hydrogel (h-CN) and used it to adsorption of various cationic (MB, Azure B, Acriflavine, and Safranin O) and anionic (RhB, eosin Y, and MO) dyes. The h-CN selectively adsorbs cationic dyes with an adsorption efficiency of 99%, because the surface charge of h-CN (zeta potential), is much more negative (63.1 mV) than pure g-C_3N_4 (30–40 mV). Furthermore, it was

Table 5.

Photocatalytic application of fullerene-based photocatalysts in organic pollutants

Photocatalyst	Pollutant	Effectiveness	Amplification factor
TiNTs/C60 TiO$_2$/C60 TiO$_2$/C60 TiO$_2$/C60 TiO$_2$/C60	Isopropanol methyl orange methylene blue methylene blue salicylic acid	99.9% (11 h) – 99.5% (1 h) 99.9% (1 h) 53 90% (2 h)	2 times than TiNTs – – 1.43 times than TiO$_2$ 1.63 times than TiO$_2$
SiO$_2$/C60 SiO$_2$/C60	methyl orange heptene	96% (25 min) 95% (100 min)	– –
C$_3$N$_4$/C60	rhodamine B	97% (1 h)	1.8 times than C$_3$N$_4$
BiOCl Bi$_2$TiO$_4$F$_2$/C60 Bi$_2$TiO$_4$F$_2$/C60 Bi$_2$MoO$_6$/C60	rhodamine B lignin Rhodamine B bromate ions	99.7% (12 h) – 90% (2 h) 1 92% (2 h)	9 times than BiOCl – 5 times than Bi$_2$TiO4F$_2$ 1.3 times than Bi$_2$MoO$_6$
LDO-AgCl/C60	Bisphenol A	90% (5 h)	2.17 times than LDO
WO$_3$/TiO$_2$/C60	methylene blue	–	–
Pt/TiO2/C60	methyl orange	80% (2 h)	1.63 times than TiO$_2$
Ag$_3$PO$_4$/C60	acid red	90% (1 h)	3.5 times than Ag$_3$PO$_4$
Fe$_2$O$_3$/C60	phenol	98.9% (80 min)	–

observed that the active surface area is much higher for h-CN (190 m^2/g) than for pure g-C$_3$N$_4$ (approximately 50 m^2/g). Chemically modified versions of g-C$_3$N$_4$ containing oxygen functional groups (-OH, -COOH and -NO$_3$) were also used to remove dyes from water (Liu et al. 2015; Kim et. al. 2016; Ming et al. 2014; Dong et al. 2014). The oxidized g-C$_3$N$_4$ shows better dispersion in aqueous media, which increases the efficiency of dye removal. Zhang et al. (2018) compared the adsorption capacity and photocatalytic remediation of g-C$_3$N$_4$, graphene aerogel-TiO$_2$ (TiO$_2$-GA) and g-C$_3$N$_4$-TiO$_2$-GA nano-composite. The g-C$_3$N$_4$-TiO$_2$-GA adsorbed 96.5% of the methylene blue dye from the aqueous environment with higher efficiency than the other composites (TiO$_2$-GA and g-C$_3$N$_4$). The high adsorption potential of g-C$_3$N4-TiO$_2$-GA was attributed to the impregnation of g-C$_3$N$_4$, which increases the porosity and thus the adsorption of the material. Younis et al. (2016) investigated the removal of various dyes (methyl orange (MO), methylene blue (MB) and crystal violet (CV)), using CaO and g-C$_3$N$_4$ based nanocomposites They showed that the copolymer exhibited higher affinity towards MB adsorption (1915.8 μmol/g) than other adsorbents.

Zhu et al. (2017, 2018) studied the adsorption of heavy metal ions (e.g., Pb (II)) using g-C$_3$N$_4$. The higher adsorption capacity of g-C$_3$N$_4$ at higher pH may be attributed to pH-dependent changes in surface charge. At low pH, due to the high concentration, H$^+$ ions compete with heavy metal ions for active sites on the g-C$_3$N$_4$

surface. In addition, the g-C_3N_4 surface assumes a positive charge because the free electron pairs act as proton acceptors and therefore repel heavy metal ions and have a reduced affinity for metal ions. However, at higher pH, a negative charge is formed on the surface of g-C_3N_4 and it effectively attracted positively charged metal ions, which are strongly adsorbed through electrostatic interactions.

Photocatalysis based on g-C_3N_4 in the presence of solar energy has been found to be extremely attractive for the degradation of a range of pharmaceutical chemicals, including antibiotics (Khan et al. 2018; Li et al. 2019; Chen et al. 2019). Deng et. al. (2018) described the degradation of ciprofloxacin using Ag- and P-doped g-C_3N_4 and coupled to the nanophotocatalyst $BiVO_4$ under visible light irradiation. Degradation of ciprofloxacin was mainly caused by photogenerated electron holes and superoxide anions, with some contribution from hydroxyl radicals. Wang et al. (2018a) used polyester fiber on g-C_3N_4 support and performed photodegradation of sulfonamide group antibiotics. Zhu et. al (2018) used Fe_3O_4/g-C_3N_4 photocatalyst to degrade several antibiotics such as tetracycline, ciprofloxacin, gatifloxacin, tetracycline hydrochloride and enrofloxacin hydrochloride. Also naproxen and diclofenac sodium were efficiently degraded to CO_2 and H_2O using g-C_3N_4 based photocatalysts (Wang et al. 2018).

2. Membranes and membrane processes

Membrane separation processes in recent decades have become one of the non-conventional techniques used to solve fresh water scarcity issues from alternative resources (Madhura et al. 2018). In comparison with conventional water and wastewater treatment processes, they are environmentally friendly and energy efficient. Moreover, they can be used in combination with conventional methods as well as single stage processes (Bodzek 2019). Crucial features of membrane water treatment and water reclamation include high automation level, compact installation sizes, lower consumption of chemicals and module configuration enabling flexible design (Bodzek 2019). Ideal membrane should characterize with controllable pore size, high hydraulic permeability, high selectivity and chemical resistance in wide pH range. The dependence between membrane selectivity and permeability is a serious challenge for membrane technologies exploitation. Membranes fouling and lifetime of membranes themselves affect energy consumption and complicates design and exploitation of the overall treatment system (Bodzek 2019). The efficiency of membrane systems depends mainly on a membrane material and a membrane thickness as well as on membrane physicochemical properties.

Different membrane techniques like reverse osmosis (RO), nanofiltration (NF), ultrafiltration (UF), microfiltration (MF), electro-dialysis, membrane distillation an extraction, pervaporation, capacitive deionization and forward osmosis (FO) can be used to water and wastewater treatment (Bodzek 2019; Elimelech and Phillip 2011).

Despite relatively good recognition and advantageous features of water and wastewater treatment, including operational costs, environmental impact and limited possibilities of water pretreatment as well as used membrane recovery, the growing interest in development and modification of these processes is observed (Miller et al. 2014). The crucial area of research in membrane water and wastewater treatment is focused on the development of novel, semipermeable membranes of improved separation efficiency and antifouling character (Elimelech and Phillip 2011; Qu et al. 2013). The next generation of membranes should met requirements of treatment of specific water types by their proper design, what includes structure, hydrophilicity, porosity, charge and thermal and mechanical stabilities as well as introduction of novel features like antibacterial and photocatalytic properties, which allow for the decrease of cleaning frequencies and elongate membrane lifetime (Bodzek et al. 2021b).

2.1. Conventional and novel membrane materials

Currently, most membrane techniques use film composite (TFC) membranes with of polyamide (PA) skin layer. Typical TFC membrane comprises of three layers (Fig. 6): dense, polyamide retention layer (skin/active layer), porous support usually made of polysulphone (PSF) or polyethersulphone (PES) and non-woven fabric for mechanical stability enhancement. Different methods of optimization of structure and chemical nature of TFC polyamide membranes are used in order to increase their separation efficiency and anti-fouling properties. Typical methods cover change of type and concentration of monomer during interfacial polymerization (IP), modification of a membrane surface and final processing of manufactured membrane (Feng et al. 2014; Arena et al. 2011). However, many of these methods allows for insignificant improvement of separation properties, while permeability of water of currently used TFC membranes remains relatively low. Except for that, other disadvantages of commercial TFC membranes are low selectivity and high affinity to fouling (Matin et al. 2011) as well as mechanical and chemical instability (Lee et al. 2011).
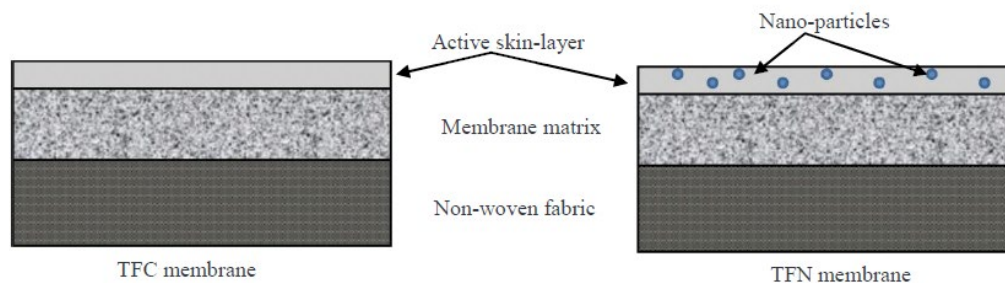

Figure 6.
The schemes of structures of thin film composite (TFC) membrane and thin film nanocomposite (TFN) membrane

The significant improvement of TFC membrane, developed in 2007, relied on introduction of porous zeolite nano-particles (NaA) of pore size about 0.4 nm to PA skin layer during IP process (Dong et al. 2016). In the membrane structure, which was named as thin film nano-composite (TFC), porous zeolite nano-particles assured preferable water transportation pathways, lowered hydraulic resistance and influenced on retention of dissolved salts. In Figure 6 the structures of thin film composite (TFC) membrane and thin film nano-composite membrane (TFN) are compared (Bodzek et al. 2021b).

In recent years the growing interest in the use of nano-materials to development of next generation of membranes (TFN) of advanced antifouling and anti-scaling properties for water and wastewater treatment has been observed (Altintas et al. 2016; Werber et al. 2016; Song et al. 2018; Anand et al. 2018; Shen et al. 2014; Hinds et al. 2004; Manawi et al. 2016; Goh et al. 2016). Significant improvements of TFC semi-permeable composite membranes in use today, involve the incorporation of nano-particles into the polymeric or ceramic active layer (Jeong et al. 2007) which allows for improvement of membrane structure and efficiencies. The most popular materials used for membrane modifications are: zeolites, metals, metal oxides, silica, and carbon-based materials (Song et al. 2018; Anand et al. 2018), i.e. graphene, graphene oxide and nanotubes (CNT) (Hinds et al. 2004; Manawi et al. 2016). In the TFN membrane structure, nano-particles provide preferential pathways for water transport, lower hydraulic resistance and higher dissolved salt retention. The production of membranes with nano-particles is based either on introduction of nano-materials to active layer of TFC membranes by means surface modification method or on their introduction to membrane matrix during phase inversion production process (Madhura et al. 2018; Qu et al. 2013).

2.2. Membranes with zeolites and metal/metal oxides nanoparticles

Nano-zeolites are the most often used in TFN membrane preparation, as they allow for formation of more permeable, negatively charged and thicker active layer of polyamide (Lind et al. 2009), large specific surface, hydrothermal stability and high number of micropores. The permeability of TFN membranes containing zeolite is almost twice as high as the one of conventional TFC membranes (without zeolite), because the small, hydrophilic pores of the nano-zeolite create preferential channels for water transport. Moreover, NaCl retention coefficient remains unchanged i.e. 94% (Dong et al. 2016). Nano-zeolites have also been used as antibacterial substances carriers, including Ag^+ ions, which give antifouling properties to a membrane (Dong et al. 2016). The addition of zeolite nano-particles can be simply adapted to existing membranes manufacturing lines, which are originally designed to production of polyamide TFC membranes (Qu et al. 2013). Hence, TFN membranes with zeolite have gained early commercialization stage (e.g. zeolite based membranes LG Nano-

H2O®). QuantumFlux TFN membranes for seawater desalination by RO method are also available on the market (Qu et al. 2013).

Nano-silica is material of narrow particles pore size distribution and large specific surface. Its introduction to a membrane structure improves membrane lifetime and chemical resistance. Kebria et al. (2015) have prepared TFN NF membranes by adding nano-SiO_2 to membrane casting solution. The water flux has equaled 13.3 $L/m^2 \cdot h$, but the removal of crystal violet have slightly decreased in comparison with the reference membrane. Yin et al. (2012) have found that by using mesoporous SiO_2 particles of pore size up to 3 nm, TFN membranes of increased water flux can be obtained, whereas the retention remains unchanged compared to reference TFC membranes. Composite UF membranes made of polyvinylidene fluoride and polysulfone (PES) containing nano-SiO_2 are highly stable at high temperature and more selective in water treatment (Yu et al. 2009; Ahn et al. 2008).

The incorporation of **nano-titanium dioxide (TiO_2) nanoparticles** into TFC membranes improves the antibacterial, anti-fouling, and photocatalytic properties, as well as membrane permeability, and NaCl retention from 70% to 84% (Mollahosseini and Rahimpour 2014; Lee et al. 2008a). When the concentration of nano-TiO_2 exceeds 5 wt%, the permeate/water flux increases at the expense of reduced retention, suggesting the formation of defects in the active layer. After UV irradiation, TFN membranes containing nano-TiO_2 can degrade organic substances and inactivate microorganisms, which reduces organic and biological fouling. Kowalik-Klimczak et al. (2018) have presented results of the research on the modification of PA membranes with the use of TiO_2 and ZnO nano-particles, in order to make the membranes resistant to biofouling. Modified membranes with nano-ZnO reveal stronger antibacterial properties than membranes modified with nano-TiO_2. Hoseinin et al. (2017) have used TiO_2 nano-particles containing different amounts of cobalt (12–15 nm) to prepare photocatalytic membranes made of PES by means of phase inversion. Permeability tests have confirmed, that the addition of TiO_2 nano-particles containing 1.34 wt.% Co to PES matrix improves 2,4-dichlorophenol degradation and permeate flux. The best separation results (flux: 7.62 $L/m^2 h$ and retention: 96.62%) have been reached for a membrane containing 1wt.% of Co/TiO_2 nano-particles (1.34 wt.%), which has been radiated with visible light. Esfahani et al. (2015) have investigated properties of UF membrane made of PSF with admixture of nano-TiO_2 and single-walled CNTs. The results have shown that the membrane changes its properties in dependence of the amount of introduced nano-particles. When the ration of nano-TiO_2 and single-walled CNTs equals 1:1 (1 wt.% in total), the obtained membrane characterizes with the highest permeability, the highest humic acid retention coefficient and anti-fouling character.

Zinc oxide (ZnO) is one of very important photocatalyst and antibacterial material. Advantageous features of nano-ZnO are low costs and high surface to volume ratio. Due to these characteristics, it is used in modification of TFC membranes. Moreover, introduction of nano-ZnO to a membrane matrix may solve fouling of the membranes (Madhura et al. 2018). The recent research have shown that UF membranes

made of a mixture of ZnO nano-particles and PVC characterize with higher hydrophilicity, what results in high water flux (Rabiee et al. 2015). Composite hollow fiber NF membranes have been modified by introducing ZnO nano-spheres to poly(piperazyn-amide) layer during interfacial polymerization (Li et al. 2016), which reduces agglomeration of nano-particles and improves dispersion. The results have shown that modified membranes of low concentration of ZnO nano-spheres (1.5 wt.%) have characterized with higher flux (33.8 L/m²·h) and good retention of $MgSO_4$ (92.2%). ZnO nano-spheres have also allowed for better resistance of NF composite membrane to chlorine in regard to reference membrane, which have not contained ZnO. Novel composite membranes composed of chitosan/ZnO nano-particles (CS/nano-ZnO) have been prepared by casting of solution containing all components, whereas nano-ZnO have been disperses in chitosan matrix (Li et al. 2010b). The results of the research have shown that nano-ZnO influences on mechanical properties of CS/nano-ZnO membrane and antibacterial resistance of membranes containing 6–10 wt.% of ZnO toward *Bacillus subtilis*, *Escherichia coli* and *Staphylococcus aureus* is significantly improved.

Membranes made of **nano-ferric oxide** and mixed polymers, i.e. PES and polyaniline nanoparticles have been prepared using phase inversion method and the amount of nano-particles has been changed (Madhura et al. 2018). It has been noticed, that membrane containing 0.1wt.% of nano-particles reveals the maximum removal of cupper(II) at the lowest pure water flux. It is caused by the fact, that nano-particles placed in surface pores of a membrane during its preparation block the pores entrance. The research with scanning electron microscope and atomic force microscope have showed, that separation mechanism is based on adsorption. Szymański et al. (2018), by using wet phase inversion method, have prepared PES membranes modified with nano-particles of Fe_3O_4–trisodium citrate (FeCTNC). It has been found that the addition of 1 and 2 wt.% of FeCTNC results in the maximum permeate flux obtained during UF of pure water in refer to results obtained for non-modified membrane. The analysis of fouling in BSA presence have shown, that membranes modified with 1 and 3 wt.% of FeCTNC characterize with much improved permeate flux in reference to non-modified membranes. In case of membranes modified with higher amount of FeCTNC (4 wt.%) the significant fouling has been observed.

Nano-particles and ions of silver are used to modification of membranes and biofouling prevention (Maheswari et al. 2012). Such the effect is obtained due to release of Ag^+ ions and generation of products containing reactive oxygen species (Zhang et al. 2016c). Ben-Sasson et al. (2014) have presented a novel method of introduction of Ag nano-particles on the surface of TFC RO membrane. The reaction of silver salt with a reducer on a membrane has resulted in uniform and irreversible coating of the surface with Ag nano-particles. Retention of salts as well as surface roughness, hydrophilicity and zeta potential have remained unchanged after Ag nano-particles introduction, while slight decrease in permeability (to 17%) has been observed. The layer of nano-particles formed at the membrane surface has resulted in strong antibacterial properties, what has been confirmed by 75% reduction of amount of three

species of model bacteria attached to the surface. Yang (2009) has proposed modification of RO membrane surface as well as spacers in the membrane module with nano-Ag layer. Modified membranes and spacers have been tested in regard to their antifouling properties in flat sheet module operated. The obtained results have shown that flux decrease during filtration has been much lower in case of coated membrane than in case of non-modified one, while the retention of salts has been slightly higher. Additionally, the antibacterial effect of membranes coated with Ag has been obtained and neither on the membrane nor on spacer any growth of bacteria has been detected, while bacteria cells attached to the membrane has been quickly deactivated.

Zodrow (2009) has introduced silver nano-particles to the UF membrane made of PSF (nAg-PSF) in order to make the membrane efficiently resistant to wide range of bacteria, including *Escherichia coli* K12, *Pseudomonas mendocina* KR1 and bacteriophages MS2. The introduced nano-silver has also increased the membrane's hydrophilicity making it less susceptible to another type of fouling. Antibacterial UF membranes made of PSF have been prepared by introduction of different silver nano-particles to the casting solution (Mollahosseini et al. 2012). Additionally, SEM analysis has also shown, that addition of silver nano-particles causes decrease of pores entrance. The filtration of bacteria containing solution has showed that membrane with smaller silver nano-particles possesses better antibacterial activity. Mozia et al. (2018) have investigated the impact of titanate nanotubes modified with silver (Ag/TNT) on transport and antibacterial properties of UF membranes made of PES formed by means of wet phase inversion method. In order to determine antibacterial efficiency of Ag/TNT the research with *Escherichia coli* and *Staphylococcus epidermidis* used as model bacteria has been carried out. The highest antibacterial activity and permeability have been revealed by membranes containing 11. 13 wt.% of Ag, whereas for non-modified membranes any zone of antibacterial activity has not been observed. In order to minimize biofouling, MF membranes made of PES has been modified by silver nano-particles (AgNps) (Ferreira et al. 2015). Antibacterial properties have been analyzed in refer to *Pseudomonas fluorescens* with 20-30% limitation of activity of microorganisms. Also bacteria of coli group removal rates have been established at 99.9 and 99.999% for non-modified and modified membranes, respectively.

2.3. Membranes made of carbon-based nano-materials

Membranes made of carbon-based nano-materials i.e. carbon nanotubes (CNT) (Das et al. 2014b; Goh et al. 2013; Tian et al. 2015), graphene based nanomaterials (Goh and Ismail 2015; Akin et al. 2014), i.e. nanoporous graphene (NPG) (Goh and Ismail 2015; Akin et al. 2014; Surwade et al. 2015; Cohen-Tanugi and Grossman 2015) and graphene oxide (GO) (Wang et al. 2016; Hu and Mi 2013) are possess huge potential in sustainable development of membrane technologies, especially in regard to desalination and water and wastewater treatment. They have also been found to be very promising membrane materials, due to their unique and advantageous features

like water transport rate through films containing CNT, NPG and GO (Bodzek et al. 2020c; Holt et al. 2006; Abraham et al. 2017). Retention properties of films containing carbon based nano-materials are strongly dependent on size of channels to water transport as well as on chemical modifications (e.g. presence of functional groups) (Holt et al. 2006; Abraham et al. 2017). Unique hybridization features of carbon based nano-materials enable preparation of membranes for different separation processes. Novel composite membranes to desalination and water and wastewater treatment made of CNT, NPG and GO can be divided into two categories (Bodzek et al. 2020c):

- Membranes made only of CNT, GO or NPG, known also as freestanding,
- Polymeric membranes modified with CNT, GO or NPG.

In the first group nano-material is directly used as a separation layer, while in the second it is used to modification of membrane surface or nano-particles are introduced to polymeric matrix.

Freestanding membranes made of GO/NPG may be described as a set of nano-sheets, which are arranges in a series of layers, packed and situated one on another and properly distanced from each other (Miller et al. 2014). Water/solvent molecules are transported through neighbour hooding nano-channels, while dissolved substances are retained. The effective thickness of one nano-sheet of GO/NPG equals 0.5 nm, while the site thickness may vary from hundreds of nanometres to dozens of micrometres (Hu and Mi 2013). Freestanding GO/NPG membranes are flexible and mechanically stable (Smith et al. 2019; You et al. 2016; Nair et al. 2012). The water permeability and selectivity of "free-standing" membranes depend on the GO/NPG nanostructure. i.e. the pore size of NPG and the spacing between GO sheets (Bodzek et al. 2020b,c), whereby increasing the porosity and distances between nano-sheets can increase the permeability of GO/NPG membranes. The spacing between nano-sheets can be increased when immersed in a polar liquid (e.g., NaOH), but also decreased by reducing GO or by covalently bonding GO sheets to small-molecule compounds (Yuan et al. 2017). For example, GO membrane after carboxylation with glycine (GO-COOH) reveals higher retention of salt and permeability as negative GO-COOH surface favours electrostatic repulsion, characterizes with increase hydrophilicity and higher number of channels for water transport (Yuan et al. 2017). Hydroxyl and epoxy functional groups attached to GO/NPG nanosheets have also been shown to be responsible for maintaining sheet spacing (Bodzek et al. 2020b,c). "Free-standing" membranes made of GO, approximately 10 nm thick, can be used in water desalination with 100% salt retention, whereas water permeation is twice as high as one observed for commercial RO membrane (Song et al. 2018; Nicolaï et al. 2014). Table 6 shows examples of the characteristics and performance of free-standing GO/NPG membranes (Bodzek and Konieczny 2021).

Xu et al. (2013) have use vacuum filtration technique to form GO/TiO$_2$ membranes by introduction of TiO$_2$ nano-particles between GO nano-sheets. It has been found that TiO$_2$ nano-particles interact with GO nano-sheets what finally elongates distance between nano-sheets and enlarges channels dedicated to water transport through the membrane. GO-TiO$_2$ nanofiltration membranes have characterize with complete

Table 6.

Effectiveness of GO/NPG free-standing membranes (Bodzek and Konieczny 2021)

Membrane type	Process/ conditions	Flux	Retention
GO/PAA/PAN	NF/5 bar	0,84 L/m²hbar	43,2% Na^+, 92,6% Mg^{2+}
GO/PSF	NF/3,4 bar	27,6 L/m²hbar	46% Na_2SO_4, 93–95% rhodamine
GO-COOH	NF/1,5 MPa	–	48,2% NaCl, 91,3% Na_2SO_4
GO-PAN nano-fibres	NF/1-3 bar	2 L/m²hbar	56,7% Na_2SO_4, 100% Kongo red
GO on various matrix	NF/5 bar	21,8 L/m²hbar	>99% dyes, ~20–60% salts
GO/PVDF	UF	80–100 L/m²hbar	Natural organic matter
Nanoporous graphene	RO/17 kPa	106 g/m²s	~100% monovalent ions

PAA – polyallamine; PAN – polyacrylonitrile; PSF – polysulfone, PVDF – poly(vinylidene fluoride).

retention of methyl and rhodamine B what confirms they usability to removal of dyes from water.

Two main types of **carbon nanotube (CNT) freestanding membranes** may be distinguished, i.e. isoporous and buckypaper ones (Sears et al. 2010). The main advantages of such CNT membranes are the presence of very large porous 3D net and large specific surface.

Iso-porous CNT membranes form vertically aligned cylindrical pores in an impermeable matrix (e.g., polymer film), and fluid flow occurs only through the hollow interiors of the CNTs (Hinds et al. 2004). They have fluid flux 2–3 orders of magnitude higher than the one resulted from fluids flow theory. It has also been noted that CNT selectivity and fluids flow control through CNT pores may be increased by CNT edges functionalization (Sears et al. 2010). Holt et al. (2006) have examined isoporous CNT membranes of pore size 2 nm and they have stated that water flux is three orders of magnitude higher than the value predicted by hydrodynamic model and several times higher than the one determined for polycarbonate commercial membranes. Hummer et al. (2001) have shown that the chain of water particles may permeate fast, frictionless through CNT, what results from hydrogen bonds present in water particles chain, which are introduced to hydrophobic interior of CNT, while interactions between carbon and water particles occurring inside CNT are insignificant. Thomas and McGaughey (2009) have been found, that increase of CNT diameter from 0.66 to 0.93 nm decreases retention ions from 100 to 95%. Baek et al. (2014) prepared iso-porous membranes by incorporating CNTs, with a pore diameter of

4.8 nm, into a polymeric epoxy matrix. The modified membrane had almost 3 times higher performance compared to commercial UF membranes with similar retention (78% and 82%, respectively). The modified membranes showed better bioresistance and bacterial reduction (approximately 2 log) than the control UF membrane.

"Bucky paper" CNT membranes can be described as the random distributed CNTs in a non-woven paper-like structure (Sears et al. 2010). In BP-CNT membranes, CNTs are hold by means of Van der Waals forces, which are responsible for strong aggregation of CNTs, thus they form coherent structure of high specific surface arranged in a large 3D lattice. Peng et al. (2007) created "free-standing" CNT membranes using vacuum filtration of a suspension of oxidized SWCNTs through a polycarbonate membrane. After immersion in ethanol, the ultra-thin films were removed from polycarbonate (PC) support to form CNT membranes with average thicknesses of tens to hundreds of nm. Dumée et al. (2010, 2011) have prepared freestanding CNT membranes to direct contact membrane distillation (DCMD). They have characterized with higher porosity (90%), hydrophobicity (contact angle 113°), heat flux (2.7 kW/m^{2}h) and salt retention equal 99% and distillate flux 12 kg/m^{2}h (seawater 35 g NaCl/L) in comparison with polytetrafluoroethylene (PTFE) membrane. Bhadra et al. (2013) have used MWCNTs functionalized with –COOH groups to preparation of freestanding CNT membrane dedicated to membrane distillation (MD). The use of MWCNTs with carboxylic groups increases polarity and interaction between membrane surface and water vapor, what results in the increase of desalination. Distillate flux equal 19.2 kg/m^{2}h measured for MWCNT membrane is higher than the one obtained for conventional membranes made of PVDF.

A modification of polymeric membranes may be made by introduction of a nano-material either to a membrane's surface or to casting solution followed by membrane formation from the mixture of a polymer and a nano-material (Bodzek et al. 2020c).

Modification of a membrane surface may be performed by direct introduction of nano-material by means of layer by layer method, vacuum filtration (Wang et al. 2016; Hu and Mi 2014) or interfacial polymerization (IC) with TFC membrane surface resulting in formation of TFN membrane (Yang et al. 2018). Nano-material can also be bundled with membrane surface by means of covalent (Perreault et al. 2014), electrostatic (Choi et al. 2013) or coordination bonding. Modification of polymeric or ceramic membrane surface using graphene and its derivatives may improve membrane properties, including antifouling and antibacterial ones (Liu et al. 2011). Additionally, membranes with modified surface are more resistant to chlorine, while the effectiveness of membrane process is maintained. Modification of membrane surface requires relatively low amount of nano-material, what is economically beneficial and limits the impact of nano-material production on environment.

Membranes from PAN **containing GO** show high retention of dyes (about 100% for Congo red) and moderate retention of divalent ions (about 56.7% for Na$_2$SO$_4$), and water permeability approximately 2 L/m^{2}hbar (Wang et al. 2016). Similarly, PSF membrane containing covalently bounded GO nanosheets had water permeabilities ranging from 8 to 27.6 L/m^{2}hbar, with relatively low retention of mono- and divalent

ions (6-46%) and high retention of dyes (93–95%) (Xu et al. 2016b). On the other hand, ceramic membranes made of alumina coated with polydopamine and containing GO on the surface showed a high capacity of 48.4 l/m2h, with a NaCl retention of 99.7% (Hu and Mi 2013). Carboxylic and amine groups on GO surface are responsible for negative charge of GO particles dispersed in water. Kim et al. (2013) have coated membrane surface with negatively charged GO nano-particles and next deposited positively charged functionalized with amine groups GO layer on the negative layer. The modified membrane has revealed high water flux equal to 28 L/m^2·h and 98% retention of salt. Choi et al. (2013) have modified polyamide (PA) membrane surface with GO and amine functionalized GO (aGO) nano-sheets. The modified membrane has shown good resistance to chlorine degradation due to the presence of protective GO layer on PA membrane surface. Also, the resistance to fouling of modified membrane has significantly increase and the flux has been 10% higher, while NaCl retention measured during filtration of water solution containing 2,000 mg/L of salt has decreased by 0.7%.

One of the main issue in membrane exploitation to water treatment is fouling, which significantly limits the wide use of membrane technologies. NPG and GO reveal ability to inactivate bacteria in direct contact with their cells (Lee et al. 2008b; Liang et al. 2009), by initiation of physical damage of cell's membrane (Liu et al. 2011) followed by eventual extraction of lipids out of the cell (Tu et al. 2013). Perreault et al. (2014) have investigated the impact of modification of membrane with GO to improve the antibacterial features of thin film composite (TFC) membranes made of PA. GO nano-sheets have been bonded with membrane surface using amide and carboxylic groups interactions. It has been shown that 65% of *E.Coli* cells becomes deactivated during direct contact with the membrane within 1 hour. Such the antibacterial behaviour of the modified membrane does not cause any loses in its transport properties. Sun et al. (2015) have presented research describing preparation of composite membranes made of CA modified with graphene containing silver nano-particles (GO-AgNP) of anti-biofouling properties. Composite GO-AgNP membranes efficiently prevent bacteria growth and formation of biofilm on the membrane surface causing 86% *Escherichia coli* inactivation after 2 hours contact the membrane. Ma et al. (2017) have introduced copper nano-particles (CuNPs) on polyamide RO membrane in order to decrease its biofouling. Zhang et al. (2013a) have connected GO with oxidized CNT to modify PVDF membrane. Modified GO-CNT membrane has shown much higher hydrophilicity and antifouling properties than membranes modified only with GO or only with CNT. Water flux of membranes modified with GO and CNT in weight ratio equal 1:1 has been increased by 252% in comparison with PVDF reference membrane.

Due to difficulties with preparation of membranes containing vertically oriented CNT, many researchers have focused on preparation of **TFN membranes based on CNT**, in which CNT are introduced to retention layer (e.g. during IP of polyamide) (Xue et al. 2016; Chan et al. 2016). As CNT are hydrophobic and non-reactive, what often causes incompatibility with polymeric matrices, a number of methods of chemical

or physical modification have been developed to improve CNT dispersion in coating solution (Park et al. 2010). Among them the use of an acid is found to be the most efficient method as it allows to form hydroxyl (-OH) and carboxylic (-COOH) groups at CNT ends making them more hydrophilic and more reactive (Balasubramanian and Burghard 2005). Functionalized CNT may be next introduced to thin skin layer made of polyamide (Xue et al. 2016), what may significantly influence on physico-chemical properties of membranes (e.g. hydrophilicity, porosity, charge density and additional water channels) (Yin et al. 2015). A number of research have also shown that TFN membranes based on CNT characterize with improved antifouling properties (Manawi et al. 2016) as CNT possess strong antibacterial properties.

Chan et al. (2013) have introduced positively and negatively charged CNT using vacuum filtration to produce high quality RO membranes. The obtained CNT containing membranes have characterized with four times higher water permeability (1.3 $L/m^2 \cdot h \cdot bar$ for TFN vs. 0.3 $L/m^2 \cdot h \cdot bar$ for TFC) and retention almost identical than non-modified membranes (98.6% for TFN vs 97.6% for TFC). Xue et al. (2016) have functionalized MWCNTs with three different functional groups, i.e. carboxylic (-COOH), hydroxyl (-OH) and amine ($-NH_2$) ones, and next they prepared TFN membranes. At the optimum concentration 0.01% of MWCNT, all membranes have revealed higher permeability of pure water and higher retention of salts. Among three types of MWCNTs membranes, TFN MWCNT-OH membrane has revealed the highest water flux and Na_2SO_4 retention equal to 41.4 $L/m^2 \cdot h$ and 97,6%, respectively. Amini et al. (2013) have modified TFC PA membrane surface with MWCNTs functionalized with amine (0.01, 0.05 and 0.1%) using IP technique. The high retention of salt and water permeability have been observed during testing of modified membranes in forward osmosis (FO) process with 10 mM NaCl solution as a feed and 2 M NaCl solution as a draw solution. It has been found that permeate flux of modified membrane is 160% higher than the one of conventional TFC membrane.

The most widely used method to introduction of carbon nanomaterials into the **polymer membrane matrix** is the phase inversion process (Bodzek et al. 2020b, c, 2021b). The wet phase inversion method is mainly used to obtain ultrafiltration or microfiltration membranes, while the dry phase inversion method is used for nanofiltration and RO membranes. The introduction of carbon nano-materials to polymeric membrane matrix influences on its structure and antibacterial properties as well as hydrophilicity, retention and mechanical strength (Zhang et al. 2013b; Ganesh et al. 2013; Zhao et al. 2013a, b; Aba et al. 2015; Chung et al. 2017; Lee et al. 2013; Yu et al. 2013; Xu et al. 2014). In comparison with conventional membranes (without nano-material), surface of modified membrane characterize with dense pore structure. The significant increase of membrane hydrophilicity results in increased water permeation of modified membrane. Hence, the introduction of carbon nano-materials creates the opportunity of membranes exploitation in dry state without permeability affection, what is especially important in regard to membrane resistance to microorganisms and enhances transport.

Lee et al. (2013) have explained the role of nano-materials in membrane casting process by means of phase inversion. When nanomaterial is absent, polymer solution quickly solidifies at phase boundary between polymer and non-solvent during phase separation due to concentration gradient and fast interaction of all components. In non-stable spots of forming polymeric surface damages and scratches can appear due to constant shrinking caused by desolvatation. The introduction of hydrophilic substances (nano-materials) to casting solution increases its hydrophilicity and influences on the exchange rate between solvent and non-solvent during phase separation, and thus more porous membrane structure is formed. As a result, number of damages and macro-holes are minimized. The use of small amounts of functionalized nano-materials leads to increase of porosity and pore size of a membrane, but only to some critical point. It has been found that if the amount of nano-material exceeds 0.5%, the porosity of membrane noticeably decreases (Xu et al. 2014; Yin et al. 2013). This trend correspond to permeability tests results, which also increases with nano--material addition up to critical point, after exceedance of which it starts to decrease. This decrease is related with pores blocking and decrease of their size caused by high concentration of nanomaterial in membrane matrix. The high content of nano--material increases solution viscosity, slows down precipitation and leads to formation of dense skin layer on a surface accompanied with formation of wider pores, size of which increase with distance from skin layer (Liu et al. 2011).

The research carried out by Lai et al. (2016) has shown the increase of permeate flux and retention of salt caused by non-functionalized GO to PSF support covered with polyamide layer. Membranes prepared with casting solution containing 0.3wt% GO have characterized with retention of Na_2SO_4, Mg_2SO_4, $MgCl_2$ and NaCl equal 95.2, 91.1, 62.1 and 59.5%, respectively. Zinadini et al. (2014) have prepared NF GO/PES membranes of different GO doses. The research on membrane resistance to fouling during filtration of powdered milk solution (8,000 mg/L) has shown that the membrane containing 0.5 wt% GO possesses the best resistance to biofouling. Additionally, this membrane characterizes with high permeate flux (ca. 65.2 kg/m^{2}h) and high dye retention (99%). Zhao et al. (2013a) have produced modified UF membranes of GO/PVDF type, which characterize with increased permeate flux and BSA retention equal 26.5 L/m^{2}h and 44.3%, respectively. Membranes are also less vulnerable to fouling due to high hydrophilicity (the contact angle of modified membrane is 61° lower than one of reference PVDF membrane 73°) and characterize with proper surface morphology.

By using phase inversion technique, Lee et al. (2013) have prepared GO/PSF membrane to treat wastewater in membrane bioreactor (MBR). The authors have found that introduction of 1wt% of GO nano-particles to polymeric matrix decreases membrane fouling and decreases chemical membrane cleaning frequency 5 times. GO increases hydrophilicity of membrane matrix and limits biofouling, due to low energy interaction between feed and membrane surface. Additionally, negative charge of membrane surface decreases adhesion forces and accumulation of substances responsible for biofouling. It may allow for production of GO based membranes of high fouling resistance, which can be used to treat wastewater in MBR.

Fryczkowska (2018) has presented results of research on the use of ultrafiltration composite GO-PAN membranes containing 0.8, 4.0 and 7.7 wt% of GO in PAN matrix to remove dyes (Indigo – IS; methylene blue – MB and anionic dyes thymol blue – TB; Congo red – CR) from industrial wastewater. Composite GO/PAN membranes can be used to complete removal of anionic TB and CR dyes, while cationic dyes (IS and MB) are removed in 60–95%.

In order to limit membranes biofouling, GO-Ag composites are introduced to membrane casting solution further processed in phase inversion method. Modified membranes reveal higher permeability and improved hydrophilic and mechanical properties in reference to non-modified membranes. Improved antibacterial features and prevention of biofilm formation are especially observed and confirmed by conventional inhibition and anti-adhesive bacterial tests. Wu et al. (2017) have bonded silver nano-particles with GO nano-sheets forming PSF membranes of different silver content (0.00–1.00 wt.%) by means of phase inversion method. The optimum amount of silver in GO, for which the best membrane performance has been observed, has been equal to 0.5 wt.%, what has been confirmed by lower contact angle, higher capacity and porosity. Additionally, surface of modified membrane has characterized with higher NOM and bacterial fouling resistance in comparison with reference membrane.

3. Final remarks and development opportunities

A number of research on the use of nanomaterials to adsorption of organic and inorganic contaminants have been performed. The most investigated and preferable materials are nanosorbents made of metal oxides, especially iron, and carbon-based nanomaterials, first of all nanotubes. Chemical modification often changes character of nano-sorbents surface, what significantly improves adsorption abilities. Recently, an increasing interest in removal of metal ions from aquatic environment by means of composite nano-adsorbents have been observed, due to their potential use in industrial scale. Properties of nanocomposites surface can be modified in regard to specific requirements, what assures their proper selectivity. There are no reports to date on the commercial applications of nanoadsorbents in water and wastewater treatment. The difficulties of regenerating depleted nano-particles and their toxicity to living organisms are cited as reasons. The reduction of production costs and a thorough review of the environmental impact of nano-adsorbents are crucial for the development of nano-materials-based water treatment technologies.

Novel composite membranes containing NPG/GO and CNT can be divided into two categories:
- membranes made only of carbon nano-materials known as freestanding membranes,
- polymeric/ceramic membranes modified with these nano-materials.

Modification of polymeric membranes can be made either by introduction of nano-material on a membrane surface or its addition to a membrane casting solution followed by membrane formation from a mixture of a polymer and a nano-material.

Polymeric or ceramic membranes containing NPG/GO and CNT used in pressure-driven processes characterize with very high water/permeate flux and possess unique antifouling and antibacterial properties as well as high mechanical and thermal stability. The capacity of nano-membranes is higher than one of conventional RO or NF membranes, while retention of low molecular weight compounds is similar. The efficiency of membranes containing NPG/GO and CNT is beneficial in regard to removal of dyes, separation of monovalent ions from bivalent ones and dewatering of water-solvent mixtures. Additionally, membranes containing carbon based nano-materials have been successfully applied to pervaporation, forward osmosis, capacitive deionization, electro-dialysis or in photocatalytic membrane formation due to their stability and high efficiency.

The future development of membranes containing NPG/GO and CNT should be focused on separation efficiency improvement using different production strategies and more attention should be given to their potential disadvantages like mechanical instability, aggregation, non-uniform distribution and surface damages. Additionally, scaling up related with industrial production of commercial ultrathin membranes of high capacity made of graphene is one of the greatest scientific and technical challenges. If successful, the use of such membranes at industrial scale will lead to significant energy saving in RO installation as well as in other processes. The key to success is to find the balance between production costs and manufacture simplicity. Additionally, such membranes should be resistant to fouling and scaling, what assures high flux long term operation and savings in operational and capital costs. Moreover, the release of nano-materials from membrane and their eventual toxicity should be carefully investigated, especially in regard to their practical use in desalination processes.

REFERENCES

Aba N.F.D., Chong J.Y., Wang B., Mattevi C. and Li K. (2015) Graphene oxide membranes on ceramic hollow fibers – Microstructural stability and nanofiltration performance. Journal of Membrane Science 484, 87–94.

Abraham J., Vasu K.S., Williams C.D., Gopinadhan K., Su Y., Cherian C.T., Dix J., Prestat E., Haigh S.J., Grigorieva I.V., Carbone P., Geim A.K. and Nair R.R. (2017) Tunable sieving of ions using graphene oxide membranes. Nature Nanotechnology 12, 546–545, DOI: 10.1038/nnano.2017.21.

Adeleye A.S., Conway J.R., Garner K., Huang Y., Su Y., Keller A.A. (2016) Engineered nanomaterials for water treatment and remediation: Costs, benefits, and applicability. Chemical Engineering Journal 286, 640–662, DOI: 10.1016/j.cej.2015.10.105.

Ahmad A., El-Nour K.A., Ammar R.A.A. and Al-Warthan A. (2012) Carbon nanotubes, science and technology part (I) structure, synthesis and characterization. Arabian Journal of Chemistry 5, 1–23, DOI: 10.1016/J.ARABJC.2010.08.022.

Ahn J., Chung W.-J., Pinnau I. and Guiver M.D. (2008) Polysulfone/silica nanoparticle mixed-matrix membranes for gas separation. Journal of Membrane Science 314, 123–133, DOI: 10.1016/j.memsci.2008.01.031.

Akhbarizadeh R., Shayesterfar M.R. and Darezereshki E. (2014) Competitive removal of metals from wastewater by maghemite nanoparticles: a comparison between simulated wastewater and AMD. Mine Water Environment 33, 89–96, DOI: 10.1007/s10230-013-0255-3.

Akin I., Zor E., Bingol H. and Ersoz M. (2014) Green synthesis of reduced graphene oxide/ polyaniline composite and its application for salt rejection by polysulfonebased composite membranes. Journal of Physical Chemistry B 118, 5707–5716, DOI: 10.1021/jp5025894.

Al-Hamadani Y.A.J., Chu K.H., Son A., Heo J., Her N., Jang M., Park C.M. and Yoon Y. (2015) Stabilization and dispersion of carbon nanomaterials in aqueous solutions: a review. Separation and Purification Technology 156, 861–874, DOI: 10.1016/j.seppur.2015.11.002.

Ali I. (2012) New generation adsorbents for water treatment. Chemical Review 112(10), 5073–5091, DOI: 10.1016/j.impact.2016.09.004.

Altintas Z., Chianella I., Da Ponte G., Paulussen S., Gaeta S. and Tothill I.E. (2016) Development of functionalized nanostructured polymeric membranes for water purification. Chemical Engineering Journal 300, 358–366, DOI: 10.1016/j.cej.2016.04.121.

Amini M., Jahanshahi M. and Rahimpour A. (2013) Synthesis of novel thin film nanocomposite (TFN) forward osmosis membranes using functionalized multi-walled carbon nanotubes. Journal of Membrane Science 435, 233–241, DOI: 10.1016/j.memsci.2013.01.041.

Anand A., Unnikrishnan B., Mao J.-Y., Lin H.-J. and Huang C.-C. (2018) Graphene-based nanofiltration membranes for improving salt rejection, water flux and antifouling – A review. Desalination 429, 119–133, DOI: 10.1016/j.desal.2017.12.012.

Anandan S., Kathiravan K., Murugesan V. and Ikuma Y. (2009) Anionic (IO_3^-) non-metal doped TiO_2 nanoparticles for the photocatalytic degradation of hazardous pollutant in water. Catalysis Commununications 10, 1014–1019, DOI: 10.1016/j.catcom.2008.12.054.

Anitha K., Namsani S. and Singh J.K. (2015) Removal of heavy metal ions using a functionalized single-walled carbon nanotube: a molecular dynamics study. The journal of physical chemistry A 119, 8349–8358, DOI: 10.1021/acs.jpca.5b03352.

Arena J.T., McCloskey B., Freeman B.D. and McCutcheon J.R. (2011) Surface modification of thin film composite membrane support layers with polydopamine: enabling use of reverse osmosis membranes in pressure retarded osmosis. Journal of Membrane Science 375, 55–62, DOI: 10.1016/j.memsci.2011.01.060.

Baek Y., Kim C., Seo D.K., Kim T., Lee J.S., Kim Y.H., Ahn K.H., Bae S.S., Lee S.C., Lim J., Lee and K. Yoon J. (2014) High performance and antifouling vertically aligned carbon nanotube membrane for water purification. Journal of Membrane Science 460, 171–177, DOI: 10.1016/j.memsci.2014.02.042.

Bai S., Shen X., Zhong X., Liu Y., Zhu G., Xu X. and Chen K. (2012) One-pot solvothermal preparation of magnetic reduced graphene oxideferrite hybrids for organic dye removal. Carbon 50, 2337–2346, DOI: 10.1016/j.carbon.2012.01.057.

Bai X., Wang L., Wang Y., Yao W. and Zhu Y. (2014) Enhanced oxidation ability of g-C_3N_4 photocatalyst via C60 modification. Applied Catalysis B: Environmental 152–153, 262–270, DOI: 10.1016/j.apcatb.2014.01.046.

Balasubramanian K. and Burghard M. (2005) Chemically functionalized carbon nanotubes. Small 1, 180–192, DOI: 10.1002/smll.200400118.

Ballesteros E., Gallego M. and Valcárcel M. (2000) Analytical potential of fullerene as adsorbent for organic and organometallic compounds from aqueous solutions. Journal of Chromatography A 869, 101–110, DOI: 10.1016/S0021-9673(99)01050-X.

Bazrafshan E., Mostafapour F.K., Hosseini A.R., Raksh A.K. and Mahvi A.H. (2013) Decolorisation of reactive red 120 dye by using single-walled carbon nanotubes in aqueous solutions. Journal of Chemistry 2013, DOI: 10.1155/2013/938374.

Belver C., Bedia J., Gómez-Avilés A., Peñas-Garzón M. and Rodriguez J.J. (2019) Semiconductor Photocatalysis for Water Purification. [In:] Micro and Nano Technologies, Nanoscale Materials in Water Purification, Editor(s): Thomas S., Pasquini D., Leu S.-Y., Gopakumar D.A. Ch. 22, 581–651, DOI: 10.1016/B978-0-12-813926-4.00028-8.

Ben-Sasson M., Lu X., Bar-Zeev E., Zodrow K.R., Nejati S., Qi G.,. Giannelis E.P. and Elimelech M. (2014) In situ formation of silver nanoparticles on thin-film composite reverse osmosis membranes for biofouling mitigation. Water Research 62, 260–270, DOI: 10.1016/j.watres.2014.05.049.

Bhadra M., Roy S. and Mitra S. (2013) Enhanced desalination using carboxylated carbon nanotube immobilized membranes. Separation and Purification Technology 120, 373–377, DOI: 10.1016/j.seppur.2013.10.020.

Bodzek M. (2019) Membrane separation techniques – removal of inorganic and organic admixtures and impurities from water environment – review. Archives of Environmental Protection 45(4), 4–19, DOI: 10.24425/aep.2019.130237.

Bodzek M. (2022) Nanoparticles for water disinfection by photocatalysis: A review. Archives of Environmental Protection 48(1), 3–17, DOI: 10.24425/aep.2022.140541.

Bodzek M. and Konieczny K. (2021) Nanomaterials in membrane water desalination. Desalination and Water Treatment 214, 155–180, DOI: 10.5004/dwt.2021.26657.

Bodzek M., Konieczny K. and Kwiecińska-Mydlak A. (2020a) The application of nanomaterial adsorbents for the removal of impurities from water and wastewaters: a review. Desalination and Water Treatment 185, 1–26, DOI: 10.5004/dwt.2020.25454.

Bodzek M., Konieczny K. and Kwiecińska-Mydlak A. (2020b) The application of nanotechnology and nanomaterials in water and wastewater treatment. Membranes, photocatalysis and disinfection. Desalination and Water Treatment 186, 88–106, DOI: 10.5004/dwt.2020.25231.

Bodzek M., Konieczny K. and Kwiecińska-Mydlak A. (2020c) Nanotechnology in water and wastewater treatment. Graphene – the nanomaterial for next generation of semipermeable membranes. Critical Reviews in Environmental Science and Technology 50(15), 1515–1579, DOI: 10.1080/10643389.2019.1664258.

Bodzek M., Konieczny K. and Kwiecińska-Mydlak A. (2021a) Nano-photocatalysis in water and wastewater treatment. Desalination and Water Treatment 243, 51–74, DOI: 10.5004/dwt.2021.27867.

Bodzek M., Konieczny K. and Kwiecińska-Mydlak A. (2021b) New generation of semipermeable membranes with carbon nanotubes for water and wastewater treatment: Critical review. Archives of Environmental Protection 47(3), 3–27, DOI: 10.24425/aep.2021.138460.

Bokare V., Jung J.-L., Chang Y.-Y. and Chang Y.-S. (2013) Reductive dechlorination of octachlorodibenzo-p-dioxin by nanosized zerovalent zinc: modeling of rate kinetics and congener profile. Journal of Hazardous Materials 250, 397–402, DOI: 10.1016/j.jhazmat.2013.02.020.

Borrego B., Lorenzo G., Mota-Morales J.D., Almanza-Reyes H., Mateos F., López-Gil E., de la Losa N., Burmistrov V.A., Pestryakov A.N. and Brun A. (2016) Potential application of silver nanoparticles to control the infectivity of Rift Valley fever virus in vitro and in

vivo. Nanomedicine: Nanotechnology, Biology and Medicine Nanomedicine 12, 1185––1192, DOI: 10.1016/j.nano.2016.01.021.

Bradder P., Ling S.K., Wang S. and Liu S. (2010) Dye adsorption on layered graphite oxide. Journal of Chemical and Engineering Data 56, 138–141, DOI: 10.1021/je101049g.

Buruga K., Song H., Shang J., Bolan N., Jagannathan T.K. and Kim K.-H. (2019) A review on functional polymer-clay based nanocomposite membranes for treatment of water. Journal of Hazardous Materials 379, 120584, DOI: 10.1016/j.jhazmat.2019.04.067.

Chae S.-R., Hotze E.M. and Wiesner M.R. (2014) Possible Applications of Fullerene Nanomaterials in Water Treatment and Reuse. [In:] Micro and Nano Technologies, Nanotechnology Applications for Clean Water (Second Edition), Editor(s): Anita Street, Richard Sustich, Jeremiah Duncan, Nora Savage, William Andrew Publishing, Ch.21, 329–338, DOI: 10.1016/B978-1-4557-3116-9.00021-4.

Chan W.-F., Chen H.-Y., Surapathi A., Taylor M.G., Shao X., Marand E. and Johnson J.K. (2013) Zwitterion functionalized carbon nanotube/polyamide nanocomposite membranes for water desalination. ACS Nano 7, 5308–5319, DOI: 10.1021/nn4011494.

Chan W.-F., Marand E. and Martin S.M. (2016) Novel zwitterion functionalized carbon nanotube nanocomposite membranes for improved RO performance and surface anti-biofouling resistance. Journal of Membrane Science 509, 125–137, DOI: 10.1016/j.memsci.2016.02.014.

Chatterjee S., Lee M.W. and Woo S.H. (2010) Adsorption of congo red by chitosan hydrogel beads impregnated with carbon nanotubes. Bioresource Technology 101, 1800–1806, DOI: 10.1016/j.biortech.2009.10.051.

Chen D., Xie Z., Zeng Y., Lv W., Zhang Q., Wang F., Liu G. and Liu H. (2019) Accelerated photocatalytic degradation of quinolone antibiotics over Z-scheme $MoO_3/g\text{-}C_3N_4$ heterostructure by peroxydisulfate under visible light irradiation: mechanism; kinetic; and products. Journal of the Taiwan Institute of Chemical Engineers 104, 250–259, DOI: 10.1016/j.jtice.2019.08.007.

Chen H., Gao B. and Li H. (2015) Removal of sulfamethoxazole and ciprofloxacin from aqueous solutions by graphene oxide. Journal of Hazardous Materials 282, 201–207, DOI: 10.1016/j.jhazmat.2014.03.063.

Cheng X., Kan A.T. and Tomson M.B. (2005) Uptake and sequestration of naphthalene and 1,2-dichlorobenzene by C60. Journal of Nanoparticle Research 7, 555–567, DOI: 10.1007/s11051-005-5674-z.

Choi W., Choi J., Bang J. and Lee J.H. (2013) Layer-by-layer assembly of graphene oxide nanosheets on polyamide membranes for durable reverse-osmosis applications. ACS Applied Materials Interfaces 5, 12510–12519, DOI: 10.1021/am403790s.

Chung Y.T., Mahmoudi E., Mohammad A.W., Benamor A., Johnson D. and Hilal N. (2017) Development of polysulfone-nanohybrid membranes using ZnO-GO composite for enhanced antifouling and antibacterial control. Desalination 402, 123–132, DOI: 10.1016/j.desal.2016.09.030.

Cohen-Tanugi D. and Grossman J.C. (2015) Nanoporous graphene as a reverse osmosis membrane: recent insights from theory and simulation. Desalination 366, 59–70, DOI: 10.1016/j.desal.2014.12.046.

Cohen-Tanugi D., McGovern R.K., Dave S.H., Lienhard J.H. and Grossman J.C. (2014) Quantifying the potential of ultra-permeable membranes for water desalination. Energy & Environmental Science 7, 1134–1141, DOI: 10.1039/C3EE43221A.

Collivignarelli M.C., Abbà A., Benigna I., Sorlini S. and Torretta V. (2018) Overview of the main disinfection processes for wastewater and drinking water treatment plants. Sustainability 10, 86, DOI: 10.3390/su1001008.

Crane R.A., Dickinson M., Popescu I.C. and Scott T.B. (2011) Magnetite and zero-valent iron nanoparticles for the remediation of uranium contaminated environmental water. Water Research 45, 2931–2942, DOI: 10.1016/j.watres.2011.03.012.

Crini G. and Lichtfouse E. (2019) Advantages and disadvantages of techniques used for wastewater treatment. Environmental Chemistry Letters 17, 145–155, DOI: 10.1007/s10311-018-0785-9.

Crini G., Lichtfouse E., Wilson L. and Morin-Crini N. (2019) Conventional and non-conventional adsorbents for wastewater treatment. Environmental Chemistry Letters 17, 195–213, DOI: 10.1007/s10311-018-0786-8.

Das R., Ali M.E., Abd Hamid S.B., Ramakrishna S. and Chowdhury Z.Z. (2014b) Carbon nanotube membranes for water purification: a bright future in water desalination. Desalination 336, 97–109, DOI: 10.1016/j.desal.2013.12.026.

Das R., Hamid S.B.A., Ali E.M., Ismail A.F., Annuar M.S.M. and Ramakrishna S. (2014a) Multifunctional carbon nanotubes in water treatment: the present, past and future. Desalination 354, 160–179, DOI: 10.1016/j.desal.2014.09.032.

Deng Y., Tang L., Feng C., Zeng G., Wang J., Zhou Y., Liu Y., Peng B. and Feng H. (2018) Construction of plasmonic Ag modified phosphorous-doped ultrathin g-C_3N_4 nanosheets/$BiVO_4$ photocatalyst with enhanced visible-near-infrared response ability for ciprofloxacin degradation. Journal of Hazardous Materials 344, 758–769, DOI: 10.1016/j.jhazmat.2017.11.027.

Ding S., Huang W., Zhou B., Peng P., Hu W., Long M. and Huang G. (2017) The mechanism of enhanced photocatalytic activity of SnO_2 through fullerene modification. Current Applied Physics 17, 1547–1556, DOI: 10.1016/j.cap.2017.07.008.

Dong G., Ai Z. and Zhang L. (2014) Efficient anoxic pollutant removal with oxygen functionalized graphitic carbon nitride under visible light. RSC Advances 4, 5553–5560, DOI: 10.1039/C3RA46068A.

Dong L.-X., Huang X.-C., Wang Z., Yang Z., Wang X.-M. and Tang C.Y. (2016) A thin-film nanocomposite nanofiltration membrane prepared on a support with in situ embedded zeolite nanoparticles. Separation and Purification Technology 166, 230–239, DOI: 10.1016/j.seppur.2016.04.043.

Dumee L., Campbell J.L., Sears K., Schutz J., Finn N., Duke M. and Gray S. (2011)The Impact of hydrophobic coating on the performance of carbon nanotube bucky paper membranes in membrane distillation. Desalination 283, 64-67, DOI: 10.1016/j.desal.2011.02.046.

Dumée L.F., Sears K., Schütz J., Finn N., Huynh C., Hawkins S., Duke M. and Gray S. (2010) Characterization and evaluation of carbon nanotube Bucky-Paper membranes for direct contact membrane distillation. Journal of Membrane Science 351, 36–43, DOI: 10.1016/j.memsci.2010.01.025.

Elimelech M. and Phillip W.A. (2011) The future of seawater desalination: energy, technology, and the environment. Science 333, 712–717, DOI: 10.1126/science.1200488.

Engates K.E. and Shipley H.J. (2011) Adsorption of Pb, Cd, Cu, Zn, and Ni to titanium dioxide nanoparticles: effect of particle size, solid concentration, and exhaustion. Environmental Science and Pollution Research 18, 386–395, DOI: 10.1007/s11356-010-0382-3.

Esfahani M.R., Lyler T.J., Stretz H.A. and Wells M.J.M. (2015) Effects of a dual nanofiller, nano-TiO2 and MWCNT, for polysulfone-based nanocomposite membranes for water purification. Desalination 372, 47–56, DOI: 10.1016/j.desal.2015.06.014.

Fabrega J., Luoma S.N., Tyler C.R., Galloway T.S. and Lead J.R. (2011) Silver nanoparticles: behaviour and effects in the aquatic environment. Environmental International 37, 517––531, DOI: 10.1016/j.envint.2010.10.012.

Fagan R., McCormack D.E., Dionysiou D.D. and Pillai S.C. (2016) A review of solar and visible light active TiO2 photocatalysis for treating bacteria, cyanotoxins and contaminants of emerging concern. Materials Science in Semiconductor Processing 42, 2–14, DOI: 10.1016/j.mssp.2015.07.052.

Fan H., Zhao X., Yang J., Shan X., Yang L., Zhang Y., Li X. and Gao M. (2012) ZnO–graphene composite for photocatalytic degradation of methylene blue dye. Catalysis Communications 29, 29–34, DOI: 10.1016/j.catcom.2012.09.013.

Fan J., Guo Y., Wang J. and Fan M. (2009) Rapid decolorization of azo dye methyl orange in aqueous solution by nanoscale zerovalent iron particles. Journal of Hazardous Materials 166, 904–910, DOI: 10.1016/j.jhazmat.2008.11.091.

Fang Z., Chen J., Qiu X., Qiu X., Cheng W. and Zhu L. (2011) Effective removal of antibiotic metronidazole from water by nanoscale zero-valent iron particles. Desalination 268, 60–67, DOI: 10.1016/J.DESAL.2010.09.051.

Feng L., Cao M., Ma X., Zhu Y. and Hu C. (2012) Superparamagnetic high-surface- area Fe3O4 nanoparticles as adsorbents for arsenic removal. Journal of Hazardous Materials 217––218, 439–446, DOI: 10.1016/j.jhazmat.2012.03.073.

Feng C., Ju X., Li M., Yang T. and Gao C. (2014) Studies on a novel nanofiltration membrane prepared by cross-linking of polyethyleneimine on polyacrylonitrile substrate. Journal of Membrane Science 451, 103–110, DOI: 10.1016/J.MEMSCI.2013.10.003.

Ferreira A.M., Roque É.B., Fonseca F.V.D. and Borges C.P. (2015) High flux microfiltration membranes with silver nanoparticles for water disinfection. Desalination and Water Treatment 56, 3590–3598, DOI: 10.1080/19443994.2014.1000977.

Fryczkowska B. (2018) The application of ultrafiltration composite GO/PAN membranes for removing dyes from textile wastewater. Desalination and Water Treatment 128, 79–88, DOI: 10.5004/dwt.2018.2259.

Ganesh B.M., Isloor A.M. and Ismail A.F. (2013) Enhanced hydrophilicity and salt rejection study of graphene oxide-polysulfone mixed matrix membrane. Desalination 313, 199–207, DOI: 10.1016/J.DESAL.2012.11.037.

Ganguly P., Byrnea C., Subramanianc G. and Suresh C.P. (2018) Antimicrobial activity of photocatalysts: Fundamentals, mechanisms, kinetics and recent advances. Applied Catalysis B: Environmental 225, 51–75, DOI: 10.1016/j.apcatb.2017.11.018.

Gao Y., Li Y., Zhang L., Huang H., Hu J., Shah S.M. and Su X. (2012) Adsorption and removal of tetracycline antibiotics from aqueous solution by graphene oxide. Journal of Colloid and Interface Science 368, 540–546, DOI: 10.1016/j.jcis.2011.11.015.

Gehrke I., Geiser A. and Somborn-Schulz A. (2015) Innovations in nanotechnology for water treatment. Nanotechnology Science and Applications 8, 1–17, DOI: 10.2147/NSA. S4377.

George R., Bahadur N., Singh N., Singh R., Verma A. and Shukla A.K. (2016) Environmentally benign TiO$_2$ nanomaterials for removal of heavy metal ions with interfering ions present in tap water. Materials Today: Proceedings 3, 162–166, DOI: 10.1016/j.matpr.2016.01.051.

Ghadim E.E., Manouchehri F., Soleimani G., Hosseini H., Kimiagar S. and Nafisi S. (2013) Adsorption properties of tetracycline onto graphene oxide: equilibrium, kinetic and thermodynamic studies. PLoS One, 8(11), DOI: 10.1371/journal.pone.0079254.

Goh P.S. and Ismail A.F. (2015) Graphene-based nanomaterial: the state-of-the-art material for cutting edge desalination technology. Desalination 356, 115–128, DOI: 10.1016/j.desal.2014.10.001.

Goh P.S., Ismail A.F. and Hilal N. (2016) Nano-enabled membranes technology: Sustainable and revolutionary solutions for membrane desalination? Desalination 380, 100–104, DOI: 10.1016/j.desal.2015.06.002.

Goh P.S., Ismail A.F. and Ng B.C. (2013) Carbon nanotubes for desalination: performance evaluation and current hurdles. Desalination 308, 2–14, DOI: 10.1016/j.desal.2012.07.040.

Gomez-Solís C., Ballesteros J., Torres-Martínez L., Juárez-Ramírez I., Torres L.D., Zarazua-Morin M.E. and Lee S.W. (2015) Rapid synthesis of ZnO nano-corncobs from Nital solution and its application in the photodegradation of methyl orange. Journal of Photochemistry and Photobiology A: Chemistry A 298, 49–54, DOI: 10.1016/j.jphotochem.2014.10.012.

Gupta V., Agarwal S. and Saleh T.A. (2011a) Chromium removal by combining the magnetic properties of iron oxide with adsorption properties of carbon nanotubes. Water Research 45, 2207–2212, DOI: 10.1016/j.watres.2011.01.012.

Gupta K., Bhattacharya S., Chattopadhyay D., Mukhopadhyay A., Biswas H., Dutta J., Ray N.R. and Ghosh U.C. (2011b) Ceria associated manganese oxide nanoparticles: synthesis, characterization and arsenic(V) sorption behavior. Chemical Engineering Journal 172, 219–229, DOI: 10.1016/j.cej.2011.05.092.

Gupta V.K. and Saleh T.A. (2013) Sorption of pollutants by porous carbon, carbon nanotubes and fullerene- An overview. Environmental Science and Pollution Research 20, 2828––2843, DOI: 10.1007/s11356-013-1524-1.

Hao L., Song H., Zhang L., Wan X., Tang Y. and Lv Y. (2012) SiO_2/graphene composite for highly selective adsorption of Pb(II) ion. Journal of Colloidal Interface Science 369, 381––387, DOI: 10.1016/j.jcis.2011.12.023.

Hao R., Wang G., Tang H., Sun L., Xu C. and Han D. (2016) Template-free preparation of macro/mesoporous g-C_3N_4/TiO_2 heterojunction photocatalysts with enhanced visible light photocatalytic activity. Applied Catalysis B-environmental 187, 47–58, DOI: 10.1016/J.APCATB.2016.01.026.

Hartono T., Wang S., Ma Q. and Zhu Z. (2009) Layer structured graphite oxide as a novel adsorbent for humic acid removal from aqueous solution. Journal of Colloid & Interface Science 333, 114–119.

Hinds B.J., Chopra N., Rantell T., Andrews R., Gavalas V. and Bachas L.G. (2004) Aligned multiwalled carbon nanotube membranes. Science 303, 62–65, DOI: 10.1126/SCIENCE.1092048.

Holt J.K., Park H.G., Wang Y., Stadermann M., Artyukhin A.B., Grigoropoulos C.P., Noy A. and Bakajin O. (2006) Fast mass transport through sub-2-nanometer carbon nanotubes. Science 312, 1034–1037, DOI: 10.1126/science.1126298.

Hoseini S.N., Pirzaman A.K., Aroon M.A. and Pirbazari A.E. (2017) Photocatalytic degradation of 2, 4-dichlorophenol by Co-doped TiO2 (Co/TiO_2) nanoparticles and Co/TiO_2 containing mixed matrix membranes. Journal of Water Process Engineering 17, 124–134, DOI: 10.1016/j.jwpe.2017.02.015.

Hu J., Chen G. and Lo I.M. (2006) Selective removal of heavy metals from industrial wastewater using maghemite nanoparticle: performance and mechanism. Journal of Environmental Engineering 132, 709–715, DOI: 10.1061/(ASCE)0733-9372(2006)132:7(709).

Hu J., Lo I. and Chen G. (2004) Removal of Cr (VI) by magnetite. Water Science & Technology 50, 139–146, DOI: 10.2166/wst.2004.0706.

Hu M. and Mi B. (2013) Enabling graphene oxide nanosheets as water separation membranes. Environmental Science and Technology 47, 3715–3723, DOI: 10.1021/es400571g.

Hu M. and Mi B. (2014) Layer-by-layer assembly of graphene oxide membranes via electrostatic interaction. Journal of Membrane Science 469, 80–87, DOI: 10.1016/j.memsci.2014.06.036.

Hua M., Zhang S., Pan B., Zhang W., Lv L. and Zhang Q. (2012) Heavy metal removal from water/wastewater by nanosized metal oxides: a review. Journal of Hazardous Materials 211–212, 317–331, DOI: 10.1016/j.jhazmat.2011.10.016.

Huang Z-H., Zheng X., Lv W., Wang M., Yang Q-H. and Kang F. (2011) Adsorption of lead(II) ions from aqueous solution on low-temperature exfoliated graphene nanosheets. Langmuir 27, 7558–7562, DOI: 10.1021/la200606r.

Hummer G., Rasaiah J.C. and Noworyta J.P. (2001) Water conduction through the hydrophobic channel of a carbon nanotube. Nature 414, 188–190, DOI: 10.1038/35102535.

Hur J., Shin J., Yoo J. and Seo Y-S. (2015) Competitive adsorption of metals onto magnetic graphene oxide: comparison with other carbonaceous adsorbents, The Scientific World Journal, Article ID 836287, 11 pages, DOI: 10.1155/2015/836287.

Hyung H. and Kim J-H. (2008) Natural organic matter (NOM) adsorption to multi-walled carbon nanotubes: effect of NOM characteristics and water quality parameters. Environmental Science & Technology 42, 4416–4421, DOI: 10.1021/es702916h.

Jeong B.H., Hoek E.M., Yan Y., Subramani A., Huang X., Hurwitz G., Ghosh A.K. and Jawor A. (2007) Interfacial polymerization of thin film nanocomposites: a new concept for reverse osmosis membranes. Journal of Membrane Science 294, 1–7, DOI: 10.1016/j.memsci.2007.02.025.

Ji L.L., Chen W., Duan L. and Zhu D.Q. (2009) Mechanisms for strong adsorption of tetracycline to carbon nanotubes: a comparative study using activated carbon and graphite as adsorbents. Environmental Sciience & Techology 43, 2322–2327, DOI: 10.1021/es803268b.

Kalhapure R.S., Sonawane S.J., Sikwal D.R., Jadhav M., Rambharose S., Mocktar C. and Govender T. (2015) Solid lipid nanoparticles of clotrimazole silver complex: an efficient nano antibacterial against Staphylococcus aureus and MRSA. Colloids Surfaces: B Biointerfaces 136, 651–658, DOI: 10.1016/j.colsurfb.2015.10.003.

Karimi M.A., Hatefi-Mehrjardi A., Mohammadi S.Z., Mohadesi A., Mazloum-Ardakani M., Kabir A.A., Kazemipour M. and Afsahi N. (2012) Solid phase extraction of trace amounts of silver (I) using dithizone-immobilized alumina-coated magnetite nanoparticles prior to determination by flame atomic absorption spectrometry. International Journal of Environmental Analytical Chemistry 92, 1325–1340, DOI: 10.1080/03067319.2011.563385.

Kebria M.R.S., Jahanshahi M. and Rahimpour A. (2015) SiO2 modified polyethyleneimine-based nanofiltration membranes for dye removal from aqueous and organic solutions. Desalination 367, 255–264, DOI: 10.1016/j.desal.2015.04.017.

Khajeh M., Laurent S. and Dastafkan K. (2013) Nanoadsorbents: classification, preparation, and applications (with emphasis on aqueous media). Chemical Review 113, 7728–7768, DOI: 10.1021/cr400086v.

Khan M.A., Mutahir S., Wang F., Zhen H., Lei W., Xia M., Ouyang Y. and Muhmood T. (2018) Synthesis of environmentally encouraged, highly robust pollutants reduction 3-D system consisting of Ag/g-C$_3$N$_4$ and Cu-complex to degrade refractory pollutants. Journal of Photochemistry and Photobiology A: Chemistry 364, 826–36, DOI: 10.1016/j.jphotochem.2018.04.035.

Kim S.G., Hyeon D.H., Chun J.H., Chun B.H. and Kim S.H. (2013) Novel thin nanocomposite RO membranes for chlorine resistance. Desalination and Water Treatment 51, 6338––6345, DOI: 10.1080/19443994.2013.780994.

Kim S.Y., Oh J., Park S., Shim Y. and Park S. (2016) Production of metal-free composites composed of graphite oxide and oxidized carbon nitride nanodots and their enhanced pho-

tocatalytic performances. Chemistry European Journal 22, 5142–5145, DOI: 10.1002/chem.201505100.

Klein S.A. and Pawlik B.M. (2012) The removal of arsenic from water using natural iron oxide minerals. Journal of Cleaner Production 29–30, 208–213, DOI: 10.1016/j.jclepro.2012.01.029.

Kowalik-Klimczak A., Stanisławek E., Kacprzyńska-Gołacka J., Bednarska A., Osuch-Słomka E. and Skowroński J. (2018) The polyamide membranes functionalized by nanoparticles for biofouling control. Desalination and Water Treatment 128, 243–252, DOI: 10.5004/DWT.2018.22868.

Krishnaraj C., Ramachandran R., Mohan K. and Kalaichelvan P. (2012) Optimization for rapid synthesis of silver nanoparticles and its effect on phytopathogenic fungi. Spectrochimica Acta A 93, 95–99, DOI: 10.1016/j.saa.2012.03.002.

Kroto H.W., Heath J.R., O'brien S.C., Curl R.F. and Smalley R.E. (1985) C60: buckminsterfullerene. Nature 318, 162–163, DOI: 10.1038/318162a0.

Kuiken T. (2010) Cleaning up contaminated waste sites: is nanotechnology the answer? Nano Today 5, 6–8, DOI: 10.1016/J.NANTOD.2009.11.001.

Kumar S., Nair R.R., Pillai P.B., Gupta S.N., Iyengar M.A.R. and Sood A.K. (2014) Graphene oxide–$MnFe_2O_4$ magnetic Nanohybrids for efficient removal of lead and arsenic from water. ACS Applied Materials & Interfaces 6, 17426–17436, DOI: 10.1021/am504826q.

Kuppusamy S., Palanisami T., Megharaj M., Venkateswarlu K. and Naidu R. (2016) Ex-Situ Remediation Technologies for Environmental Pollutants: A Critical Perspective. [In:] P. de Voogt (ed.), Reviews of Environmental Contamination and Toxicology. Springer Switzerland 2016, 236, 117–192, DOI: 10.1007/978-3-319-20013-2_2.

Lai G.S., Lau W.J., Goh P.S., Ismail A.F., Yusof N. and Tan Y.H. (2016) Graphene oxide incorporated thin film nanocomposite nanofiltration membrane for enhanced salt removal performance. Desalination 387, 14–24, DOI: 10.1016/j.desal.2016.03.007.

Lakshmipathiraj P., Narasimhan B., Prabhakar S. and Raju G.B. (2006) Adsorption of arsenate on synthetic goethite from aqueous solutions. Journal of Hazardous Materials 136, 281–287, DOI: 10.1016/j.jhazmat.2005.12.015.

Lee C., Wei X., Kysar J.W. and Hone J. (2008b) Measurement of the elastic properties and intrinsic strength of monolayer graphene. Science 321, 385–388, DOI: 10.1126/science.1157996.

Lee H.S., Im S.J., Kim J.H., Kim H.J., Kim J.P. and Min B.R. (2008a) Polyamide thin-film nanofiltration membranes containing TiO_2 nanoparticles. Desalination 219, 48–56, DOI: 10.1016/j.desal.2007.06.003.

Lee J., Chae H.R., Won Y.J., Lee K., Lee C.H., Lee H.H., Kim I.C. and Lee J.M. (2013) Graphene oxide nanoplatelets composite membrane with hydrophilic and antifouling properties for wastewater treatment. Journal of Membrane Science 448, 223–230, DOI: 10.1016/j.memsci.2013.08.017.

Lee K.P., Arnot T.C. and Mattia D. (2011) A review of reverse osmosis membrane materials for desalination—development to date and future potential. Journal of Membrane Science 370, 1–22, DOI: 10.1016/j.memsci.2010.12.036.

Lee Y-C. and Yang J-W. (2012) Self-assembled flower-like TiO_2 on exfoliated graphite oxide for heavy metal removal. Journal of Industrial and Engineering Chemistry 18(3), 1178–1185, DO: 10.1016/j.jiec.2012.01.005.

Li C., Che H., Liu C., Che G., Charpentier P.A., Xu W.Z., Wang X. and Liu L. (2019) Facile fabrication of g-C3N4 QDs/BiVO4 Z-scheme heterojunction towards enhancing photodegradation activity under visible light. Journal of the Taiwan Institute of Chemical Engineers 95, 669–681, DOI: 10.1016/j.jtice.2018.10.011.

Li H., Shi W., Zhu H., Zhang Y., Du Q. and Qin X. (2016) Effects of zinc oxide nanospheres on the separation performance of hollow fiber poly(piperazine-amide) composite nanofiltration membranes. Fibers and Polymers 17, 836–846, DOI: 10.1007/s12221-016-6219-z.

Li L.-H., Deng J.-C., Deng H.-R., Liu Z.-L. and Xin L. (2010b) Synthesis and characterization of chitosan/ZnO nanoparticle composite membranes. Carbohydrate Research 345, 994––998, DOI: 10.1016/j.carres.2010.03.019.

Li Q., Lam M.H.W., Wu R.S.S. and Jiang B. (2010a) Rapid magnetic-mediated solid-phase extraction and pre-concentration of selected endocrine disrupting chemicals in natural waters by poly(divinylbenzene-co-methacrylic acid) coated Fe_3O_4 core-shell magnetite microspheres for their liquid chromatography-tandem mass spectrometry determination. Journal of Chromatography A 1217, 1219–1226, DOI: 10.1016/j.chroma.2009.12.035.

Li S.L., Wang W., Yan W.L. and Zhang W.X. (2014) Nanoscale zero-valent iron (nZVI) for the treatment of concentrated Cu(II) wastewater: a field demonstration. Environmental Science: Processes Impacts 16, 524–533, DOI: 10.1039/C3EM00578J.

Li X., Lenhart J.J. and Walker H.W. (2011) Aggregation kinetics and dissolution of coated silver nanoparticles. Langmuir 28, 1095–1104, DOI: 10.1021/la202328n.

Li Y.H., Di Z.C., Ding J., Wu D.H., Luan Z.K. and Zhu Y.Q. (2005) Adsorption thermodynamic, kinetic and desorption studies of Pb^{2+} on carbon nanotubes. Water Research 39, 605–609, DOI: 10.1016/j.watres.2004.11.004.

Li Y.H., Ding J., Luan Z.K., Di Z.C., Zhu Y.F., Xu C.L., Wu D.H. and Wei B.Q. (2003) Competitive adsorption of Pb^{2+}, Cu^{2+} and Cd^{2+} ions from aqueous solutions by multiwalled carbon nanotubes. Carbon 41, 2787–2792, DOI: 10.1016/S0008-6223(03)00392-0.

Li Y-H., Wang S., Wei J., Zhang X., Xu C., Luan Z., Wu D. Wei B. (2002) Lead adsorption on carbon nanotubes. Chemical Physics Letters 357, 263–266, DOI: 10.1016/S0009-2614(02)-00502-X.

Liang J., Huang Y., Zhang L., Wang Y., Ma Y., Guo T. and Chen Y. (2009) Molecular-level dispersion of graphene into poly(vinyl alcohol) and effective reinforcement of their nanocomposites. Advanced Functional Materials 19, 2297–2302, DOI: 10.1002/adfm.200801776.

Lin D.H., Xing B.S. (2008) Adsorption of phenolic compounds by carbon nanotubes: role of aromaticity and substitution of hydroxyl groups. Environmental Science & Technology 42, 7254–7259, DOI: 10.1021/es801297u.

Lin Y., Xu S. and Li J. (2013) Fast and highly efficient tetracyclines removal from environmental waters by graphene oxide functionalized magnetic particles. Chemical Engineering Journal 225, 679–685, DOI: 10.1016/j.cej.2013.03.104.

Lind M.L., Ghosh A.K., Jawor A., Huang X.F., Hou W., Yang Y. and Hoek E.M.V. (2009) Influence of zeolite crystal size on zeolite polyamide thin film nanocomposite membranes. Langmuir 25, 10139–10145, DOI: 10.1021/la900938x.

Liu F., Abed M.R.M. and Li K. (2011) Preparation and characterization of poly(vinylidene fluoride) (PVDF) based ultrafiltration membranes using nano γ-Al_2O_3. Journal of Membrane Science 366, 97–103, DOI: 10.1016/j.memsci.2010.09.044.

Liu F., Chung S., Oh G. and Seo T.S. (2012) Three-dimensional graphene oxide nanostructure for fast and efficient water-soluble dye removal. ACS Applied Materials & Interfaces 4, 922–927, DOI: 10.1021/am201590z.

Liu H., Ma S., Shao L., Liu H., Gao Q., Li B., Fu H., Fu S., Ye H., Zhao F. and Zhou J. (2020) Defective engineering in graphitic carbon nitride nanosheet for efficient photocatalytic pathogenic bacteria disinfection. Applied Catalysis B: Environmental 261, DOI: 10.1016/j.apcatb.2019.118201.

Liu J., Li W., Duan L., Li X., Ji L., Geng Z., Huang K., Lu L., Zhou L., Liu Z., Chen W., Liu L., Feng S. and Zhang Y. (2015) A graphene-like oxygenated carbon nitride material for improved cycle-life lithium/sulfur batteries. Nano Letters 15, 5137–5142, DOI: 10.1021/acs.nanolett.5b01919.

Liu S., Zeng T.H., Hofmann M., Burcombe E., Wei J., Jiang R., Kong J. and Chen Y. (2011) Antibacterial activity of graphite, graphite oxide, graphene oxide, and reduced graphene oxide: membrane and oxidative stress. ACS Nano 5, 6971–6980, DOI: 10.1021/nn202451x.

Lofrano G., Carotenuto M., Libralato G., Domingos R.F., Markus A., Dini L., Gautam R.K., Baldantoni D., Rossi M., Sharma S.K., Chattopadhyaya M.C., Giugni M. and Meric S. (2016) Polymer functionalized nanocomposites for metals removal from water and wastewater: an overview. Water Research 92, 22–37, DOI: 10.1016/j.watres.2016.01.033.

Long Y., Lu Y., Huang Y., Peng Y., Lu Y., Kang S. and Mu J. (2009) Effect of C60 on the photocatalytic activity of TiO_2 nanorods. Journal of Physical Chemistry C 113, 13899–13905, DOI: 10.1021/jp902417j.

Lu C. and Chiu H. (2006) Adsorption of zinc(II) from water with purified carbon nanotubes. Chemical Engineering Science 61, 1138–1145, DOI: 10.1016/J.CES.2005.08.007.

Lu C., Chiu H. and Bai H. (2007) Comparisons of adsorbent cost for the removal of zinc (II) from aqueous solution by carbon nanotubes and activated carbon. Journal of Nanoscience and Nanotechnology 7, 1647–1652, DOI: 10.1166/jnn.2007.349.

Lu C., Chung Y-L. and Chang K-F. (2005) Adsorption of trihalomethanes from water with carbon nanotubes. Water Research 39, 1183–1189, DOI: 10.1016/j.watres.2004.12.033.

Lu C. and Liu C. (2006) Removal of nickel(II) from aqueous solution by carbon nanotubes. Journal of Chemical Technology and Biotechnology 81, 1932–1940, DOI: 10.1002/jctb.1626.

Lu F. and Astruc D. (2018) Nanomaterials for removal of toxic elements from water. Coordination Chemistry Reviews 356, 147–164, DOI: 10.1016/j.ccr.2017.11.003.

Luo T., Cui J., Hu S., Huang Y. and Jing C. (2010) Arsenic removal and recovery from copper smelting wastewater using TiO_2. Environmental Science & Technology 44, 9094–9098, DOI: 10.1021/es1024355.

Ma J., Yang M., Yu F. and Zheng J. (2015) Water-enhanced removal of ciprofloxacin from water by porous graphene hydrogel. Scientific Reports 5, DOI: 10.1038/srep13578.

Ma W., Soroush A., Van Anh Luong T. and Rahaman S. (2017) Cysteamine- and graphene oxide-mediated copper nanoparticle decoration on reverse osmosis membrane for enhanced anti-microbial performance. Journal of Colloid and Interface Science 501, 330––340, DOI: 10.1016/j.jcis.2017.04.069.

Madadrang C.J., Kim H.Y., Gao G.H., Wang N., Zhu J., Feng H., Gorring M., Kasner M.L. and Hou S.F. (2012) Adsorption behavior of EDTA-graphene oxide for Pb (II) removal. ACS Applied Materials & Interfaces 4, 1186–1193, DOI: 10.1021/am201645g.

Madhura L., Singh S., Kanchi S., Sabela M. and Bisetty K. (2018) Nanotechnology based water quality management for wastewater treatment. Environmental Chemistry Letters 17, 65–121, DOI: 10.1007/s10311-018-0778-8.

Maheswari P., Prasannadevi D. and Mohan D. (2012) Preparation and performance of silver nanoparticle incorporated polyetherethersulfone nanofiltration membranes. High Performance Polymers 25, 174–187, DOI: 10.1177/0954008312459865.

Mak S.-Y. and Chen D.-H. (2004) Fast adsorption of methylene blue on polyacrylic acid-bound iron oxide magnetic nanoparticles. Dyes Pigments 61, 93–98, DOI: 10.1016/j.dyepig.2003.10.008.

Manawi Y., Kochkodan V., Ali Hussein M., Khaleel M.A., Khraisheh M. and Hilal N. (2016) Can carbon-based nanomaterials revolutionize membrane fabrication for water treatment and desalination? Desalination 391, 69–88, DOI: 10.1016/j.desal.2016.02.015.

Mani A.D., Reddy P.M.K., Srinivaas M., Ghosal P., Xanthopoulos N. and Subrahmanyam C. (2015) Facile synthesis of efficient visible active C-doped TiO_2 nanomaterials with high surface area for the simultaneous removal of phenol and Cr(VI). Materials Research Bulletin 61, 391–399, DOI: 10.1016/j.materresbull.2014.10.051.

Mansoori G.A., Rohani.Bastami T., Ahmadpour A. and Eshaghi Z. (2008) Environmental application of nanotechnology. Annual Review of Nano Research 2(2), 393–438, DOI: 10.1142/9789812790248_0010.

Mashhadizadeh M.H. and Amoli-Diva M. (2013) Atomic absorption spectrometric determination of Al^{3+} and Cr^{3+} after preconcentration and separation on 3-mercaptopropionic acid modified silica coated-Fe_3O_4 nanoparticles. Journal of Analytical Atomic Spectrometry 28, 251–258, DOI: 10.1039/C2JA30286A.

Matin A., Khan Z., Zaidi S.M.J. and Boyce M.C. (2011) Biofouling in reverse osmosis membranes for seawater desalination: phenomena and prevention. Desalination 281, 1–16, DOI: 10.1016/j.desal.2011.06.063.

Mercer K.L. and Tobiason J.E. (2008) Removal of arsenic from high ionic strength solutions: effects of ionic strength, pH, and preformed versus in situ formed HFO. Environmental Science & Technology 42, 3797–3802, DOI: 10.1021/ES702946S.

Miller S., Shemer H. and Semiat R. (2014) Energy and environmental issues in desalination. Desalination 366, 2–8, DOI: 10.1016/j.desal.2014.11.034.

Ming L., Yue H., Xu L. and Chen F. (2014) Hydrothermal synthesis of oxidized gC3N4 and its regulation of photocatalytic activity. Journal of Materials Chemistry A 2, 19145–19149, DOI: 10.1039/C4TA04041D.

Mohan D., Singh K.P. and Singh V.K. (2008) Wastewater treatment using low cost activated carbons derived from agricultural byproducts — a case study. Journal of Hazardous Materials 152, 1045–1053, DOI: 10.1016/j.jhazmat.2007.07.079.

Mollahosseini A. and Rahimpour A. (2014) Interfacially polymerized thin film nanofiltration membranes on TiO_2 coated polysulfone substrate. Journal of Industrial and Engineering Chemistry 20, 1261–1268, DOI: 10.1016/j.jiec.2013.07.002.

Mollahosseini A., Rahimpour A., Jahamshahi M., Peyravi M. and Khavarpour M. (2012) The effect of silver nanoparticle size on performance and antibacteriality of polysulfone ultrafiltration membrane. Desalination 306, 41–50, DOI: 10.1016/j.desal.2012.08.035.

Mozia S., Jose M., Sienkiewicz P., Szymański K., Darowna D., Zgrzebnicki M. and Markowska-Szczupak A. (2018) Polyethersulfone ultrafiltration membranes modified with hybrid Ag/titanate nanotubes: physicochemical characteristics, antimicrobial properties and fouling resistance. Desalination and Water Treatment 128, 106–118, DOI: 10.5004/dwt.2018.22602.

Mueller N., Braun J., Bruns J., Cernik M.,. Rissing P, Rickerby D. and Nowack B. (2012) Application of nanoscale zero valent iron (NZVI) for groundwater remediation in Europe. Environmental Science & Pollution Research 19, 550–558, DOI: 10.1007/s11356-011-0576-3.

Murugesan P., Moses J.A. and Anandharamakrishnan C. (2019) Photocatalytic disinfection efficiency of 2D structure graphitic carbon nitride-based nanocomposites: a review. Journal of Materials Science 54, 12206–12235, DOI: 10.1007/s10853-019-03695-2.

Nair R., Wu H., Jayaram P., Grigorieva I. and Geim A. (2012) Unimpeded permeation of water through helium-leak–tight graphene-based membranes. Science 335, 442–444, DOI: 10.1126/science.1211694.

Nandi D., Basu T., Debnath S., Ghosh A.K., De A. and Ghosh U.C. (2013) Mechanistic insight for the sorption of Cd(II) and Cu(II) from aqueous solution on magnetic Mn-doped Fe(III) oxide nanoparticle implanted graphene. Journal of Chemical & Engineering Data 58, 2809–2818, DOI: 10.1021/JE4005257.

Nicolaï A., Sumpter B.G. and Meunier V. (2014) Tunable water desalination across Graphene oxide framework membranes. Physical Chemistry Chemical Physics 16, 8646–8654, DOI: 10.1039/c4cp01051e.

Ozmen M., Can K., Arslan G., Tor A, Cengeloglu Y. and Ersoz M. (2010) Adsorption of Cu(II) from aqueous solution by using modified Fe_3O_4 magnetic nanoparticles. Desalination 254, 162–169, DOI: 10.1016/j.desal.2009.11.043.

Palit S. (2021) Application of nanotechnology in the energy industry, green sustainability and the visionary future. Academia Letters Article 2326, DOI: 10.20935/AL2326.

Pan Y., Liu X., Zhang W., Liu Z., Zeng G., Shao B., Liang Q., He Q., Yuan X., Huang D. and Chen M. (2020) Advances in photocatalysis based on fullerene C60 and its derivatives: Properties, mechanism, synthesis, and applications. Applied Catalysis B: Environmental 265, DOI: 10.1016/j.apcatb.2019.118579.

Pandey N., Shukla S.K. and Singh N.B. (2017) Water purification by polymer nanocomposites: an overview. Nanocomposites 3(2), 47–66, DOI: 10.1080/20550324.2017.1329983.

Park O.-K., Kim N.H., Lau K.-T. and Lee J.H. (2010) Effect of surface treatment with potassium persulfate on dispersion stability of multi-walled carbon nanotubes. Materials Letters 64, 718–721, DOI: 10.1016/j.matlet.2009.12.048.

Park Y., Singh N.J., Kim K.S., Tachikawa T., Majima T. and Choi W. (2009) Fullerol-titania charge-transfer-mediated photocatalysis working under visible light. Chemistry 15, 10843–10850, DOI: 10.1002/chem.200901704.

Pastrana-Martinez L.M., Morales-Torres S., Likodimos V., Figueiredo J.L., Faria J.L., Falaras P. and Silva A.M. (2012) Advanced nanostructured photocatalysts based on reduced graphene oxide–TiO_2 composites for degradation of diphenhydramine pharmaceutical and methyl orange dye. Applied Catalisis B: Environmental 123, 241–256, DOI: 10.1016/j.apcatb.2012.04.045.

Peng X., Jin J., Ericsson E.M. and Ichinose I. (2007) General method for ultrathin free-standing films of nanofibrous composite materials. Journal of the American Chemical Society 129, 8625–8633, DOI: 10.1021/ja0718974.

Perreault F., Tousley M.E. and Elimelech M. (2014) Thin-film composite polyamide membranes functionalized with biocidal graphene oxide nanosheets. Environmental Science &Technology Letters 1, 71–76, DOI: 10.1021/ez4001356.

Petronella F., Truppi C., Ingrosso A., Placido T., Striccoli M., Curri M.L., Agostiano A. and Comparelli R. (2016) Nanocomposite materials for photocatalytic degradation of pollutants. Catalysis Today 281, 85–100, DOI: 10.1016/j.cattod.2016.05.048.

Pishnamazi M., Nakhjiri A. T., Taleghani A. S., Ghadiri M., Marjani A. and Shirazian S. (2020) Computational modelling of drug separation from aqueous solutions using octanol organic solution in membranes. Scientific Reports 10, 1–12, DOI: 10.1038/s41598-020-76189-w.

Qi K., Selvaraj R., Al Fahdi T., Al-Kindy S., Kim Y., Wang G., Tai C.W. and Sillanpaa M. (2016) Enhanced photocatalytic activity of anatase-TiO_2 nanoparticles by fullerene modification: a theoretical and experimental study. Applied Surface Science 387, 750–758, DOI: 10.1016/j.apsusc.2016.06.134.

Qu X., Alvarez P.J.J. and Li Q. (2013) Applications of nanotechnology in water and wastewater treatment. Water Research 47, 3931–3946, DOI: 10.1016/j.watres.2012.09.058.

Quang D.V., Sarawade P.B., Jeon S.J., Kim S.H., Kim J-K., Chai Y.G. and Kim H.T. (2013) Effective water disinfection using silver nanoparticle containing silica beads. Applied Surface Science 266, 280–287, DOI: 10.1016/j.apsusc.2012.11.168.

Rabiee H., Vatanpour V., Farahani M.H.D.A. and Zarrabi H. (2015) Improvement in flux and antifouling properties of PVC ultrafiltration membranes by incorporation of zinc oxide (ZnO) nanoparticles. Separation and Purification Technology 156, 299–310, DOI: 10.1016/j.seppur.2015.10.015.

Ramos M.A.V., Yan W., Li X.Q., Koel B.E. and Zhang W.X. (2009) Simultaneous oxidation and reduction of arsenic by zero-valent iron nanoparticles: understanding the significance of the core-shell structure. The Journal of Physical Chemistry C 113, 14591–14594, DOI: 10.1021/jp9051837.

Rao G.P., Lu C. and Su F. (2007) Sorption of divalent metal ions from aqueous solution by carbon nanotubes: a review. Separation and Purification Technology 58, 224–231, DOI: 10.1016/j.seppur.2006.12.006.

Ren D., Colosi L.M. and Smith J.A. (2013) Evaluating the sustainability of ceramic filters for point-of-use drinking water treatment. Environmental Science & Technology 47, 11206–11213, DOI: 10.1021/es4026084.

Ren D. and Smith J.A. (2013) Retention and transport of silver nanoparticles in a ceramic porous medium used for point-of-use water treatment. Environmental Science & Technology 47, 3825–3832, DOI: 10.1021/es4000752.

Ren X., Chen C., Nagatsu M. and Wang X. (2011) Carbon nanotubes as adsorbents in environmental pollution management: a review. Chemical Engineering Journal 170 (2–3), 395–410, DOI: 10.1016/j.cej.2010.08.045.

Runowski M. (2014) Nanotechnology – nanomaterials, nanoparticles and multifunctional nanostructures core/coating type. Chemik 68, 766–775.

Ryu A., Jeong S.-W., Jang A. and Choi H. (2011) Reduction of highly concentrated nitrate using nanoscale zero-valent iron: effects of aggregation and catalyst on reactivity. Applied Catalysis B Environmental 105, 128–135, DOI: 10.1016/j.apcatb.2011.04.002.

Santhosh C., Velmurugan V., Jacob G., Jeong S.K., Grace A.N. and Bhatnagar A. (2016) Role of nanomaterials in water treatment applications: a review. Chemical Engineering Journal 306, 1116–1137, DOI: 10.1016/j.cej.2016.08.053.

Sarma G.K., Gupta S.S. and Bhattacharyya K.G. (2019) Nanomaterials as versatile adsorbents for heavy metal ions in water: a review. Environmental Science and Pollution Research 26, 6245–6278, DOI: 10.1007/s11356-018-04093-y.

Sears K., Dumée L., Schütz J., She M., Huynh C., Hawkins S., Duke M. and Gray S. (2010) Recent developments in carbon nanotube membranes for water purification and gas separation. Materials 3, 127–149, DOI: 10.3390/ma3010127.

Sharma S. and Bhattacharya A. (2017) Drinking water contamination and treatment techniques. Applied Water Science (2017) 7, 1043–1067, DOI: 10.1007/s13201-016-0455-7.

Sharma Y.C., Srivastava V., Singh V.K., Kaul S.N. and Weng C.H. (2009) Nano-adsorbents for the removal of metallic pollutants from water and wastewater. Environmental Technology 30, 583–609, DOI: 10.1080/09593330902838080.

Sheela T., Nayaka Y.A., Viswanatha R., Basavanna S. and Venkatesha T.G. (2012) Kinetics and thermodynamics studies on the adsorption of Zn(II), Cd(II) and Hg(II) from aqueous solution using zinc oxide nanoparticles. Powder Technology 217, 163–170, DOI: 10.1016/j.powtec.2011.10.023.

Shen Y.-X., Saboe P.O, Sines I.T., Erbakan M. and Kumar M. (2014) Biomimetic membranes: a review. Journal of Membrane Science 454, 359–381, DOI: 10.1016/j.memsci.2013.12.019.

Shi X., Ruan W., Hu J., Fan M., Cao R. and Wei X. (2017) Optimizing the removal of rhodamine B in aqueous solutions by reduced graphene oxide-supported nanoscale zerovalent iron (NZVI/RGO) using an artificial neural network-genetic algorithm (ANN-GA). Nanomaterials 7, 134, DOI: 10.3390/nano7100309.

Shipley H.J., Engates K.E. and Grover V.A. (2013) Removal of Pb(II), Cd(II), Cu(II), and Zn(II) by hematite nanoparticles: effect of sorbent concentration, pH, temperature, and exhaustion. Environmental Science and Pollution Research 20, 1727–1736, DOI: 10.1007/s11356-012-0984-z.

Sitko R., Turek E., Zawisza B., Malicka E., Talik E., Heimann J., Gagor A., Feist B. and Wrzalik R. (2013) Adsorption of divalent metal ions from aqueous solutions using graphene oxide. Dalton Transactions 42, 5682–5689, DOI: 10.1039/C3DT33097D.

Smith A.T., LaChance A.M., Zeng S., Liu B. and Sun L. (2019) Synthesis, properties, and applications of graphene oxide/reduced graphene oxide and their nanocomposites. Nano Materials Science 1, 31–47, DOI: 10.1016/j.nanoms.2019.02.004.

Sondi I. and Salopek-Sondi B. (2004) Silver nanoparticles as antimicrobial agent: a case study on E. coli as a model for Gram-negative bacteria. Journal of Colloids Interface Science 275, 177–182, DOI: 10.1016/j.jcis.2004.02.012.

Song N., Gao X., Mac Z., Wanga X., Weia Y. and Gao C. (2018) A review of graphene-based separation membrane: Materials, characteristics, preparation and applications. Desalination 437, 59–72, DOI: 10.1016/J.DESAL.2018.02.024.

Sreeprasad T., Maliyekkal S.M., Lisha K. and Pradeep T. (2011) Reduced graphene oxide–metal/metal oxide composites: facile synthesis and application in water purification. Journal of Hazardous Materials 186, 921–931, DOI: 10.1016/j.jhazmat.2010.11.100.

Stafiej A. and Pyrzynska K. (2007) Adsorption of heavy metal ions with carbon nanotubes. Separation and Purification Technology 58, 49–52, DOI: 10.1016/j.seppur.2007.07.008.

Sun X.F., Qin J., Xia P.F., Guo B.B., Yang C.M., Song C. and Wang S.G. (2015) Graphene oxide–silver nanoparticle membrane for biofouling control and water purification. Chemical Engineering Journal 28(1), 53–59, DOI: 10.1016/j.cej.2015.06.059.

Surwade S.P., Smirnov S.N., Vlassiouk I.V., Unocic R.R., Veith G.M., Dai S. and Mahurin S.M. (2015) Water desalination using nanoporous single-layer graphene. Nature Nanotechnology 10, 459–464, DOI: 10.1038/nnano.2015.37.

Szymański K., Sienkiewicz P., Darowna D., Jose M., Szymańska K. and Mozia S. (2018) Investigation on polyethersulfone membranes modified with Fe_3O_4 – trisodium citrate nanoparticles. Desalination and Water Treatment 128, 265–271, DOI: 10.5004/dwt.2018.22871.

Tesh S.J. and Scott T.B. (2014) Nano-composites for water remediation: a review. Advanced Materials 26(35), 6056–6068, DOI: 10.1002/adma.201401376.

Thomas J.A. and McGaughey A.J.H. (2009) Water flow in carbon nanotubes: transition to subcontinuum transport. Physical Review Letters 102, DOI: 10.1103/PHYSREVLETT.102.184502.

Tian M., Wang Y.N. and Wang R. (2015) Synthesis and characterization of novel high-performance thin film nanocomposite (TFN) FO membranes with nanofibrous substrate reinforced by functionalized carbon nanotubes. Desalination 370, 79–86, DOI: 10.1016/j.desal.2015.05.016.

Tosco T., Papini P.M., Viggi C.C. and Sethi R. (2014) Nanoscale zerovalent iron particles for groundwater remediation: a review. Journal of Cleaner Production 77, 10–21, DOI: 10.1016/j.jclepro.2013.12.026.

Tratnyek P.G., Salter A.J., Nurmi J.T. and Sarathy V. (2010) Environmental applications of zerovalent metals: iron vs. zinc. In: Nanoscale materials in chemistry: environmental applications. ACS Publications 165–178, DOI: 10.1021/bk-2010-1045.ch009.

Trivedi P. and Axe L. (2000) Modeling Cd and Zn sorption to hydrous metal oxides. Environmental Science & Technology 34, 2215–2223, DOI: 10.1021/es010703w.

Tu Y., Lv M., Xiu P., Huynh T., Zhang M., Castelli M. et al. (2013) Destructive extraction of phospholipids from Escherichia coli membranes by graphene nanosheets. Nature Nanotechnology 8, 594–601, DOI: 10.1038/nnano.2013.125.

Tyagi I., Gupta V., Sadegh H., Ghoshekandi R. and Makhlouf A.S.H. (2017) Nanoparticles as adsorbent; a positive approach for removal of noxious metal ions: a review. Science Technology and Development 34, 95–214, DOI: 10.3923/std.2015.195.214.

Tycko R., Haddon R.C., Dabbagh G., Glarum S.H., Douglass D.C. and Mujsce A.M. (1991) Solid-state magnetic resonance spectroscopy of fullerenes. Journal of Physical Chemistry 95, 518–520, DOI: 10.1021/j100155a006.

Vasudevan S. and Lakshmi J. (2012)The adsorption of phosphate by graphene from aqueous solution. RSC Advances 2, 5234–5242, DOI: 10.1039/C2RA20270K.

Wang F., Wang Y., Feng Y., Zeng Y., Xie Z., Zhang Q., Su Y., Chen P., Liu Y., Yao K., Lv W. and Liu G. (2018) Novel ternary photocatalyst of single atom-dispersed silver and carbon quantum dots co-loaded with ultrathin g-C_3N_4 for broad spectrum photocatalytic degradation of naproxen. Applied Catalysis B: Environmental 221, 510–520, DOI: 10.1016/j.apcatb.2017.09.055.

Wang H., Yuan X.Z., Wu Y., Huang H.J., Zeng G.M., Liu Y., Wang X.L., Lin N.B. and Qi Y. (2013a) Adsorption characteristics and behaviors of graphene oxide for Zn(II) removal from aqueous solution. Applied Surface Science 279, 432–440, DOI: 10.1016/j.apsusc.2013.04.133.

Wang J., Zhang P., Liang B., Liu Y., Xu T., Wang L., Cao B. and Pan K. (2016) Graphene oxide as an effective barrier on a porous nanofibrous membrane for water treatment. Applied Materials & Interfaces 8, 6211–6218, DOI: 10.1021/acsami.5b12723.

Wang S., Ng C.W., Wang W., Li Q. and Hao Z. (2012a) Synergistic and competitive adsorption of organic dyes on multiwalled carbon nanotubes. Chemical Engineering Journal 197, 34–40, DOI: 10.1016/j.cej.2012.05.008.

Wang X., Cai W., Lin Y., Wang G. and Liang C. (2010) Mass production of micro/nanostructured porous ZnO plates and their strong structurally enhanced and selective adsorption performance for environmental remediation. Journal of Materials Chemistry 20, 8582––8590, DOI: 10.1039/C0JM01024C.

Wang X., Lu J. and Xing B. (2008) Sorption of organic contaminants by carbon nanotubes: influence of X adsorbed organic matter. Environmental Science & Technology 42, 3207–3212, DOI: 10.1021/es702971g.

Wang X., Tian H., Yang Y., Wang H., Wang S., Zheng W. and Liu Y. (2012b) Reduced graphene oxide/CdS for efficiently photocatalystic degradation of methylene blue. Journal of Alloys and Compounds 524, 5–12, DOI: 10.1016/j.jallcom.2012.02.058.

Wang Y., Liang S., Chen B., Guo F., Yu S. and Tang Y. (2013b) Synergistic removal of Pb(II), Cd(II) and humic acid by Fe_3O_4@mesoporous silica–graphene oxide composites. PLoS One 8(6), e65634, DOI: 10.1371/journal.pone.0065634.

Wen Z., Zhang Y. and Dai C. (2014) Removal of phosphate from aqueous solution using nanoscale zerovalent iron (nZVI). Colloids and Surfaces A: Physicochemical and Engineering Aspects 457, 433–440, DOI: 10.1016/j.colsurfa.2014.06.017.

Werber J.R., Osuji C.O. and Elimelech M. (2016) Materials for next-generation desalination and water purification membranes. Nature Reviews Materials 1, 16018, DOI: 10.1038/natrevmats.2016.18.

Wu C-H. (2007) Adsorption of reactive dye onto carbon nanotubes: equilibrium, kinetics and thermodynamics. Journal of Hazardous Materials 144, 93–100, DOI: 10.1016/j.jhazmat.2006.09.083.

Wu Q., Chen G.E., Sun W.G, Xu Z.L., Konga Y.P., Zheng X.P. and Xu S.J. (2017) Bio-inspired GO-Ag/PVDF/F127 membrane with improved anti-fouling for natural organic matter (NOM) resistance. Chemical and Engineering Journal 313, 450–460, DOI: 10.1016/j.cej.2016.12.079.

Xie G., Xi P., Liu H., Chen F., Huang L., Shi Y., Hou F., Zeng Z., Shao C. and Wang J. (2012) A facile chemical method to produce superparamagnetic graphene oxide–Fe_3O_4 hybrid composite and its application in the removal of dyes from aqueous solution. Journal of Materials Chemistry 22, 1033–1039, DOI: 10.1039/C1JM13433G.

Xu C., Cui A., Xu Y. and Fu X. (2013) Graphene oxide–TiO_2 composite filtration membranes and their potential application for water purification. Carbon 62, 465–471, DOI: 10.1016/j.carbon.2013.06.035.

Xu K., Feng B., Zhou C. and Huang A. (2016b) Synthesis of highly stable graphene oxide membranes on polydopamine functionalized supports for seawater desalination. Chemical Engineering Science 146, 159–165.

Xu P., Zeng G.M., Huang D.L., Feng C.L., Hu S., Zhao M.H., Lai C., Wei Z., Huang C., Xie G.X. and Liu Z.F. (2012) Use of iron oxide nanomaterials in wastewater treatment: a review. Science of The Total Environment 424, 1–10, DOI: 10.12691/ijebb-9-1-2.

Xu T.Y., Zhu R.L., Zhu J.X., Liang X.L., Zhu G.Q., Liu Y., Xu Y. and He H.P. (2016a) Fullerene modification of Ag_3PO_4 for the visible-light-driven degradation of acid red 18. RSC Advances 6, 85962–85969, DOI: 10.1039/C6RA18657B.

Xu Z., Zhang J., Shan M., Li Y., Li B., Niu J., Zhou B. and Qian X. (2014) Organosilane functionalized graphene oxide for enhanced antifouling and mechanical properties of polyvinylidene fluoride ultrafiltration membranes. Journal of Membrane Science 458, 1–13.

Xue S.-M., Xu Z.-L., Tang Y.-J. and Ji C.-H. (2016) Polypiperazine-amide nanofiltration membrane modified by different functionalized multiwalled carbon nanotubes (MWCNTs). ACS Applied Materials & Interfaces 8, 19135–19144, DOI: 10.1021/acsami.6b05545.

Yang H.-L., Lin J. C.-T. and Huang C. (2009) Application of nanosilver surface modification to RO membrane and spacer for mitigating biofouling in seawater desalination. Water Research 43, 3777–3786.

Yang K. and Xing B.S. (2010) Adsorption of organic compounds by carbon nanomaterials in aqueous phase: Polanyi theory and its application. Chemical Reviews 110, 5989–6008, DOI: 10.1021/cr100059s.

Yang K., Zhu L. and Xing B. (2006) Adsorption of polycyclic aromatic hydrocarbons by carbon nanomaterials. Environmental Science and Technology 40, 1855–1861, DOI: 10.1021/es052208w.

Yang Z., Ma X.H. and Tang C.Y. (2018) Recent development of novel membranes for desalination. Desalination 434, 37–59, DOI: 10.1016/J.DESAL.2017.11.046.

Yannoni C.S., Johnson R.D., Meijer G., Bethune D.S. and Salem J.R. (1991) 13C NMR study of the C60 cluster in the solid state: molecular motion and carbon chemical shift anisotropy. Journal of Physical Chemistry 95, 9–10, DOI: 10.1021/j100154a005.

Yao Y., Bing H., Feifei X. and Xiaofeng C. (2011) Equilibrium and kinetic studies of methyl orange adsorption on multiwalled carbon nanotubes. Chemical Engineering Journal 170, 82–89, DOI: 10.1016/j.cej.2011.03.031.

Yean S., Cong L., Yavuz C.T., Mayo J.T., Yu W.W., Kan A.T., Colvin V.L. and Tomson M.B. (2005) Effect of magnetite particle size on adsorption and desorption of arsenite and arsenate. Journal of Materials Research 20, 3255–3264, DOI: 10.1557/jmr.2005.0403.

Yin J. and Deng B.L. (2015) Polymer-matrix nanocomposite membranes for water treatment. Journal of Membrane Science 479, 256–275, DOI: 10.1016/j.memsci.2014.11.019.

Yin J., Kim E.-S., Yang J. and Deng B. (2012) Fabrication of a novel thin-film nanocomposite(TFN) membrane containing MCM-41 silica nanoparticles (NPs) for water purification. Journal of Membrane Science 423, 238–246, DOI: 10.1016/J.MEMSCI.2012.08.020.

Yin J., Zhu G. and Deng B. (2013) Multi-walled carbon nanotubes (MWNTs)/polysulfone (PSU) mixed matrix hollow fiber membranes for enhanced water treatment. Journal of Membrane Science 437, 237–248, DOI: 10.1016/j.memsci.2013.03.021.

You Y., Sahajwalla V., Yoshimura M. and Joshi R.K. (2016) Graphene and graphene oxide for desalination. Nanoscale 8, 117–119, DOI: 10.1039/C5NR06154G.

Younis S.A., Abd-Elaziz A. and Hashem A. (2016) Utilization of a pyrrole derivative based antimicrobial functionality impregnated onto CaO/g-C_3N4 for dyes adsorption. RSC Advances 6, 89367–89379, DOI: 10.1039/C6RA10143G.

Yu F., Ma J. and Bi D. (2015) Enhanced adsorptive removal of selected pharmaceutical antibiotics from aqueous solution by activated graphene. Environmental Science Pollution. Research International 22, 4715–4724, DOI: 10.1007/s11356-014-3723-9.

Yu L., Zhang Y., Zhang B., Liu J., Zhang H. and Song C. (2013) Preparation and characterization of HPEI-GO/PES ultrafiltration membrane with antifouling and antibacterial properties. Journal of Membrane Science 447, 452–462.

Yu R.-F., Chi F.-H., Cheng W.-P. and Chang J.-C. (2014) Application of pH, ORP, and DO monitoring to evaluate chromium(VI) removal from wastewater by the nanoscale zerovalent iron (nZVI) process. Chemical Engineering Journal 255, 568–576, DOI: 10.1016/j.cej.2014.06.002.

Yu S., Zuo X., Bao R., Xu X., Wang J. and Xu J. (2009) Effect of SiO_2 nanoparticle addition on the characteristics of a new organic–inorganic hybrid membrane. Polymer 50, 553–559, DOI: 10.1016/j.polymer.2008.11.012.

Yuan Y., Gao X., Wei Y., Wang X., Wang J., Zhang Y. and Gao C. (2017) Enhanced desalination performance of carboxyl functionalized graphene oxide nanofiltration membranes. Desalination 405, 29–39, DOI: 10.1016/j.desal.2016.11.024.

Zhang C., Hu Z. and Deng B. (2016c) Silver nanoparticles in aquatic environments: physiochemical behavior and antimicrobial mechanisms. Water Research 88, 403–427, DOI: 10.1016/j.watres.2015.10.025.

Zhang J., Xu Z., Shan M., Zhou B., Li Y., Li B., Niu J. and Qian X. (2013b) Synergetic effects of oxidized carbon nanotubes and graphene oxide on fouling control and anti-fouling mechanism of polyvinylidene fluoride ultrafiltration membranes. Journal of Membrane Science 448, 81–92, DOI: 10.1016/j.memsci.2013.07.064.

Zhang J.-J., Fang S.-S., Mei J.-Y., Zheng G.-P., Zheng X.-C. and Guan X.-X. (2018) High efficiency removal of rhodamine B dye in water using g-C_3N_4 and TiO_2 cohybridized 3D graphene aerogel composites. Separation and Purification Technology 194, 96–103, DOI: 10.1016/j.seppur.2017.11.035.

Zhang L., Huang T., Zhang M., Guo X. and Yuan Z. (2008) Studies on the capability and behavior of adsorption of thallium on nano-Al_2O_3. Journal of Hazardous Materials 157, 352–357, DOI: 10.1016/j.jhazmat.2008.01.005.

Zhang S., Shao Y., Liu J., Aksay I.A. and Lin Y. (2011) Graphene-polypyrrole nanocomposite as a highly efficient and low cost electrically switched ion exchange for removing ClO_4^- from wastewater. ACS Applied Materials & Interfaces 3, 3633–3637, DOI: 10.1021/am200839m.

Zhang W., Wu B., Xu H., Liu H., Wang M., He Y. and Pan B. (2016a) Nanomaterials-enabled water and wastewater treatment. NanoImpact 3–4, 22–39, DOI: 10.1016/j.impact.2016.09.004.

Zhang Y., Zhang X., Cheng C., Zhao J., Ma L., Sun S. and Zhao C. (2013a) Polyethersulfone enwrapped graphene oxide porous particles for water treatment. Chemical Engineering Journal 215, 72–81, DOI: 10.1016/j.cej.2012.11.009.

Zhang Y., Zhou Z., Shen Y., Zhou Q., Wang J., Liu A.R., Liu S.Q. and Zhang Y.J. (2016b) Reversible assembly of graphitic carbon nitride 3D network for highly selective dyes absorption and regeneration. ACS Nano 10, 9036–9043, DOI: 10.1021/acsnano.6b05488.

Zhao C., Xu X., Chen J. and Yang F. (2013a) Effect of graphene oxide concentration on the morphologies and antifouling properties of PVDF ultrafiltration membranes. Journal of Environmental and Chemical Engineering 1, 349–354, DOI: 10.1016/j.jece.2013.05.014.

Zhao H., Wu L., Zhou Z., Zhang L. and Chen H. (2013b) Improving the antifouling property of polysulfone ultrafiltration membrane by incorporation of isocyanate-treated Graphene oxide. Physical Chemistry Chemical Physics 15, 9084–9092, DOI: 10.1039/c3cp50955a.

Zhao L., Xue F., Yu B., Xie J., Zhang X., Wu R., Wang R., Hu Z., Yang S-T. and Luo J. (2015) TiO_2–graphene sponge for the removal of tetracycline. Journal of Nanoparticle Research 17, 16, DOI: 10.1007/s11051-014-2825-0.

Zhu L., You L., Wang Y. and Shi Z. (2017) The application of graphitic carbon nitride for the adsorption of Pb^{2+} ion from aqueous solution. Materials Research Express 4, 075606, DOI: 10.1088/2053-1591/aa7903.

Zhu Z., Huo P., Lu Z., Yan Y., Liuc Z., Shi W., Li C. and Dong H. (2018) Fabrication of magnetically recoverable photocatalysts using g-C3N4 for effective separation of charge carriers through like-Z-scheme mechanism with Fe3O4 mediator. Chemical Engineering Journal 331, 615–625, DOI: 10.1016/J.CEJ.2017.08.131.

Zinadini S., Zinatizadeh A.A., Rahimi M., Vatanpour V. and Zangeneh H. (2014) Preparation of a novel antifouling mixed matrix PES membrane by embedding graphene oxide nanoplates. Journal of Membrane Science 453, 292–301, DOI: 10.1016/j.memsci.2013.10.070.

Zodrow K., Brunet L., Mahendra S., Li D., Zhang A., Li Q. and Alvarez P.J.J. (2009) Polysulfone ultrafiltration membranes impregnated with silver nanoparticles show improved biofouling resistance and virus removal. Water Research 43, 715–723, DOI: 10.1016/j.watres.2008.11.014.

Jakub Copik*, Edyta Kudlek, Mariusz Dudziak, Martyna Kaczmarek

Silesian University of Technology, jakub.copik@polsl.pl; e-mail*: jakub.copik@polsl.pl

The use of ultrasound to remove 4-tert octylphenol by hydrogen peroxide assistance

ABSTRACT: Endocrine disrupting compounds (EDCs) was recognized as a large group of diverse contaminants which are widely spread in environmental compartments. According to the literature reports, they have a significant impact on human health even in very small doses thus recently, removing EDCs from the aquatic environment attract the attention of many researchers. 4-tert octylphenol (OP) is a compound identified as EDCs that causes many harmful health effects such as reduction of testosterone and sperm production. Moreover, it can significantly affect the reproductive system. OP is widely used in dispersants, detergents, emulsifiers, wetting agents, and solubilizers. Literature data showed, that conventional wastewater treatment methods can be not sufficiently effective in EDCs removal, so other techniques should be developed.

In this study, the removal effectiveness of OP from the urban sewage treatment plant synthetic effluent by using ultrasound was evaluated. Furthermore, the effect of hydrogen peroxide addition was determined. Research revealed that the degradation rate of OP was proportional to the amplitude, sonication time, and hydrogen peroxide dosage. To evaluate the process effectiveness, the gas chromatography method (GC-MS) was used preceded by solid-phase extraction (SPE). The analysis has shown that after 45 min of sonication removal of OP reached 88%. Research revealed also that combined ultrasonication and hydrogen peroxide dosage were more effective than these methods used as a single process. At the dosage of 12 mg L^{-1} hydrogen peroxide, OP removal was 57% while in the combined process it was enhanced by 10% during 1 min sonication.

KEYWORDS: ultrasound, hydrogen peroxide, Endocrine disrupting compounds, wastewater treatment, advanced oxidation processes, AOPs

Introduction

As a consequence of anthropogenic activity, many undesirable substances are released into the environment. Nowadays, they can be identified in water even at very

low concentrations due to the development of analytical techniques. In recent years, the attention of scientists has attracted a wide group of organic pollutants recognized as contaminants of emerging concern including endocrine-disrupting compounds (EDCs) (Bohdziewicz et al. 2016; Gavrilescu et al. 2015; Kudlek 2018). These substances were found in various matrixes, such as water, wastewater, soils, sediments, sludges, gases, aerosols, and even body fluids and tissues (Metcalfe et al. 2022). Noteworthy, these substances could be harmful to human health even in very low concentrations. EDCs are known as substances able to block or mimic hormones that are responsible for the proper functioning of the human body. Moreover, contact with ECDs can lead to alterations in the endocrine system and affect other human body systems (Vieira et al. 2021). 4-tert octylphenol (OP) which is a common endocrine-disrupting chemical used in many consumer products such as epoxy resins and polycarbonate plastic can cause serious health problems. For instance exposure to OP is associated with neonatal size reduction at birth, and idiopathic infertility (Chen et al. 2013; Lv et al. 2016). Furthermore, it was reported in the literature that OP exposure could lead to problems with brain development (Tran et al. 2020). OP reduced bromodeoxyuridine (BrdU. OP is widely spread in the aquatic environment. It could be found in surface waters, groundwaters, bottled water, and in biological matrices such as human urine, breast milk, blood, and food (Acir and Guenther 2018).

Literature data showed that conventional treatment such as adsorption, flocculation, and coagulation can be ineffective and time-consuming in OP degradation unlike advanced oxidation processes (AOPs) which were found to be an interesting and effective alternative in many micropollutants removal (Ahmedchekk at et al. 2021; Dudziak et al. 2018; Kudlek 2018; Kudlek et al. 2017). Recently acoustic cavitation as one of the AOPs was found to be effective in the removal of many harmful substances such as bacteria, fungi, dyes, viruses, algae, polycyclic aromatic hydrocarbons (PAHs) as well as pesticides, pharmaceuticals and personal care products (PPCPs) and industrial chemicals. Also, OP was effectively removed from distilled water, seawater, natural water, and sewage water by Ahmedchekk at et al. (Ahmedchekkat et al. 2021). They proved that after 60 min sonication at 278 kHz OP was eliminated at the level of 90%. Acoustic cavitation phenomena (ultrasonication) is described as the formation, growth, and implosion of bubbles generated by periodic pressure changes in the medium caused by ultrasonic waves (Yasui 2018). During bubble collapse several sonochemical and hydrodynamic effects can occur, namely hydroxyl radicals formation, the occurrence of shear stresses, microjets, high temperature, pressure, and shock waves. Due to these effects, harmful substances could be eliminated (Dular et al. 2016; Merouani et al. 2015; Zhang et al. 2011). Nowadays, to increase the efficiency of the treatment there is a tendency to combine this technology with other AOPs such as ozone addition, UV irradiation or hydrogen peroxide treatment (Gągol et al. 2018).

The aim of this study was to evaluate the efficiency of OP ultrasonic treatment from urban sewage treatment plant synthetic effluent at different operational parameters. The effect of hydrogen peroxide addition (H_2O_2) combined with sonication on OP degradation was also examined.

1. Materials and methods

1.1. Experimental setup, materials and reagents

The OP standard (purity higher than 99%) used in the study was purchased from Sigma-Aldrich (Poznan, Poland). The experimental setup used in the research consists of an ultrasonic system, a cooling setup to prevent overheating, and stirrer. In the study, ultrasonic processor Sonics VCX 500 (Vibra Cell Sonics, Sonics & Materials, USA) with a maximum power of 500 W and frequency of 20 kHz was used. Primarily, the effect of ultrasonication as a single process on the OP removal process was investigated. In the second stage, a 30% solution of analytical grade hydrogen peroxide (H_2O_2) obtained from Stanlab (Lublin, Poland) was added to the treated solution at different dosages. In all experiments, 13 mm diameter titanium sonotrode was immersed at a fixed depth of 2 cm. The experiments were carried out at different levels of intensity, the volume of the sample and dosage of oxidant. Moreover, sonication time during the treatment varied from 1 to 45 min. Literature data shown that ultrasonic technique could be effective even at short time (Ahmedchekkat et al. 2021; Pokhalekar and Chakraborty 2016).

The concentration of OP in the tested urban sewage treatment plant synthetic effluent was maintained at the level of 0.5 mg L^{-1}, the temperature of the samples was kept at a constant level of 20°C and the volume of the treated samples varied from 50 to 250 mL. The concentration of OP which was added to the water matrix was relatively high to increase the measurement precision. In the prepared samples basic physicochemical parameters were determined, namely pH, turbidity, UV absorbance, and conductivity.

1.2. Gas chromatography analysis

The effect of contaminant reduction was evaluated using a gas chromatograph (GC) 7890B provided by Perlan Technologies (Warsaw, Poland). Gas chromatography analysis was preceded by Solid Phase Extraction (SPE) Method using Superclean^{TM} ENVI^{TM} – 18 tubes were applied with an Octadecylsilane (C_{18}) as a cartridge bed. In the conditioning and washing phase, 5 mL of Acetonitrile (ACN) and 5 mL of Methanol (MeOH), and 5 mL of deionized water were used, respectively. During elution, 1.5 mL of ACN and MeOH were employed. The negative pressure during the SPE process was set to 5–10 kPa, while the flow rate was 1 mL/min. During GC analysis, the temperature of the ion trap was 150°C, the ion source was 230°C, and the oven temperature was 80 to 300°C. The flow rate of Helium, which was used as a carrier gas was kept at 1.1 mL min^{-1}. Each sample were measured two times and the degradation rate of OP was calculated based on the average peak areas obtained in GC analysis which were compared to the data collected during calibration.

1.3. Biological assay

Samples after mentioned AOPs were subjected to toxicological analysis using Lemna sp. Growth Inhibition Test. According to OECD Guideline 221 (OECD 2006), toxicity was assessed based on plants morphological changes after 7 days of exposure to 6000 lux light at the 25°C temperature. After this period, *Lemna minor* frond number could change as a result of contact with post-treated samples. In the study, toxicity *E* was calculated as a percentage of inhibition of the *Lemna minor* growth following equation 1:

$$E = \frac{L_c - L_t}{L_c} \cdot 100$$

where:
E – toxicity, %,
L_c – number of fronds in the control sample,
L_t – number of fronds in the tested sample.

Toxicity measurement were performed two times – at 5 and 15 min of post – treated sample exposure and in the study the average values are presented. Obtained results allowed to classify the toxicity values to particular toxicity classes according to Dudziak and Werle (Dudziak and Werle 2013).
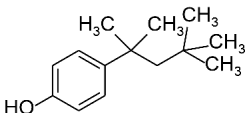
2. Results and discussion

2.1. Effect of ultrasound intensity and sonication time on OP removal

Before the samples sonication, basic physicochemical parameters of the solution containing 0.5 mg L^{-1} were measured. The properties of OP and water solution with added contaminant are listed in Table 1.

In the study, relatively high intensities from 10 to 75 W cm^{-2} were used which corresponds to 20–100% of maximum device amplitude. To evaluate the influence of this parameter on OP removal efficiency by ultrasound, 0.5 mg L^{-1} concentration of the contaminant was used, and the samples were sonicated for 1 min. As expected, It was noted that ultrasound intensity is proportional to the degradation rate of solution. As illustrated in figure 1. at the intensity of 10 W cm^{-2} removal of OP was the lowest and it was 1%. Increasing the intensity to 23, 41, and 57 W cm^{-2} resulted in a degradation rate equal to 3 20, and 29%, respectively. Maximum degradation of OP (38%) was obtained at 75 W cm^{-2}.

Table 1.

Selected physicochemical properties of OP, and tested samples before treatment

OP properties	
Compound name	4-tert-octylphenol
CAS no.	140-66-9
Molecular formula	$C_{14}H_{22}O$
Chemical structure	
Molecular weight, g mol^{-1}	206.32
Water solubility, g L^{-1}	0.01
Vapour pressure, mmHg	0.0005
Melting point, °C	79–82
Boiling point at 4 mmHg, °C	150
Properties of tested sample	
pH	7.0
Turbidity, NTU	0.8
Color, mg Pt L^{-1}	9
UV absorbance	0.02
Conductivity, µS cm^{-1}	688

Obtained relation between degradation rate and intensity is common in the literature data (Al-Juboori et.al 2015; Copik et al. 2021; Lim et al. 2014). It is connected with the increase of bubble collapsing events and more hydroxyl radicals generation. Moreover, at a higher amplitude, bubble collapse is more violent due to changes in bubble collapse time, pressure in the bubble, and the transient temperature (Ahmed-chekkat et al. 2021; Thompson and Doraiswamy 1999). Results indicated also, that sonication time was proportional to the OP removal efficiency in treated samples (Fig. 1). After 45 min of the treatment, the degradation rate of OP was 88% while after 15 and 30 min it was respectively 45 and 68%. The effectiveness of the process was proved by the decrease in conductivity of the treated samples (from 688 to 630 µS cm^{-1} at the sonicated time of 45 min.). Moreover, the pH value increased from 7.0 to 7.6 which indicates the improvement of water matrix quality. However, it was noted that the treated time was proportional to the turbidity and color values which may be related to some intermediates generation. Toxicity analysis showed that after 1 min of sonication, solution toxicity decreased from 60% (toxic) to 40% (low-toxic). After 45 min the post-treated solution was non-toxic (the toxicity effect decreased to 20%).

2.2. Effect of sample volume and H_2O_2 dosage on OP removal

It is well known fact, that a decrease in the operating volume during sonication is attributed to the increase of ultrasound power density, thus degradation of contaminants could be faster. Moreover, decreased volume is related to the occurrence of areas where the cavitation activity is low (dead zones). The presence of the dead zones could be increased during usage of horn-type ultrasound equipment, due to the non-uniform distribution of the ultrasound field which is located mainly close to the probe (Desai et al. 2008). It was proved in the literature, that power density could be the most significant parameter to control harmful substances removal efficiency (Zhang et al. 2011).

To evaluate the volume of the treated solution influence on OP degradation, the sonicated sample volume was set to 50, 100, 150, and 250 mL. The volume used in the study corresponds to 1.52, 0.76, 0.51, and 0.30 W mL^{-1} power densities. As expected, it can be seen from the Figure 3, that also in this study, the OP removal from the solution was inversely proportional to the volume of the sample. After 1 min ultrasonication of 50 mL sample degradation rate was equal to 50% while the sonication of 250 mL sample resulted in 16% OP removal. Furthermore, toxicity analysis revealed that the toxic effect in post-treated samples decreased from 60% (toxic) to 40% (low-toxic).

In the last stage of the treatment, the effect of H_2O_2 addition was examined, both as a single process and combined with 1 min ultrasound treatment (H_2O_2 + US) (Fig. 4). The dosage of the oxidant varied from 3 to 12 mg L^{-1}. The study revealed that as the H_2O_2 concentration increases during ultrasonication, the degradation rate of OP also increased. Moreover, the research provided further evidence that ultrasonication could enhance the treatment efficiency of other AOPs.
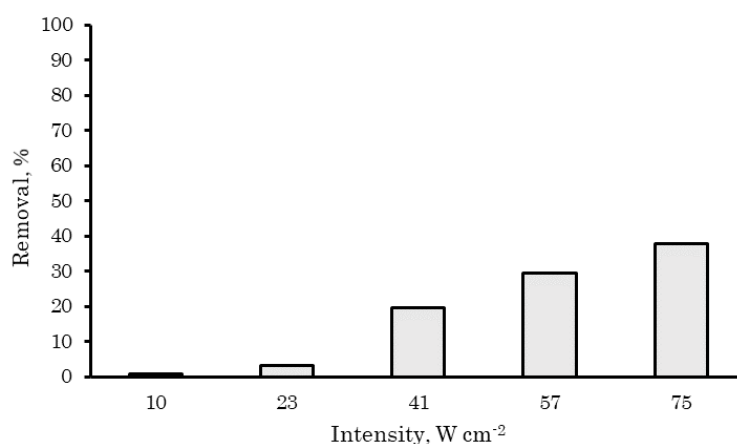

Figure 1.
Effect of ultrasound intensity on OP removal from synthetic urban sewage treatment plant effluent
(time 1 min., volume of the sample 100 ml, pH = 7.0, initial OP concentration
0.5 mg L^{-1}, temperature 20°C 20 kHz frequency)

Degradation of OP by H_2O_2 addition varied from 53 to 58% while treatment by using H_2O_2 + US as a combined process resulted in the enhanced degradation rate of OP. At 12 mg L^{-1} degradation rate was 10% higher and it was equal to 68%. However, during using ultrasonication as a single process, the degradation rate of OP was lower (29%) than in treatment by H_2O_2 dosage alone. As commonly recognized, acoustic cavitation phenomena is related to hydroxyl radicals (OH'), and H_2O_2 formation during bubble implosion in so-called compression phase following the equations (Doosti et al. 2012; Nie et al. 2008).

$$H_2O \rightarrow H' + OH' \tag{1}$$

$$H' + OH' \rightarrow H_2O \tag{2}$$

$$H' + H' \rightarrow H_2 \tag{3}$$
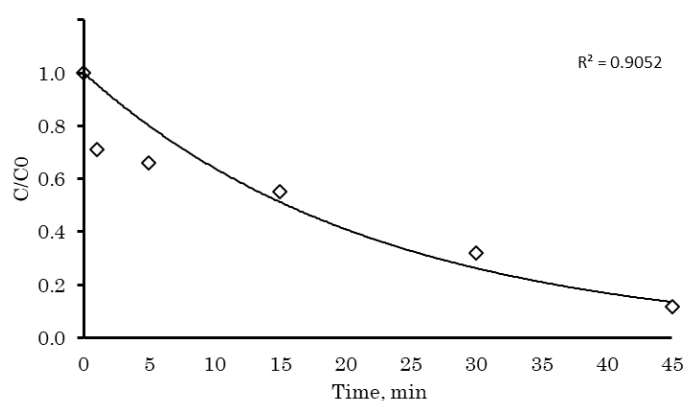
$$OH' + OH' \rightarrow H_2O_2 \tag{4}$$

Figure 2.
Effect of ultrasound sonication time on OP removal from synthetic urban sewage treatment plant effluent (volume of the treated sample 100 ml, pH = 7.0, 57 W cm^{-2} intensity, initial OP concentration 0.5 mg L^{-1}, temperature 20°C 20 kHz frequency)

The hydroxyl radicals (OH') are generated mainly in the bubble interior in which very high temperature and pressure conditions occur. As a result of the reaction between (OH'), H_2O_2 can be produced (mainly at the bubble-liquid interface), however formed H_2O_2 amount was not evaluated in this study. Due to the very high oxidation potential of these compounds, they can directly remove organic pollutants. The H_2O_2 addition to the treated samples could be treated as its secondary source, and it is considered in literature data as one of the most effective additives enhancing ultrasonication.
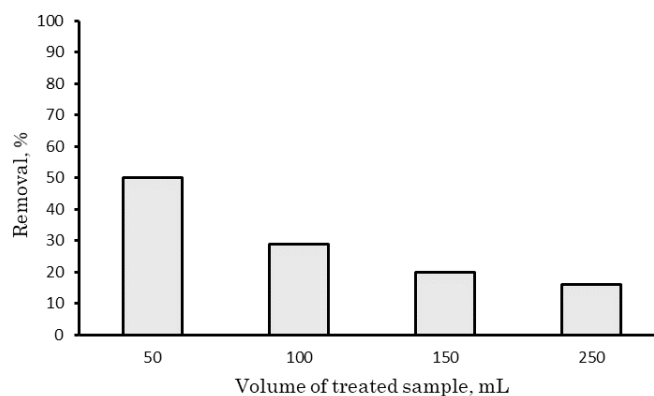
Figure 3.
Effect of treated sample volume on OP removal from synthetic urban sewage treatment plant effluent by using
ultrasonication (volume of the treated sample 100 ml, pH = 7.0, 57 W cm^{-2} intensity,
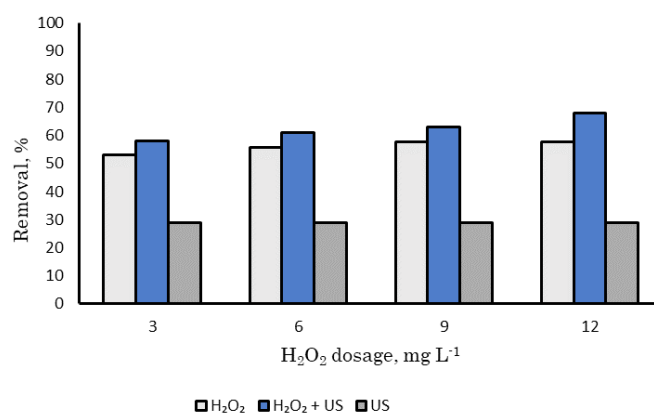*1 min sonication time, initial OP concentration 0.5 mg L^{-1}, temperature 20°C 20 kHz frequency)*

Figure 4.
Effect of H$_2$O$_2$ dosage on OP removal from synthetic urban sewage treatment plant effluent by using
ultrasonication (volume of the treated sample 100 ml, pH = 7.0, 57 W cm^{-2} intensity,
1 min sonication time, initial OP concentration 0.5 mg L^{-1}, temperature 20°C 20 kHz frequency)

Conclusions

To conclude, OP is one of the EDCs which could be very harmful to human health even at small doses. It can be released to the different matrices of the environment as a result of anthropogenic processes and urbanization. Importantly it could not be removed effectively from water by using classical treatment methods. The study revealed that ultrasonic treatment could be an effective method for OP removal from the urban sewage treatment plant synthetic effluent. The research emphasized that H$_2$O$_2$ addition

to the ultrasonicated solution increased the OP removal efficiency from the solution which was proved by toxicological analysis. The degradation rate of OP during ultrasonication was proportional to the ultrasound intensity, sonication time, and dosage of the oxidant. Although ultrasonication is considered a promising technology, further research is needed for its further development such as scaling it up and high energy requirements. Moreover, attention should be paid to intermediates identification which could be generated during the process, which may be harmful to human health.

REFERENCES

Acir I.H. and Guenther K. (2018) Endocrine-disrupting metabolites of alkylphenol ethoxylates – A critical review of analytical methods, environmental occurrences, toxicity, and regulation. Science of the Total Environment 635, 1530–1546, DOI: 10.1016/j.scitotenv.2018.04.079.

Ahmedchekkat F., Chiha M., Al Bsoul A. and Hailat M. (2021) Sonochemical degradation of 4-tert octylphenol in aqueous solutions: Ideal acoustic frequency, influencing parameters, and desert sand particles synergy. Desalination and Water Treatment 217, 307–319, DOI: 10.5004/dwt.2021.26892.

Al-Juboori R. A., Aravinthan V. and Yusaf T. (2015) Impact of pulsed ultrasound on bacteria reduction of natural waters. Ultrasonics Sonochemistry 27, 137–147, DOI: 10.1016/j.ultsonch.2015.05.007.

Bohdziewicz J., Dudziak M., Kamińska G. and Kudlek E. (2016) Chromatographic determination and toxicological potential evaluation of selected micropollutants in aquatic environment—analytical problems. Desalination and Water Treatment 57(3), 1361–1369, DOI: 10.1080/19443994.2015.1017325.

Chen M., Tang R., Fu G., Xu B., Zhu P., Qiao S. and Wang X. (2013) Association of exposure to phenols and idiopathic male infertility. Journal of Hazardous Materials 250–251, 115––121, DOI: 10.1016/j.jhazmat.2013.01.061.

Copik J., Kudlek E. and Dudziak M. (2021) Removal of PAHs from Road Drainage System by Ultrasonication. Environmental Sciences Proceedings 9(1), 4, DOI: 10.3390/environsciproc2021009004.

Desai V., Shenoy M.A. and Gogate P.R. (2008) Ultrasonic degradation of low-density polyethylene. Chemical Engineering and Processing: Process Intensification 47(9–10), 1451–1455, DOI: 10.1016/j.cep.2008.02.003.

Doosti M.R., Kargar R. and Sayadi M.H. (2012) Water treatment using ultrasonic assistance: A review. Ecology 2(2), 96–110.

Dudziak M., Kudlek E. and Burdzik-Niemiec E. (2018) Decomposition of micropollutants and changes in the toxicity of water matrices subjected to various oxidation processes. Desalination and Water Treatment 117, 181–187, DOI: 10.5004/dwt.2018.22233.

Dudziak M. and Werle S. (2013) Ocena toksyczności osadów ściekowych oraz produktów ubocznych powstających podczas ich zgazowania. Przemysł Chemiczny 92(7), 1350––1353.

Dular M., Griessler-Bulc T., Gutierrez-Aguirre I., Heath E., Kosjek T., Krivograd Klemenčič A. and Kompare B. (2016) Use of hydrodynamic cavitation in (waste)water treatment. Ultrasonics Sonochemistry, 29(October 2017), 577–588, DOI: 10.1016/j.ultsonch.2015.10.010.

Gągol M., Przyjazny A. and Boczkaj G. (2018) Wastewater treatment by means of advanced oxidation processes based on cavitation – A review. Chemical Engineering Journal 338, 599–627, DOI: 10.1016/j.cej.2018.01.049.

Gavrilescu M., Demnerová K., Aamand J., Agathos S. and Fava F. (2015) Emerging pollutants in the environment: Present and future challenges in biomonitoring, ecological risks and bioremediation. New Biotechnology 32(1), 147–156, DOI: 10.1016/j.nbt.2014.01.001.

Kudlek E. (2018) Decomposition of contaminants of emerging concern in advanced oxidation processes. Water (Switzerland) 10(7), DOI: 10.3390/w10070955.

Kudlek E., Dudziak M., Kamińska G. and Bohdziewicz J. (2017) Kinetics of the Photocatalytic Degradation of Selected Organic Micropollutants in the Water Enviroment. Inżynieria Ekologiczna 18(2), 75–82, DOI: 10.12912/23920629/68341.

Lim M., Son Y. and Khim J. (2014) The effects of hydrogen peroxide on the sonochemical degradation of phenol and bisphenol A. Ultrasonics Sonochemistry 21(6), 1976–1981, DOI: 10.1016/j.ultsonch.2014.03.021.

Lv S., Wu C., Lu D., Qi X., Xu H., Guo, J., … and Zhou Z. (2016). Birth outcome measures and prenatal exposure to 4-tert-octylphenol. Environmental Pollution 212, 65–70, DOI: 10.1016/j.envpol.2016.01.048.

Merouani S., Hamdaoui O., Rezgui Y. and Guemini M. (2015) Modeling of ultrasonic cavitation as an advanced technique for water treatment. Desalination and Water Treatment 56(6), 1465–1475, DOI: 10.1080/19443994.2014.950994.

Metcalfe C.D., Bayen S., Desrosiers M., Muñoz G., Sauvé S. and Yargeau V. (2022) Methods for the analysis of endocrine disrupting chemicals in selected environmental matrixes. Environmental Research 206(June 2021), DOI: 10.1016/j.envres.2021.112616.

Nie M., Wang Q. and Qiu G. (2008) Enhancement of ultrasonically initiated emulsion polymerization rate using aliphatic alcohols as hydroxyl radical scavengers. Ultrasonics Sonochemistry 15(3), 222–226, DOI: 10.1016/j.ultsonch.2007.03.010.

OECD (2006) Test No. 221: Lemna sp. Growth Inhibition Test. Guideline for Testing Chemicals 1–26. [Online] http://www.oecd-ilibrary.org/environment/test-no-221-lemna-sp-growth-inhabition-test_9789264016194-en (Accessed: 2022-05-25).

Pokhalekar P. and Chakraborty M. (2016) Degradation of bisphenol A and 4-tert-octylphenol: a comparison between ultrasonic and photocatalytic technique. Desalination and Water Treatment 57(22), 10370–10377, DOI: 10.1080/19443994.2015.1041053.

Thompson L.H. and Doraiswamy L. K. (1999) Sonochemistry: Science and engineering. Industrial and Engineering Chemistry Research 38(4), 1215–1249, DOI: 10.1021/ie9804172.

Tran D.N., Jung E.M., Yoo Y.M. and Jeung E.B. (2020) 4-tert-Octylphenol Exposure Disrupts Brain Development and Subsequent Motor, Cognition, Social, and Behavioral Functions. Oxidative Medicine and Cellular Longevity 2020, DOI: 10.1155/2020/8875604.

Vieira W.T., De Farias M.B., Spaolonzi M.P., Da Silva M.G.C. and Vieira M.G.A. (2021) Latest advanced oxidative processes applied for the removal of endocrine disruptors from aqueous media – A critical report. Journal of Environmental Chemical Engineering 9(4), DOI: 10.1016/j.jece.2021.105748.

Yasui K. (2018) Acoustic Cavitation and Bubble Dynamics. http://www.springer.com/series/15634 (Accessed: 2022-05-25).

Zhang K., Gao N., Deng Y., Lin T. F., Ma Y., Li L. and Sui M. (2011) Degradation of bisphenol-A using ultrasonic irradiation assisted by low-concentration hydrogen peroxide. Journal of Environmental Sciences 23(1), 31–36, DOI: 10.1016/S1001-0742(10)60397-X.

Apurva Goel

Independent Researcher, Pune, Maharashtra, India; e-mail: apurva.goel@gmail.com

Application of circular economy in E-waste management – a review with an Indian perspective

ABSTRACT: The current rate at which natural resources are being extracted to meet the demands of the growing population is not sustainable for future generations. The linear economy approach based on the take-make-dispose ideology is being replaced by the circular economy (CE) approach to manage the demand and create a balance between the available resources. The concept of circular economy is believed to be very relevant for E-products and E-waste as it strives to design out the waste by better products, practices, and business models.

This paper aims to study how CE can be applied in E-waste management with the implementation of various concepts like the 3Rs, reverse logistics, and urban mining. As the study is focused on India, the current E-waste management practices and legislation support have been discussed in this paper. The paper further explains the complexities prevalent in the E-waste management system in India due to the presence of a huge informal sector primarily responsible for the collection and disposal of E-waste. Finally, the paper present certain strategies that could be helpful to overcome the challenges in the successful implementation of the Circular economy in E-waste management in India.

KEYWORDS: circular economy, e-waste, urban mining, reverse logistics

Introduction

People all around the world are facing detrimental effects due to environmental issues like climate change, deforestation, air and water pollution, soil erosion and contamination and depletion of natural resources. These issues not only impact the environment but also restrict the sustainable development of social and economic growth. Over the last 50 years, the global population has increased at a tremendous rate from 3.7 billion in 1970 to over 7.8 billion people in 2020 (Gill and Verma 2021). To satisfy the needs of the growing population and the upliftment of standard of living, the demand for natural resources is increasing. The linear economy model fol-

lowed by most industries has tripled the rate of extraction and processing of natural resources leading to the scarcity and the threat of total exhaustion of these resources.

Organizations have realized that the linear economy approach, based on the concept of 'Take-Make and Dispose', is not sustainable and creates an imbalance in the supply chain of the natural resources. The companies following the linear economic model extract the factory inputs from the environment, use energy and human resources to manufacture a product and sell it to a consumer who then disposes it into the environment after a single use (Goyal et al. 2018). This model is not sustainable in the long term and will create a major deficit of natural resources and also overlook the great value which is embedded in the used material (Ravindra and Mor 2019).

Governing bodies around the world are realizing the growing stress that the planet earth is facing, and hence they are focusing on developing various models and approaches that could lead to the sustainable development of society. One such model that has become popular is the Circular Economy (CE) (Tiwari et al. 2019). Figure 1 shows the linear economy and the circular economy models.

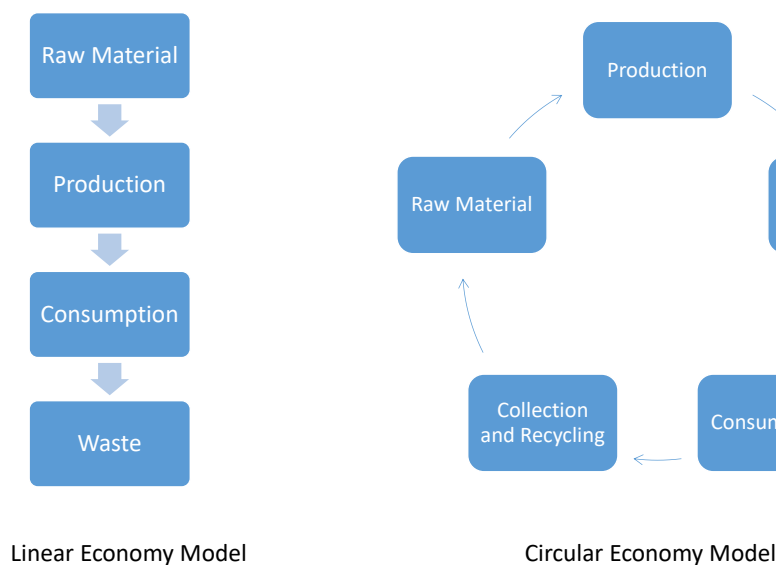Linear Economy Model   Circular Economy Model

Figure 1.
The Linear economy model vs the circular economy model

The electronic and electrical industry is the world's largest growing production commerce. As the production of electric and electronic equipment (EEE) increases, the waste generated during the manufacturing and the usage by the consumers also increases. Electronic waste (E-waste) comprises wastes generated from used electronic devices and household appliances like discarded computers, office electronic equipment, entertainment device, electronics, mobile phones, television sets, and re-

frigerators, which are not fit for their original intended use and are destined for recovery, recycling or disposal (Thagela 2019; Shagun and Arora 2013; Tiwari et al. 2019).

Increasing at a rate of 3–4% every year, E-waste is one of the fastest-growing waste categories on earth. According to the Global E-waste Monitor 2020 report, a record 53.6 million metric tons (Mt) of electronic waste were generated worldwide in 2019 (Forti et al. 2020). India generated 3.2 million tons of E-waste in 2019, ranking third after China (10.1 million tons) and the United States (6.9 million tons) (Mehta 2020; Herat 2021).

E-waste is a non-homogenous waste consisting of a variety of components across different categories and a range of constituents being labeled as hazardous and non-hazardous. It contains many precious metals like iron, copper, gold, silver, aluminum, manganese, chromium, and zinc along with various rare earth elements (Ahirwar and Tripathi 2021) that can be recovered by recycling E-waste. The rate at which these abiotic resources are extracted is significantly higher than the rate of their formation in nature. In India, despite the formulation of various policies and setup of infrastructure for the E-waste management, the actual figures for formal collection and recycling (only 10–15% of the total generation) are not satisfactory which can be attributed to various reasons like gaps in the policy developed, public awareness, lack of research in the cost-efficient recovery methods, etc. (Garg and Adhana 2019). The CE model approach promotes recycling the waste, identifying and quantifying precious and perilous substances and improving the recuperation of minerals to build up a sustainable solution for E-waste management in a developing country like India (Barapatre and Rastogi 2021).

This paper is divided into the following sections- Introduction to circular economy, situation analysis of the E-waste generation in India, the various impact it has on human health, detailed discussions on the legislation initiatives towards application of the CE in the E-waste management and the challenges faced. Finally, the paper also discusses some strategic approaches which can help to improve and fill the gaps in the CE approaches towards E-waste management in India.

1. Materials and methods

The methodology adopted in the paper is conceptual in nature. Extensive research of various research papers, books, articles, reports from the publication databases and the internet was conducted on topics related to the circular economy, E-waste, urban mining, reverse logistics etc. After an extensive review of the literature, the problems faced by developing countries like India with regards to E-waste management were identified and certain strategies were formulated to fill the gaps and promote the success of CE in E-waste management.

2. Circular Economy

There are various definitions of the CE model available in the literature. It has a close association with various concepts like the green economy, industrial ecology and industrial symbiosis (Cecchin et al. 2020). According to the World Economic Forum & Ellen MacArthur Foundation (2016), a circular economy is a systemic approach to economic development designed to benefit businesses, society, and the environment. It is a concept that eventually reduces the EEE consumption rate while circulating the waste material within the system for the longest possible time and minimizing and eliminating their re-generation via smarter product designing and business modeling (Parajuly 2017). CE is accompanied by three principles called the circular economy principles. The first principle is to preserve and enhance natural capital stock through restoration and regeneration. The focus of the second principle is to achieve resource efficiency in both biological and technical cycles. The third principle promotes the elimination of negative externalities in the environment (Camacho-Otero et al. 2018).

Figure 2 shows the chronological analysis of the main concepts of the CE and sustainability. All the concepts emerged from the Carrying Capacity term coined by Odum (1953). The new concepts like the Extended Producer Responsibility (EPR) and Integrated Product Policy (IPP) are based on the thought of how to effectively use the available resources to meet the current and future demands. The latest of the
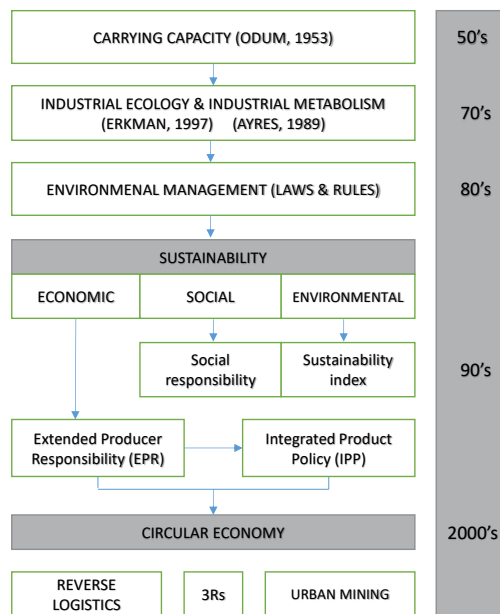

Figure 2.
Chronological analysis of sustainability and the
circular economy (Xavier et al. 2019)

concepts, CE also promotes sustainable development and effective use of the available resources. The 3Rs, Reverse logistics and Urban mining are the most important methodologies that support the success of the CE (Xavier et al. 2019).

2.1. Reverse logistics

Reverse logistics also referred to as "aftermarket supply chain" in the circular economy is the process of collecting and aggregating products, components, or materials at the end-of-life from the point of consumption and managing the reverse flow to their origins where they can be recycled, reused, or disposed of (Fig. 3) (De Mattos et al. 2018). Take-back programs, warranties and product defect returns, all require reverse logistics to get the product from the consumer back to the manufacturer (Jayaraman and Luo 2007).
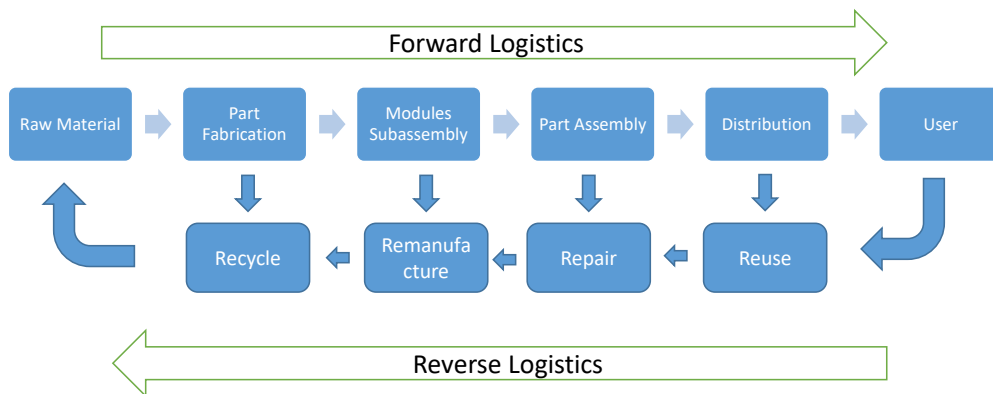

Figure 3.
The conceptual framework of the concept of reverse logistics

2.2. 3R (Reduce, Reuse and Recycle)

The core principle of the CE is the 3R concept of reduce, reuse and recycle used in the efficient management of the waste and improving the resource efficiency that promotes the return of the secondary resources into the product lifecycle, and reduces the waste emissions (Awan et al. 2020).

Reducing the usage of resources and eliminating the waste/pollution during the manufacturing, distribution and consumption of products.

Reusing the scrap material diligently in the workplace itself. Reusing the discarded products after the repair, refurbishment as the product itself, or using parts from it as spare parts for other products.

Recycling the waste into the raw material for making a new product.

The 3R-based CE approach promotes sustainable economic growth and decouples the relation between economic development and increased use of biotic and abiotic resources.

2.3. Urban mining of E-waste

Urban mining is the process of recovering the rare and precious metals from the discarded E-waste of a society (Arya and Kumar 2020). The scarcity of rare and precious metal resources and the limitation of the earth to reproduce them have led to the emergence of urban mining to recover the critical materials from the E-waste.

For the success of the urban mining process, the manufacturers must produce recyclable products (Xavier et al. 2019). Also, the E-waste collection system should be in place along with the advanced technology-based recycling centers where the precious reusable materials can be recovered from the waste.

Figure 4.
Model showing the integrated urban mining at the core of a CE (Tesfaye et al. 2017)

Figure 4 shows integrated urban mining at the core of a circular economy model that closes the metals loop, recovers energy, and manages environmental issues related to hazardous materials from the E-waste (Tesfaye et al. 2017). As shown in

the figure, collection, preprocessing and recovery are the three basic stages in urban mining. The first stage of collection is highly dependent on the collection systems that are in place and also on the consumer awareness as they have to return the End of Life (EOL) EEEs (including the smallest of them) to the collection centers for recycling. Organizations need to run campaigns to spread awareness among the people about the E-waste and why it needs to be sent (particularly the mobile phones and tablets as they are bought/upgraded quite often) to a recycling facility instead of stockpiling them at home. Incentives like free pickup or free coupons should be complemented to the people if they hand over their EOL EEEs to the collection centers.

The second stage, i.e. preprocessing includes manual dismantling of the equipment and segregating based on the type of materials present in it. It is then followed by a mechanical process like shredding where the E-waste is broken down into smaller pieces (Khaliq et al. 2014). The pieces are then segregated as metallic and non-metallic using different techniques like eddy current, screening, magnets etc. The separated pieces are then compacted and pelletized to provide them as a feed to the smelting units to recover the valuable resources from them (Kaya 2018).

The last stage of recovery is highly complex and requires highly advanced technologies to process the waste and recover the different resources from it. Currently, hydro- and pyro- and electro-metallurgical techniques are used by various industries for metal recovery (Cui and Zhang 2008).

3. E-waste generation in India

Indian electronic industry has developed as the fastest growing industry in terms of production, consumption and export of electronics. With the advancement in the IT sector, personal computers have become tools to utilize the technology (Borthakur and Govind 2018). A study by KPMG and ASSOCHAM identified that computer equipment accounts for almost 70 percent of E-waste in India, followed by telecom/phones (12 percent), electrical equipment (8 percent) and medical equipment (7 percent) (Garg and Adhana 2019). Therefore a large part of E-waste comprises computer waste which contains large amounts of hazardous substances like lead, cadmium, mercury, beryllium, brominated flame retardants (BFR), polyvinyl chloride and phosphor compounds (Thagela 2019).

The magnitude in which the E-waste generation is increasing in India is way ahead the pace at which it is collected and recycled. The policies in India have driven the setup of formal recycling facilities resulting in the establishment of 407 authorized recyclers having a capacity of treating approximately 1.18 million Mt annually. But in India, there is an existence of a huge informal sector that handles E-waste and the formal recycling facilities remain underutilized.

Informal recycling is a big sector in India, where thousands of people make their living from the recovery of valuable metals by breaking and burning the equipment /PCB's. Small independent workshops carry on this business in India, where there is no control on emissions and discharge of pollutants. The small-scale local scrap dealers collect the E-waste and then break, shred and burn it to extract the precious metals – elements for reselling (Vats and Singh 2014).

4. Impact of E-waste on human health and environment

E-waste comprises a diverse combination of poisonous elements which can have irreversible impacts on the environment and human health. The treatment/recovery of the E-waste becomes very complex due to the presence of hazardous materials like lead, mercury, cadmium, nickel, hexavalent chromium and brominated flame retardants (BRFs) (Olubanjo et al. 2015).

According to the Global E-waste Monitor 2019 (Forti et al. 2020) out of the total E-waste generated worldwide only 17.4% are formally collected and recycled while the remaining 82.6% end up in the dumps or the landfills or traded in illegal markets. The informal recycling methods like open burning, incineration, acid stripping of metals and acid baths generate many byproducts like dioxins, furans and heavy metals into the environment. The physiological and health impacts of these on humans are many, but children and women are more vulnerable to its effects (Awasthi et al. 2016).

The informal recycling units of E-waste are primarily engaged in the extraction of precious metals like gold, silver, copper, and lead. There is a standard process that begins with the dismantling of components, wet chemical processing and incineration (Ashiq et al. 2019). It involves unscientific and crude methods for resource recovery and is carried out by unskilled people. This entire mechanism is hazardous and leads to direct exposure of manual labor to harmful chemicals affecting their health and leading to chronic illness. The informal recycling units incinerate the E-waste material without proper exhaust systems which has dangerous impacts on the workers' health. Additionally, during the process, the most dangerous fumes and chemicals are released into the environment. Also, the acids released during the extraction process are disposed into the vicinity without adequate precautions polluting the air and water. Subsequently, rainwater washes off toxic substances to the low-lying areas and agricultural lands causing bioaccumulation in crops (Sethurajan et al. 2019). The polluted groundwater has the impact of polluting underwater or aquatic life. Therefore recycling of E-waste not only causes occupational hazards but also environmental damage which reaches from near to far off areas (Boralkar 2006).

5. Legislation initiatives in India towards E-waste management

Before 2011, E-waste was covered under the Hazardous Waste Management (HWM) Rules only. In 2011 the E-waste (Management and Handling) Rules were enacted under the Environmental Protection Act 1986 and became active from 1st May 2012 (Ghosh et al. 2016). It was for the first time, the concept of EPR was introduced, making the manufacturers liable for the entire product life cycle of the product till it is safely disposed of. The rules enabled the recovery and reuse of the useful materials from the E-waste, safe disposal of hazardous substances and enforced the safe handling, transporting, storing and recycling of the E-waste (Ganguly 2016).

In 2016, the E-waste (Management) Rules were enacted in supersession of the 2011 Rules and came into effect on 1st October 2016. With these rules, the Producer Responsibility Organization (PRO) was introduced as an additional channel for the implementation of EPR by Producers (Awasthi et al. 2018). Hence, the manufacturers, dealers, refurbishers, and PROs were all covered under these rules. Also, the 2016 rules expanded their applicability to cover consumables, components and the spare parts of EEE in addition to the equipment already covered.

In 2018, the E-waste Management Rules of 2016 were amended by governing bodies to further improve and facilitate effective E-waste management in India in an environment-friendly way. These amendments were made to further formalize the E-waste recycling sector by channelizing the E-waste generated in the country to the authorized dismantlers and recyclers (Sharma and Hussain 2018).

As per the amended rules, the collection targets under the provision of EPR have been revised with effect from 1st October 2017. According to the revised targets, in 2017–2018 the collection target was 10% of the total waste generated with a 10% increase every year until the year 2023. After 2023, the collection target has been fixed at 70% of the total E-waste generated. This would ensure more effective management of the E-waste and will be monitored by the Central Pollution Control Board (CPCB) of India (Sharma and Hussain 2018).

6. Challenges faced in India during E-waste management

The key to efficient waste management is to ensure proper segregation of waste at the source and to ensure that the waste goes through different streams of recycling and resource recovery (Lahiry 2017). However, waste management operates as a fragmented industry in India with a lack of collection, segregation and monitoring systems. Even though 407 recycling facilities (as of 2019–2020) with a capacity of 11.10 MT are established, most of them are not even running at their 50% capacity (MEITY 2021). The majority of the E-waste gets recycled in the informal sector using

unscientific treatment methods. This in turn leads to hazards like environmental degradation, water pollution, soil pollution, and air pollution. Some of the major challenges faced in India are given below.

6.1. Waste leakage

Lack of monitoring systems results in the leakage of collected E-waste from the authorized dismantlers and recyclers to the informal sector. Due to this, a significant quantity of E-waste ends up being recycled by the informal sector (MEITY 2021). Another major source of the leakage is the auction held by the bulk consumers (Govt. departments, ministry companies, MNCs, etc.), wherein, due to the lack of monitoring of the bidding agencies, the collected waste ends up at the informal recyclers.

6.2. Fragmented product lifecycle management

The policies in India concerning E-waste management are enacted to cover the entire product life cycle of a product, but the approach of the producers is mainly restricted to just meeting the collection and recycling targets. The manufacturing industries and the EOL management systems like the PROs exist are two independent units. The outsourcing of the producer's responsibility to manage the EOL of the products to the third, limits this process to just documenting the numbers to meet the targets. The primary intention of the policies to bring a change in the product design, reuse of resources, and improve the overall resource efficiency is neglected.

6.3. Lack of awareness amongst people

The majority of the population in India does not realize the importance of the proper disposal of E-waste. They are not aware of why they should dispose of their E-waste through a proper channel (Turaga et al. 2019). Though during the last 3 to 4 years, with a lot of campaigns being run and e-disposal centers being opened, some percentage of the population has become aware about the importance of routing the E-waste to an authorized channel. However, the system and processes dealing with E-waste in India still need a lot of work to be done.

6.4. Lack of monitoring systems

There is a huge gap in E-waste monitoring systems in India. There should be a digital platform in place that could monitor the E-waste collection right from the

---

time it is collected, till it is completely recycled, including its transfer from one party to another through the value chain (Balaji 2020).

6.5. High investment cost in setting up recycling facilities

The advanced technologies used for the recycling of E-waste requires a very high investment cost. Most organizations find the investment into such technologies risky considering the fact that out of the total E-waste generated in India only 10–15% gets collected through the formal channels.

7. CE and E-waste in India – way forward

E-waste is considered one of the rich sources of secondary raw materials and can contribute towards resource security and environmental sustainability (Wang 2019; MEITY 2021). From the above sections, it can be concluded that though the legislation in India has enforced certain rules to improve resource efficiency and reduce E-waste, however, there are many challenges that the organizations have to face which have resulted in only 10% collection and recycling of the total E-waste generated through authorized channels (Turaga et al. 2019). For a successful CE model, the most important step is to collect and monitor the E-waste generated and channelize it to proper recycling centers, where it can be mined for useable materials, or recycled into new products or disposed of in an environmentally friendly manner. Taking this into consideration, the following prepositions are proposed to streamline the E-waste handling processes and promote the success of CE in E-waste management in India.

7.1. Integration of informal sector with the formal one

To eliminate the health and environment hazards due to the informal recovery methods, it is necessary to integrate the informal sector with the formal one. There is an urgent requirement to develop a connection between scrap vendors involved in door-to-door collection of E-waste and the formal collection centers to ensure that total E-waste generated get channelized through a formal sector. Various small-scale initiatives by many non-profit organizations are established in different cities of India to bridge this gap. Some of these initiatives are given below:

1. **Sanshodhan**: An E-waste Exchange Program. It is a global company headquartered in Hyderabad, India, and has partners in Europe, the US and Australia. This Digital-PRO system allows the users to dispose of their E-waste through

the digital E-waste Exchange (EWX) platform which is being incubated at T-Hub, India's leading incubator by the Telangana government (TheCityFix Labs India 2019).

2. **Saahas Zero Waste**: It is a non-profit organization founded by Wilma Rodriguez based in Bangalore that works towards scientific and sustainable disposal of electronic waste. It is authorized as a Producer Responsibility Organization (PRO) to assist producers and manufacturers in fulfilling their Extended Producer Responsibility (EPR). It works on the principle of the Reverse logistics chain for E-waste from the end-consumer to formal E-waste recyclers (Saahas Zero Waste, n.d.).

3. **Kabadiwalla Connect**: It is a Chennai-based firm that uses its technology platform to leverage the already existing informal infrastructure toward a more efficient waste management system and apply the circular economy approach (Hande 2019).

7.2. Awareness among the customers

Customer is the key in product life cycle of any product that goes through the three stages, i.e., manufacture, use and EOL. Customer's decision decides the effectiveness of the circular economy in E-waste management, whether the product will be going through repair or reuse cycle or will end up for recycling at the EOL. The customer's decision depends on existing infrastructure and awareness that leads them to repair or reuse the products instead of simply discarding them. Hence is highly important to provide information and increase publicity on the current recycling practices to increase public awareness. Customer awareness about E-waste management will drive their decisions to explore the different options available to them like repair, reuse, exchange, sending to the E-waste collection centers, etc., than discarding them with the regular waste or stockpiling. These decisions impact how the EOL products are handled, which in turn affect the collection, resource recovery, and the success of the implementation of the circular economy (Parajuly et al. 2020). For small EOL devices like mobile phones, provisions should be made available to the customers at public places like the shopping mall, community centers etc., to hand over the old devices easily in exchange for some incentives.

Financial assistance should be given to the NGOs and the associated environmentalists for conducting awareness campaigns. The most effective role can be played by dealers of EEE. They should be given the formal responsibility of informing consumers about the right methods of disposal of EOL EEE at the time of selling the products.

7.3. Increasing the life span of the products

Circular Economy also encourages the reduction of waste generation. The companies, in order to fulfill their monetary gains, are manufacturing the products with a shorter life span which has encouraged the users to use and throw attitude. For the success of the circular economy model, companies should not be allowed to manufacture products with EOL for less than 10 years. An increase in the life span of EEE would decrease the quantity of E-waste thereby changing the use and throw attitude of consumers and producers.

7.4. EOL tracking by the producers

Most manufacturing industries rely on their digital systems to track the warranty and extended warranty of the EEE. Once the warranty and extended warranty are over, no tracking is done further on the customers and product. The manufacturers can use the current digital systems and extend them to track the EEE till they reach EOL. Once the EEE is about to reach its EOL, they can contact the customer and make them aware of the nearest disposal centers or provide them a free pickup facility so that the product reaches the correct channel and is safely processed further.

7.5. Incentives on the usage of recycled material

Certain norms/incentives should be set by the government, to encourage the industries to use recycled materials in their products while maintaining the quality of the products. This will not only ensure resource security but also generate a demand for recycled material in the market.

Along with this, to encourage the customer to buy products with recycled materials or easily recyclable ones, incentives in form of some percentage of Goods and Service Tax (GST) relaxation can be given to them. Once the market demand for secondary recycled material generates in the market, the leakage of the E-waste at various channels will reduce and the existing recycling centers will be used at full capacity.

Conclusions

E-waste is one of the fastest-growing waste which contains a significant amount of valuable and hazardous substances. The rate at which the minerals used in the e-products is extracted is way ahead the rate at which they are formed in nature. If

current practices are continued, in no time a deficit of these minerals will be formed. The circular economy is a model which aims at reducing, recycling and mining valuable substances from waste.

India is one of the IT hubs in the world and ranks 3rd in the world in the E-waste generation. Realizing the health and environmental hazards caused by the improper disposal of E-waste, the legislation in India has enacted various rules and policies to promote the recycling and mining of E-waste. However, due to the dominance of a huge informal sector handling the E-waste, and the lack of monitoring of the collection and transportation systems, the actual collection and recycling rate by the formal sector is just around 10%.

To successfully apply the CE principles in E-waste management, some strategies can be applied like integration of the informal sector with the formal one, running customer awareness programs to change the customer behavior towards E-waste, mandating the manufacturers to increase the life span of the products to at least 10 years, applying the digital technologies to track the EOL products and set up a reverse logistics system to collect them back.

A change in the customer behavior and setting up better collection systems with centralized monitoring will ensure the safe and environmentally safe disposal of the E-waste along with the recovery and utilization of the secondary raw materials. India also needs to invest in advanced recycling technologies to mine the intricate valuable material from the E-waste leading towards circular growth in electronic production and sustainable access to the resources.

REFERENCES

Ahirwar R. and Tripathi A.K. (2021) E-waste management: A review of recycling process, environmental and occupational health hazards, and potential solutions. Environmental Nanotechnology, Monitoring & Management 15, DOI: 10.1016/j.enmm.2020.100409.

Arya S. and Kumar S. (2020) Bioleaching: urban mining option to curb the menace of E-waste challenge. Bioengineered 11(1), 640–660, DOI: 10.1080/21655979.2020.1775988.

Ashiq A., Kulkarni J. and Vithanage M. (2019) Hydrometallurgical recovery of metals from E-waste. Electronic waste management and treatment technology, 225–246, DOI: 10.1016/B978-0-12-816190-6.00010-8.

Awan U., Kanwal N.and Bhutta M.K.S. (2020) A literature analysis of definitions for a circular economy. Logistics Operations and Management for Recycling and Reuse, 19–34, DOI: 10.1007/978-3-642-33857-1_2.

Awasthi A.K., Wang M., Wang Z., Awasthi M.K. and Li J. (2018) E-waste management in India: A mini-review. Waste Management & Research 36(5), 408–414, DOI: 10.1177/0734242X18767038.

Awasthi A.K., Zeng X. and Li J. (2016) Relationship between E-waste recycling and human health risk in India: a critical review. Environmental Science and Pollution Research 23(18), 18945–18946, DOI: 10.1007/s11356-016-7304-y.

Balaji R. (2020) India lacks localised solutions to manage E-waste: Pranshu Singhal of Karo Sambhav. [Online] https://yourstory.com/socialstory/2020/03/india-electronic-waste -management-recycling-karo-sambhav/amp (Accessed: 2022-04-22).

Barapatre S. and Rastogi M. (2021) E-waste Management: A Transition Towards a Circular Economy. [In:] Baskar C. et al. (eds.), Handbook of Solid Waste Management, Springer.

Borthakur A. and Govind M. (2018) February. Management of the challenges of electronic waste in India: an analysis. [In:] Proceedings of the Institution of Civil Engineers-Waste and Resource Management 171(1), 14–20, DOI: 10.1680/jwarm.17.00035.

Camacho-Otero J., Boks C. and Pettersen I. N. (2018) Consumption in the circular economy: A literature review. Sustainability 10(8), DOI: 10.3390/su10082758.

Cecchin A., Salomone R., Deutz P., Raggi A. and Cutaia L. (2020) Relating industrial symbiosis and circular economy to the sustainable development debate. [In:] Industrial symbiosis for the circular economy, 1–25), DOI: 10.1007/978-3-030-36660-5_1.

Cui J., Zhang L. (2008) Metallurgical recovery of metals from electronic waste: A review. Journal of hazardous materials 158(2-3), 228–256, DOI: 10.1016/j.jhazmat.2008.02.001.

De Mattos C.A. and De Albuquerque T.L.M. (2018) Enabling factors and strategies for the transition toward a circular economy (CE). Sustainability 10(12), DOI: 10.3390/su10124628.

Ellen MacArthur Foundation (2016) Circular Economy in India: Rethinking growth for long-term prosperity. Ellen MacArthur Foundation. [Online] https://ellenmacarthurfoundation.org/circular-economy-in-india (Accessed: 2022-06-21).

Forti V., Balde C.P., Kuehr R. and Bel G. (2020) The Global E-waste Monitor 2020: Quantities, flows and the circular economy potential. United Nations University/United Nations Institute for Training and Research, International Telecommunication Union, and International Solid Waste Association, Bonn, Geneva and Rotterdam.

Ganguly R. (2016) E-waste management in India-An overview. International Journal of Earth Sciences and Engineering 9(2), 574–588.

Garg N. and Adhana D. (2019) E-waste management in India: a study of current scenario. International Journal of Management, Technology and Engineering 9(1), 2791–2803.

Ghosh S.K., Debnath B., Baidya R., De D., Li J., Ghosh S.K., Zheng L., Awasthi A.K., Liubarskaia M.A., Ogola J.S. and Tavares A.N. (2016) Waste electrical and electronic equipment management and Basel Convention compliance in Brazil, Russia, India, China and South Africa (BRICS) nations. Waste Management & Research 34(8), 693–707, DOI: 10.1177/0734242X16652956.

Gill K. and Verma I. (2021) Circular economy: A review of global practices and initiatives with special reference to India. FOCUS: Journal of International Business 8(1), 187–205, DOI: 10.17492/jpi.focus.v8i1.

Goyal S., Esposito M. and Kapoor A. (2018) Circular economy business models in developing economies: lessons from India on reduce, recycle, and reuse paradigms. Thunderbird International Business Review 60(5), 729–740, DOI: 10.1002/tie.21883.

Hande S. (2019) The informal waste sector: a solution to the recycling problem in developing countries. Field Actions Science Reports. The Journal of Field Actions (Special Issue 19), 28–35. [Online] http://journals.openedition.org/factsreports/5143 (Accessed: 2022-05-12).

Herat S. (2021) E-waste management in Asia Pacific region: review of issues, challenges and solutions. Nature Environment and Pollution Technology 20(1), 45–53, DOI: 10.46488/NEPT.2021.V20I01.005.

Jayaraman V. and Luo Y. (2007) Creating competitive advantages through new value creation: a reverse logistics perspective. Academy of Management Perspectives 21(2), 56–73, DOI: 10.5465/amp.2007.25356512.

Kaya M. (2018) Current WEEE recycling solutions. [In:] Waste electrical and electronic equipment recycling. Woodhead Publishing, 33–93, DOI: 10.1016/b978-0-08-102057-9.00003-2.

Khaliq A., Rhamdhani M.A., Brooks G. and Masood S. (2014) Metal extraction processes for electronic waste and existing industrial routes: a review and Australian perspective. Resources 3(1), 152–179, DOI: 10.3390/resources3010152.

Kush S.A. and Arora A. (2013) Proposed solution of E-waste management. International Journal of Future Computer and Communication 2(5), 490–493, DOI: 10.7763/IJFCC.2013.V2.212.

Lahiry S. (2017) India's Challenges in Waste Management. [Online] https://www.downtoearth.org.in/blog/waste/india-s-challenges-in-waste-management-56753 (Accessed: 2022-04-06).

Mehta, Sejal (2020) The why and how of disposing electronic waste. [Online] https://india.mongabay.com/2020/08/explainer-the-why-and-how-of-disposing-electronic-waste/ (Accessed: 2021-11-15).

MEITY (2021) Circular Economy in Electronics and Electrical Sector. Ministry of Electronics and Information TechnologyGovernment of India, New Delhi. [Online] https://www.meity.gov.in/writereaddata/files/Circular_Economy_EEE-MeitY-May2021-ver7.pdf (Accessed: 2021-11-15).

Odum E.P. and Barrett G.W. (1971) Fundamentals of ecology (Vol. 3, p. 5). Philadelphia: Saunders.

Olubanjo K., Osibanjo O. and Chidi N. (2015) Evaluation of Pb and Cu contents of selectedcomponent parts of waste personal computers. J. Appl. Sci. Environ. Manag. 19(3), 470–477, DOI: 10.4314/jasem.v19i3.17.

Parajuly K. (2017) Circular economy in E-waste management: Resource recovery and design for end-of-life (Doctoral dissertation, University of Southern Denmark).

Parajuly K., Fitzpatrick C., Muldoon O. and Kuehr R. (2020) Behavioral change for the circular economy: A review with focus on electronic waste management in the EU. Resources, Conservation & Recycling: X 6, DOI: 10.1016/j.rcrx.2020.100035.

Ravindra K. and Mor S. (2019) E-waste generation and management practices in Chandigarh, India and economic evaluation for sustainable recycling. Journal of Cleaner Production 221, 286–294, DOI: 10.1016/j.jclepro.2019.02.158.

Saahas Zero Waste n.d. Ewaste Management and Recycling Services. [Online] https://saahaszerowaste.com/E-waste-management-recycling-services/ (Accessed: 2022-04-06).

Sethurajan M., Van Hullebusch, E.D., Fontana D., Akcil A., Deveci H., Batinic B., ... and Kuchta K. (2019) Recent advances on hydrometallurgical recovery of critical and precious el-ements from end of life electronic wastes-a review. Critical reviews in environmental science and technology 49(3), 212–275, DOI: 10.1080/10643389.2018.1540760.

Sharma M., Joshi S. and Govinda K. (2021) Issues and solutions of electronic waste urban mining for circular economy transition: An Indian context. Journal of Environmental Management 290, DOI: 10.1016/j.jenvman.2021.112373.

Sharma R. and Hussain S. (2018) India: E-waste Management In India. [Online] https://www.mondaq.com/india/waste-management/695996/E-waste-management-in-india (Accessed: 2021-11-15).

Tesfaye F., Lindberg D., Hamuyuni J., Taskinen P. and Hupa L. (2017) Improving urban mining practices for optimal recovery of resources from E-waste. Minerals Engineering 111, 209–221, DOI: 10.1016/j.mineng.2017.06.018.

Thagela M. (2019) E-waste: Adverse impact on health & environment. International Journal of Advanced Research in Management and Social Sciences 8(10), 11–21.

TheCityFix Labs India (2019) Sanshodhan's E-waste platform offers a guilt-free solution to get rid of old electronics sustainably. [Online] https://yourstory.com/socialstory/2019/02/sanshodhan-E-waste-disposal-platform-n79izniqwh/amp (Accessed: 2021-11-15).

Tiwari D., Raghupathy L., Khan A.S. and Dhawan N.G. (2019) A Study on the E-waste Collection Systems in Some Asian Countries with Special Reference to India. Nature Environment and Pollution Technology 18(1), 149–156.

Turaga R.M.R., Bhaskar K., Sinha S., Hinchliffe D., Hemkhaus M., Arora R., Chatterjee S., Khetriwal D.S., Radulovic V., Singhal P. and Sharma, H. (2019) E-waste management in India: Issues and strategies. Vikalpa: The Journal for Decision Makers 44(3), 127–162, DOI: 10.1177/0256090919880655.

Wang X. (2019) System Simulation Optimization of Resource and Environmental Effects of Circular Economy. Nature Environment & Pollution Technology 18(5), 1573–1578.

Xavier L.H., Giese E.C., Ribeiro-Duthie A.C. and Lins F.A.F. (2019) Sustainability and the circular economy: A theoretical approach focused on E-waste urban mining. Resources Policy 74, DOI: 10.1016/j.resourpol.2019.101467.

Maciej Mróz

Warsaw School of Economics, Poland; e-mail: maciej.mroz@sgh.waw.pl

The impact of hard coal prices on selected wind-power-related metal prices

ABSTRACT: The energy transition gather pace. In the light of ambitious plans for further use of renewable energy sources (RES), the strong demand for non-energy materials critical for RES is highly expected. Also, energy production is currently more and more substitutable, i.e. electricity can be produced by burning coal or, for example, from wind or solar farms as well. Therefore, there is a noticeable potential link between two completely different groups of commodities: energy, and metals which are widely used in the energy sector as well. Hence, the main purpose of this study is to examine the impact of hard coal prices on 5 selected wind-power-related metal prices with econometric approach. Thus, we are looking for new insights in terms of relationships between hard coal prices and significant metals for wind-power-technology, that potentially have been established or strengthened in the recent years. In the light of increasing uncertainty and significant risk of resources price volatility there is a widespread belief that it is necessary to study such relationships. However, vast literature devoted to this matter focus mostly on oil and metals used in clean energy technologies prices. Hence, the econometric models such as Autoregressive Distributed Lag (ARDL) or dynamic Error Correction Model (ECM) are employed to examine the impact of hard coal prices on selected wind-power-related metal prices.

KEYWORDS: coal, metals, wind energy, ARDL, ECM

Introduction

The United Nations Framework Convention on Climate Change (UNFCCC) Paris Agreement has been announced as a crucial step towards combating the global threat of climate change. That agreement sets out a goal of reducing global warming to well below 2, preferably to 1.5 degrees Celsius, compared to pre-industrial levels (United Nations Framework Convention on Climate 2021). This agreement was adopted by 196 Parties at COP21 in Paris on 12 December 2015, although it entered into force on 4 November 2016 (European Commission 2021).

The Paris Agreement is perceived as a landmark in the climate change process, as it provides for a common undertaking of all nations to make ambitious efforts to counteract and adapt to climate change (United Nations Framework Convention on Climate 2021). One of the key elements in this action against climate change is development of renewable energy sources (RES). Thus, developing renewable energy is main strategy in line with the Paris Agreement (IRENA 2021). Therefore, RES are currently being developed rapidly by a large number of countries (see e.g. 3), and are expected to be developed further in the future (Baron 2016; The Government of Japan 2021).

Therefore, the continued use of RES determines significant growth in demand for such metals as zinc, nickel, copper, cobalt, chromium or aluminum instead of traditional fossil fuels, namely crude oil, natural gas or coal. Hence, a global shift from energy commodities towards metals used in clean energy technologies strongly suggests a causality supply-demand relationship between them (Shao and Zhang 2020). Moreover, other economic factors determine how they will be priced further as well. By example, metal manufacture is highly energy-intensive (Hammoudeh et al. 2004). Therefore, higher production costs, and previously extraction costs, should be directly reflected in increasing clean energy metal prices. Furthermore, the crude oil price is impacting the metal industry due to transportation costs as well (influence channel) (Dutta 2018; Korhonen and Ledyaeva 2010).

Therefore, in current literature the number of studies on the link between energy commodities, especially crude oil, and the metal markets is still increasing see, for instance (Shao and Zhang 2020; Balcilar et al. 2017; Chaudhuri 2001; Chen and Xu 2019; Juvenal and Petrella 2014; Shahzad et al. 2019; Singhal et al. 2019; Tiwaria and Sahadudheen 2015). However, the relationships in these studies have been examined from different standpoints, thereby leading to the use of different methodologies and final results. For example, Baffes (Korhonen and Ledyaeva 2010) estimated the ratio of pass-through of crude oil price changes to the prices of 35 other internationally traded primary commodities. He presented evidence that precious metals are strongly affected by the changes in crude oil price. In turn, in their research based on Granger causality tests, Bakhat and Würzburg (Bakhat and Würzburg 2013) documented that adjustments to positive and negative deviations from the long-run equilibrium are asymmetric for copper in the short-run, while the adjustments for aluminum and nickel are symmetric. Also, Reboredo and Ugolini (Reboredo and Ugolini 2016) assess the impact of downward/upward oil price movements on metal prices: six industrial metals (aluminum, copper, lead, nickel, tin and zinc) and four precious metals (gold, silver, palladium and platinum). They indicate that large downward and upward oil price movements had spillover effects on these metals during the pre- and post-financial crisis periods.

However, among the wide range of already existing research and publications, other energy resources like coal is a relatively poorly explored area. Despite oil continuing to play the leading role, coal is also important. Indeed, as substitutability of energy sources is increasing, i.e. electricity can be produced by burning coal and can

also be generated by wind and solar farms as well. Thus, the relationship between coal and metals used in clean energy technologies prices is also strongly justified. On the other hand, it should be noticed that hard coal prices are not the only determinant of metal prices, and their levels are predominantly determined by other supply and demand factors, e.g. the degree of depletion of ore deposits of these minerals and consumption in other sectors of the economy. Additionally, it should be borne in mind that the prices of metallurgical coal using in manufacturing differ significantly from the prices of hard coal which is used in electricity production. However, the proposed analysis in this paper aims to capture the statistical impact which will potentially allow the use of these results in the future, e.g. for forecasting metal prices.

Therefore, in light of the above, the aim of this article is to examine the impact of the prices of hard coal, on 5 selected wind-power-related metal prices in the over six-year term of the Paris Agreement period with econometric approach. However, due to the multitude of variables in this research, for the sake of transparency as well as greater clarity in the interpretation of the results, the relationships are examined individually with coal-metal models.

This paper is organized as follows. Section 2 contains data description and presents ARDL-ECM methodology. Section 3 contains the results of the research based on coal prices and wind-power-related metal prices. Section 4 contains a discussion while section 5 provides conclusions and prospects for further research.

1. Materials and methods

In this research the dynamic data (time-series) is used for hard coal prices (Richards Bay) and selected wind-power-related metal prices, namely aluminum, chromium, cobalt, copper and zinc. All these metals are quoted on the Shanghai Metals Market (SMM) and the time span is from the 14 December 2015 to 13 December 2021 (weekly data; 6 years; Fig. 1). All financial data are sourced form Reuters database. Due to stabilize the variance of the time-series the logarithmic transformation is applied.

Table 1 presents the basic statistics of each variable. By example, the skewness for copper, cobalt, chromium, aluminum and coal is positive (greater than 0) and shows an obvious right-skewed distribution, while the skewness zinc is negative that means left-skewed distribution. The Jarque-Bera test statistic shows that coal and metal prices reject the normal distribution assumption. All these time series are non-stationary on the levels, however, the first differences between them are stationary (Table 3 in annex; ADF (Phillips and Perron 1988) and Phillips-Perron (PPT) (Reboredo 2013) tests).

The research is conducted with the econometric models such as Autoregressive Distributed Lag (ARDL) or dynamic error correction model (ECM) which are em-
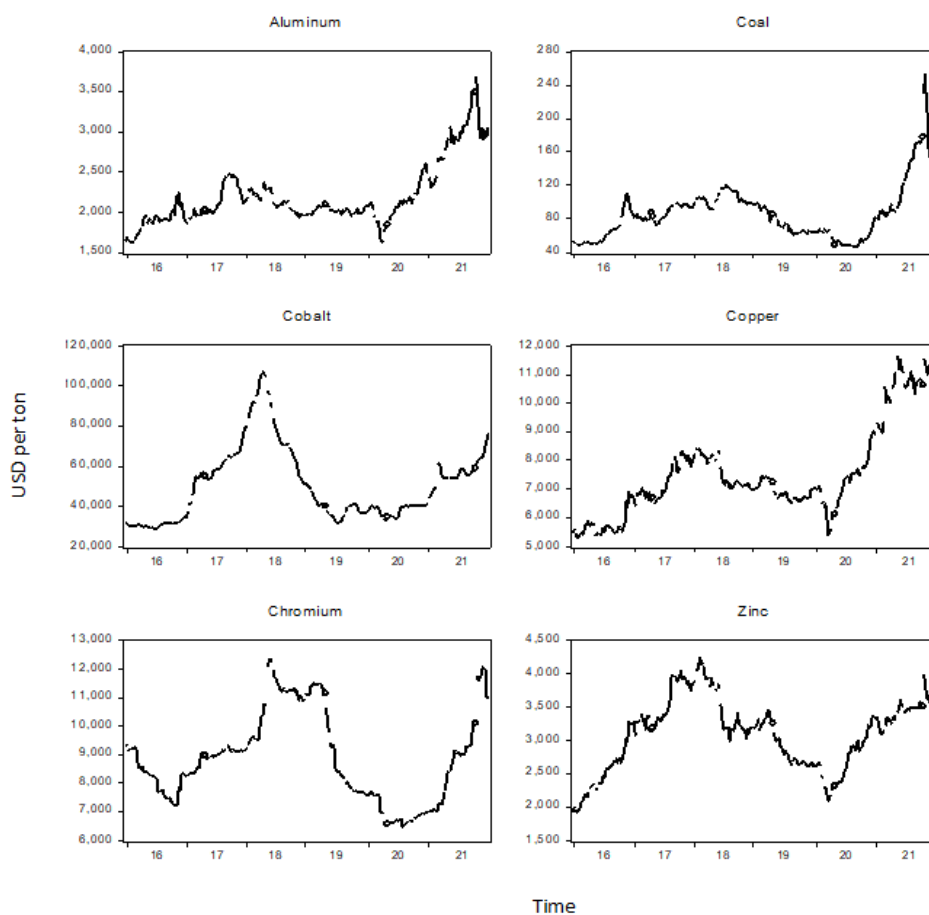
Figure 1.
Time-series for copper, coal, cobalt, chromium, aluminum and zinc 2015-2021
(in USD per ton)

Table 1.

Statistic of time-series

Variable	Mean	Median	Min.	Max.	Std. Dev.	Ex. kurtosis	Jarque-Bera Test	Skewness
Zinc	3,099.8	3194.0	1,916.8	4,237.6	536.91	−0.6606	5.82092	−0.15228
Copper	7,549.6	7134.4	5,312.1	11,638	1,611.6	0.21121	42.7447	0.97996
Cobalt	50,450	44313	28,335	10,745	18,401	0.59957	51.5919	1.0405
Chromium	8,886.5	8840.7	6,474.7	12,362	1,578.6	−0.8002	16.2746	0.45803
Aluminum	2,195.0	2062.9	1,618.2	3,675.8	391.24	1.9592	138.866	1.4820
Coal	86.965	82.535	46.500	254.00	33.475	4.2169	319.093	1.6753

Notes: Ex. Kurtosis is the kurtosis minus 3.

Table 2.

Unit roots tests

Variable	Augmented Dickey-Fuller test for unit root		Phillips-Perron test for unit root	
	Levels	First Difference	Levels	First Difference
Coal	−1.233	−9.665	−1.777	−13.331
Aluminium	−1.550	−9.443	−1.776	−15.619
Chromium	−1.534	−9.187	−1.604	−13.976
Cobalt	−1.195	−7.355	−1.209	−9.919
Copper	−1.471	−10.525	−1.454	−16.409
Zinc	−0.070	−10.612	−0.344	−17.351

ployed to examine the short and long-run causality between these variables. The ARDL methodology allows to perform analysis if there is I(0) or I(1) level integration, but not I(2) or higher.

All models in this research are coal-metal equations as below:

$$ARDL(p,q): M_t = \beta_0 + \sum_{i=1}^{p} \beta_i M_{t-i} + \sum_{i=0}^{q} \delta_i C_{t-i} + \varepsilon_t \tag{1}$$

$$ARDL: \Delta M_t = \beta_0 + \sum_{i=1}^{p} \lambda_i \Delta M_{t-i} + \sum_{i=0}^{q} \delta_i \Delta C_{t-i} + \varphi_1 M_{t-1} + \varphi_2 C_{t-1} + \vartheta_t \tag{2}$$

$$ECM: \Delta M_t = \beta_0 + \sum_{i=1}^{p} \lambda_i \Delta M_{t-i} + \sum_{i=0}^{q} \delta_i \Delta C_{t-i} + \varphi z_{t-1} + \vartheta_t \tag{3}$$

where:
M_t – selected metal price,
C_t – coal price,
p,q – number of lags,
$\beta_0, \lambda_i, \delta_i, \varphi_1, \varphi_2$ – coefficients,
$\varepsilon_t, \vartheta_t$ – error term.

2. Results

Firstly, each metal-coal pair have been tested for number of lags. Therefore, using the Akaike Information Criterion (AIC), the Bayesian Schwarz Criterion (BIC) and

Hannana-Quinna Criteria (HQC), we found the appropriate lag order for each pair (aluminum: 1 lag; copper: 1 lag; chromium: 2 lags; zinc: 1 lag; cobalt: 2 lags; here AIC is used as main criteria) (Tables 3–7).

Table 3.

Lag selection for aluminum

Lag	LL	AIC	HQIC	SBIC
0	130.032	−1.00813	−.996924	−.980276
1	1,008.44	−7.89327*	−7.85965*	−7.80971*
2	1,011.12	−7.88283	−7.82681	−7.74357
3	1,013.87	−7.87296	−7.79453	−7.67799
4	1,016.58	−7.8628	−7.76196	−7.61212
5	1,020.14	−7.8594	−7.73615	−7.55302

Notes: *Level of significant; LL – Langrange Multiplier; AIC – Akaike Information Criterion; SBIC – Bayesian Information Criterion; HQIC – Hannan–Quinn Information Criterion.

Table 4.

Lag selection for copper

Lag	LL	AIC	HQIC	SBIC
0	68.6351	−.524686	−.513481	−.496833
1	982.944	−7.69247*	−7.65886*	−7.60891*
2	986.646	−7.69013	−7.6341	−7.55086
3	988.578	−7.67384	−7.59541	−7.47887
4	990.787	−7.65974	−7.5589	−7.40906
5	995.088	−7.66211	−7.53885	−7.35572

Notes: *Level of significant; LL – Langrange Multiplier; AIC – Akaike Information Criterion; SBIC – Bayesian Information Criterion; HQIC – Hannan–Quinn Information Criterion.

Table 5.

Lag selection for chromium

Lag	LL	AIC	HQIC	SBIC
0	90.4841	−.696725	−.68552	−.668872
1	1062.58	−8.31954	−8.28592	−8.23598*
2	1070.03	−8.34673*	−8.29071*	−8.20747
3	1073.71	−8.34419	−8.26576	−8.14922
4	1075.81	−8.32919	−8.22835	−8.07852
5	1076.33	−8.30185	−8.17859	−7.99546

Notes: *Level of significant; LL – Langrange Multiplier; AIC – Akaike Information Criterion; SBIC – Bayesian Information Criterion; HQIC – Hannan–Quinn Information Criterion.

Table 6.

Lag selection for zinc

Lag	LL	AIC	HQIC	SBIC
0	119.781	−.927413	−.916208	−.89956
1	973.732	−7.61993	−7.58632*	−7.53637*
2	979.363	−7.63278*	−7.57675	−7.49351
3	981.21	−7.61582	−7.53739	−7.42085
4	982.16	−7.59181	−7.49097	−7.34113
5	984.189	−7.57629	−7.45304	−7.26991

Notes: *Level of significant; LL – Langrange Multiplier; AIC – Akaike Information Criterion; SBIC – Bayesian Information Criterion; HQIC – Hannan–Quinn Information Criterion.

Table 7.

Lag selection for cobalt

Lag	LL	AIC	HQIC	SBIC
0	−62.4491	.507473	.518678	.535326
1	957.153	−7.48939	−7.45578	−7.40583
2	993.338	−7.74282*	−7.68679*	−7.60355*
3	996.455	−7.73587	−7.65743	−7.54089
4	996.94	−7.70819	−7.60735	−7.45751
5	1000.72	−7.70648	−7.58323	−7.4001

Notes: *Level of significant; LL – Langrange Multiplier; AIC – Akaike Information Criterion; SBIC – Bayesian Information Criterion; HQIC – Hannan–Quinn Information Criterion.

Further, we started with the analysis of the ARDL model (bound testing) in order to study the cointegration of variables in individual countries. In other words, we checked whether there are long-term relationships between the analyzed variables: coal → metal.

Results shows that this long-term relationship exists only in case of coal-chromium pair (F statistic 11.29975; t statistic –3.635052). In other four pairs, the calculated F and t statistics are lower than the critical values for the I(0) variables what means that we cannot reject the null hypothesis about the lack of relationship between these variables. Taken together, the results presented in Table 8 show that there is cointegration – a long-term relationship (steady-state equilibrium) – only between one of five coal-metal pair (coal-chromium).

Having a confirmed cointegration or non-contegration in case of each pair, we estimate the equations coefficients. Standard ARDL models are used in case of aluminum, zinc, copper, cobalt while the ARDL-ECM for chromium, where the long-run equilibrium is identified (Table 9). For the appropriate model with lags selection, the Akaike info criterion is used. Therefore, lags for coal and metals are not the same in case of all models.

Table 8.
ARDL bounds test for coal and metals

Statistics	Decision	Stats	value	I(0)*	I(1)*
Coal → Aluminium ARDL(1,1)	No cointegration	F	1.720238	4.94	5.73
		t	−0.103035	−2.86	−3.22
Coal → Zinc ARDL(1,0)	No cointegration	F	2.874782	4.94	5.73
		t	−2.063837	−2.86	−3.22
Coal → Copper ARDL(1,0)	No cointegration	F	0.366264	4.94	5.73
		t	−0.257885	−2.86	−3.22
Coal → Cobalt ARDL(2,2)	No cointegration	F	1.881946	4.94	5.73
		t	−1.888836	−2.86	−3.22
Coal → Chromium ARDL(2,2)	Cointegration	F	11.29975	4.94	5.73
		t	−3.635052	−2.86	−3.22

Notes: *5% level of significant

Table 9.
Estimation results of short and long-term coefficients for ARDL and ECM

Statistics	emct-1	Coal	Coal(-1)	Coal(-2)	Metal(-1)	Metal(-2)	Const.
Coal → Aluminium ARDL		0.05245 (0.1328)	−0.06103 (0.0722)		0.99841 (0.0000)		0.05212 (0.5957)
Coal → Zinc ARDL		0.00571 (0.4563)			0.96989 (0.0000)		0.21900 (0.0211)
Coal → Copper ARDL		−0.00275 (0.6909)			0.99694 (0.0000)		0.04203 (0.6303)
Coal → Cobalt ARDL		0.06343 (0.0575)	−0.10882 (0.0341)	0.056265 (0.0939)	1.46447 (0.0000)	−0.47716 (0.0000)	1.61046 (0.1085)
Coal → Chromium ARDL-ECM	−0.03507 (0.0000)	0.12772 (0.0000)	−0.19463 (0.0000)	0.090440 (0.0006)	1.11103 (0.0000)	−0.14610 (0.0151)	0.21508 (0.0043)

Notes: values in brackets are p-value for significant.

In case of coal → aluminum, there is only ARDL model presented (short-run relationship), however, the first lag is statistically significant (5% level of significant). Thus, we assume that coal is not impacting the aluminum price in the short term. Similarly, in case of coal → zinc and coal → copper. On the other hand, there is an evidence that cobalt is impacted by hard coal prices (coal → cobalt) in the short term (one lag; DL(1)). However, this is the short-run relationship due to the fact that no cointegration is detected.

In case of coal → chromium relationship, there is the confirmation of the that in case of both short- and long-run relationship (all p-values below 5% of significant) that means strong causal relationship in this case. Thus, the model for coal → chromium should include 2 lags for coal and 2 for chromium.

Finally, the stability check for models have been test by using CUSUM and CU-SUM squared tests (see Annex). All models are stable if we use CUSUM tests while CUSUM squared shows exceeds in case of all metals with the exception of zinc. That suggest that all models without zinc are not stable in time.

3. Discussion

Since the Paris Agreement was adopted on 12 December 2015, nearly all countries around the world have agreed to take action with regard to the climate and to reduce the global temperature to well below 2 degrees Celsius (°C) this century compared to pre-industrial levels, and reach a target of 1.5 °C. Importantly, most of them declared in their Nationally Determined Contributions renewables, which include quantified renewable energy targets. Thus, further development of RES determines the demand for non-renewable resources, such as metals used in clean energy technologies gradually excluding traditional fossil fuels. This provides the basis for the analysis of possible causal relationships.

The empirical results obtained from this research provide clear evidence that hard coal price may affect selected wind-power-related metals prices, however its impact is radically different and it depends on the metals. The number of strong causal relationships detected in this research is only one (chromium). Nevertheless, there is also evidence that short-run causality exists in case of cobalt as well.

Other analysis shows that fuel-metal relationships depends on the type of the fuel e.g. there is the evidence that crude oil price impacts the metal prices (Shao and Zhang 2020). However, it also vary on metals used in this research (the results show that crude oil price has non-linear Granger causality with lithium, cobalt, manganese, antimony, cadmium, molybdenum, and tellurium). It suggest that our results may arise in near future while the energy transition gather pace. For example, as the Paris Agreement becomes more stringent, along with the progressive implementation of national goals, this can be expected to ensure the intensification of the existing causal relationships and the emergence of new ones.

Conclusions

A possible prospect for further research on this issue is analysis of these relationships in the future. In this context, as the decisions of the Paris Agreement should be reviewed every five years, the causal dependencies may emerge or intensify in the future (over the next five years). Consequently, there is broad scope for testing this

kind of relationship in the future, especially if it could be important for policymakers, for example concerning energy security (Mróz 2021). Additionally, the broader context with other clean energy metal prices should be also explored.

It should be also noticed that Covid-19 may be perceived as a main factor significantly affecting possible causal relationships in recent period. However, a proper assessment of this impact will not be possible until the future.

On the other hand, potential in this kind of research is also visible for vector autoregressive (VAR) and vector error correction (VECM) models. Hence, this type of the research should be explored.

REFERENCES

Bakhat M. and Würzburg K. (2013) Co-integration of Oil and Commodity Prices: A Comprehensive Approach. Economies for energy. Working Paper WP FA05/2013.

Balcilar M., Bekiros S. and Gupta R. (2017) The role of news-based uncertainty indices in predicting oil markets: a hybrid nonparametric quantile causality method. Empirical Economics 53(3), 879–889, DOI: 10.1007/s00181-016-1150-0.

Baron R. (2016) Energy Transition after the Paris Agreement: Policy and Corporate Challenges. [In:] Background paper for the 34th Round Table on Sustainable Development, 28–29 September 2016. OECD.

BP, Statistical Review of World Energy 2021, 70th edition. [Online] https://www.bp.com/content/dam/bp/business-sites/en/global/corporate/pdfs/energy economics/statistical-review/bp-stats-review-2021-full-report.pdf (Accessed: 2021-09-03).

Chaudhuri K. (2001) Long-Run Prices of Primary Commodities and Oil Prices. Applied Economics 33(4), 531–38.

Chen R. and Xu J. (2019) Forecasting volatility and correlation between oil and gold prices using a novel multivariate GAS model. Energy Economics 78, 379–391, DOI: 10.1016/j.eneco.2018.11.011.

Dutta A. (2018) Impacts of oil volatility shocks on metal markets: A research note. Resources Policy 55, 9–19, DOI: 10.1016/j.resourpol.2017.09.003.

European Commission. Paris Agreement. [Online] https://ec.europa.eu/clima/eu-action/international-action-climate-change/climate-negotiations/paris-agreement_en (Accessed: 2021-10-07).

Hammoudeh S., Dibooglu S. and Aleisa E. (2004) Relationships among U.S. oil prices and oil industry equity indices. International Review of Economics & Finance 13(4), 427–453.

IRENA. Renewable Energy and Climate Pledges: Five Years After the Paris Agreement. [Online] https://www.irena.org//media/Files/IRENA/Agency/Publication/2020/Dec/IRENA_NDC_update_2020.pdf (Accessed: 2021-10-10).

Juvenal L. and Petrella I. (2014) Speculation in the Oil Market. J. of Applied Economics 30(4), 621–649, DOI: 10.1002/jae.2388.

Korhonen I., Ledyaeva S. (2010) Trade linkages and macroeconomic effects of the price of oil. Energy Economics 32(4), 848–856.

Mróz M. (2021) The energy security trap The European Union perspective. [In:] The Economics of Sustainable Transformation. A. Szelągowska, A. Pluta-Zaremba (Eds.), Routledge: UK, London.

Phillips P.C.B. and Perron P. (1988) Testing for a unit root in time series regressions. Biometrica 75, 335–346.

Reboredo J.C. (2013) Is gold a safe haven or a hedge for the US dollar? Implications for risk management. Journal of Banking & Finance 37(8), 2665–2676, DOI: 10.1016/j.jbank-fin.2013.03.020.

Reboredo J.C. and Ugolini A. (2016) The impact of downward/upward oil price movements on metal prices. Resources Policy 49, 129–141, DOI: 10.1016/j.resourpol.2016.05.006.

Shahzad S.J.H., Rehman M.U. and Jammazi R. (2019) Spillovers from oil to precious metals: quantile approaches. Resources Policy 61, 508–521, DOI: 10.1016/j.resour-pol.2018.05.002.

Shao L. and Zhang H. (2020) The impact of oil price on the clean energy metal prices: A multi-scale perspective. Resource Policy 68, 1–11, DOI: 10.1016/j.resourpol.2020.101730.

Singhal S., Choudharyb S. and Biswal P.C. (2019) Return and volatility linkages among International crude oil price, gold price, exchange rate and stock markets: Evidence from Mexico. Resource Policy 60, 255–261, DOI: 10.1016/j.resourpol.2019.01.004.

The Government of Japan. The Long-term Strategy under the Paris Agreement. [Online] https://unfccc.int/sites/default/files/resource/The%20Long-term%20Strategy%20under%20the%20Paris%20Agreement.pdf (Accessed: 2021-09-03).

Tiwaria A.K. and Sahadudheen I. (2015) Understanding the nexus between oil and gold. Resource Policy 46, 85–91, DOI: 10.1016/j.resourpol.2015.09.003.

United Nations Framework Convention on Climate. The Paris Agreement. [Online] https://unfccc.int/process-and-meetings/the-paris-agreement/the-paris-agreement (Accessed: 2021-10-07).

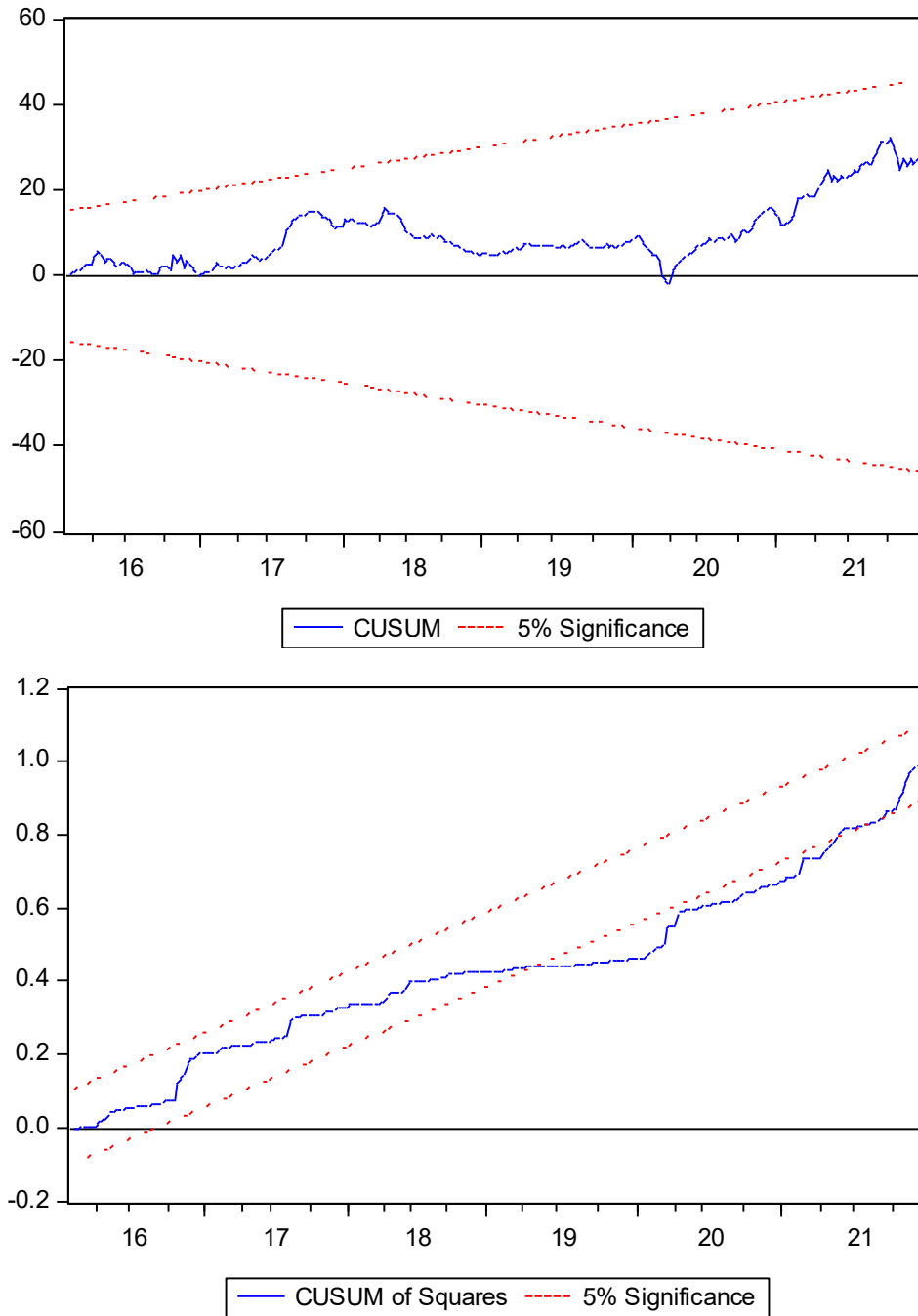### Annex 1. CUSUM and CUSUM square test for stability

Figure 1.
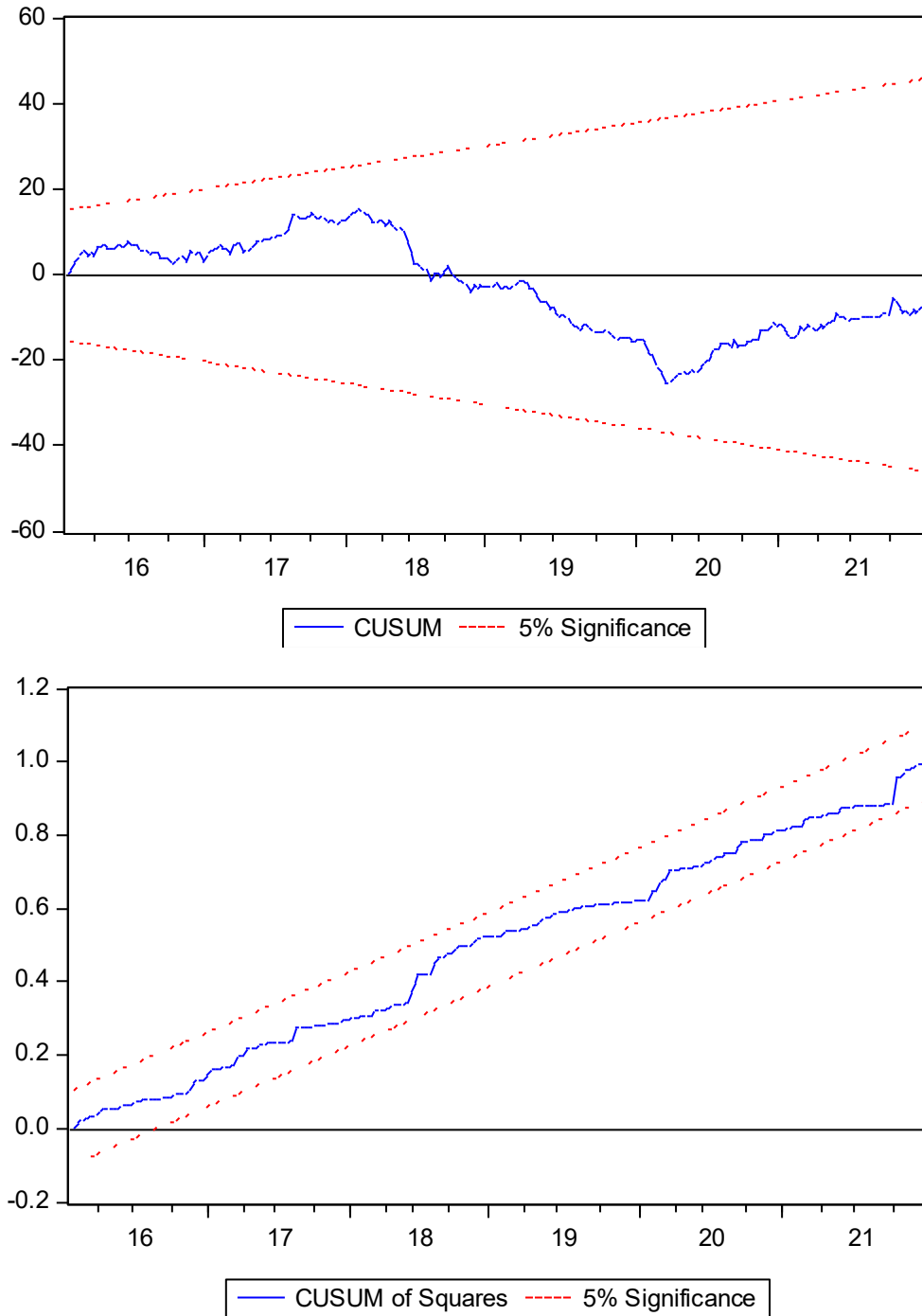CUSUM (upper) and CUSUM square (lower) test for stability for aluminium

Figure 2.
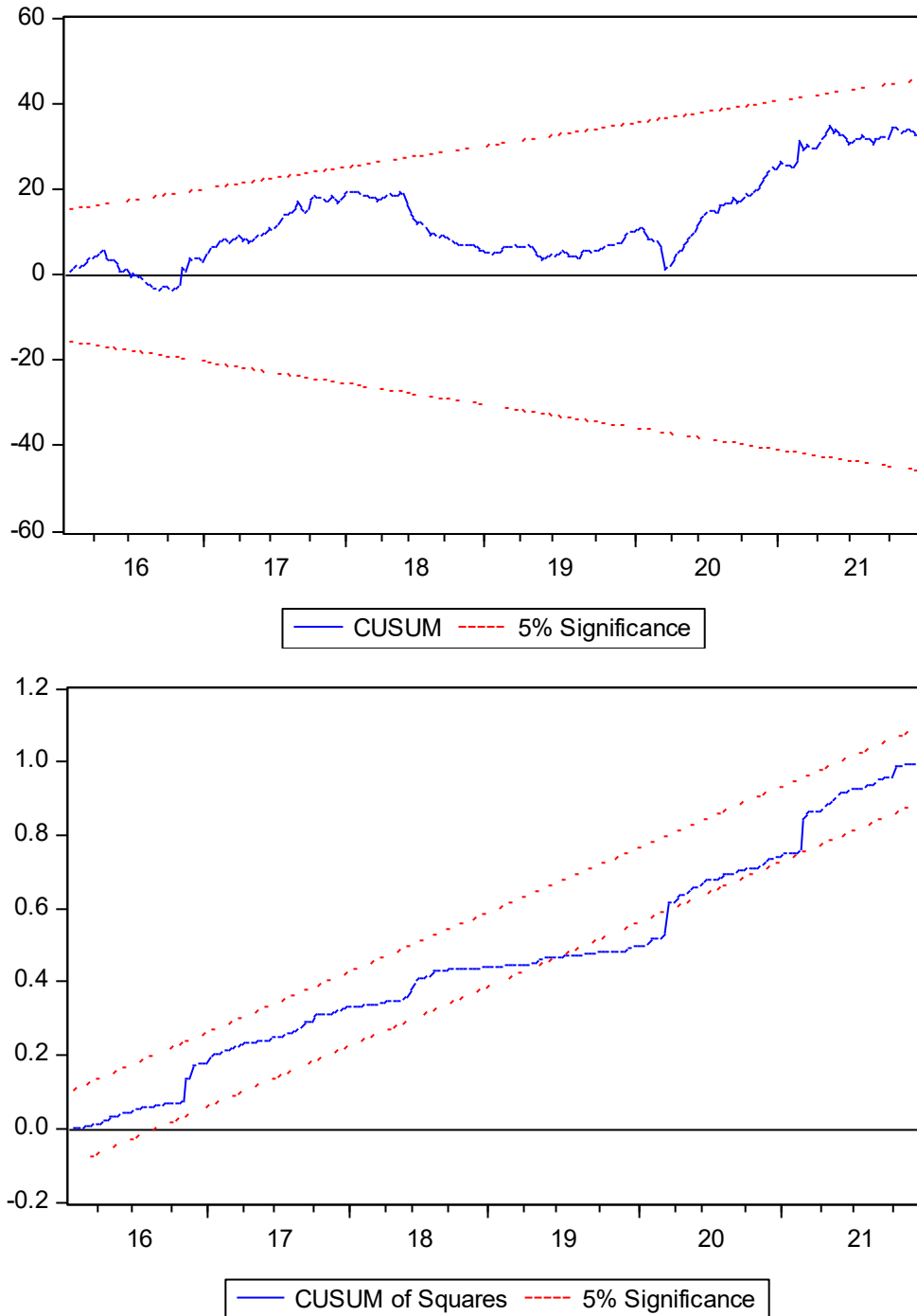*CUSUM (upper) and CUSUM square (lower) test for stability for zinc*

Figure 3.
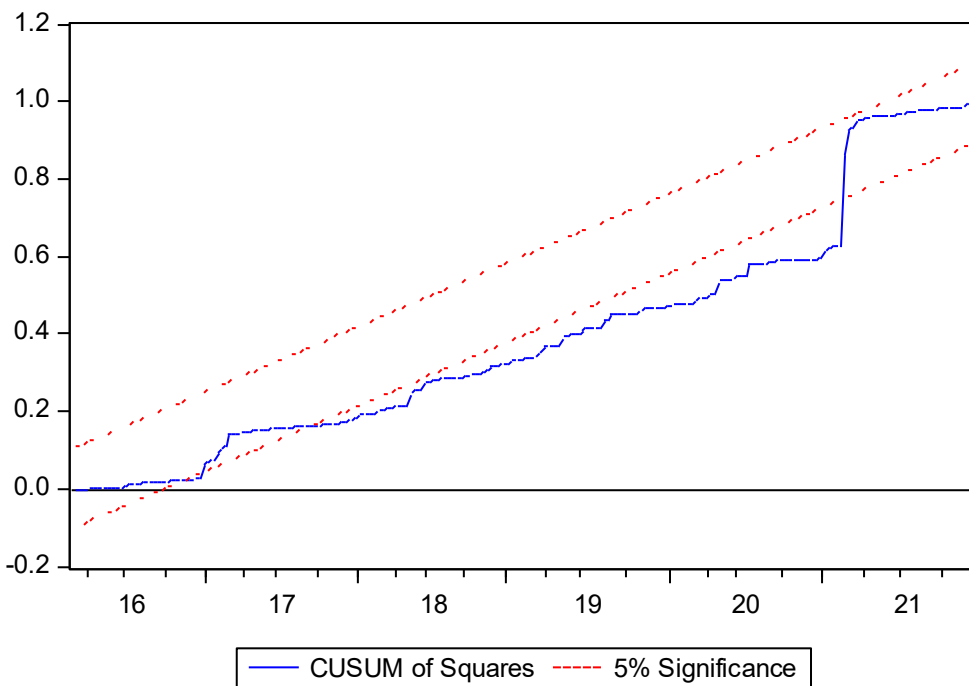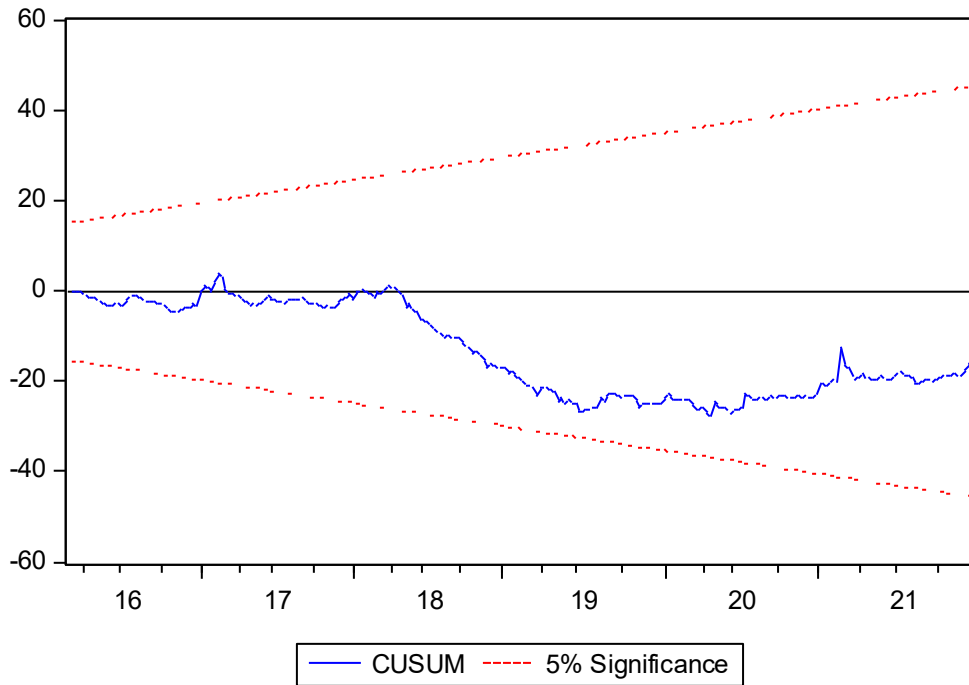*CUSUM (upper) and CUSUM square (lower) test for stability for copper.*

Figure 4.
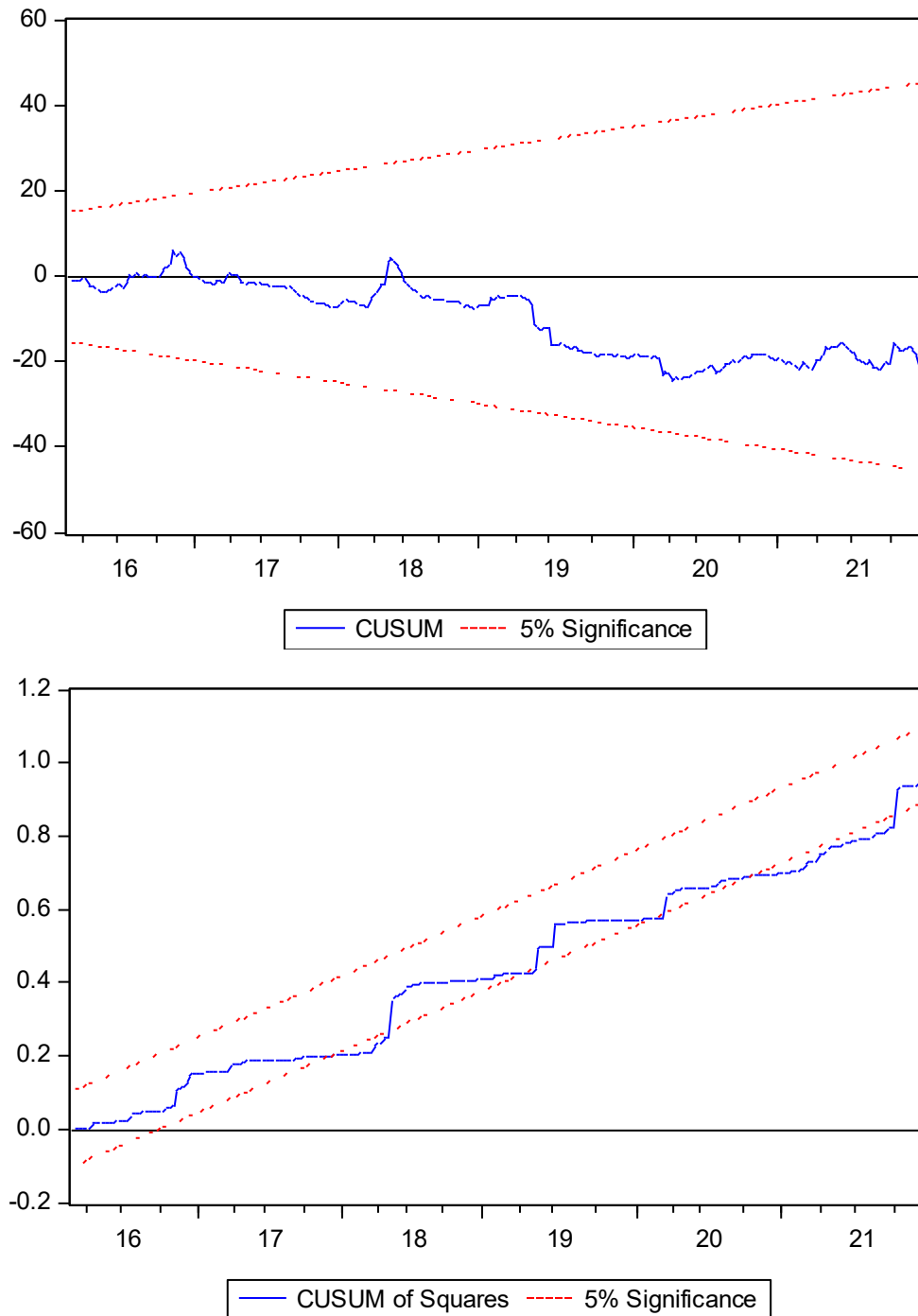*CUSUM (upper) and CUSUM square (lower) test for stability for cobalt*

Figure 5.
CUSUM (upper) and CUSUM square (lower) test for stability for chromium

Beata Pospiech

Częstochowa University of Technology, Poland; e-mail: beata.pospiech@pcz.pl

Application of Polymer Inclusion Membranes for the selective removal of copper from model leach liquor of waste Printed Circuit Boards (PCBs)

ABSTRACT: Waste printed circuit boards (PCBs) contain many various metals and their effective recycling is very important. In this work, an effective process based on the application of polymer inclusion membranes (PIMs) for selective recovering of copper(II) from the synthetic leach liquor of PCBs was developed. For the first time, trihexyl(tetradecyl)phosphonium thiosalicylate [PR4][TS] was used as the ion carrier of copper(II). Environmentally friendly ionic liquid was proposed as a new carrier for synthesis of polymer membranes. The results proved that transport Cu(II) into 0.5 M sulphuric acid is efficient and selective. The obtained results showed that the recovery factor of Cu(II) ion from synthetic leach liquor containing mixture of various metals was over 91 %.

KEYWORDS: electronic waste, printed circuits boards (PCBs), copper, heavy metals

Introduction

Printed circuit boards (PCBs) are present in every electronic and electric equipments. PCBs contain many various metals such as copper, tin, nickel, lead, iron, silver, gold, etc. We can find many literature reports on the recovery of metals from PCBs using various methods such as: (1) leaching by inorganic acid (Le et al. 2011; Choubey et al. 2015; Park et al. 2021; De Andrade et al. 2021), (2) extraction of metal ions (Zhu et al. 2012; Panda et al. 2020), (2) separation using membrane processes (Kavitha and Palanivelu 2012). The method of recovering metals from waste should be ecological and environmentally friendly. PCBs contain approximately 28% metals (about 16% Cu, 2% Al and 0.5% Ni, 5% Fe 2000 ppm Ag, 150 ppm Au and other metals) and 23% plastics (Burat and Özer 2018; Cui and Zhang 2008). Leach liquors of PCBs contain many heavy metals. The examples of aqueous solutions obtained after leaching in various conditions are presented in Table 1. As can be seen, various

leaching agents were using for the recovery of valuable metals from waste. Jadhav and Hocheng (2015) reported that hydrochloric acid is less corrosive than nitric acid and sulfuric acid. Furthermore, this acid has the ability to dissolve valuable metals from metallic waste. Therefore, hydrochloric acid can be recognized as the effective leaching agent for the recovery of metals from PCBs.

The separation process of metal ions from aqueous solutions requires application of the appropriate methods and reagents. This is essential stage in hydrometallurgical processing. The separation process of copper(II) from the solutions containing other metals should be highly effective. A number of researchers reported that transport of metal ion through polymer inclusion membranes (PIMs) have potential applications as alternatives to solvent extraction duo to their low cost, long term stability, economical utilization of carriers, good selectivity, easy design and operation as well as easily satisfying environmental pollution regulations (Pospiech and Kujawski 2015). A typical PIM consists of a polymer, a plasticizer and an ion carrier to facilitate the selective transport of metal ion. The choice of the ion carrier is crucial to ensure the selectivity and efficiency (Güel et al 2011; Jaqub et al. 2021). Therefore, the looking for the new, effective and ecological components of the membranes for the separation of heavy metal ion is very needed and important.

Copper, cobalt and nickel are commonly found in the aqueous solutions in the case of the recovery of metals from various wastes by hydrometallurgical processes. PIMs with different ion carriers were studied for Cu(II) recovery from multi-component solutions. For instance, Wang et al. (2000, 2016, 2017) studied transport of metal ions across PIM system with 2-hydroxy-5-nonylacetophenone oxime (LIX 84I) and di(2-ethylhexyl) phosphoric acid (D2EHPA) as carriers for the simultaneous separation of Cu(II) from solutions containing multiple cations. Kavitha and Palanivelu (2012) reported recovery of Cu(II), Pb(II), Ni(II) from digested e-waste through PIM with D2EHPA.

In this work, for the first time trihexyl(tetradecyl)phosphonium thiosalicylate [PR4][TS] was used as the ion carrier of copper(II). This ionic liquid (IL) can be called green solvent due to melting point below 100°C, high thermal stability, negligible vapor pressure as well as low toxicity. Generally, ILs are classified as environmentally friendly substances. They have many advantages and applications as the effective extractants/carriers of metal ions and solvents (Fisher et al. 2011, Fuerhacker et al. 2012, Pospiech and Kujawski 2015; R. Leyma et. al. 2016; Lukomska et al. 2018).

In this work, [PR4][TS] was used as up-to-date carrier of copper(II) for synthesis of polymer inclusion membranes (PIMs). The aim of the present work is to study the influence of the hydrochloric acid concentration in the aqueous solution on the effective and selective recovery of copper(II) from the aqueous source phase containing nickel(II), iron(II) and zinc(II).

Table 1.

Composition of selected leach liquors of waste PCBs

Leaching agent	Composition of solution after leaching	Ref.
3.5 M HNO_3	42.11 g/L Cu, 2.12 g/L Fe, 4.02 g/L Pb, 1.58 g/L Zn, and 0.4 g/L Ni	Le et al. 2011
3 M HNO_3	22.97 g/L Cu, 6.3 mol/L HNO_3	Choubey 2015
1.2 mol/L H_2SO_4 and 10.0 vol% of H_2O_2	16.66 g/L Cu, 0.1 g/L Pb, 0.64 g/L Al, 0.13 g/L Fe, and 0.79 g/L Ca	Kumar et al. 2014
3 M HNO_3	21,12 g/L Cu (96%), 0.52 g/L Pb, 0.91 g/L Al, 0.13 g/L Fe and 1.7 g/L Ca	Kumar et al. 2014
2 M/L HCl and Cl_2 as oxidant	Results of the leaching: 71% of Cu, 98% of Zn, 96% of Sn, 96% of Pb	Kim et al. 2011

1. Materials and methods

Inorganic chemicals, i.e. copper(II) chloride ($CuCl_2 \cdot 2H_2O$), nickel(II) chloride ($NiCl_2 \cdot 6H_2O$), zinc(II) chloride ($ZnCl_2$), iron chloride ($FeCl_3$), hydrochloric acid (HCl), sulfuric acid (H_2SO_4), were of analytical grade and were purchased from POCh (Gliwice, Poland). Organic reagents, i.e. trihexyl(tetradecyl)phosphonium thiosalicylate [PR4][TS] (purity≥97%), cellulose triacetate (CTA), dichloromethane, 2-nitrophenyl octyl ether (NPOE), were of analytical reagent grade (Aldrich).

1.1. Polymer Inclusion Membranes (PIMs)

PIMs were prepared as reported in the earlier papers (Pospiech 2015; Makowka and Pospiech 2019 2020). The solution of cellulose triacetate (CTA) containing 1.25 g CTA/100 cm^3 of dichloromethane was prepared. 0.1 M solution of the ion carrier ([PR4][TS]) in chloromethane was used for synthesis of PIM. 2-nitrophenyl octyl ether (NPOE) was applied as the plasticizer. Dichloromethane was used as the solvent for the each membrane component (CTA, NPOE and carrier). The membrane was obtained as a result of evaporation of dichloromethane from a mixture containing CTA, NPOE and carrier.

1.2. Transport experiment

Transport experiment was described in the previous papers (Pospiech 2015; Makowka and Pospiech 2019, 2020). The volume of the source phase and the receiving

phase was 100 cm^3, respectively. The membrane surface was 12.56 cm^2. The source and the receiving phases were pumped with a peristaltic pump (PP1B-05A type, Zalimp, Poland). The concentrations of Cu(II), Ni(II), Fe(III), Zn(II) were analyzed by the plasma emission spectrometer MP-AES 4200 (Agilent).

The transport process of metal ions was described by a first-order reaction in metal ion concentration (Danesi 1984). To calculate the k value (rate constant), a plot of $\ln(c/c_i)$ versus time was prepared (c – concentration of metal ion after 12 h; c_i – initial concentration of metal). The permeability coefficient (P) was calculated as:

$$P = \frac{V}{A}k \left[\frac{m}{s}\right]$$

(1)

where:
- V – volume of the aqueous phase,
- A – the surface of PIM. The initial flux (J_i) was calculated as:

$$J_i = Pc_i \left[\frac{mol}{m^2s}\right]$$

(2)

2. Results

The composition of synthetic leach liquor was presented in Table 2. At first, the effect of hydrochloric acid concentration in the source phase on the selective recovery of copper(II) from the mixture of metal ions was investigated using transport across PIM containing 20 wt.% CTA, 30 wt.% [PR4][TS], 50 wt.% NPOE. The concentration of hydrochloric acid in this aqueous phase was varied between 0.5 mol/L to 3 mol/L. The results are presented in figure 1, which shows the kinetics dependence of $\ln(c/c_i)$ versus time for the transport of Cu(II) depending on hydrochloric acid concentration in the aqueous solution. The linear relation of $\ln c/c_i$ versus time shows the facilitated mechanism of Cu(II) transport across PIM. Other metals were not detected in the receiving phase, which proves the high selectivity of the process. Table 3 shows kinetic parameters such as the rate constant (k), the permeability coefficient (P) and recovery factor (%, RF).

The next part of the investigation concerned the effect of sulphuric acid concentration in the receiving phase on the transport of metal ion from the source phase. The concentration of sulfuric acid in this aqueous phase was varied between 0.1 mol/L to 2 mol/L. The results are presented in Table 4. As can be observed, the high concentration of sulphuric acid in the receiving phase is not favorable for the transport of Cu(II). The highest initial flux of Cu(II) reached the value of 44.5 µmol/m^{2}s for 0.5 M H$_2$SO$_4$ as the receiving phase. Table 4 shows kinetic parameters of the transport of

Table 2.

Composition of synthetic leach liquor of PCBs

Metal	Concentration [mol/dm^3]
Cu(II)	0.01
Ni(II)	0.001
Fe(III)	0.001
Zn(II)	0.001

Table 3.

Kinetic parameters for transport of Cu(II) from synthetic leach liquor.

The receiving phase: 0.5 M H$_2$SO$_4$

[HCl] [mol/dm^3]	Rate constant, k, [h-1]	Permeability coefficient, P [μmol/s]	Recovery factor [%]
0.5	0.052	1.16	47.4
1.0	0.127	2.80	77.6
2.0	0.184	4.06	89.1
3.0	0.202	4.45	91.5

Figure 1.
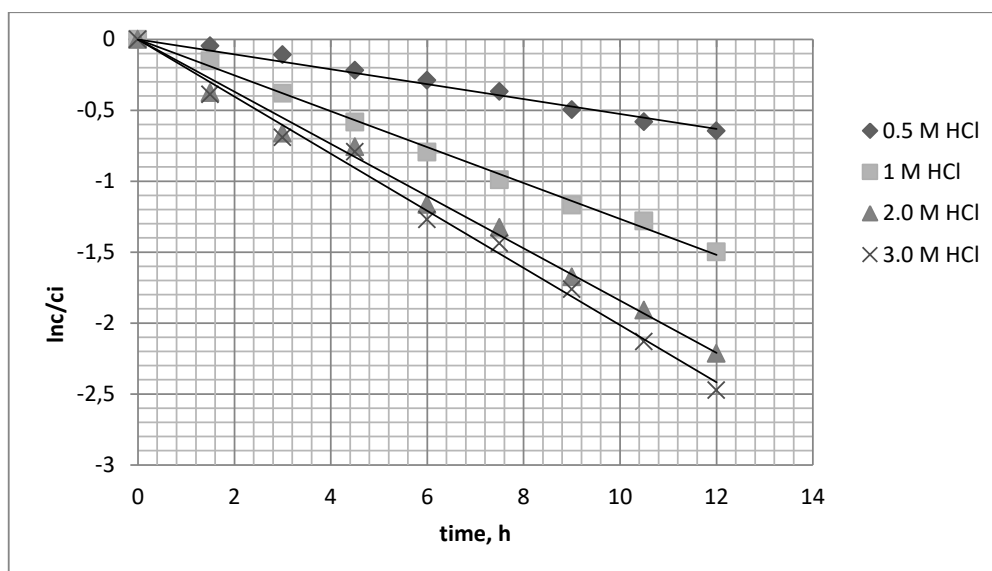
Relationship of ln(c/c$_i$) vs. time for Cu(II) transport across PIM with [PR4][TS]. The receiving phase: 0.5 M H$_2$SO$_4$

Cu(II). These results showed that transport of metal ions into the receiving phase was depended on the concentration of H_2SO_4 in the receiving phase. The recovery of copper(II) decreased when the concentration of H_2SO_4 was above 0.5 M.

Table 4.

Kinetic parameters for transport of Cu(II) from HCl solutions in depending on H_2SO_4 concentration in the receiving phase. PIM: 20 wt.% CTA, 30 wt.% [PR4][TS], 50 wt.% NPOE. The receiving phase: H_2SO_4

$[H_2SO_4]$ [mol/dm^3]	Rate constant, k [h-1]	Permeability coefficient, P [μm/s]	Recovery factor [%]	J_i [μmol/m^{2}s]
0.1	0.178	3.94	87.8	39.4
0.5	0.202	4.45	91.5	44.5
1.0	0.184	4.07	89.0	40.7

The stability of the PIM containing 20 wt.% CTA, 30 wt.% [PR4][TS], 50 wt.% NPOE was evaluated on the basis of the permeability values obtained from three sequential experiments in which the membrane was used under the following experimental conditions: 0.01 M Cu(II), 0.001 Ni(II), 0.001 Fe(II), 0.001 Zn(II) in 3 M HCl as the source phase, the receiving phase: 0.5 M H_2SO_4. The membrane was taken away from the cell and washed in deionized water. There were three repeated membrane transport experiments which used the same membrane. The permeability coefficient of Cu(II) ion varied slightly after three cycles of 12 h each. As before, other metals were not detected in the receiving phase. In Table 5, the variation of the permeability coefficient of Cu(II) observed during all three experiments is shown. As can be seen, the permeability coefficients for Cu(II) decreased from 4.45 to 3.82 μm/s.

Table 5.

Effect of cycles number for Cu(II) transport across PIMs on permeability coefficient. PIM: 20 wt.% CTA, 30 wt.% [PR4][TS], 50 wt.% NPOE

Cycle number	Permeability coefficient, P [μm/s]
1	4.45
2	4.35
3	3.82

3. Discussion

Based on the literature review (Lee et al. 2018), it can be concluded that hydrochloric acid can be used to metals leaching from waste PCBs. Review of literature shows that copper is the major metal of each leach liquor independently of the leaching agent (Table 1). The results show that significant amount of Cu as well as small amount of Ni, Fe and Zn were leached. Hydrochloric acid was one of the most effective leaching agents. A careful review of the literature shows that the recovery of copper(II) using PIM containing [PR4][TS] has been not to perform so far. Membrane containing 20 wt.% CTA, 30 wt.% [PR4][TS], 50 wt.% NPOE can be used for the selective recovering Cu(II) from leach liquors of PCBs containing Zn(II), Ni(II) and Fe(III). As can be observed, when the hydrochloric acid concentration increased, the values of the rate constants and the initial fluxes of Cu(II) also increased. The highest permeability coefficient of Cu(II) reached the values 4.45 μm/s for 3 mol/L HCl. It can also noted the increase of the recovery factor of Cu(II) with increasing concentration of HCl in the source phases from value 47.4% for 0.5 M HCl to value 91.5% for 3 mol/L HCl. The high concentration of hydrochloric acid in the source phase promotes the transport of Cu(II) into 0.5 mol/L H_2SO_4. Copper ions exist as the anionic chlorocomplexes in the concentrated HCl (Zhu et al. 2012) and are favored by the ion carrier containing in the PIM. It indicates that in this case anion exchange mechanism of transport occurs, because Cu(II) forms stable anionic chlorocomplexes in the source phase at high chloride ion concentration. The maximum transport of Cu(II) ions was obtained by using the membrane containing 1 mol/dm^3 of [PR4][TS]. The resulting membrane contained 20 wt.% CTA, 30 wt.% [PR4][TS], 50 wt.% NPOE. It is worth noting that the solubility of carrier in NPOE is limited and PIM is more viscous at very high carrier concentration (Pospiech 2015, 2021). Experimental studies allow to determine the appropriate composition of the membrane in the given process conditions.

Conclusions

PIMs are useful for the selective separation of copper (II) ion from the synthetic leach liquors of PCBs. Polymer membrane based on CTA (polymer matrix) with the ionic liquid [PR$_4$][TS] can be successfully used in the selectively recovering Cu(II) from the aqueous solutions containing Ni(II), Zn(II), and Fe(III) in hydrochloric acid solution. The results of the presented investigations proved that transport Cu(II) into 0.5 M sulfuric acid as the receiving phase was very fast and efficient. The highest flux of Cu(II) was obtained for the transport through PIM containing: 20 wt.% CTA, 30 wt.% [PR4][TS], 50 wt.% NPOE. The obtained results showed that recovery factor of Cu(II) ions from mixture containing Ni(II), Fe(III) and Zn(II) was over 91%.

REFERENCES

Andrade L.M., de Carvalho M.A., Caldas M.P.K., Espinosa D. and Tenòrio J. (2021) Recovery of copper and silver of Printed Circuit Boards from obsolete computers by one-step acid leaching. Detritus 4, 86–91, DOI: 10.31025/2611-4135/2021.14056.

Burat F. and Özer M. (2018) Physical separation route for printed circuit boards. Physicochemical Problems of Mineral Processing 54, 554–566, DOI: 10.5277/ppmp1858.

Cui J. and Zhang L. (2008) Metallurgical recovery of metals from electronic waste: a review. Journal of Hazardous Materials 158, 228–256.

Choubey P.K., Panda R., Jha M.K., Lee J.Ch. and Pathak D.D. (2015) Recovery of copper and recycling of acid from the leach liquor of discarded Printed Circuit Boards (PCBs). Separation and Purification Technology 156(2), 269–275, DOI: 10.1016/j.seppur.2015.10.012.

Danesi P.R. (1984) Separation of metal species by supported liquid membranes. Separation Science Technology 19(11–12), 857–894, DOI: 10.1080/01496398408068598.

Fisher L., Falta T., Koellensperger G., Stojanovic A. and Kogelnig D. (2011) Ionic liquids for extraction of metals and metal containing compounds from communal and industrial waste water. Water Research 45, 4601–4614, DOI: 10.1016/j.watres.2011.06.011.

Fuerhacker M., Haile T.M., Kogelnig D., Stojanovic A. and Keppler B. (2012) Application of ionic liquids for the removal of heavy metals from wastewater and activated sludge. Water Science Technology 65(10), 1765–1773, DOI: 10.2166/wst.2012.907.

Güel R., Antico E., Kolev S.D. and Benavente J. (2011) Development and characterization of polymer inclusion membranes for the separation and speciation of inorganic as species. Journal of Membrane Science 383(1), 88–95, DOI: 10.1016/j.memsci.2011.08.037.

Jadhav U. and Hocheng H. (2015) Hydrometallurgical recovery of metals from large printed circuit board pieces. Scientific Reports 5(1), DOI: 10.1038/srep14574.

Jaqub M., Eren B. and Eyupoglu V. (2021) Prediction of heavy metals removal by polymer inclusion membranes using machine learning techniques. Water Environment Journal 35, 1073–1084, DOI: 10.1111/wej.12699.

Kavitha N. and Palanivelu K. (2012) Recovery of copper through polymer inclusion membrane with di(2-ethylhexyl) phosphoric acid as carrier from e-waste. Journal of Membrane Science 415–416, 663–669, DOI: 10.1016/j.memsci.2012.05.047.

Kim E.Y., Kim M.S., Lee J.Ch., Jeong J. and Pandey B.D. (2011) Leaching kinetics of copper from waste printed circuit boards by electro-generated chlorine in HCl solution. Hydrometallurgy 107(3–4), 124–132, DOI: 10.1016/j.hydromet.2011.02.009.

Kumar M., Jae-Chun Lee J.Ch., Kim M.S., Jeong J. and Yoo K. (2014) Leaching of metals from waste printed circuit boards (WPCBs) using sulfuric and nitric acids. Environmental Engineering and Management Journal 13(10), 2601–2607, DOI: 10.30638/eemj.2014.290.

Le H., Jeong J., Lee J.Ch., Pandey B.D., Yoo J.M. and Huyunh T.H. (2011) Hydrometallurgical Process for Copper Recovery from Waste Printed Circuit Boards (PCBs). Mineral Processing and Extractive Metallargy Review 32(2), 90–104, DOI: 10.1080/08827508.2010.530720.

Li H., Eksteen J. and Oraby E. (2018) Hydrometallurgical recovery of metals from waste printed circuit boards(WPCBs): Current status and perspectives – A review. Resources, Conservation & Recycling 139, 122–139, DOI: 10.1016/j.resconrec.2018.08.007.

Leyma R., Platzer S., Jirsa F., Kandioller W. and Krachler R. (2016) Novel thiosalicylate-based ionic liquids for heavy metal extractions. Journal of Hazardous Materials 314, 164–171. DOI: 10.1016/j.jhazmat.2016.04.038.

Lukomska A., Wisniewska A., Dabrowski Z. and Domanska U. 2020. Liquid-liquid extraction of cobalt(II) and zinc(II) from aqueous solutions using novel ionic liquids as an extractants. Journal Molecular Liquids 307, DOI: 10.1016/j.molliq.2020.112955.

Makowka A. and Pospiech B. (2019) Synthesis of polymer inclusion membranes (PIM) based on cellulose triacetate (CTA) for recovery lanthanum(III) from aqueous solutions. AUTEX Research Journal 19(3), 288–292, DOI: 10.1515/aut-2018-0056.

Makowka A. and Pospiech B. (2020) Studies on extraction and competitive permeation of cerium(III) and lanthanum(III) using Cyphos IL 104 as selective extraction and ion carrier. Separation Science Technology 55(12), 2193–220, DOI: 10.1080/01496395.2019.1584635.

Noguyen V.H.N. and Lee M.S. (2020) Separation of Co(II), Cu(II), Ni(II) and Mn(II) from synthetic hydrochloric acid leaching solution of spent lithium ion batteries by solvent extraction, Physicochemical Problems of Mineral Processing 56(4), 599–610, DOI: 10.37190/ppmp/122784.

Panda R., Jha M.K., Pathak D.D. and Gupta R. (2020) Recovery of Ag, Cu, Ni and Fe from the nitrate leach liquor of waste ICs. Minerals Engineering (158), DOI: 10.1016/j.mineng.2020.106584.

Park Y., Eom Y., Yoo K., Jha M.K (2021) Leaching of copper from waste-printed circuit boards (PCBs) in sulfate medium using cupric ion and oxygen. Metals 11: 1369. DOI: 10.3390/met11091369.

Pospiech B. and Kujawski W. (2015) Ionic liquids as selective extractants and ion carriers of heavy metal ions from aqueous solutions utilized in extraction and membrane separation. Reviews in Chemical Engineering 31(2), 179–191, DOI: 10.1515/revce-2014-0048.

Pospiech B. (2015) Studies on extraction and permeation of cadmium(II) using Cyphos IL 104 as selective extractant and ion carrier. Hydrometallurgy 154, 88–94, DOI: 10.1016/j.hydromet.2015.04.007.

Pospiech B. and Makowka A. (2021) Application of plasticized cellulose triacetate membranes for recovery and separation of cerium(III) and lanthanum(III). AUTEX Research Journal, DOI: 10.2478/aut-2021-0019.

Wang L., Paimin R., Cattrall R., Shen W. and Kolev S.D. (2000) The extraction of cadmium(II) and copper(II) from hydrochloric acid solutions using an Aliquat 336/PVC membrane. Journal of Membrane Science 176(1), 105–112, DOI: 10.1016/S0376-7388(00)00436-1.

Wang D., Hu J., Liu D., Chen Q. and Li J. (2016) Evidence on the 2-nitrophenyl octyl ether (NPOE) facilitating copper(II) through polymer inclusion membranes. Journal of Membrane Science 501(1), 228–235, DOI: 10.1016/j.memsci.2015.12.013.

Wang D., Hu J., Liu D., Chen Q. and Li J. (2017) Selective transport and simultaneous separation of Cu(II), Zn(II) and Mg(II) using a dual polymer inclusion membrane system. Journal of Membrane Science 524, 205–213, DOI: 10.1016/j.memsci.2016.11.027.

Zhu Z., Zhang W. and Cheng C.Y. (2012) A synergistic solvent extraction system for separating copper from iron in high chloride concentration solutions. Hydrometallurgy 113–114, 155–159, DOI: 10.1016/j.hydromet.2011.12.016.

Edyta Strzelec

AGH University of Science and Technology, Poland; e-mail: strzelec@agh.edu.pl

Fermentation as a way of glycerin waste management towards lactic acid production

ABSTRACT: This work investigates the potential conversion of waste glycerin (other names: glycerol, glycerine) from biodiesel production into lactic acid (LA). After biodiesel production it is necessary to manage wastes e.g. glycerine. Waste glycerin is metabolized by microorganisms from the *Lactobacillus* family. Waste glycerine was used as a substrate for cultivation of several lactic acid bacteria (LAB). Among the screened microorganisms, *Lactobacillus rhamnosus*, ATCC7469; *Lactobacillus* plantarum, ATCC 8014; *Lactobacillus delbrueckii* WLP677 was identified as the most promising producer of LA. Therefore, it could be demonstrated that glycerol is a promising raw material for the production of lactic acid and could serve as a feedstock for the sustainable largescale production of lactic acid.

KEYWORDS: biotechnology, lactic acid, waste management, environmental protection

Introduction

Glycerin waste from biofuel production or food waste in the form of molasses, whey and other raw materials is an excellent material for further use in chemical processes. (Hofvendahl 2000; Krishna 2019).

Various paths enabling the maximum management of waste or its transformation into chemically and universally useful products have been searched for a long time (Mostafa 2012).

So far, the most attractive seems to be the production of lactic acid as a mer for polymerization into PLA (polylactic acid). This fits perfectly into the circular economy cycle, because looking at waste disposal, it tries to add a new technology for their processing to the already existing technologies for obtaining main products. On the example of glycerin, the entire cycle is presented in the following scheme (Ohleyer 1985; Senedese 2015; Sreenath 2001).
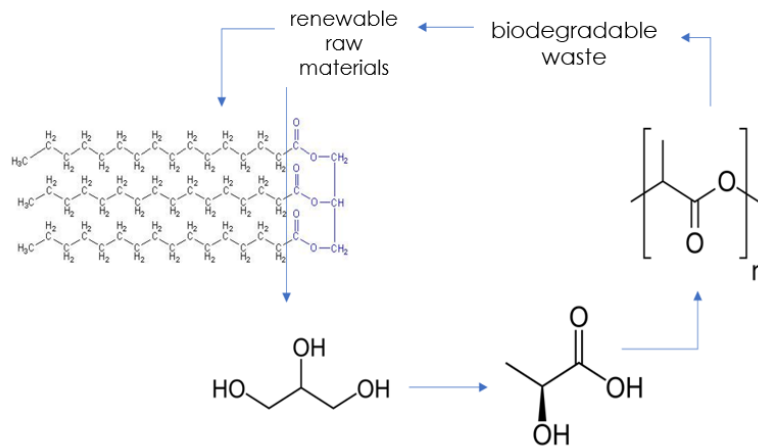
Figure 1.
Circular economy cycle with waste from biodiesel production

Lactic acid is an organic acid widely used in industrial applications. In the recent years, the interest towards lactic acid recovery from fermentation broth increases. This interest is caused by increasing in the demand of pure, naturally produced lactic acid. The most important applications are as a preservative and acidulant in foods, as a controlled delivery of drugs in pharmaceutical agents, as a precursor for production of polymer in plastic industries and in leather tanning and textile dyeing. World demand for lactic acid is estimated as $150 million (100,000 tones). About 50% of the
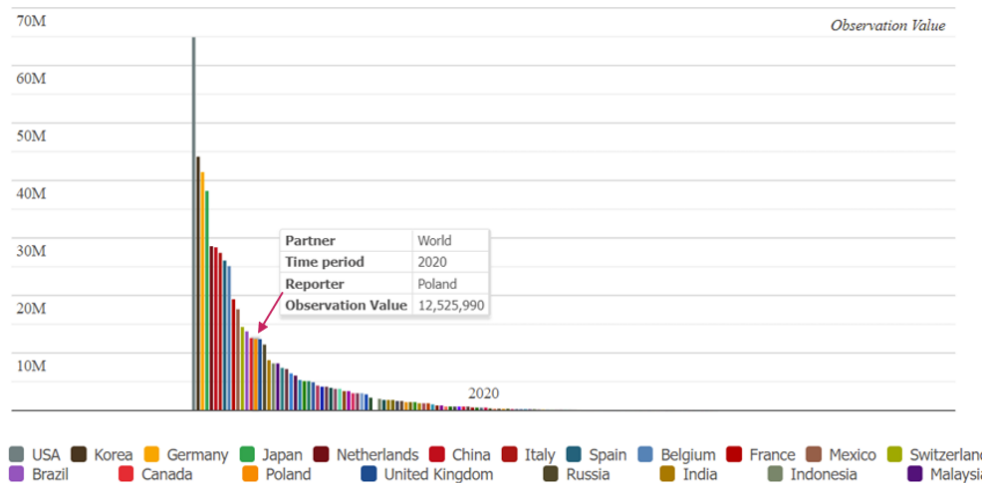

Figure 2.
Lactic acid – import in 2020 (from TrendEconomy) – Poland – 12,525,990 million US$
[units – US dollar; M – a million]

market is in food and beverage applications which are a mature and stable market. (Datta 2006; Lin 2020; Sreenath 2001; Tsapekos 2020; Wee 2006).

Fermentation is the important process for manufacturing of products with desirable biochemical characteristics with the aid of microorganisms or enzymes. Fermentation plays at least six the most important roles:

- enrichment of the diet through development of a diversity of flavours, aromas and textures in food substrates,
- preservation of food via lactic acid, ethanol, acetic acid and alkaline fermentations,
- biological upgrading of food substrates with proteins, essential amino acids, fatty acids and vitamins,
- detoxification in the course of food fermentation,
- saving cooking time and fuel requirements,
- biocatalysis in bioprocesses (for example production of lactic acid and others chemical compound).

LAB from ancient times have been used in production of traditional foodstuffs. LAB are important microorganisms involved in manufacturing various dairy products such as yogurt, kefir, cheese, butter and so on. The latter account for about 20% of the global output of fermented products. LAB can be divided into two groups depending on optimal growth temperature: mesophilic (20–30°C) and thermophilic (30–45°C). The flavour, texture and consistency may vary considerably when mesophilic or thermophilic cultures are used. Dairy industry mainly consumes starter cultures selected and maintained by subcultivation in milk.

The raw materials used as input material are above all cheap and readily available. They include: starch, whey, molasses, glycerin and others. Currently, lignocellulosic materials such as starch and cellulose are very popular due to their low cost and the fact that they are renewable. The starchy raw materials include: sorghum, corn, cassava, potatoes and many others. The problem, however, is that these materials have to be hydrolyzed to fermentable sugars, which are mainly glucose. On the other hand, cellulosic materials are used in fermentation in a fairly similar way to starch, but they often contain more complex molecules that must be broken down into fermentable fragments before fermentation (RedCorn et al. 2016).

Current research among scientists covers the production of lactic acid from pure cellulose by simultaneous saccharification and fermentation (SSF i.e. *simultaneous saccharification and* fermentation is a process that combines enzymatic hydrolysis with fermentation to obtain value-added products in a single step) from corn, waste paper or wood. In addition, wheat bran, straw or alfalfa fibers are tested for the production of lactic acid or other chemically attractive substances (Lee et al. 2004)

Some industrial wastes such as whey, molasses and glycerin are interesting substrates for the production of lactic acid. Whey is the main by-product of the dairy industry and contains lactose (sugar), protein, fat and mineral salts, which are elements quite important in fermentation into lactic acid using biocatalysts (bacteria). Molasses, on the other hand, is left over from the sugar manufacturing process and

usually contains a large amount of sucrose. The literature shows that the most common bacteria dealing with molasses in fermentation are *Escherichia coli, Lactobacillus delbrueckii*.

Glycerin, on the other hand, as one of these innovative ideas for its use as a raw material in fermentation, is used in cosmetics and pharmacy, and in other industries (Dobson et al. 2012; Sittijuda et al. 2021). However, the problem with glycerin begins when the post-process glycerin from the production of biodiesel is used, which is not purified. Only it undergoes the process of methanol recovery, which can be even 7–10%, which deactivates the biocatalysts used in fermentation.
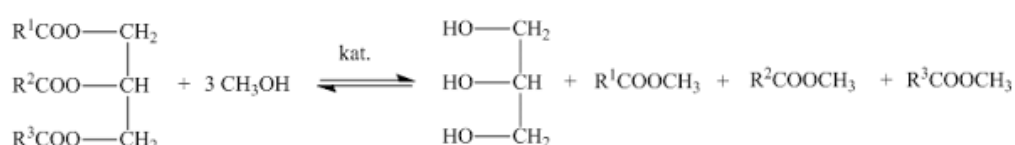
$$R^1COO-CH_2 \qquad \qquad HO-CH_2$$
$$R^2COO-CH \ + \ 3\,CH_3OH \ \underset{}{\overset{kat.}{\rightleftharpoons}} \ HO-CH \ + \ R^1COOCH_3 \ + \ R^2COOCH_3 \ + \ R^3COOCH_3$$
$$R^3COO-CH_2 \qquad \qquad HO-CH_2$$

Figure 3.
Scheme of the transesterification reaction with the use of methyl alcohol

The transesterification reaction shows the production of a biocomponent for biodiesel using oily substances as a raw material and alcohol with NaOH as a catalyst. The oily substance can be:

- substances of plant origin,
- substances of animal origin,
- used oils, used frying fats.

As can be seen from the reaction, according to data provided by refineries producing biofuels, one ton of raw material produces about two hundred kilograms of crude glycerol. It is subjected to a multi-stage purification process, thanks to which technical and pharmaceutical glycerin is obtained (Sittijuda et al. 2021).

2. Materials and methods

Many fermentation parameters in bioreactor have a significant effect in the growth and metabolic production of lactic acid such as temperature, pH, agitation speed, dissolved oxygen level etc. Growth kinetic study of the microbial cultures can be used to estimate the cost-effective production of lactic acidic large scale (Huang 2021; Mostafa 2012).

In case study, the bacteria were cultured in MRS medium in Erlenmeyer flasks. The medium temperature was adjusted according to the proposed temperature for the optimum growth of the respective organism, 37°C for the *L. plantarum*, 32°C for

L. rhamnosus and 37°C for *L. delbrueckii*. For each strain, several parallel fermentations were carried out with different conditions to obtain the highest cell growth.

In this study, he tries to use crude glycerol, only subjected to the alcohol recovery process, for economic reasons, i.e. cleaning costs. The purification process in its essence consists in decolorization of glycerol, vacuum distillation, the stage of purification on activated carbon beds and its deodorization. The cost of the crude glycerol purification steps mentioned influenced the decision to use crude, de-alcoholised glycerin.

Focusing on laboratory work, an element of innovation in experiments is the use of bacteria from publicly available sources. It is economical from the point of view of larger technologies where production costs have to be reduced. In addition, the research includes work on the optimization of parameters and the use of raw, unpurified, waste glycerin to reduce the costs of further processing, treatment or disposal. It seems to be needed nowadays by the greater awareness of the society.

In the available literature, research is being conducted on the possibilities of bacteria capable of processing waste compounds. However, these are usually genetically modified microorganisms, therefore their price is high. The research so far is based on the bacteria: *Escherichia coli* and selected *Lactobacillus* strains. This study shows that not only modified bacteria metabolize difficult waste compounds, but also those derived from cheap sources of dairy products. Their breeding and parameters are adapted to the low technological regime, thanks to which the process can be decidedly more economical.

3. Results

The influence of the medium on Lactobacillus strains is quite large. They are usually picky microorganisms with high nutritional and temperature requirements. Bacteria achieve their optimal growth on the third day of cultivation, and usually then their number is maximum. After this stage, bacterial growth slightly decreases over time.

The glycerol waste from petrochemical industry was used as carbon source for lactic acid production. Different bacteria from *Lactobacillus* family were tested for their growth behavior and lactic acid production ability. Effects of some parameters such as temperature, inoculum size, substrate dilution, has not yet been thoroughly tested for selected bacteria. This research is under preparation. On the other hand, the data collected from the preliminary measurement tests show that the optimal growth temperature of bacteria allows for their maximum number and during fermentation they allow the conversion of glycerin to lactic acid, which requires confirmation by HPLC. The research focused on the temperature parameter, which is practically the most important. (Abedi 2020; Coehlo 2011; Rojan 2006; Shamala 1988).
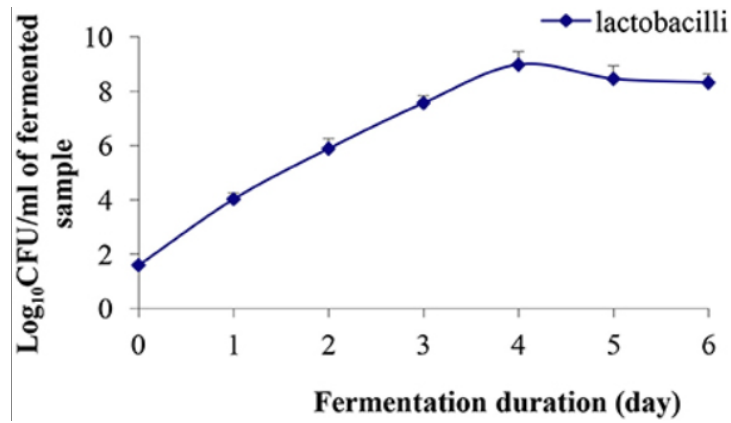
Figure 4.
An example of the influence of temperature on the growth of bacteria
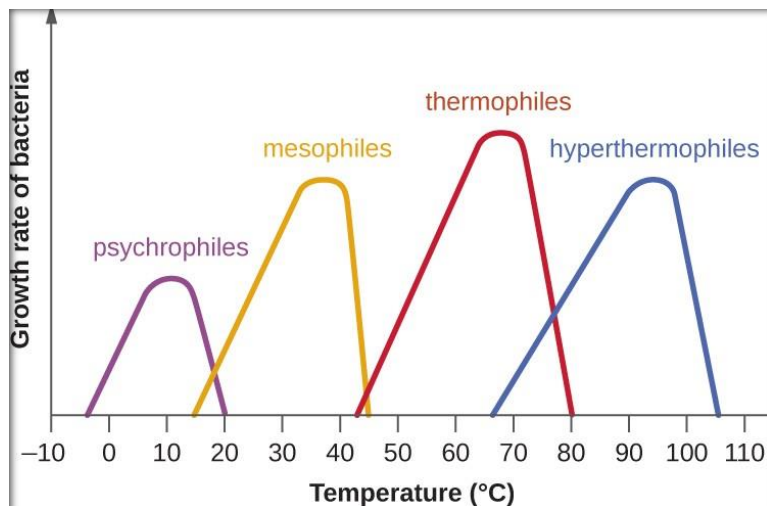
Figure 5.
Bacteria temperature tolerance chart

Preliminary tests were performed using appropriate concentrations of glycerol. The influence of the amount of glycerol on the growth of selected bacteria as well as the influence of temperature and time on the metabolism of the raw material was investigated.

The graphs below show the results obtained in individual fermentations with the use of glycerol as a raw material (in various concentrations) as a function of temperature.

For *Lactobacillus plantarum* and various glycerol concentrations:

Figure 6.
Lactobacillus plantarum growth on MRS medium with glycerol (0,25; 0,5; 2; 5%)

For *Lactobacillus rhamnosus* and various glycerol concentrations:

Figure 7.
Lactobacillus rhamnosus growth on MRS medium with glycerol (0,25; 0,5; 2; 5%)
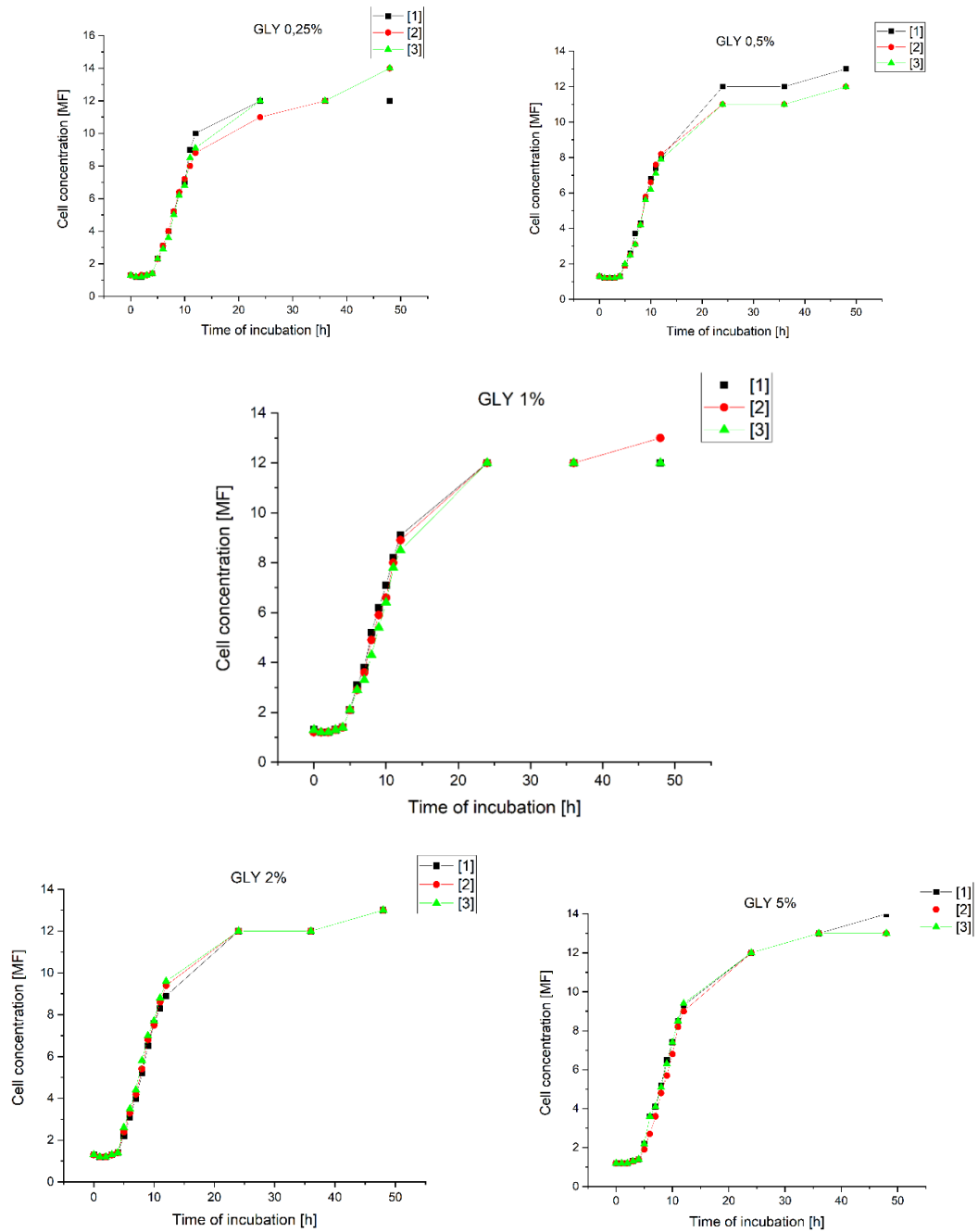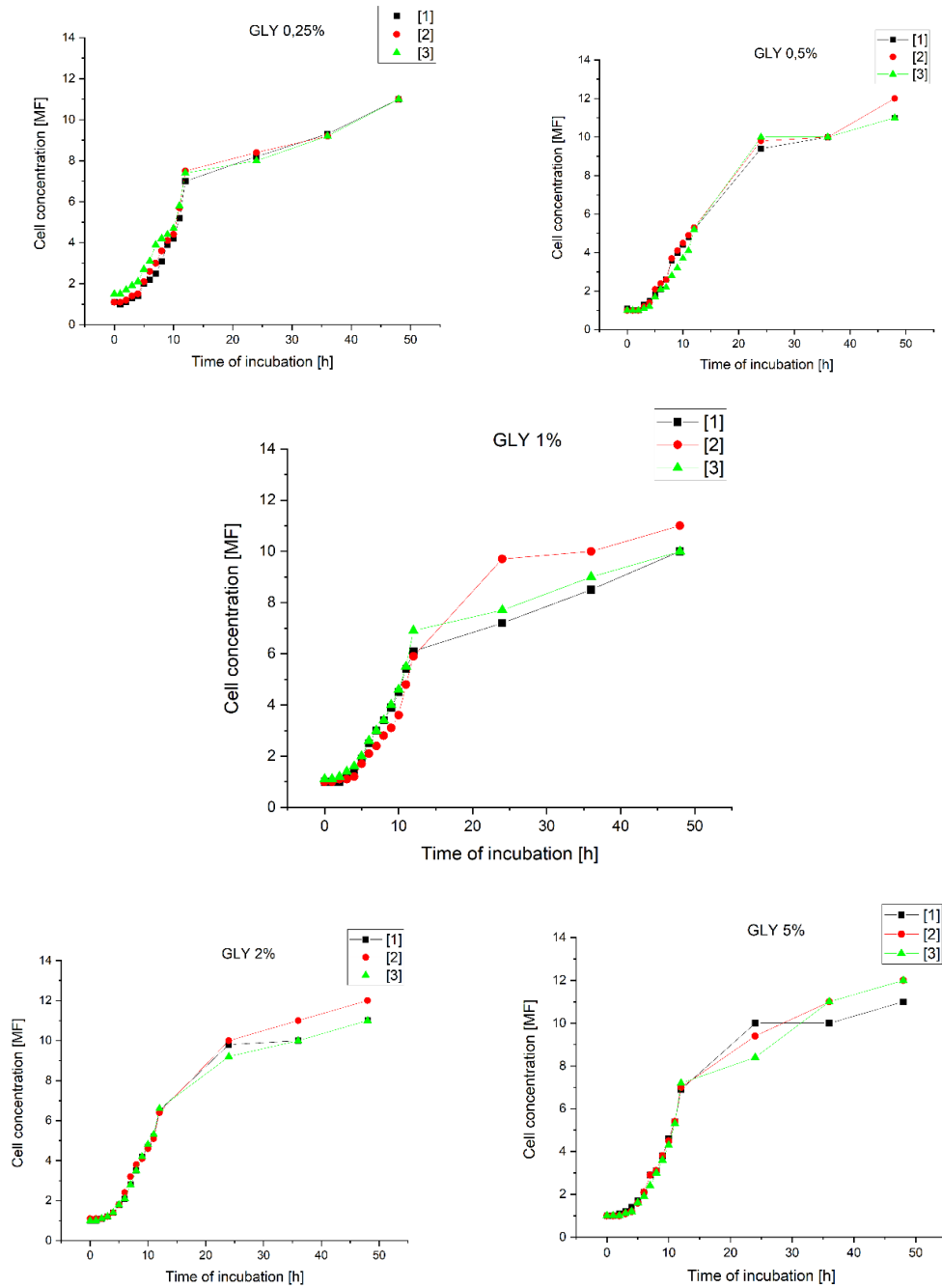
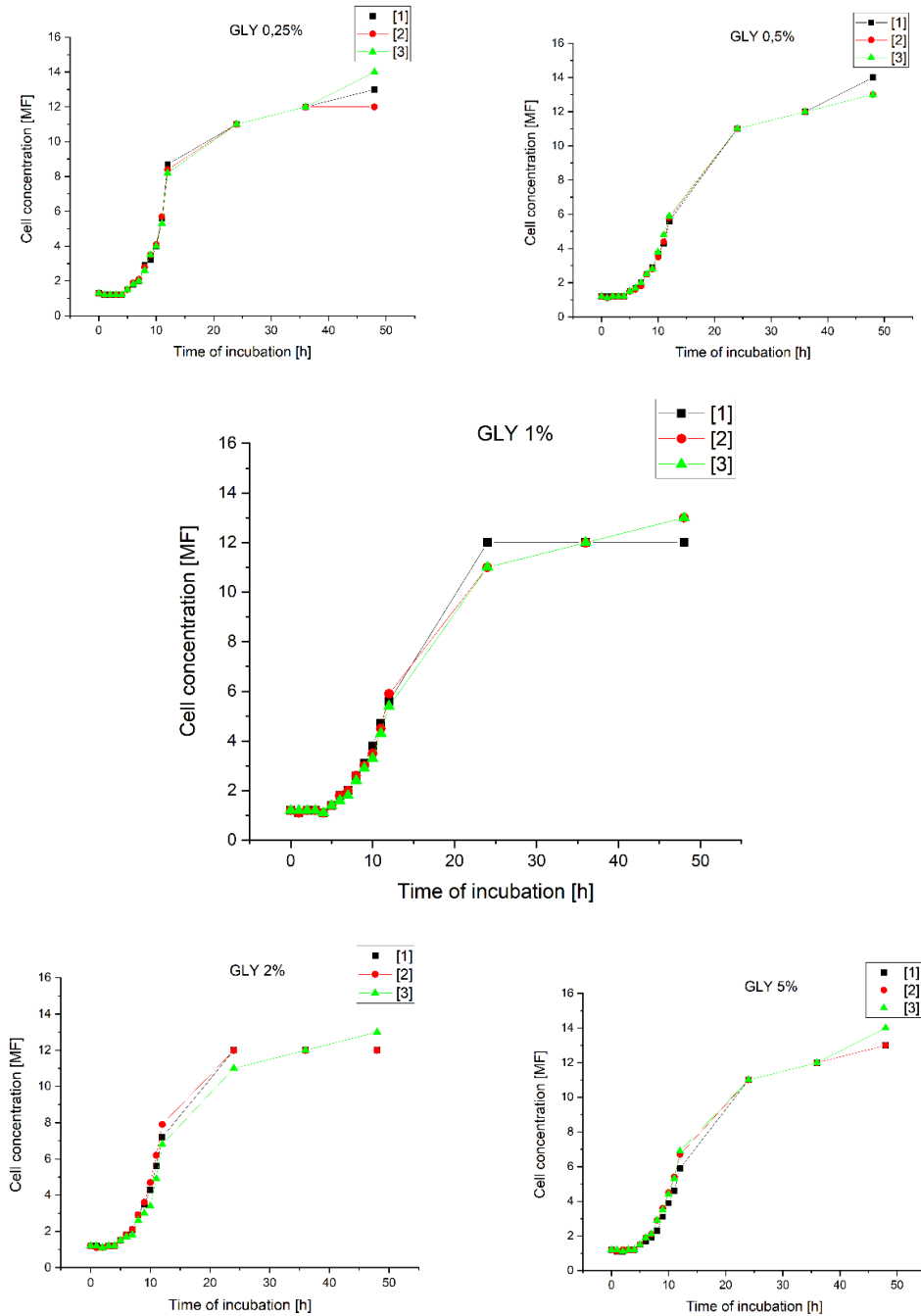For *Lactobacillus delbrueckii* and various glycerol concentrations:

Figure 8.
Lactobacillus delbrueckii growth on MRS medium with glycerol (0,25; 0,5; 2; 5%)

An example of the use of bacteria with the use of glycerin and other raw materials that are a source of carbon for bacteria is presented in the table 1 below:

Table 1.

Examples of the amount of produced lactic acid for selected bacteria

Organism	LA [g/L]
Lb. delbrueckii ATCC 9649	58
Lb. plantarum NRRL B-531	17
Lb. rhamnosus ATCC 10863	17

LAB (*lactic acid bacteria*) represent a diverse microbial group united by the ability to produce lactic acid from various substrates. The first pure culture of LAB, now known as Lactococcus lactis, was isolated in 1873 by Lister. Originally the term "lactic acid bacteria" denoted "milk souring organisms," but it came out of use after publication of the monograph by Orla-Jensen (1919) formulating the principles of modern LAB classification. Taxonomic affiliation of the bacteria based on cellular morphology, mode of glucose fermentation, growth temperatures and range of sugar utilization distinguished four core genera: *Lactobacillus*, *Leuconostoc*, *Pediococcus* and *Streptococcus* (Al-Dhabi et al. 2020; Zhang et al. 2021).

Glycerol is a cheap, abundant, and simple molecule, which can be taken up into the microbial cell by facilitated diffusion, and a number of microorganisms have metabolic pathways that can convert glycerol into different metabolic intermediates. This is because glycerol is found abundantly in nature in the form of triglycerides, the chemical combinations of glycerol and fatty acids (Sittijuda et al. 2021).

In addition, glycerol is a highly reduced carbon source , which means that it can be used as a platform for the anaerobic production of chemicals of a reduced nature. Dissimilation of glycerol in microorganisms, in fermentative metabolism, is strictly linked to their ability to produce the highly reduced product 1,3-PD (propanediol). This process involves two pathways which are responsible for the metabolism of the carbon substrate. These pathways are widely known but not fully understood and this is a limiting factor in fermentative studies (El-Sheshtawy et al. 2022; Lee et al. 2004).

Because of LAB (lactic acid bacteria) beneficial properties, their correct identification is vital for further industrial and medical use. LAB are Gram-positive rods and cocci characterized by the absence of catalase, tolerance to low pH values and lack of spore formation. LAB produce ATP (energy carrier) predominantly by fermentation of sugars. The distinctive feature of LAB is production of lactic acid. They are chemotrophic microorganisms deriving necessary energy from oxidation of chemical compounds, especially sugars. There are two fermentation pathways: homofermentative and heterofermentative. Homofermentative bacteria produce lactic acid as the major metabolite through glycolysis or Embden-Meyerhof-Parnas pathway generating two

moles of lactate per mole of glucose. Pentoses and gluconate are not fermented by microorganisms via obligate homofermentative pathway due to lack of enzyme (Lech et al. 2019; Sittijuda et al. 2021). In turn, heterofermentative microorganisms using pentose phosphoketolase pathway produce lactate, CO_2 and ethanol. LAB are applied in food production and preservation from the ancient times. Nowadays, LAB find wide use in various areas such as synthesis of chemicals and pharmaceuticals or manufacturing of probiotics for agriculture and medicine. Nevertheless, food industry remains to be the domain of broad LAB application. LAB strains were granted "Qualified Presumption of Safety" and "Generally Regarded as Safe" status by the European Food Safety Authority (EFSA) and Food and Agriculture Organization of the United Nations (FAO), respectively. They are used in manufacturing of dairy, meat, baking and vegetable products all over the world. These bacteria also allay product allergenicity and ensure longer preservation of fermented foods. LAB can be involved in the delivery of functional biomolecules and ingredients into high quality gluten-free cereal products. In the seafood industry, LAB are usually applied for product conservation, with the exception of traditional fish sauces in Southeast Asia. In recent years, novel fish products with various flavour and biochemical characteristics have been developed (Dobson et al. 2012; Lee et al. 2004).

For lactic acid to be commercially attractive, economically efficient and environmentally sound manufacturing processes are needed for its production. Recent announcements of new lactic acid production plants by major chemical and agrochemical companies might usher in new technologies for the efficient, low-cost manufacture of lactic acid and its derivatives for new applications (RedCorn et al. 2016).

4. Discussion

The results of this work show that the bacteria used in the fermentations are suitable biocatalysts for the production of LA from glycerin. As can be seen in the graphs, glycerin does not inhibit the growth of bacteria (despite the fact that it is a triple-substituted alcohol hydroxyl group). It can also be stated on the basis of other articles that selected bacteria metabolized glycerin in their life processes. Also, it should be emphasized that the successive increase of the concentration in subsequent experiments has its grounds confirmed by these tests. The MRS broth medium, which was used for the development of microorganisms, coped perfectly with the parameters and conditions of breeding.

This work showed that the production of LA in a liquid medium with the addition of glycerin with the participation of *L. rhamnosus, L. delbrueckii, L. plantarum* can be considered as very a promising and suitable process that could then be incorporated into a biorefinery concept. Therefore, future research should be directed to studying the effects of higher concentrations of crude glycerin and on development bioreac-

tors able to simultaneously recover lactic acid and have the possibility of recycling bacteria which, after fermentation, are still suitable as biocatalysts for subsequent processes (which was shown in the graphs in the last phase of their growth).

Conclusions

According to this article, the importance of lactic acid can be observed due to its wide use and obtaining from waste materials from the petrochemical and food industries. The literature describes many of the uses of lactic acid, such as cosmetics, pharmaceuticals, chemicals, food, and more recently in medicine. The greatest demand is in food and polymer applications. Lactic acid produced by the fermentation process has several advantages: low substrate costs, production temperature and energy consumption. However, the production of lactic acid is still limited by the final production cost which is associated with a downstream process which requires many steps and makes the process expensive. Therefore, it is imperative to develop more efficient and cost-effective technologies.

Rising consumer awareness with respect to the need for recyclability, green packaging, and sustainability is driving significant demand globally. Unlike conventional plastic, PLA does not take decades to degrade, and as such, reduces adverse environmental impact.

REFERENCES

Abedi E. and Hashemi S.M.B. (2020) Lactic acid production – producting microorganisms and substrates sources-state of art. Heliyon 6(10), DOI: 10.1016/j.heliyon.2020.e04974.

Al-Dhabi N.A., Esmail G.A. and Arasu M.V. (2020) Co-Fermentation of Food Waste and Municipal Sludge from the Saudi Arabian Environment to Improve Lactic Acid Production by *Lactobacillus rhamnosus* AW3 Isolated from Date Processing Waste. Sustainability 12(17), DOI: DOI:10.3390/su12176899.

Coelho L.F., Lima C.J.B., Rodovalho C.M., Bernardo M.P. and Contiero J. (2011) Lactic Acid Production by new *Lactobacillus plantarum* LMISM6 grown in molasses: optimization of medium composition. Brazilian Journal of Chemical Engineering 28(01), 27–36.

Datta R. and Henry M. (2006) Rewiev Lactic acid: recent advances in products, processes and technologies-a review. Jurnal of Chemical Technology and Biotechnology 81, 1119–1129.

Dobson R., Gray V. and Rumbold K. (2012) Microbial utilization of crude glycerol for the production of value-added products. Journal Industry Microbiology and Biotechnology 9, 217–226.

El-Sheshtawy H.S., Fahim I., Hosny M. and El-Badry M.A. (2022) Optimization of lactic acid production from agro-industrial wastes produced by *Kosakonia cowanii*. Current Research in Green and Sustainable Chemistry 5, DOI: 10.1016/j.crgsc.2021.100228.

Hofvendahl K. and Hahn-Hagerdal B. (2000) Factors affecting the fermentative lactic acid production from renewable resources. Enzyme and Microbial Technology 26, 87–107, DOI: 10.1016/s0141-0229(99)00155-6.

Huang S., Xu Y., Yu B., Wang L., Zhou C. and Ma Y. (2021) A Review of the Recent Developments in the Bioproduction of Polylactic Acid and Its Precursors Optically Pure Lactic Acids. Molecules 26, DOI: 10.3390/molecules 26216446.

Krishna B.S., Nikhilesh G.S.S., Tarun B., Saibaba K.V.N. and Gopinadh R. (2019) Industrial production of lactic acid and its applications. Int. J. Biotech. Res 1(1), 42–54.

Lech M. and Trusek A. (2019) Selection of batch process conditions for microbiological production of lactic acid using waste whey. Chemical and Process Engineering 40(1), 67–76, DOI: 10.24425/cpe.2019.125101.

Lee S-M., Koo Y-M. and Lin J. (2004) Production of Lactic Acid from Paper Sludge by Simultaneous Saccharification and Fermentation. Advances Biochemistry Engineering and Biotechnology 87, 173–194, DOI: 10.1007/b94365.

Lin H-T.V., Huang M-Y., Kao T-Y., Lu W-J., Lin H-J. and Pan C-L. (2020) Production of Lactic Acid from Seaweed Hydrolysates via Lactic Acid Bacteria Fermentation. Fermentation 6(1), DOI: 10.3390/fermentation6010037.

Mostafa S.S.M., Shalaby E.A. and Mohamoud G.I. (2012) Cultivating Microalgae in Domestic Wastewater for Biodiesel Production. Notulae Scientia Biologicae 4(1), 56–65, DOI: 10.15835/nsb417298.

Ohleyer E., Blanch H.W. and Wilke C.R. (1985) Continuous production of Lactic Acid in a Cell Recycle Reactor. Applied Biochemistry and Biotechnology 11, 317–332, DOI: 10.1007/BF02798444.

RedCorn R. and Engelberth A. S. (2016) Identifying conditions to optimize lactic acid production from food waste co-digested with primary sludge. Biochemical Engineering Journal 105(A), 205–213, DOI: 10.1016/j.bej.2015.09.014.

Rojan P.J., Nampoothiri K.M. and Pandey A. (2006) Fermentative production of lactic acid from biomass: an overview o process developments and future perspectives. Applied Microbiology and Biotechnology 74, 524–534, DOI: 10.1007/s00253-006-0779-6.

Senedese A.L.C., Filho R.M. and Macciel M.R.W. (2015) L-Lactic Acid Production by *Lacctobacillus rhamnosus* ATCC 10863. The Scientific World Journal 2015, DOI: 10.1155/2015/501029.

Shamala T.R. and Sreekantiah K.R. (1988) Fermentation of starch hydrolysates by *Lactobacillus plantarum*. Journal of Industrial Microbiology 3, 175–178.

Sittijunda S., Sitthikitpanya N., Plangklang P. and Reungsang A. (2021) Two-Stage Anaerobic Codigestion of Crude Glycerol and Micro-Algal Biomass for Biohydrogen and Methane Production by Anaerobic Sludge Consortium. Fermentation 7, DOI: 10.3390/fermentation7030175.

Sreenath H.K., Moldes A.B., Koegel R.G. and Straub R.J. (2001) Lactic Acid Production by Simultaneous Saccharification and Fermentation of Alfalfa Fiber. Journal of Bioscience and Bioengineering 92(6), 518–523, DOI: 10.1016/S1389-1723(01)80309-1.

Tsapekos P., Alvarado-Morales M., Baladi S., Bosma E.F. and Angelidaki I. (2020) Fermentative Production of Lactic Acid as a Sustainable Approach to Valorize Household Bio-Waste. Frontiers in Sustainability 1, DOI: 10.3389/frsus.2020.00004.

Wee Y-J., Kim J-N. and Ryu H-W. (2006) Biotechnological Production of Lactic Acid and Its Recent Applications. Food Technology and Biotechnology 44(2), 163–172.

Zhang Z., Tsapekos P., Alvarado-Morales M. and Angelidaki I. (2021) Impact of storage duration and micro-aeroic conditions on lactic acid production from food waste. Bioresource Technology 323, DOI: 10.1016/j.biortech.2020.124618.

Magdalena Osial[1,2], Paulina Pietrzyk[1], Weronika Urbańska[3],*

[1] *University of Warsaw, Poland*

[2] *Institute of the Fundamental Technological Research, Polish Academy of Sciences, Poland*

[3] *Wrocław University of Science and Technology, Poland; e-mail*: weronika.urbanska@pwr.edu.pl*

Tetracycline pollution treatment – current trends in water remediation

ABSTRACT: Water pollution caused by antibiotics is a global environmental problem leading to the spread of antibiotic-resistant bacterial strains, and adverse effects on health and ecosystems. One of the most widespread antibiotics in the soil and water is tetracycline, often used in veterinary treatment. Over 75% of this drug is exerted with biological fluids and gets to the environment. There are many solutions proposed to deal this problem, where the recent literature presents various aspects of tetracycline (TC), including monitoring techniques, TC degradation, and its removal from wastewater. In this work, we present a concise overview of the TC treatment techniques, especially with the solutions that are based on nanotechnology.

KEYWORDS: water pollution, antibiotics, water remediation, wastewater treatment, tetracycline

Introduction

Recent industry progress drastically affected the environment causing the release of toxic compounds to the soil and water (Philip et al. 2018; Rathi et al. 2021; Inyinbor et al. 2017). Besides many emerging contaminants, many of them can also be found in drinking water, personal care products, and food. One of the largest groups of emerging contaminants is antibiotics, widely used to treat several diseases at both human and animal treatment. Due to their wide application, their metabolites easily get to the environment (Song et al. 2010; Łukaszewicz et al. 2017). Moreover, the fast and easy migration of such compounds to drinking water may also have severe consequences for public health. Antibiotics are released to the surface water, seawater, groundwater, soil, and sludge, easily exposed to the biota. Extensive antibiotics use results in developing antibiotic-resistant ABR bacteria strains, becoming a serious problem and difficult to defeat (Ventola 2015; Kongkham et al. 2020). ABR of bacteria

leads to the fast spread of diseases (Aslam et al. 2018). The pharmaceuticals used to defeat bacterial infections, and their metabolites in the aquatic environment affect all organisms. Antibiotics can also accumulate in vegetables, aquatic plants, crops, animals, and even animal-derived products like milk, honey, and meat (Gothwal and Shashidhar 2014).

Several types of antibiotics have different therapeutic properties and mechanisms of action in the body, differing the chemical composition. The most common ones are: aminoglycosides, β-lactams, carbapenems, chloramphenicol, fluoroquinolones, glycopeptides, lincomycin, macrolides, monobactams, polyenes, polypeptides, quinolones, rifamycin, tetracyclines, and sulfonamides (Gothwal & Shashidhar 2014), while the tetracycline (TC) is one of the most spread in the environment (Manyi-Loh et al. 2018; Hejduk et al. 2021). This antibiotic is widely used for bacterial infections treatment in humans and animals and for agricultural purposes. Over 75% of TCs are excreted in an active form with the urine and feces, directly affecting the whole ecosystem. Though tetracycline-based antibiotics presented in figure 1 reveal benefits to health dealing with severe bacterial infections. Its overuse is associated with the ABR bacterial strains development, allergic reactions, and significant fluctuations in environmental microflora in humans and animals.
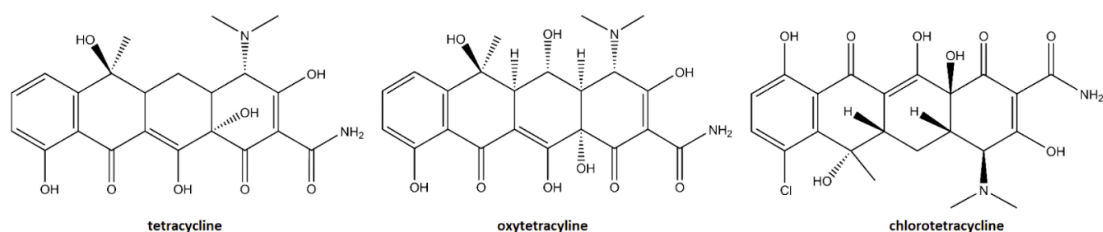
Figure 1.
Structures of tetracycline, oxytetracycline, and chlortetracycline

In Soares et al. (2021), it is presented that tetracycline negatively impacts the health of the bees affecting their gut microbiota (Soares et al. 2021). Tetracycline exposure is also associated with decreased relative abundances of several bee species. In Zhao et al. (2015) the complexity of the tetracycline reactions leading to the toxic degradation products is presented, where the UV light and free radicals are the main factors affecting TC structure that are toxic to zebrafish embryos. It confirms the huge need for the removal of these compounds from the water to avoid contact with organisms (Zhao et al. 2020).

Tetracycline has adverse effects on intestinal epithelial cells. It causes a barrier disruption in even small concentrations ranging from 15 to 150 μg mL^{-1} (Gokulan et al. 2017). Another research refers to the negative impacts on eye retinal cells (Salimiaghdam et al. 2022). The most important influence for humans and other animals is antibiotic resistance development. The scientist's study influences TC for larva honey

bees. The results are disturbing, where the lethal dose of the half population is about 125.25 μg mL^{-1} (Aljedani. 2021). TC poses a severe threat to sea animals; for example, tilapia, this antibiotic disrupts the work of the gills, oxidation stress, and induces various inflammatory reactions (Xu et al. 2022).

1. Strategies towards the TC treatment

Since TC is one of the main antibiotic-based contaminants in aquatic systems, its treatment is highly needed. Although antibiotics and their metabolites are monitored and easily detected, there is still a lack of systemic solutions preventing the environment from pollution with these contaminants. Many techniques are used to decrease the TC and its metabolites in an environment, including ozonation, Fenton process, photolysis, sonolysis/sonochemical oxidation, microbial treatment, enzymatic degradation, and adsorption. Each method has its merits and demerits. The best strategy would be highly effective, low-cost, environmentally friendly, and scalable to be applied on an industrial scale. The most commonly used are based on the TC degradation within the free radicals or UV-light in the presence of chemical factors. Generally, the degradation of TC leads to the breakdown of this molecule to the secondary metabolites that are supposed to be less toxic than the primary compound.

1.1. Catalytic and photocatalytic degradation of TC

Ozone is much more efficient than chloride, making it one of the most effective techniques in wastewater treatment, where the ozone is used to remove organic pollutants or inactivate pathogens by producing highly reactive radicals (Iakovides et al. 2019). This highly reactive gas reacts via cycloaddition to double bonds like C = C, C = N, N = N, and generation of HO• radicals that affect molecules. In case of the tetracycline treatment, the ozonation can be boosted within the catalysts (Nawrocki and Kasprzyk-Hordern 2010). Literature refers many different catalysts like metal oxide semiconductors and composites like silica ore supported silicate ore supported Co_3O_4 (Luo et al. 2018), Ce-doped $Mn_3Gd_{7-x}Ce_x(SiO_4)_6O_{1.5}$ (Fu et al. 2019), ZnO (Mohsin et al. 2021), ZnO/γ-Fe_2O_3 (Semeraro et al. 2020), CeO_2–TiO_2) (Zhu et al. 2012), Bi_2WO_6 (Lu et al. 2021). In (Olusegun et al. 2021) Olusegun et al. proposed application of superparamagnetic iron oxide nanoparticles offering high efficiency TC photodegradation.

Besides the ozonation, another method is the Fenton process based on the reaction between the Fe^{2+} ion and hydrogen peroxide, leading to the generation of free radicals affecting other molecules. Fenton-like reactions can also be used where copper or cobalt ions can be used instead of iron. In (Yamal-Turbay et al. 2013) tetracycline

degradation is performed in function of the H_2O_2 dosage. With the increase of H_2O_2, the amount of the free radical rises leading to the effective TC treatment. The Fenton catalytic process also can be enhanced by the application of various materials Fe_3O_4 nanospheres (Hou et al. 2016; Nie et al. 2020), $Fe_3O_4@SiO_2$ submicrospheres (Cai et al. 2021), carbon-bridge-modified malonamide (MLD)/g-C_3N_4 (CN) (Zhang et al. 2021), magnetic $MnFe_2O_4$ and $MnFe_2O_4$/biochar composite (Lai et al. 2019), graphene oxide (GO) and cobalt-phthalocyanine (CoPc) based magnetic composite like $Fe_3O_4@GO$-CoPc (Huang et al. 2022), magnetic polydopamine Au-Fenton catalyst ($Fe_3O_4@PDA/Au$) (Zhai et al. 2021). Literature also shows the effect of the inorganic anions and cations on the degradation of TC revealing effectiveness UV-induced Fenton process, in the following order: $HPO_4^{2-} > HCO_3^- \gg SO_4^{2-} > Cl^-$ and $Cu^{2+} \gg Ca^{2+} > Na^+$ (Han et al. 2020).

Besides many techniques, tetracycline can be adsorbed and degraded with the application of Fenton catalysts and ozone, as well as different catalysts and photocatalysts. Oxidative degradation of pharmaceutical compounds like TC using such photocatalysts is a viable option due to their simplicity and low-costs. The most popular semiconductor used for photocatalysis is TiO_2. It works under the UV light for its wide band gap of about 3.2 eV (Zhu et al. 2013) being suitable for TC degradation. Nagamine et al. refers to the effective photodegradation of TC with semiconducting CdS (Nagamine et al. 2020). SnO_2 and CeO_2 are also exploited for photodegradation of TC. The researchers used the mixed oxides consisting of cerium and tin prepared by hydrothermal methods assisted with sonication. Receiving band gap in the range of 2.78–2.91 eV and degradation of TC at the level 97% after 120 minutes (Mohammad et al. 2021).

Other photocatalytic systems are reported in the literature for tetracycline degradation, however, they are either using UV light or they are more complex, involving heterogeneous composites and hybrid systems, where one of the main component is TiO_2 responsible for effective TC degradation under the UV-light. Literature presents many composites based on TiO_2 opening possibilities to apply not only UV, but also the visible light. In He et al. 2020 highly-oriented one-dimensional (1D) MIL-100(Fe)/TiO_2 is presented. Li et al. 2018 refers the application of the CdS-TiO_2, while Djouadi et al. 2018 presents the Bi_2S_3/TiO_2–montmorillonite nanocomposites as an effective composite for TC treatment making it possible to degrade that drug in both, UV and visible range of the solar radiation. Literature also refers another composites application that are based on the other hybrids like Cu_2O–TiO_2 (Shi et al. 2016), multiwall carbon nanotubes-MWCNT/TiO_2 (Ahmadi et al. 2017), TiO_2/activated carbon (Martins et al. 2017), ternary heterogeneous BiOCl/TiO_2/sepiolite (Hu et al. 2019), ternary NCQDs-BiOBr-TiO_2 (Luo et al. 2021), 3D IO-TiO_2-CdS nanocomposite (Lv et al. 2021), AgI/N–TiO_2 (Tung et al. 2020), yolk-shell structured $Fe_3O_4@void@TiO_2$ (), ternary composites including MGO-Ce-TiO_2 (Cao et al. 2016). Zhang et al. 2022 shows the synergetic enhancement of piezo catalytic performance to remove tetracycline by $K_2Ti_6O_{13}$/TiO_2 nanocomposite including the derived free radicals mechanism of TC degradation (Zhang et al. 2022).

Besides the TiO_2 also other semiconductors can be used including CdS, zinc and ceria oxide, bismuth oxide and other metals and their oxides like $FeNi_3/SiO_2/ZnO$ (Nasseh et al. 2020), PtO-ZnO (Reda et al. 2021), $Sr-Bi_2O_3$ (Niu et al. 2013), SnO/CeO_2 (Zhang et al. 2020), and $CeO_2/Bi_2O_2CO_3$ (Lai et al. 2021), $Ag/Ag_2CO_3/BiVO_4$ (Liu et al. 2018), and $IO-TiO_2-CdS$ (Lv et al. 2021). The bandgap of these composites is suitable for effective TC treatment. Another references describe application of a tribo-positive $Fe@MoS_2$ piezocatalyst (Meng et al. 2020) as an effective material for TC degradation, while other sources propose the use of the following compounds: $In_2O_3@ZnFe_2O_4$ heterojunction (Fei et al. 2019), $FeNi_3$ (Khodadadi et al. 2018; Nasseh et al. 2018), magnetite (Lee et al. 2021), copper sulfide $Cu_{31}S_{16}$ and Cu_7S_4 nanoparticles (Ravele et al. 2021), or even composites like zinc oxide coupled with porous hydroxyapatite mineral (Bekkali et al. 2018), ZnO composite with nanocellulose (Soltani et al. 2019). Depending on the chemical composition the band gap of materials vary. Literature refers the following materials having particular band gaps for the TC treatment as well: 3.37 eV for ZnO (Rahimi et al. 2022), 1.4 eV for CuO (Kumar et al. 2020), 2.17 eV for Cu_2O (Su et al. 2018), SnO has a wide band gap of 2.7–3.2 eV (Shahvelayati et al. 2022), CeO_2 3.5 eV (Mohanty and Nayak 2021), 3.55–3.75 eV In_2O_3 (Almontasser and Parveen 2022), 2.5–3.0 eV for WO_3 (Piriyanon et al. 2021), 2.8 eV for Fe_3O_4 (Lima et al. 2020), 2.1 eV for Fe_2O_3 (Kumar et al. 2019), but within the doping this value can be changed.

Carbon based composites are also widely used for the water remediation, while their hybrids with photocatalysts boost the degradation of TC. Bera et al. in 2015 described the application of the reduced Graphene Oxide/CdS nanosheet increasing the active surface of the applied semiconductor through the use of carbon based material. Li et al. in 2016 presented synergistic effects of silver ions and carbon dots $Ag^+-CDs-Bi_2WO_6$ (Li et al. 2016), while other sources also refers enhancement of the TC degradation when the carbon based materials are incorporated into the hybrid like $WO_3/g-C_3N_4$ composite (Xiao et al. 2018), ZnO nanorods and K-Doped Exfoliated $g-C_3N_4$ nanosheets (Jin et al. 2020), needle-like SnO_2 nanoparticles anchored on exfoliated $g-C_3N_4$ (Oluwole et al. 2022), Ag_3PO_4/GO (Wu et al. 2019), metal organic frameworks could with graphene oxide $Zr/Fe-MOFs/GO$ (Wei et al. 2021), while Kakavandi et al. in 2019 presented hybrid system based on the TiO_2 decorated and magnetic nanoparticles deposited onto the activated carbon (MAC@T) coupled ultrasounds and photoassisted degradation, while literature also refers the application of activated carbon supported $ZnO/ZnWO_4$ nanocomposite (Raizada et al. 2017), and graphene oxide/calcium alginate composite fibers (Zhu et al. 2018).

Generally, photodegradation generates free radical molecules responsible for the further degradation of the compounds. For example, Sun et al. (Sun et al. 2022) used $CuyMn5-yOx/hG$ as a catalyst for the photo-assisted degradation of TC and then presented results on the toxicity of the post-treatment products. Microtox test based on the photobacterium Vibrio fischeri has shown that the application of semiconductors reduces the toxicity of the TC's photodegradation products. In (Fang et al. 2022) the TC degradation mechanism and the toxicity of TC were investigated. Studies have

shown that the biological toxicity of the photodegradation products was negligible. On the other hand, Jiao et al. (Jiao et al. 2008) showed that photodegradation can lead to toxic products when performed only by UV light without semiconductors application. Other work presented by Yang et al. (Yang et al. 2021) share the metabolic pathway of tetracycline by humic acid on III areas of the mass of the TC photodegradation products: 180–230 m/z, 230–380 m/z, and 380–450 m/z. Results pointed out that the most toxic products have an average mass equal to 201.1 m/z, where the toxicity distribution of TET transformation products first increased and then decreased with the ring destruction of the molecular structure during the oxidation process. Moreover, the medium molecular weight intermediates with bicyclic or tricyclic structures posed more significant toxicity. The indirect product of decomposition tetracycline proved to have higher toxicity than the pristine TC compound.

Based on such studies, it can be said that the use of semiconductors for photodegradation of TC enhances the decomposition of tetracycline to small, less toxic, or non-toxic molecules in comparison to bare photodegradation without semiconductors use.

2. Biodegradation

TC degradation can be also performed within the application with microorganisms (Ahmad et al. 2021). Mechanism degradation of TC is complex and may occur within several pathways like isomerisation, dehydration, substitution, and oxygenation (Chen and Huang 2011), while the mechanism can differ for different experiments. Products of metabolism TC could be more active and toxic than the original form. A part of hydrolytic products of tetracyclines have been identified as 4-epitetracycline, anhydrotetracycline, 4-epi-chlortetracycline, and 4-epi-oxytetracycline (Zhong et al. 2022).

Shao et al. 2019 refers to using stain Klebsiella sp. SQY5, while the reaction emergent nine others products. TEC was biodegraded by oxidation, ring opening hydrolysis, de-carbonylation, de-amination and de-hydroxylation step by step. In acid condition TC could undergo reversible epimerization and under aerobic condition it can undergo dehydroxylation and demethylation. Thanks to using stain Klebsiella sp. SQY5 concentration of TC decreases to 4.44 mg/L within 4 days (Shao et al. 2019). This strain is also referred to in Kümmerer 2009 revealing high effectiveness in TC treatment. C.W. Yang et al. recommend using different bacterial strains, especially suggest exploiting two strains. Above 90% of TC and derivatives were degraded in different types of sludge when the initial concentration was 2 mg mL^{-1} within 8 days. *Pseudmonas pseudoalcaligenes* and *Pseudmonas taiwanensis* in the sludge under oxygen condition containing aerobic strains show the highest yield. However, under anaerobic conditions *Bacillus flexus* and *Clostridium butyricum* are effectively degrading TC (Yang et al. 2020).

Another possibility for biodegradation of CTC derivatives is to use microalgae and bacteria by biosorption. The consortium works better than microalgae, it is resistant to CTC up to 80 mg L^{-1}, however it depends on the type of algae. Adsorption capacitance improved to 102.53 mg g^{-1} by 12 hours (Wang et al. 2022).

Chen et al. developed an anaerobic/aerobic moving-bed biofilm (A/O-MBBR) membrane bioreactors based on the bacteria. Effectiveness of removing TC estimated at 2.8 µg L^{-1} starting with concentration 10 µg L^{-1}. The authors indicate that this reactor works well in low rage concentrations of TC also in solution of various derivatives. However, concentration 500 µgL^{-1} causes destruction of the structure of the activated sludge bacteria. The antibiotics were adsorbed by activated sludge subsequently therein where the process of hydrolysis and fermentation took place. The research has shown that hydrolysis takes place under aerobic conditions during this process hydroxyl and enol groups structures on the tetraphenyl TC create a form of open-loop lipid compounds thereby increasing the toxicity (Chen et al. 2018). Leng et al. recommend using bacteria such as Stenotrophomonas maltophilia DT1. Within the addition of such bacteria the TC concentration in the solution dropped from 50 mg L^{-1} to 44.43 mg L^{-1} in four days, while after 7 days the concentration was about 2.23 mg L^{-1}. Moreover, pH rage after degradation was higher than initial pH due to the alkaline metabolites excreted by the bacteria, however the post-treatment products are less toxic than the pristine TC (Leng Y. et al. 2016).

Shi et al. proposed application of the *Arthrobacter nicotianae* OTC-16 showing that after 8 days 98.5% concentration of TET and OTC pollution can be removed from aqueous solutions and soil (Shi et al. 2021), while Chang B.V. and Ren Y.L. to biodegradation of TC used enzyme extract from mushroom compost of *Pleurotus eryngii* (Chang and Ren 2015).

3. Adsorption of tetracycline

Based on the structure of TC containing various hydroxyl-, methyl-, keto-, and dimethylamino- functional groups the effective removal of this antibiotic can be designed within the application of the materials able to interact with these groups leading to the TC efficient adsorption. There are many critical parameters for effective adsorption like surface potential, and large volume-to-ratio active area, so depending on the chemical composition of the materials and its porosity it can be effective towards the TC treatment. Literature refers to many types of materials that can work as sorbents for the removal of TC from aqueous solutions.

One of them is based on the magnetic composites, where the sorbent is combined with the magnetic material enabling the magnetic removal of the sorbent after the adsorption like α-Fe_2O_3/reduced graphene oxide that offer a large active surface (Zou et al. 2021). Zhou et al. described use of the magnetically modified powder

resin Q150 having high specific surface area, where the proposed material was more efficient than other sorbents like granule resin (GR) XAD-4, the powder activated carbon (PAC) 1240AC and the granular activated carbon (GAC) HD4000 (Zhou et al. 2012). Zhang et al. proposed an application of recyclable magnetic adsorbent based on montmorillonite ($CoFe_2O_4$/MMT) (Zhang et al. 2018), while Liu et al. described effective removal of TC with the use of magnetite (Fe_3O_4) core and a metal-organic framework (type ZIF-8) as the shell, where the composite has a large specific surface and superparamagnetic response (Liu et al. 2017).

Besides iron-based sorbents, the following group of materials that are widely used for the antibiotics removal from aqueous suspension are hydroxyapatite and its composites. Hydroxyapatite is well known for its high effectiveness towards the aqueous pollutants removal (Misra et al. 1991; Harja and Ciobanju 2018) and its composites even boost the efficiency of the TC adsorption. In Ersan et al. 2015 hydroxyapatite is used as a component of the following composites: hydroxyapatite/clay (HA-C) and hydroxyapatite/pumice (HA-P) offering high active surface and much larger efficiency of the TC binding than bare hydroxyapatite (Ersan et al. 2015). Hydroxyapatite nanopowder can also be modified with magnetic nanoparticles making it easy to remove the sorbent magnetically after the TC treatment (Babaei et al. 2016). Other solutions are based on the mesoporous zeolite-hydroxyapatite-activated palm ash (Z-HAP-AA) composites (Khanday and Hameed 2018), zinc oxide coupled with porous hydroxyapatite (Bekkali et al. 2018), or hollow hydroxyapatite microspheres decorated with small amounts of reduced graphene oxides (Zou et al. 2020).

Similarly to the hydroxyapatites, zeolites offer large surface area making them effective sorbents for TC removal from water. Kang et al. presented that the aluminum in the zeolite beta causes the efficient antibiotic uptake (Kang et al. 2011).

Sorbents can also be based on the by-products from forest and food industries like oak ash, pine bark, and mussel shell (Conde-Cid et al. 2020). Conde-Cid et al. showed that oak ash has high adsorption for all three antibiotics in the simple systems (100% of CTC, 90% of TC, and 80% of OTC). In (Guzel and Saygili 2016) the activated carbon (GPAC) adsorbent obtained by $ZnCl_2$ activation from grape processing pulp (GP) is described as a porous material for antibiotics removal from aqueous media, similarly to the activated carbons obtained from the different sources like the macadamia nut shells (Martins et al. 2015), petroleum coke-derived highly porous activated carbon (Zhang et al. 2015), corn stalk (Song et al. 2020), vine wood (Pouretedal and Sadegh 2014), or apricot nut shell (Marzbali et al. 2016). Saremi et al. present carbon-rich material produced during pyrolysis from the date palm, where the biochar is upgraded with vitamin B6 (Saremi et al. 2020), while Zhang et al. revealed efficient removal of TC from aqueous solutions within corn straw biochar (Zhang et al. 2013). Biochar can be obtained from the multiple types of biomass including pine-wood derived, soybean residue, biochar from *Eucommia ulmoides* plant (Monisha et al. 2022), *Camellia oleifera* plant (Fu et al. 2017), animal-derived chicken feathers (Li et al. 2017), and even chicken bones (Oladipo and Ifebajo 2018).

To deal with that problem also other sorbents are proposed like gel beads based on polyvinyl alcohol-copper alginate (PVA-CA) (Liao et al. 2022), mesoporous and high-surface-area NaOH-activated macroalgae carbon (Wei et al. 2022), metal-free catalysis with 3D macroscopic N-doped porous carbon nanosheets (Shen et al. 2022), microcrystalline cellulose composite aerogel doped with montmorillonite (Amaly et al. 2022), biosynthesized of SiO_2 nanoparticles (Messaoudi et al. 2022), boron nitride nanosheets (Bangari et al. 2022), magnetic, macro-reticulated cross-linked chitosan (MRC) (Oladoja et al. 2014), multi-walled carbon nanotubes (Zhang et al. 2011), clay (Figueroa et al. 2004), or $MnFe_2O_4/rGO$ (Wang et al. 2012).

Summary

Due to the global contamination of the aquatic reservoirs within pharmaceutical-based compounds like antibiotics, effective pollution treatment is highly important. Among many antibiotics, tetracycline and its metabolites are widespread pollutants in an environment, causing severe health problems that spread of antibiotic-resistant bacterial strains. This review presents the need to develop TC degradation and removal techniques that are cost-effective, efficient, and environmentally friendly. This work does not raise any substantive scientific objections and refers recent solutions described in the recent literature. One of the most common methods of TC treatment is oxidation, photodegradation, or adsorption, where each method has advantages and disadvantages. Nanocomposites based on heterostructures can improve the oxidative decomposition of pharmaceutical-based pollutants. At the same time, the hazardous byproducts can stay in an environment.

In contrast, sorbents application does not release any toxic products. Still, it requires a large amount of sorbent material use and further disposal, generating additional costs. Biodegradation of TC offers low processing costs, easy operation, and lack of secondary pollution or byproducts; however, it may lead to the proliferation of ARGs. For now, despite the progress of the pharmaceutical-based contaminants treatment, the reduction of TC pollution in an environment needs improvement. However, some materials efficiently deal with that problem and offer promising properties making them possible to be used not only towards TC, but also other pollutants.

REFERENCES

Ahmad F., Zhu D. and Sun J. (2021) Environmental fate of tetracycline antibiotics: degradation pathway mechanisms, challenges, and perspectives. Environmental Sciences Europe 33, 64, DOI: 10.1186/s12302-021-00505-y.

Ahmadi M., Motlagh H.R., Jaafarzadeh N., Mostoufi A., Saeedi R., Barzegar G. and Jorfi S. (2017) Enhanced photocatalytic degradation of tetracycline and real pharmaceutical wa-

stewater using MWCNT/TiO$_2$ nano-composite. Journal of Environmental Management 186(1), 55–63, DOI: 10.1016/j.jenvman.2016.09.088.

Aljedani D.M. (2021) Antibiotic treatment (Tetracycline) effect on bio-efficiency of the larvae honey bee (Apis mellifera jemenatica). Saudi Journal of Biological Sciences, Article in Press. DOI: 10.1016/j.sjbs.2021.11.024.

Almontasser A. and Parveen A. (2022) Tuning the structural, optical, and magnetic properties of In$_2$O$_3$ nanoparticles with an evaluation of its antibacterial efficiency via controlling the doping concentrations of Ni, Co, and Fe. Materials today communications 30, DOI: 10.1016/j.mtcomm.2021.103063.

Amaly N., El-Moghazy A.Y., Nitin N., Sun G. and Pandey P.K. (2022) Synergistic adsorption-photocatalytic degradation of tetracycline by microcrystalline cellulose composite aero-gel dopped with montmorillonite hosted methylene blue. Chemical Engineering Journal 430(3), DOI: 10.1016/j.cej.2021.133077.

Aslam B., Wang W., Arshad M.I., Khurshid M., Muzammil S., Rasool M.H., Nisar M.A., Alvi R.F., Aslam M.A., Qamar M.U., Salamat M. and Baloch Z. 2018. Antibiotic resistance: a rundown of a global crisis. Infection and drug resistance 11, 1645–1658, DOI: 10.2147/IDR.S173867.

Babaei A.A., Ahmadi K., Kazeminezhad I., Alavi S.N. and Takdastan A. (2016) Synthesis and Application of Magnetic Hydroxyapatite for Removal of Tetracycline from Aqueous Solutions. Journal of Mazandaran University of Medical Sciences 26(136), 146–159.

Bangari R.S., Yadav A., Awasthi P. and Sinha N. (2022) Experimental and theoretical analysis of simultaneous removal of methylene blue and tetracycline using boron nitride nano-sheets as adsorbent. Colloids and Surfaces A: Physicochemical and Engineering Aspects 634, DOI: 10.1016/j.colsurfa.2021.127943.

Bekkali C.E., Bouyarmane H., Karbane M.E., Masse S., Saoiabi A., Coradin T. and Laghzizil A. (2018) Zinc oxide-hydroxyapatite nanocomposite photocatalysts for the degradation of ciprofloxacin and ofloxacin antibiotics. Colloids Surf A 539, 364–370, DOI: 10.1016/j.colsurfa.2017.12.051.

Bera R., Kundu S. and Patra A. (2015) 2D Hybrid Nanostructure of Reduced Graphene Oxide–CdS Nanosheet for Enhanced Photocatalysis. ACS Applied Materials & Interfaces 7, 13251–13259, DOI: 10.1021/acsami.5b03800.

Cai H., Li X., Ma D., Feng Q., Wang D., Liu Z., Wei X., Chen K., Lin H., Qin S. and Lu F. (2021) Stable Fe$_3$O$_4$ submicrospheres with SiO$_2$ coating for heterogeneous Fenton-like reaction at alkaline condition. Science of the total environment 764, DOI: 10.1016/j.scitotenv.2020.144200.

Cao M., Wang P., Ao Y., Wang C., Hou J. and Qian J. (2016) Visible light activated photocatalytic degradation of tetracycline by a magnetically separable composite photocatalyst: Graphene oxide/magnetite/cerium-doped titania. Journal of Colloid and Interface Science 467, 129–139, DOI: 10.1016/j.jcis.2016.01.005.

Chang B.V. and Ren Y.L. (2015) Biodegradation of three tetracyclines in river sediment. Ecological Engineering 75, 272–277, DOI: 10.1016/j.ecoleng.2014.11.039.

Chen H.Y., Liu Y.D. and Dong B. (2018) Biodegradation of tetracycline antibiotics in A/O moving-bed biofilm reactor systems. Bioprocess and Biosystems Engineering 41, 47–56, DOI: 10.1007/s00449-017-1842-7.

Chen W.R. and Huang C.H. (2011) Transformation kinetics and pathways of tetracycline antibiotics with manganese oxide. Environmental Pollution 159(5), 1092–1100, DOI: 10.1016/j.envpol.2011.02.027.

Conde-Cid M., Fernandez-Sanjurjo M. J., Ferreira-Coelho G., Fernandez-Calvino D., Arias-Estevez M., Nunez-Delgado A. and Alvarez-Rodriguez E. (2020) Competitive adsorption and desorption of three tetracycline antibiotics on bio-sorbent materials in binary systems. Environmental Research 190, DOI: 10.1016/j.envres.2020.110003.

Djouadi L., Khalaf H., Boukhatem H., Boutoumi H., Kezzime A., Santaballa J.A. and Canle M. (2018) Degradation of aqueous ketoprofen by heterogeneous photocatalysis using Bi_2S_3/TiO_2–Montmorillonite nanocomposites under simulated solar irradiation. Applied Clay Science 166, 27–37, DOI: 10.1016/j.clay.2018.09.008.

Ersan M., Guler U.A., Acikel U and Sarioglu M. (2015) Synthesis of hydroxyapatite/clay and hydroxyapatite/pumice composites for tetracycline removal from aqueous solutions. Process Safety and Environmental Protection 96, 22–32, DOI: 10.1016/j.psep.2015.04.001.

Fang C., Wang S., Xu H.,and Huang Q. (2022) Degradation of tetracycline by atmospheric-pressure non-thermal plasma: Enhanced performance, degradation mechanism, and toxicity evaluation. Science of the Total Environment. 812, DOI: 10.1016/j.scitotenv.2021.152455.

Fei W., Song Y., Li N., Chen D., Xu Q., Li H., He J. and Lu J. (2019) Hollow In_2O_3@$ZnFe_2O_4$ heterojunctions for highly efficient photocatalytic degradation of tetracycline under visible light. Environmental Science: Nano 6, 3123–3132, DOI: 10.1039/C9EN00811J.

Figueroa R.A., Leonard A. and MacKay A.A. (2004) Modeling Tetracycline Antibiotic Sorption to Clays. Environmental Science & Technology 38(2), 476–483, DOI: 10.1021/es0342087.

Fu D., Chen Z., Xia D., Shen L., Wang Y. and Li Q (2017) A novel solid digestate-derived biochar-Cu NP composite activating H2O2 system for simultaneous adsorption and degradation of tetracycline. Environmental Pollution 221, 301–310, DOI: 10.1016/j.envpol.2016.11.078.

Fu J., Liu N., Mei L., Liao L., Deyneko D., Wang J., Bai Y. and Lv G. (2019) Synthesis of Ce-doped $Mn_3Gd_{7-x}Ce_x(SiO_4)_6O_{1.5}$ for the enhanced catalytic ozonation of tetracycline. Scientific Reports 9, 18734, DOI: 10.1038/s41598-019-55230-7.

Gothwal R. and Shashidhar T. (2014) Antibiotic pollution in the environment: A review. Clean soil and water 43(4), 479–489, DOI: 10.1002/clen.201300989.

Gokulan K., Cerniglia C.E., Thomas C., Pineiro S.A. and Khare S. (2017) Effects of residual levels of tetracycline on the barrier functions of human intestinal epithelial cells. Food and Chemical Toxicology 109(1), 253–263, DOI: 10.1016/j.fct.2017.09.004.

Guzal F. and Saygili H. (2016) Adsorptive efficacy analysis of novel carbonaceous sorbent derived from grape industrial processing wastes towards tetracycline in aqueous solution. Journal of the Taiwan Institue of Chemical Engineers 60, 236–240, DOI: 10.1016/j.jtice.2015.10.003.

Han C.H., Park H.D., Kim S.B., Yargeau V., Choi J.W., Lee S.H. and Park J.A. (2020) Oxidation of tetracycline and oxytetracycline for the photo-Fenton process: Their transformation products and toxicity assessment. Water research 172, DOI: 10.1016/j.watres.2020.115514.

Harjan M. and Ciobanu G. (2018) Studies on adsorption of oxytetracycline from aqueous solutions onto hydroxyapatite. Science of the Total Environment 628–629, 36–43, DOI: 10.1016/j.scitotenv.2018.02.027.

He X., Nguyen V., Jiang Z., Wang D., Zhu Z. and Wang, W.N. (2018) Highly-Oriented One-Dimensional MOF-Semiconductor Nanoarrays for Efficient Photodegradation of Antibiotics. Catalysis Science & Technology 8, 1–8, DOI: 10.1039/C8CY00229K.

Hejduk P., Warczak M., Urbańska W. and Osial M. (2021) Oczyszczanie wody z zanieczyszczeń pochodzenia farmaceutycznego (Purification of water from contaminants of pharmaceutical origin). [In:] Innowacyjna zielona gospodarka. Cz. 1. Gospodarka o obiegu

zamkniętym w systemach przemysłowych – możliwości praktycznego zastosowania, Główny Instytut Górnictwa, Katowice, Poland, 52–58.

Hou L., Wang L., Royer S. and Zhang, H. (2016) Ultrasound-assisted heterogeneous Fenton-like degradation of tetracycline over a magnetite catalyst. Journal of hazardous materials 302, 458–467, DOI: 10.1016/j.jhazmat.2015.09.033.

Hu X., Sun Z., Song J., Zhang G., Li C. and Zheng S. (2019) Synthesis of novel ternary heterogeneous BiOCl/TiO$_2$/sepiolite composite with enhanced visible-light-induced photocatalytic activity towards tetracycline. Journal of Colloid and Interface Science 533, 238–250, DOI: 10.1016/j.jcis.2018.08.077.

Huang X., Xiao J., Yi Q., Li D., Liu C. and Liu Y. (2022) Construction of core-shell Fe$_3$O$_4$@ GO-CoPc photo-Fenton catalyst for superior removal of tetracycline: The role of GO in promotion of H$_2$O$_2$ to OH conversion. Journal of environmental management 308, Advance online publication, DOI: 10.1016/j.jenvman.2022.114613.

Iakovides I.C., Michael-Kordatoub I., Moreira N.F.F., Ribeirod A.R., Fernandes T., Pereira M.F.R., Nunes O.C., Manaia C.M., Silva A.M.T. and Fatta-Kassinos D. (2019) Continuous ozonation of urban wastewater: Removal of antibiotics, antibiotic-resistant *Escherichia coli* and antibiotic resistance genes and phytotoxicity. Water Research 159, 333–347, DOI: 10.1016/j.watres.2019.05.025.

Inyinbor Adejumoke A., Adebesin Babatunde O., Oluyori Abimbola P., Adelani-Akande Tabitha A., Dada Adewumi O. and Oreofe Toyin A. (2017) Water Pollution: Effects, Prevention, and Climatic Impact. [In:] Water Challenges of Urbanizing World, London: IntechOpen. DOI: 10.5772/intechopen.72018.

Jiao S., Zheng S., Yin D., Wang L. and Chen L. (2008) Aqueous oxytetracycline degradation and the toxicity change of degradation compounds in photoirradiation process. Journal of Environmental Sciences 20(7), 806–813, DOI: 10.1016/S1001-0742(08)62130-0.

Jin C., Li W., Chen Y., Li R., Huo J., He, Q. and Wang Y. (2020) Efficient Photocatalytic Degradation and Adsorption of Tetracycline over Type-II Heterojunctions Consisting of ZnO Nanorods and K-Doped Exfoliated g-C$_3$N$_4$ Nanosheets. Industrial & Engineering Chemistry Research 59, 2860–2873, DOI: 10.1021/acs.iecr.9b06911.

Kakavandi B., Bahari N., Rezaei Kalantary R. and Dehghani Fard E. (2019) Enhanced sono-photocatalysis of tetracycline antibiotic using TiO$_2$ decorated on magnetic activated carbon (MAC@T) coupled with US and UV: A new hybrid system. Ultrasonics sonochemistry 55, 75–85, DOI: 10.1016/j.ultsonch.2019.02.026.

Kang J., Liu H., Zheng Y. M., Qu J. and Chen J. P. (2011) Application of nuclear magnetic resonance spectroscopy, Fourier transform infrared spectroscopy, UV–Visible spectroscopy and kinetic modeling for elucidation of adsorption chemistry in uptake of tetracycline by zeolite beta. Jorunal of Colloid and Interface Science 354(1), 261–267, DOI: 10.1016/j.jcis.2010.10.065.

Khanday W.A. and Hameed B.H. (2018) Zeolite-hydroxyapatite-activated oil palm ash composite for antibiotic tetracycline adsorption. Fuel 215, 499–505, DOI: 10.1016/j.fuel.2017.11.068.

Khodadadi M., Ehrampoush M., Ghaneian M., Allahresani A. and Mahvi A. (2018) Synthesis and characterizations of FeNi$_3$SiO$_2$TiO$_2$ nanocomposite and its application in photocatalytic degradation of tetracycline in simulated wastewater. J. Mol. Liq. 255, 224–232, DOI: 10.1016/j.molliq.2017.11.137.

Kongkham B., Prabakaran D. and Puttaswamy H. (2020) Opportunities and challenges in managing antibiotic resistance in bacteria using plant secondary metabolites. Fitoterapia 147, DOI: 10.1016/j.fitote.2020.104762.

Kummar P., Mathpal M.C., Parkash J., Viljoen B.C., Roos W.D. and Swart H.C. (2020) Band gap tailoring of cauliflower-shaped CuO nanostructures by Zn doping for antibacterial applications. Journal of Alloys and Compounds 832, DOI: 10.1016/j.jallcom.2020.154968.

Kumar R.R., Raj R. and Venimadhav A. (2019) Weak ferromagnetism in band-gap engineered α-$(Fe_2O_3)_{1-X}(Cr_2O_3)_X$ nanoparticles. Journal of Magnetism and Magnetic Materials 473, 119–124, DOI: 10.1016/j.jmmm.2018.10.007.

Kümmerer K. (2009) Antibiotics in the aquatic environment–A review–Part I. Chemosphere 75, 417–434, DOI: 10.1016/j.chemosphere.2008.11.086.

Lai C., Huang F., Zeng G., Huang D., Qin L., Cheng M., Zhang C., Li B., Yi H., Liu S., Li L. and Chen L. (2019) Fabrication of novel magnetic $MnFe_2O_4$/bio-char composite and heterogeneous photo-Fenton degradation of tetracycline in near neutral pH. Chemosphere 224, 910–921, DOI: 10.1016/j.chemosphere.2019.02.193.

Lai C., Xu F., Zhang M., Li B., Liu S., Yi H., Li L., Qin L., Liu X., Fu Y., An N., Yang H., Huo X., Yang X. and Yan H. (2021) Facile synthesis of CeO_2/carbonate doped $Bi_2O_2CO_3$ Z-scheme heterojunction for improved visible-light photocatalytic performance: Photodegradation of tetracycline and photocatalytic mechanism. Journal of Colloid and Interface Science 588, 283–294, DOI: 10.1016/j.jcis.2020.12.073.

Lee D., kim S., Tang K., De Volder M. and Hwang Y. (2021) Oxidative Degradation of Tetracycline by Magnetite and Persulfate: Performance, Water Matrix Effect, and Reaction Mechanism. Nanomaterials 11(9), DOI: 10.3390/nano11092292.

Leng Y., Bao J., Chang G., Zheng H., Li X., Du J. and Snow D. (2016) Biotransformation of tetracycline by a novel bacterial strain Stenotrophomonas maltophilia DT1. Journal of Hazardous Materials 318, 125–133, DOI: 10.1016/j.jhazmat.2016.06.053.

Li H., Hu J., Meng Y., Su J. and Wang X. (2017) An investigation into the rapid removal of tetracycline using multilayered graphene-phase biochar derived from waste chicken feather. Science of the Total Environment 603, 39–48, DOI: 10.1016/j.scitotenv.2017.06.006.

Li Z., Zhu L., Wu W., Wang S. and Qiang L. (2016) Highly efficient toward tetracycline under simulated solar-light by Ag+-CDs-Bi_2WO_6: Synergistic effects of silver ions and carbon dots. Applied Catalysis B: Environmental 192, 277–285, DOI: 10.1016/j.apcatb.2016.03.045.

Li W., Ding H., Ji H., Dai W., Guo J. and Du G. (2018) Photocatalytic Degradation of Tetracycline Hydrochloride via a CdS-TiO_2 Heterostructure Composite under Visible Light Irradiation. Nanomaterials 8, DOI: 10.3390/nano8060415.

Lima M.S., Cruz-Filho J.F., Noleto L.F.G., Silva L.J., Costa T.M.S. and Luz Jr. G.E. (2020) Synthesis, characterization and catalytic activity of Fe_3O_4@WO_3/SBA-15 on photodegradation of the acid dichlorophenoxyacetic (2,4-D) under UV irradiation. Journal of Environmental Chemical Engineering 8(5), DOI: 10.1016/j.jece.2020.104145.

Liao Q., Rong H., Zhao M., Luo H., Chu Z. and Wang R. (2022) Strong adsorption properties and mechanism of action with regard to tetracycline adsorption of double-network polyvinyl alcohol-copper alginate gel beads. journal of Hazardous Materials 422, DOI: 10.1016/j.jhazmat.2021.126863.

Liu H., Chen L. and Ding J. (2017) A core-shell magnetic metal organic framework of type Fe_3O_4@ZIF-8 for the extraction of tetracycline antibiotics from water samples followed by ultra-HPLC-MS analysis. Microchimica Acta 184, 4091–4098, DOI: 10.1007/s00604-017-2442-6.

Liu Y., Kong J., Yuan J., Zhao W., Zhu X., Sun C. and Xie J. (2018) Enhanced photocatalytic activity over flower-like sphere Ag/Ag_2CO_3/$BiVO_4$ plasmonic heterojunction photocat-

alyst for tetracycline degradation. Chemical Engineering Journal 331, 242–254, DOI: 10.1016/j.cej.2017.08.114.

Lu T., Gao Y., Yang Y., Ming H., Huang Z., Liu G., Zhen D., Zhang J and Hou Y. (2021) Efficient degradation of tetracycline hydrochloride by photocatalytic ozonation over Bi_2WO_6. Chemosphere 283, DOI: 10.1016/j.chemosphere.2021.131256.

Luo H., mig Y., Wu Y., Lin X. and Yan Y. (2021) Facile synthesis of PVDF photocatalytic membrane based on $NCQDs/BiOBr/TiO_2$ heterojunction for effective removal of tetracycline. Materials Science and Engineering: B 265, DOI: 10.1016/j.mseb.2020.114996.

Luo L., Zou D., Lu D., Yu F., Xin B. and Ma J. (2018) Study of catalytic ozonation for tetracycline hydrochloride degradation in water by silicate ore supported Co_3O_4. RSC Advances 8: 41109–41116, DOI: 10.1039/C8RA08402E.

Lv C., Lan X., Wang L., Dai X., Zhang M., Cui J., Yuan S., Wang, S. and Shi J. (2021) Rapidly and highly efficient degradation of tetracycline hydrochloride in wastewater by 3D IO-TiO_2-CdS nanocomposite under visible light. Environmental Technology 42, 377–387, DOI: 10.1080/09593330.2019.1629183.

Łukaszewicz P., Maszkowska J., Mulkiewicz E., Kumirska J., Stepnowski P. and Caban M. (2017) Impact of veterinary pharmaceuticals on the agricultural environment: a re-inspection. [In:] F.A. Gunther, P. de Voogt (Eds), Cham, Springer, Reviews of Environmental Contamination and Toxicology 243, 89–148.

Manyi-Loh C., Mamphweli S., Meyer E. and Okoh A. (2018) Antibiotic Use in Agriculture and Its Consequential Resistance in Environmental Sources: Potential Public Health Implications. Molecules 23(4), 795, DOI: 10.3390/molecules23040795.

Martins A.C., Cazetta A.L., Pezoti O., Souza J.R.B., Zhang T., Pilau E.J., Asefa T. and Almeida V.C. (2017) Sol-gel synthesis of new TiO_2/activated carbon photocatalyst and its application for degradation of tetracycline. Ceramics International 43(5), 4411–4418, DOI: 10.1016/j.ceramint.2016.12.088.

Meng F., Ma W., Wang T., Zhu Z., Chen Z. and Lu G. (2020) A tribo-positive $Fe@MoS_2$ piezocatalyst for the durable degradation of tetracycline: degradation mechanism and toxicity assessment. Envirionmental Science: Nano 7, 1704–1718, DOI: 10.1039/D0EN00284D.

Messaoudi N.E., Khomri M.E., Ablouh E.H., Bouich A., Lacherai A., Jada A., Lima E.C. and Sher F. (2022) Biosynthesis of SiO_2 nanoparticles using extract of Nerium oleander leaves for the removal of tetracycline antibiotic Chemosphere 287(4), DOI: 10.1016/j.chemosphere.2021.132453.

Misra D.N. (1991) Adsorption and orientation of tetracycline on hydroxyapatite. Calcified Tissue International 48, 362–367, DOI: 10.1007/BF02556156.

Mohsin M.K. and Mohammed A.A. (2021) Catalytic ozonation for removal of antibiotic oxytetracycline using zinc oxide nanoparticles. Applied Water Science 11, 9, DOI: 10.1007/s13201-020-01333-w.

Monisha R.S., Mani R.L., Sivaprakash B., Rajamohan N and Vo D.N. (2022) Green remediation of pharmaceutical wastes using biochar: a review. Environmental Chemistry Letters 20, 681–704, DOI: 10.1007/s10311-021-01348-y.

Nagamine M., Osial M., Jackowska K., Krysinski P. and Widera-Kalinowska J. (2020) Tetracycline Photocatalytic Degradation under CdS Treatment. Journal of Marine Science and Engineering 8, DOI: 10.3390/jmse8070483.

Nasseh N., Taghavi L., Barikbin B. and Nasseri M.A. (2018) Synthesis and characterizations of a novel FeNi3/SiO2/CuS magnetic nanocomposite for photocatalytic degradation of

tetracycline in simulated wastewater. Journal of Cleaner Production 179, 42–54, DOI: 10.1016/j.jclepro.2018.01.052.

Nasseh N., Panahi A.H., Esmati M., Daglioglud N., Asadi A., Rajati H. and Khodadoost F. (2020) Enhanced photocatalytic degradation of tetracycline from aqueous solution by a novel magnetically separable $FeNi_3/SiO_2/ZnO$ nano-composite under simulated sunlight: Efficiency, stability, and kinetic studies. Journal of Molecular Liquids 301, 112434––112442, DOI: 10.1016/j.molliq.2019.112434.

Nawrocki J. and Kasprzyk-Hordern B. (2010) The efficiency and mechanisms of catalytic ozonation. Applied Catalysis B: Environmental 99, 27–42, DOI: 10.1016/j.apcatb.2010.06.033.

Nie M., Li Y., He J., Xie C., Wu Z., Sun B., Zhang K., Kong L. and Liu J. (2020) Degradation of tetracycline in water using Fe_3O_4 nanospheres as Fenton-like catalysts: kinetics, mechanisms and pathways. New Journal of Chemistry 44, 2847–2857, DOI: 10.1039/D0NJ00125B.

Niu J., Ding S., Zhang L., Zhao J. and Feng C.J.C. (2013) Visible-light-mediated $Sr-Bi_2O_3$ photocatalysis of tetracycline: Kinetics, mechanisms and toxicity assessment. Chemosphere 2013, 93, 1–8, DOI: 10.1016/j.chemosphere.2013.04.043.

Martins A.C., Pezoti O., Cazetta A.L., Bedin K.C., Yamazaki D.A.S., Bandoch G.F.G., Asefa T., Visentainer J.V. and Almeida V.C. (2015) Removal of tetracycline by NaOH-activated carbon produced from macadamia nut shells: Kinetic and equilibrium studies. Chemical Engineering Journal 260, 291–299, DOI: 10.1016/j.cej.2014.09.017.

Marzbali M.H., Esmaieli M., Abolghasemi H. and Mazbali M.H. (2016) Tetracycline adsorption by H_3PO_4-activated carbon produced from apricot nut shells: A batch study. Process Safety and Environmental Protection 102, 700–709, DOI: 10.1016/j.psep.2016.05.025.

Mohammad A., Khan M.E., Cho M.H. and Yoon T. (2021) Adsorption promoted visible-light-induced photocatalytic degradation of antibiotic tetracycline by tin oxide/cerium oxide nanocomposite. Applied Surface Science 565, DOI: 10.1016/j.apsusc.2021.150337.

Mohanty B. and Nayak J. (2021) Band gap narrowing and prolongation of carrier lifetime in solution-processed CeO_2/CdS thin films for application as photoanodes in quantum dot sensitized solar cells. Ceramics International 47(18), 26144–26156, DOI: 10.1016/j.ceramint.2021.06.022.

Oladipo A.A. and Ifebajo A.O. (2018) Highly efficient magnetic chicken bone biochar for removal of tetracycline and fluorescent dye from wastewater: two-stage adsorber analysis. Journal of Environmental Management 209, 9–16, DOI: 10.1016/j.jenvman.2017.12.030.

Oladoja N.A., Adelagun R.O.A., Ahmad A.L., Unuabonah E.I. and Bello H.A. (2014) Preparation of magnetic, macro-reticulated cross-linked chitosan for tetracycline removal from aquatic systems. Coloids and Surfaces B: Biointerfaces 117, 51–59, DOI: 10.1016/j.colsurfb.2014.02.006.

Olusegun S.J., Larrea G., Osial M., Jackowska K. and Krysinski P. (2021) Photocatalytic Degradation of Antibiotics by Superparamagnetic Iron Oxide Nanoparticles. Tetracycline Case. Catalysts 11(10), DOI: 10.3390/catal11101243.

Oluwole A.O. and Olatunji O.S. (2022) Photocatalytic degradation of tetracycline in aqueous systems under visible light irridiation using needle-like SnO_2 nanoparticles anchored on exfoliated $g-C_3N_4$. Environmental Sciences Europe 34, 5, DOI: 10.1186/s12302-021-00588-7.

Piriyanon J., Takhai P., Patta S., Chankhanittha T., Senasu T., Nijpanich S., Juabrum S., Chanlek N. and Nanan S. Performance of sunlight responsive $WO_3/AgBr$ heterojunction pho-

tocatalyst toward degradation of Rhodamine B dye and ofloxacin antibiotic. Optical materials 121, DOI: 10.1016/j.optmat.2021.111573.

Philip J.M., Aravind U.K. and Aravindakumar C.T. (2018) Emerging contaminants in Indian environmental matrices – A review. Chemosphere 190, 307–326, DOI: 10.1016/j.chemosphere.2017.09.120.

Pouretedal H.R. and Sadegh N. (2014) Effective removal of Amoxicillin, Cephalexin, Tetracycline and Penicillin G from aqueous solutions using activated carbon nanoparticles prepared from vine wood. Journal of Water Process Engineering 1, 64-73, DOI: 10.1016/j.jwpe.2014.03.006.

Rathi S., Kumar S. and Vo D.V.N. (2021) Critical review on hazardous pollutants in water environment: Occurrence, monitoring, fate, removal technologies and risk assessment. Science of the Total Environment 797, DOI: 10.1016/j.scitotenv.2021.149134.

Reda M.M., Adel A.I., Mohammad W.K., Ajayb S.A. and Ibraheem A.M. (2021) Fabrication of Mesoporous PtO–ZnO Nanocomposites with Promoted Photocatalytic Performance for Degradation of Tetracycline. ACS Omega 6(9), 6438–6447, DOI: 10.1021/acsomega.1c00135.

Rahimi S.M., Panahi A.H., Moghaddam N.S.M., Allahyari E. and Nasseh N. (2022) Breaking down of low-biodegradation Acid Red 206 dye using bentonite/Fe_3O_4/ZnO magnetic nanocomposite as a novel photo-catalyst in presence of UV light. Chemical Physics Letters 794, DOI: 10.1016/j.cplett.2022.139480.

Raizada P., Kumari J. Shandilya P. and Singh P. (2017) Kinetics of photocatalytic mineralization of oxytetracycline and ampicillin using activated carbon supported ZnO/ZnWO4 nanocomposite in simulated wastewater. Desalination and Water Treatment 79, 204–213, DOI: 10.5004/dwt.2017.20831.

Ravele M.P., Oyewo O.A., Ramaila S., Mavuru L. and Onwudiwe D.C. (2021) Photocatalytic Degradation of Tetracycline in Aqueous Solution Using Copper Sulfide Nanoparticles. Catalysts 11, DOI: 10.3390/catal11101238.

Salimiaghdam N., Singh L., Schneider K., Chwa M., Atilano S.R., Nalbandian A., Limb A.G. and Kenney C.M. (2022) Effects of fluoroquinolones and tetracyclines on mitochondria of human retinal MIO-M1 cells. Experimental Eye Research 213, DOI: 10.1016/j.exer.2021.108857.

Saremi F., Miroliaei M.R., Nejad M.S. and Sheibani H. (2020) Adsorption of tetracycline antibiotic from aqueous solutions onto vitamin B6-upgraded biochar derived from date palm leaves. Journal of Molecular Liquids 318, DOI: 10.1016/j.molliq.2020.114126.

Semeraro P., Bettini S., Sawalha S., Pal S., Licciulli A., Marzo F., Lovergine N., Valli L. and Giancane G.J.N. (2020) Photocatalytic degradation of tetracycline by ZnO/γ-Fe2O3 paramagnetic nanocomposite material. Nanomaterials 10, DOI: 10.3390/nano10081458.

Shahvelayati A. S., Sheshmani S. and Siminghad M. (2022) Preparation and characterization of SnO nanoflowers with controllable thicknesses using imidazolium-based ionic liquids as green media: Visible light photocatalytic degradation of Acid Blue 19. Materials Chemistry and Physics 278, DOI: 10.1016/j.matchemphys.2021.125442.

Shao S., Hu Y., Cheng J. and Chen Y. (2019) Biodegradation mechanism of tetracycline (TEC) by strain Klebsiella sp. SQY5 as revealed through products analysis and genomics. Ecotoxicology and Environmental Safety 85, 109676–109683, DOI: 10.1016/j.ecoenv.2019.109676.

Shen Y., Zhu K., He D., Huang J., He H., Lei L. and Chen W. (2022) Tetracycline removal via adsorption and metal-free catalysis with 3D macroscopic N-doped porous carbon nanosheets: Non-radical mechanism and degradation pathway. Journal of Environmental Sciences 111, 351–366, DOI: 10.1016/j.jes.2021.04.014.

Shi Y., Yang Z., Wang B., An H., Chen Z. and Cui H. (2016) Adsorption and photocatalytic degradation of tetracycline hydrochloride using a palygorskite-supported Cu_2O–TiO_2 composite. Applied Clay Science 119(2), 311–320, DOI: 10.1016/j.clay.2015.10.033.

Shi Y., Lin H., Ma J,. Zhu R., Sun W., Lin X., Zhang J., Zheng H. and Zhang X. (2021) Degradation of tetracycline antibiotics by Arthrobacter nicotianae OTC-16. Journal of Hazardous Materials 403, DOI: 10.1016/j.jhazmat.2020.123996.

Soares K.O., de Oliveira C.J.B., Rodrigues A.E., Vasconcelos P.C., da Silva N.M.V., da Cunha Filho O.G., Madden C. and Hale V.L. (2021) Tetracycline Exposure Alters Key Gut Microbiota in Africanized Honey Bees (*Apis mellifera scutellata* x spp.). Frontiers in Ecology and Evolution 9, DOI: 10.3389/fevo.2021.716660.

Soltani R.D.C., Mashayekhi M., Naderi M., Boczkaj G., Jorfi S. and Safari M. (2019) Sonocatalytic degradation of tetracycline antibiotic using zinc oxide nanostructures loaded on nano-cellulose from waste straw as nanosonocatalyst. Ultrasonics Sonochemistry 55, 117–124, DOI: 10.1016/j.ultsonch.2019.03.009.

Song W., Ding Y., Chiou C.T. and Li H. (2010) Selected veterinary pharmaceuticals in agricultural water and soil from land application of animal manure. Journal of Environmental Quality 39(4), 1211–1217, DOI: 10.2134/jeq2009.0090.

Song Y.X., Chen S., You N., Fan H.T. and Sun L.N. (2020) Nanocomposites of zero-valent Iron@ Activated carbon derived from corn stalk for adsorptive removal of tetracycline antibiotics. Chemosphere 255, DOI: 10.1016/j.chemosphere.2020.126917.

Su J., Zhang Y., Liu L., Sun R. and Niu Q. (2018) Variation of structure and band gap for N doped Cu_2O films deposited with ceramic target. Thin Solid Films 651, 67–70, DOI: 10.1016/j.tsf.2018.02.023.

Sun Y., Xiong R., Zhang Y., Ma Y., Li Y., Ji W., Ma Y., Wang Z. (2022) Insight into synergetic mechanism of $Cu_yMn_{5-y}O_x$/hG-activated peroxydisulfate enhances tetracycline antibiotics degradation and toxicity assessment. Separation and purification Technology 293, DOI: 10.1016/j.seppur.2022.121066.

Tung M.H.T., Cam N.T.D., Thuan D.V., Quan P.V., Hoang C.V., Phuong T.T.T., Lam N.T., Tam T.T., Chi N.T.P.L., Lan N.T., Thoai D.N. and Pham T. (2020) Novel direct Z-scheme AgI/N–TiO_2 photocatalyst for removal of polluted tetracycline under visible irradiation. Ceramics International 46(5), 6012–6021, DOI: 10.1016/j.ceramint.2019.11.058.

Wang Y., Zhang, H., Chen L., Wang S. and Zhang D. (2012) Ozonation combined with ultrasound for the degradation of tetracycline in a rectangular air-lift reactor. Separation and Purification Technology 84, 138–146, DOI: 10.1016/j.seppur.2011.06.035.

Wang Y., He Y., Li X., Nagarajan D. and Chang J.S. (2022) Enhanced biodegradation of chlortetracycline via a microalgae-bacteria consortium. Bioresource Technology 343, DOI: 10.1016/j.biortech.2021.126149.

Wei F., Ren Q., Zhang H., Yang L., Chen H., Liang Z. and Chen D. (2021) Removal of tetracycline hydrochloride from wastewater by Zr/Fe-MOFs/GO composites. Royal Society of Chemistry 11, 9977–9984, DOI: 10.1039/D1RA01027A.

Wei M., Marrakchi F., Yuan C., Cheng X., Jiang D., Zafar F.F., Fu Y. and Wang S. (2022) Adsorption modeling, thermodynamics, and DFT simulation of tetracycline onto mesoporous and high-surface-area NaOH-activated macroalgae carbon. Journal of Hazardous Materials 425, DOI: 10.1016/j.jhazmat.2021.127887.

Wu F., Zhou F., Zhu Z., Zhan S. and He Q. (2019) Enhanced photocatalytic activities of Ag_3PO_4/GO in tetracycline degradation, Chemical Physics Letters 724, 90–95, DOI: 10.1016/j.cplett.2019.03.058.

Ventola C.L. (2015) The antibiotic resistance crisis: part 1: causes and threats. P & T: A Peer-reviewed. Journal for Formulary Management 40(4), 277–283.

Xiao T., Tang Z., Yang Y., Tangb L., Zhoub Y. and Zoub Z. (2018) In situ construction of hierarchical WO_3/g-C_3N_4 composite hollow microspheres as a Z-scheme photocatalyst for the degradation of antibiotics. Applied Catalysis B: Environmental 220, 417–428, DOI: 10.1016/j.apcatb.2017.08.070.

Xu Y. Ch., Liu G.H., Xu Y.H., Zhao T., Zheng H. and Tan X.Y. (2022) Physiological and transcriptomic analyses reveal the toxicological mechanism and risk assessment of environmentally-relevant waterborne tetracycline exposure on the gills of tilapia (Oreochromis niloticus). Science of The Total Environment 806(3), DOI: 10.1016/j.scitotenv.2021.151290.

Yamal-Turbay E., Jaen E., Graells M. and Perez-Moya M. (2013) Enhanced photo-Fenton process for tetracycline degradation using efficient hydrogen peroxide dosage. Journal of Photochemistry and Photobiology A: Chemistry 267, 11–16, DOI: 10.1016/j.jphotochem.2013.05.008.

Yang C.W., Liu C. and Chang B.V. (2020) Biodegradation of Amoxicillin, Tetracyclines and Sulfonamides in Wastewater Sludge. Water 12(8), DOI: 10.3390/w12082147.

Yang B., Cheng X., Zhang Y., Li W., Wang J. and Guo H. (2021) Insight into the role of binding interaction in the transformation of tetracycline and toxicity distribution. Environmental Science and Ecotechnology 8, DOI: 10.1016/j.ese.2021.100127.

Zhu H., Chen T., Liu J. and Li D. (2018) Adsorption of tetracycline antibiotics from an aqueous solution onto graphene oxide/calcium alginate composite fibers. RCS Advances 8, 2616–2621, DOI: 10.1039/C7RA11964J.

Zhu X.-D., Wang Y.-J., Sun R.-J. and Zhou D.-M. (2013) Photocatalytic degradation of tetracycline in aqueous solution by nanosized TiO_2. Chemosphere 92, 925–932, DOI: 10.1016/j.chemosphere.2013.02.066.

Zhu Y., Quan X., Chen F., Fan X. and Feng Y. (2012) CeO_2–TiO_2 Coated Ceramic Membrane with Catalytic Ozonation Capability for Treatment of Tetracycline in Drinking Water. Science of Advanced Materials 4(12), 1191–1199, DOI: 10.1166/sam.2012.1413.

Zhai X., Cheng S., Wang H., Zhang C., Li Y. and Dong W. (2021) Fast preparation of Fe_3O_4@ polydopamine/Au for highly efficient degradation of tetracycline. Chemosphere 285, DOI: 10.1016/j.chemosphere.2021.131523.

Zhang D., Yin J., Zhao J., Zhu H. and Wang C. (2015) Adsorption and removal of tetracycline from water by petroleum coke-derived highly porous activated carbon. Journal of Environmental Chemical Engineering 3(3), 1504–1512, DOI: 10.1016/j.jece.2015.05.014.

Zhang G., Liu X., Sun K., He Q., Qian T. and Yan Y. (2013) Interactions of simazine, metsulfuron-methyl, and tetracycline with biochars and soil as a function of molecular structure. Journal of Soils and Sediments 13, 1600–1610, DOI: 10.1007/s11368-013-0755-6.

Zhang J., Khan M. A., Abdo A. M., Lei W., Liao C. and Wang F. (2019) Facile hydrothermal synthesis of magnetic adsorbent $CoFe_2O_4$/MMT to eliminate antibiotics in aqueous phase: tetracycline and ciprofloxacin. Environmental Science and Pollution Research 26, 215–226, DOI: 10.1007/s11356-018-3452-6.

Zhang K., Gu S., Wu Y., Fan Q. and Zhu C. (2020) Preparation of pyramidal SnO/CeO_2 nano-heterojunctions with enhanced photocatalytic activity for degradation of tetracycline. Nanotechnology 31, 215702, DOI: 10.1088/1361-6528/ab73b4.

Zhang l., Song X., Liu X., Yang L. Pan F. and Lv J. (2011) Studies on the removal of tetracycline by multi-walled carbon nanotubes. Chemical Engineering Journal 178, 26–33, DOI: 10.1016/j.cej.2011.09.127.

Zhang S., Liu H., Gao F., Fang M., Zhang Y., Cai Y., Li K., Kong M. and Tan X. (2022) The synergetic enhancement of piezo catalytic performance to remove tetracycline by $K_2Ti_6O_{13}/TiO_2$ composite. Journal of Alloys and Compounds 900, DOI: 10.1016/j.jallcom.2021.163492.

Zhang X., Ren B., Li X., Liu B., Wang S., Yu, P., Xu Y. and Jiang G. (2021) High-efficiency removal of tetracycline by carbon-bridge-doped $g-C_3N_4/Fe_3O_4$ magnetic heterogeneous catalyst through photo-Fenton process. Journal of hazardous materials 418, DOI: 10.1016/j.jhazmat.2021.126333.

Zhao T., Zheng M., Fu C., Li G., Xionga Y., Qiua W., Zhang T., Zhanga J. and Zhenga C. (2020) Effect of low-level H2O2 and Fe(II) on the UV treatment of tetracycline antibiotics and the toxicity of reaction solutions to zebrafish embryos. Chemical Engineering Journal 394, DOI: 10.1016/j.cej.2020.125021.

Zhong S.F., Yang B., Xiong Q., Cai W.W., Lan Z.G. and Ying G. (2022) Hydrolytic transformation mechanism of tetracycline antibiotics: Reaction kinetics, products identification and determination in WWTPs. Ecotoxicology and Environmental Safety 229, DOI: 10.1016/j.ecoenv.2021.113063.

Zhou Q., Zhang M.C., Shuang C.D., Li Z.Q., Li A.M. (2012) Preparation of a novel magnetic powder resin for the rapid removal of tetracycline in the aquatic environment. Chinese Chemical Letters 23(6), 745–748, DOI: 10.1016/j.cclet.2012.01.039.

Zou R., Xu T., Lei X., Wu Q. and Xue S.(2020) Novel design of porous hollow hydroxyapatite microspheres decorated by reduced graphene oxides with superior photocatalytic performance for tetracycline removal. Solid State Sciences 99, DOI: 10.1016/j.solidstatesciences.2019.106067.

Zou S.J., Chen Y.F., Zhang Y., Wang X.F., You N. and Fan H.T. (2021) A hybrid sorbent of α-iron oxide/reduced graphene oxide: Studies for adsorptive removal of tetracycline antibiotics. Journal of Alloys and Compounds 862, DOI: 10.1016/j.jallcom.2020.158475.

Ewa Wiśniowska

Częstochowa University of Technology, Poland; e-mail: ewa.wisniowska@pcz.pl

Possibilities of potassium recovery from wastewater

ABSTRACT: The paper reviews data on potassium struvite recovery possibilities in wastewater treatment plants. The chemistry of potassium struvite precipitation and the properties of this residue have been described. Technical parameters of K-struvite recovery have been discussed, and finally, sources of necessary supplements supporting the process have been presented. In conclusion, although there is only one technical scale installation for K-struvite recovery, this technology has a great potential to be applied. Facilities similar to the MAP ones can be adapted. Because of operational costs use of waste products can be considered for supplementation of Mg or other elements. Because many factors affect K-struvite nucleation and precipitation, optimal operational conditions should be chosen experimentally in each case. New law regulations such as Regulation EU 2019/1009 of the European Parliament and of the Council of 5 June 2019 create favorable conditions for the sale of fertilizers recovered from wastewater.

KEYWORDS: potash, K-struvite, MPP, wastewater treatment plants, potassium recovery

Introduction

Potassium is the element that is crucial for plants' growth, it is among the 17 essential nutrients necessary for plants and has been classified as a macronutrient. This element is involved in such physiological plant processes as osmoregulation, protein synthesis, enzyme activation, and photosynthate translocation (Mikkelsen 2007). Good potassium nutrition of plants improves their drought tolerance, winter hardiness, and resistance to disease and insect pests (Bennett 2015).

Minerals that contain potassium are commonly called potash, and they could be, e.g., potassium chloride or potassium magnesium sulfate. Potash is used worldwide mainly to produce fertilizers (about 95%). It is primarily derived from K-rich minerals mined from underground deposits formed millions of years ago due to the evaporation of seawater. The world's biggest potash producer is Canada (30% of worldwide production), followed by Russia (17%) and Belarus (15%). In Europe, Spain and Ger-

many are potash producers, but at lower levels than the top 3 producers (Di Costanzo et al. 2021).

Potash reserves are now estimated to be about 90 years (Johansson et al. 2018); that is why potassium recovery technologies from wastes and wastewater should be of increasing interest, in addition to phosphorus compounds recycling. Economically, the nutrient recovery processes in WWTPs are still unprofitable compared to K-rock or P-rock mining. It is still cheaper to use minerals than the recovered materials for the fertilizer industry, but it changes over time. E.g., in 2007, recovering P from wastewater cost about 2000–8000 EUR per one ton, and it was practically impossible to sell it at this price. At the same time, phosphate rock costed about 35–50 $ per ton (Molinos-Senante et al. 2011). It is estimated that the ton of struvite is marketed to even 1000 EUR. The highest prices can be obtained for struvite from Pearl installations; however, more struvite (80–87%) is sold at prices below the estimated market value, it means below 250–400 EUR per ton (Muys et al. 2021). Simultaneously global spot prices for potash are at 13-year highs of 650 $ per ton. Recently the prices of fertilizers have increased significantly (Devitt et al. 2021). All these factors affect the interest in potassium and phosphorus recovery from wastewater.

Moreover, nowadays, it is more and more frequently considered that simply economic value is not enough for accessing the profits from struvite recovery. There are also other ones, e.g., phosphorus recovery involves many environmental values, such as eutrophication prevention in the receiving environment. Ecological effects are hard to evaluate, but they definitely should be considered. Also, political factors shape the interest in nutrient recovery, not only European Union policies but also a geopolitical situation, including e.g. the tense situation in Ukraine, Belarus, and Russia.

As a result of a variety of factors mentioned above, increasing interest in new technologies of struvite recovery is observed; as a result, new technologies are designed and allow for increasing recovery efficiency of this precipitate. More attention has been paid to magnesium ammonium phosphate (MAP) recovery than magnesium potassium phosphate (MPP); however, the last one is an up-and-coming alternative and should be considered when planning a circular economy in wastewater treatment plants.

1. Possibilities of potassium recovery from sewage and sludge

1.1. Chemistry of the process

The potassium struvite formula is $MgKPO_4 \cdot 6H_2O$ and is an isomorphous analog of crystalline ammonium struvite ($NH_4MgPO_4 \cdot 6H_2O$). K-struvite (magnesium potas-

sium phosphate – MPP) can be used as slow-release fertilizer in agriculture (Di Co-stanzo et al. 2021). The chemistry of K-struvite precipitation is as follows (Pervitasari et al. 2019):

$$Mg^{2+} + K^+ + PO_4^{3-} + 6H_2O \rightarrow MgKPO_4 \cdot 6H_2O$$
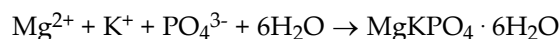
The structure of K – struvite is equivalent to magnesium ammonium phosphate, where potassium ones have replaced ammonium ions. Generally, it can be stated that struvite group compounds can be described by using the following formula:

$$A^{2+}B^+PO_4 \cdot nH_2O$$

where:

- n – can be equal from 6 to 8,
- A^{2+} – corresponds to Mg^{2+}, Cu^{2+}, Pb^{2+}, Mn^{2+} or Ni^{2+},
- B^+ – corresponds to univalent ions such as NH_4^+, K^+, Na^+, Rb^+, Cs^+ (Shih et al. 2016; Siciliano et al. 2020).

The water solubility of K-struvite is low but higher than MAP (solubility constant for MAP equal to $10^{-13.26}$, solubility constant for K-struvite in the range, according to various reports, from $10^{-11.7}$ to $10^{-13.26}$); however, it is well soluble in the acidic environment (Shih et al. 2016). Because MPP has a higher solubility than MAP in the presence of ammonium in the solution, MAP is preferable precipitated (Taragó 2017). The shape of struvite crystals is needle-like, and their length can be from 15 μm to even 3.5 mm. Compared to ammonium struvite the potassium one has a slightly higher density: 1.864 g/cm^3 (for K-struvite) vs. 1.711 g/cm^3 (for MAP) (Shih et al. 2016).

The formation of K-struvite involves two stages: nucleation and crystal growth. Nucleation is the formation of new crystals, which can occur in the absence of crystals and other solid phases or in the presence of primary crystals. The formed crystals grow until the solid/ liquid equilibrium is reached. Both nucleation and crystal growth are strongly dependent on supersaturation. High supersaturation values promote the nucleation phase, whereas low supersaturation values enhance a crystal's growth (Taragó 2017). The crystallization process is affected by various factors. The pH, molar ratios of $Mg^{2+}:NH_4^+:PO_4^{3-}$, presence of the other ions, time of reaction, and presence of other ions are of great importance.

1.2. Technical parameters of K-struvite recovery from wastewater

A comparison of technical parameters for MAP and MPP precipitation is presented in Table 1.

Comparing the MAP and MPP precipitation, both processes are strongly pH-dependent; pH value affects the amount of struvite precipitate, growth rate, sizes of

Table 1.

A comparison of technical parameters for MAP and MPP precipitation
(Katakojwala et al. 2019; Taragó Abella E. 2017; Perwitasari et al. 2019; Kim et al. 2017;

González-Morales et al. 2021; Mohamad et al. 2019; Johansson et al. 2018)

Parameter	Magnesium ammonium phosphate (MAP)	Magnesium potassium phosphate (MPP)
Optimal pH	according to various sources, MAP precipitates at a wide pH range from 7.0 to 11.5, but the most suitable is 8.0 to 9.5	according to various sources in the range of 8.5 to 10.5; experiments at higher pH values were rarely investigated; pH in the range of 9–10.5 are reported for maximum P recovery in K precipitation
Molar ratio of $A^{2+} : B^+ : PO_4^{3-}$	$Mg^{2+}:NH_4^+:PO_4^{3-}$ = 1:1:1 (or close to this proportion)	$Mg^{2+}:K^+:PO_4^{3-}$ = 1:1:1 (or close to this proportion)
Time of reaction, min.	the most frequently applied up to 4 hours	usually several hours (1.5–4), but also up to hydraulic retention time about 3.5 days
Factors disturbing struvite precipitation	concentration of Ca^{2+} or K^+ in solution, e.g. increasing molar ratio of $K^+:N-NH_4^+$ from 0.0 to 1.0 decreased ammonium nitrogen recovery from landfill leachate by 11%	presence of Mg^{2+}, Ca^{2+}, NH_4^+ and CO_3^{2-} in solution, e.g. MPP can only precipitate when the potassium concentration is much higher than ammonium
Removal effectiveness	> 90% of P removal > 70% of $N-NH_4^+$ removal	> 80–90% of P removal K removal efficiency is usually showed from the perspective of phosphorus concentration decrease

crystals, and their purity (Daegi et al. 2017). Struvite precipitation is usually performed at pH values higher than neutral, and at low pH, minimal crystals are obtained (Bayuseno et al. 2020). The optimal pH for K-struvite precipitation is reported to be between 8.5 and 10.5 (Perwitasari et al. 2019; Taragó Abella 2017). In the case of MAP, it was also stated that high pH values increase the density of the nuclei population, and as a result, smaller, heterogeneous crystals are formed (Gonzáles-Morazles 2021). As the pH increases, magnesium can be precipitated as $Mg(OH)_2$; thus, it reduces the amount of Mg^{2+} available for the process (Taragó 2017).

The availability of Mg^{2+} and PO_4^{3-} present in the solution can also be reduced due to the precipitation of another magnesium-phosphate mineral – $Mg_3(PO_4)_2 \cdot 22H_2O$, which precipitates at a pH higher than 10 (Bayuseno et al. 2020). Coexisting ions such as OH^- or CO_3^{2-} coprecipitate with Mg^{2+}, decreasing its availability for struvite precipitation (Molinoz-Senante et al. 2011). Mg^{2+} can also be precipitated (dependent on pH) as $Mg_3(PO_4)_2$, $MgHPO_4$, and $Mg(H_2PO_4)_2$. Not always increasing Mg^{2+} concentration results in larger struvite generation (Zhang et al. 2017). Excessive magnesium amounts would increase pH value and promote the formation of other magnesium phosphate precipitates. It should also be emphasized that optimal pH for struvite precipitation may vary depending on the type of liquid from which it is

precipitated, e.g., in the case of MAP, it was stated that optimal pH for wastewater was in the range 8–10, while in the case of livestock wastewater in the range of 8.0–9.0 (Zhang et al. 2017). Excess Mg^{2+} in the reaction environment, at high pH, significantly affected K-struvite recovery efficiency. In contrast, no effect has been shown for the excess dose of the K supplement (Kabadasli et al. 2022). Among the other ions, Ca^{2+} ones are the most interfering, e.g., precipitation of hydroxyapatite ($Ca_5(PO_4)_3(OH)$) was observed at pH 9.5–10.0 instead of MPP. Also, other calcium salts can be potentially formed instead of MPP, including $CaHPO_4$, $CaHPO_4 \cdot 2H_2O$, or $Ca_3(PO_4)_2 \cdot 2H_2O$ (Taragó 2017). Also, such solids as $Mg_3(PO_4)_3$, $MgNaPO_4 \cdot 7H_2O$, and $MgHPO_4 \cdot 7H_2O$ may accompany K-struvite precipitation (Kabdasli et al. 2022). According to some researchers, carbonates also affect MPP precipitation because carbonates and phosphates compete for calcium. High carbonate concentrations cause preferential calcium carbonate precipitation, making phosphates available for MPP precipitation (Taragó Abella 2017). The molar ratio of $Mg^{2+}:K^+:PO_4^{3-}$ should be near the theoretical value of 1:1:1. Underdosing any of the ingredients decrease the recovery rates of K and P. Excessive concentrations of, e.g., Mg^{2+} are not preferable because of higher, unreasonable costs (Taragó Abella 2017). Some authors, however, indicate that a K:P molar ratio over 3 was necessary to form MPP at an efficiently high concentration of phosphorus (Nakao 2017).

Also, organic acids (such as citric acid, acetic acid, and succinic acid) have been recognized as affecting struvite precipitation (Bayuseno et al. 2020). The research works concerning MAP struvite crystallization; however, it should also be considered in the case of MPP precipitation because the presence of the organic acids can retard the growth of the crystals.

Na^+ ions present in the reaction environment can additionally affect K-struvite recovery. As observed by Huang et al. (Huang et al. 2018), when Na: K molar ratio was higher than ten, the precipitation of Na was more than the precipitation of K when performed K-struvite recovery from urine. It is crucial in the case of wastewater that contains Na^+. It was also stated that the presence of ammonium in the solution disturbs potassium recovery, and K can only precipitate if the potassium concentration is much higher than ammonium. It is commonly accepted that MPP precipitation and recovery should be performed after releasing ammonium from the wastewater or rejected water stream, resulting in, e.g., biological denitrification (Johansson et al. 2018). In some installations, however, this phenomenon can be applied for the recovery of the mixed struvite material containing both MAP and MPP (Soares et al. 2017).

Among other factors, suspended solids concentration is indicated as the one affecting struvite precipitation. Suspended solids can act as nucleation seeds. It is also well known that seed crystals have a positive influence on struvite growth, and adding them shortens the nucleation time and increases the crystal growth rate (Zhang 2017).

Opinions on the influence of the temperature on struvite formation indicate that the temperature has a relatively more minor effect on struvite precipitation than pH. Still, it can significantly affect the growth rate and solubility of struvite crystals, and because of this, it should also be considered when someone designs struvite recovery

installation from wastewater (Gonzáles-Morazles 2021). E.g., Perwitasari et al. (Perwitasari et al. 2019) have indicated that temperature is a significant factor in the mass yield of K-struvite crystals. In the case of recovery of MPP from source-separated human urine, the effect of temperature was insignificant on K-struvite solubility within the range of 24–90°C.

The formation of struvite can also be affected by technical factors such as turbulent flow or stirring. The stirring rate may control the nucleation and crystal growth of struvite. When the stirring rate is higher, the nucleation of struvite occurs rapidly (Perwitasari 2019).

The data given above indicate that despite theoretical consideration, there is a need to choose struvite precipitation parameters experimentally, e.g., using the jar tests.

1.3. Waste products for potassium and magnesium supplementation in wastewater

Potassium concentration in domestic wastewater is estimated to be 13–20 mgK/dm^3 (Perwitasari 2019). In the case of a wastewater treatment plant that receives about 50,000 m^3 of daily sewage load, potassium is about 0.65–1.0 tons, and the annual is equal to 231,4–356 tons. It provides favorable conditions for the recovery of this element. Potassium can also be recovered from reject water in a wastewater treatment plant. In this type of wastewater, potassium is concentrated, and the concentration of this element can be about 250 mgK/dm^3 (Johansson 2018).

Another alternative for potassium recovery is to recover this element from industrial wastewater rich in K. Concentrations of potassium in various types of wastewater are presented in Table 2.

Table 2.
K-rich wastewater which could be used for recovery of potassium (Arienzo et al. 2008)

Type of wastewater	Potassium content [g/m^3]
Cheese whey	1,680
Lactic/casein whey	1,660
Piggery	500–1,000
Wineries	250
Olive oil	10,000–200,000
Municipal wastewater	13–20

The problem with the recovery of potassium from wastewater is that the concentration of the Mg in wastewater is usually lower than K, and supplementation of the magnesium salts is necessary. Different types of reagents can be used to supplement Mg. To supplement Mg^{2+} e.g., $MgCl_2·6H_2O$, MgO, $Mg(OH)_2$ can be added. The sequence for precipitate's phosphorus by various Mg sources has been found as follows:

$MgCl_2 > MgSO_4 > MgO > Mg(OH)_2 > MgCO_3$ (Rodlia et al. 2020). Using magnesium reagents could not be economically effective (Fattah et al. 2013).

Except for commercial magnesium salts, different Mg-rich by-products can also be used, such as magnesite, brucite, products of thermal treatment of meat waste, and bone meal. Also, MgO-saponification wastewater and seawater have been tested for this purpose (Myllymäki 2020; Fattah et al. 2013). Experiments conducted by Fattah et al. (Fattah et al. 2013) have also successfully applied as Mg source reject waters from desalination plants. As potential wastes, dairy, swine, or poultry wastes have been suggested. An interested K source can also be potash brine. Some authors have also suggested the concentrates from membrane processes applied for landfill leachates treatment (Wang 2012).

In the case of potassium recovery, supplementation of phosphorus or potassium can also be necessary. Sewage, sewage sludge, and manures contain less potassium to make the simultaneous recovery of potassium and phosphate a compelling alternative to MAP recovery. It is possible to supplement K as KCl, K_2SO_4, or other potassium compounds. However, the interesting option is to use waste materials, e.g., substratum, in the co-fermentation process. Potential K-rich wastes for co-fermentation and simultaneous supplementation of potassium are listed in Table 3.

Table 3.

K-rich waste materials which could be used for supplementation of K in sewage sludge (Arienzo 2008; Godlewska & Becher 2021)

Type of waste material	Potassium content
Oat (stem)	16.3 g/kg$_{d.m.}$
Rye (stem)	13.6 g/kg$_{d.m.}$
Molasses	up to 24 g/kg
Potato pulp	8.6 g/kg$_{d.m.}$
Sewage sludge	4.06 g/kg

When wastewater is used for K-struvite recovery pH of the reject waters or wastewater should be corrected. As supplements for pH increase frequently, $Ca(OH)_2$ or NaOH are used, affecting K-struvite precipitation. To reduce the amount of reagents required to raise pH, CO_2 stripping is recommended if possible (Cerillo et al. 2014; Siciliano et al. 2020).

When we plan to recover K from waste materials or wastewater, we should focus on heavy metals concentrations. Some researchers consider it a problem; however, previous experiences have indicated that it could be a problem only in WWTPs, to which some industrial wastewater inflow. In the case of other types of waste materials, specific pollutants should be monitored, including e.g., veterinary drugs (Taragó 2017).

1.4. Reactors for struvite precipitation and the struvite yield

Various types of reactors (crystallizers) can be used for K-struvite recovery from wastewater. They are of the same kind as the MAP process. As has rightly been said (Zhang et al. 2017), crystallizers can be divided into three types based on air agitation, water agitation, and mechanical agitation type. The first type of crystallizer is equipped with an aeration system that mixes the solution and simultaneously strips CO_2. As a result, efficient mixing is achieved, and an increase in pH value. In the water agitation type crystallizers, mixing is performed, e.g., by changing the direction of the solution flow or changing the flow velocity. The third type of reactor is equipped with various constructions of impellers – simple to operate but of relatively high energy consumption (Zhang et al. 2017). Crystallizers can work as batch reactors or as continuous ones.

Until now, only one full-scale K-struvite precipitation installation has been applied. The facility in Putten (the Netherlands) treats more than 100,000 m^3 of calf manure per year. In this installation, calf manure is divided into two streams – solid and liquid. Liquid one is processed to recover MPP. At first, the BNR activated sludge process is applied to remove organic carbon and nitrogen, and then phosphate and potassium-rich effluent is supplemented by MgO. Mechanically stirred tanks are used for the procedure. The advantage of MgO use is increasing the pH of the manure to the value in the range of 8.5 – 9.0. Precipitated MPP is separated in lamella separators. It allows for about 95% P recovery efficiency (Schuiling and Andrade, 1999; Desmidt et al. 2015).

As the full-scale process for K-recovery also, the REM-NUT process is indicated. The process is applied to remove phosphate, ammonium, and potassium from low concentration effluents. REM-NUT unit consists of ion exchange units. NaCl is used for the regeneration of the ion exchangers. Caustic soda and $MgCl_2$ are applied to form MAP and MPP from regeneration liquids. However, this technology is considered significantly expensive compared to the other ones (Piveteau 2018).

1.5. Law quality requirements for struvite type fertilizers

New regulations concerning, among others, struvite type fertilizers will apply in European Union as of 16 July 2022. They are introduced by the Regulation EU 2019/1009 of the European Parliament and of the Council of 5 June 2019, laying down rules on the making available on the market of EU fertilizing products and amending Regulations (EC) No 1069/2009 and (EC) No 1107/2009 and repealing Regulation (EC) No 2003/2003 (Regulation 2019). The regulation, among others, introduces limits for toxic contaminants in fertilizers recovered from wastewater to guarantee a high level of soil protection and reduce environmental and health risks. It also, what is of high importance in significantly harmonizing EU fertilizer legislation. It makes easier the use and trade flows of such fertilizers.

Conclusions

Based on the short review given in the chapter, it can be concluded that:

1. Potassium recovery processes should be of greater interest; economic, political, and environmental reasons support it.
2. Despite theoretical considerations in particular cases, experimental design methods, including e.g., jar test, should match optimal operational conditions for installations.
3. At present, the main limitations of K-recovery are the high price of MPP compared to mineral potash and the necessity to supplement Mg to achieve the right Mg:P:K proportion. The problem is also to achieve MPP without amendments of other magnesium and phosphorus salts.
4. More attention should be paid to using waste products as a source of the elements necessary for MPP recovery because they could be a solution to the problem of Mg supplementation. Some Mg sources, e.g., molasses or oat stems, can be used.
5. Because of the higher concentrations of K reject water should be considered a preferable sewage stream for K-recovery. Experience at industrial scale indicates that K-recovery is a promising technology in processing K-rich wastewater, e.g., from piggery, olive oil production, or selected dairy wastewater.
6. The reactors used for MAP recovery can be adapted for K recovery, and both processes can be applied in wastewater treatment plants.
7. New law regulations such as Regulation EU 2019/1009 of the European Parliament and of the Council of 5 June 2019 create favorable conditions for the sale of fertilizers recovered from wastewater.

REFERENCES

Arienzo M., Christen E., Quaile W.C. and Kumar A. (2008) A review of the fate of potassium in the soil-plant system after land application of wastewaters. Journal of Hazardous Materials 164(2–3), 415–22.

Bayuseno A.P., Perwitasari D.S., Muryanto S., Tauviqirrahman M. and Jamari J. (2020) Kinetics and morphological characteristics of struvite (MgNH4PO4.6H2O) under the influence of maleic acid. Heliyon 6(3), DOI: 10.1016/j.heliyon.2020.e03533.

Bennett A.M. (2015) Potential for potassium recovery as K-struvite. MAS Thesis. The University of British Columbia, Vancouver.

Cerillo M., Palatsi J., Comas J., Vicens J. and Bonmati A. (2014) Struvite precipitation as a technology to be integrated in a manure anaerobic digestion treatment plant – removal efficiency, crystal characterization and agricultural assessment. Journal of Chemical Technology and Biotechnology 90(6), 1135–1143, DOI: 10.1002/jctb.4459.

Daegi K., Min K.J., Lee K., Yu M.S. and Park K.Y. (2017) Effects of pH, molar ratios and pre-treatment on phosphorus recovery through struvite crystallization from effluent of anaerobically digested swine wastewater. Environmental Engineering Research 22(1), 12–18, DOI: 10.4491/eer.2016.037.

Desmidt E., Ghyselbrecht K., Zhang Y., Pinoy L., van der Bruggen B., Verstraete W., Rabaey K. and Meesschaert B. (2015) Global phosphorus scarcity and full-scale P-recovery techniques – a review, Crtical Reviews in Environmental Science and Technology 45(4), 336–384.

Devitt P., Jadhav R. and Samora R. (2021) Potash importers brace for prolonged price rally after sanctions on Belarus. [Online] https://www.reuters.com/markets/commodities/potash-importers-brace-prolonged-price-rally-after-sanctions-belarus-2021-12-21/ (Accessed: 2022-02-27).

Di Costanzo N., Cesaro A., Di Capua F. and Esposito G. (2021) Exploiting the nutrient potential of anaerobically digested sewage sludge: a review. Energies 14(23), DOI: 10.3390/en14238149.

Fattah K.P., Shabani S. and Ahmed A. (2013) Use of desalinated reject water as a source of magnesium for phosphorus recovery. International Journal of Chemical Engineering and Applications 4(3), 165–168, DOI: 10.7763/IJCEA.2013.V4.286.

Godlewska A.M. (2021) The effect of waste materials on the content of some macroelements in test plants. Journal of Ecological Engineering 22(4), 167–174, DOI: 10.12911/22998993/134046.

González-Morales C., Fernández B., Molina F.J., Naranjo-Fernández D., Matamoros-Veloza A. and Camargo-Valero M. (2021) Influence of pH and temperature on struvite purity and recovery from anaerobic digestate. Sustainalbility 13, DOI: 10.3390/su131910730.

Huang H., Li J., Li B., Zhang D., Zhao N. and Tang S. (2018) Comparison of different K-struvite crystallization processes for simultaneous potassium and phosphate recovery from source-separated urine. Science of the Total Environment 651 (1), 787–795, DOI: 10.1016/j.scitotenv.2018.09.232.

Johansson S., Ruscalleda M., Saerens B. and Colprim J. (2018) Potassium recovery from centrate: taking advantage of autotrophic nitrogen removal for multi-nutrient recovery. Journal of Chemical Technology & Biotechnology 94(3), 819–829, DOI: 10.1002/jctb.5828.

Kabdaşli I., Kuşçuoğlu S., Tünay O. and Siciliano A. (2022) Assessment of K-struvite precipitation as a means of nutrient recovery from source separated human urine. Sustainability 14(3), DOI: 10.3390/su14031082.

Katakojwala R., Kumar A.N., Chakraborty D. and Venkata Mohan S. (2019) Valorization of sugarcane waste: prospects of the biorefinery. [In:] Industrial and Municipal Sludge. Emerging Concerns and Scope of Resource Recovery, Prasad M.N.V., de Campos Favas P.J., Ventaka Mohan S., (Eds.), Butterworth-Heinemann: 47–60.

Kim D., Min K.J., Lee K., Yu M.S. and Park K.Y. (2017) Effects of pH, molar ratios and pre-treatment on phosphorus recovery through struvite crystallization from effluent of anaerobically digested swine wastewater. Environmental Engineering Research 22(1), 12–18, DOI: 10.4491/eer.2016.037.

Mikkelsen R.L. (2007) Managing potassium for organic crop production. HortTechnology 17(4), 455–460, DOI: 10.21273/HORTTECH.17.4.455.

Mohamad D., Azmil A., Hafiz P.M. and Aeslina A.K. (2019) Study on the effect of potassium on struvite precipitation in synthetic landfill leachate. Asian Journal of Water, Environment and Pollution 16(4), 77–80, DOI: 10.3233/AJW190050.

Molinos-Senante M., Hernandez-Sancho F., Sala-Garrido R. and Garrido-Baserba M. (2011) Economic feasibility study for phosphorus recovery processes. Ambio 40(4), 408–416, DOI: 10.1007/s13280-010-0101-9.
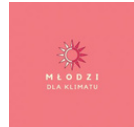
Muys M., Phukan R., Brader G., Samad A., Moretti M., Haiden B., Pluchon S., Roest K., Vlaeminck S.E. and Spiller M. (2021) A systematic comparison of commercially produced struvite: quantities, qualities and soil-maize phosphorus availability. Science of the Total Environment 756, DOI: 10.1016/j.scitotenv.2020.143726.

Myllymäki P., Pesonen J., Nurmesniemi E., Romar H., Tynjälä P., Hu T. and Lassi U. (2020) The use of industrial waste materials for the simultaneous removal of ammonium nitrogen and phosphate from the anaerobic digestion reject water. Waste and Biomass Valorisation 11, 4013–4020, DOI: 10.1007/s12649-019-00724-8.

Nakao S., Nishio T. and Kanjo Y (2017) Simultaneous recovery of phosphorus and potassium as magnesium potassium phosphate from synthetic sewage sludge effluent. Environmental Technology 38(19), 2416–2426, DOI: 10.1080/09593330.2016.1264485.

Perwitasari D.S., Muryanto S., Tauviqirrahman M., Jamari J. and Bayuseno A.P. (2019) Optimization of key parameters in struvite (K) production for phosphorus and potassium recovery using a batch crystallizer. RASĀYan Journal of Chemistry 12(2), 787–795, DOI: 10.31788/RJC.2019.1225125.

Piveteau S. (2017) Optimizing hydrolysis and acidogenesis in order to dissolve and recover phosphorus in organic effluents upstream from methane production. Organic chemistry. Université Rennes 1, NNT: 2017REN1S123. [Online] https://tel.archives-ouvertes.fr/tel-01800084/document (Accessed: 2022-02-27).

Regulation (EU) 2019/1009 of the European Parliament and of the Council of 5 June 2019 laying down rules on the making available on the market of EU fertilising products and amending Regulations (EC) No 1069/2009 and (EC) No 1107/2009 and repealing Regulation (EC) No 2003/2003 (Text with EEA relevance) O.J.L. 17, 25.6.2019, 1–114.

Rodlia W., Ikhlas N., Pandebesie E.S., Bagastyo A.Y. and Herumurti W. (2020) The effect of mixing rate on struvite recovery from the fertilizer industry. [In:] IOP Conf. Series: Earth and Environmental Science 506, DOI: 10.1088/1755-1315/506/1/012013.

Schiuling R.D. and Andrade A. (1999) Recovery of struvite from calf manure. Environmental Technology 20, 765–768.

Shih K. and Yan H. (2016) Chapter 26: The crystallization of struvite and its analog (K-struvite) from wase streams for nutrient recycling. [In:] Prasad M.N.V., Shih K. (Eds.), Environmental materials and waste, Academic Press.

Siciliano A., Limonti C., Curcio G.M. and Molinari R. (2020) Advances in struvite precipitation technologies for nutrient removal and recovery from aqueous waste and wastewater. Sustainability 12, DOI: 10.3390/su12187538.

Soares A., Czajkowska J., Colprim J., Gali A., Johannson S., Masic A., Marchi A., McLeod A., Nenov V., Ruscalleda M. and Siwiec T. (2017) Chapter 17: Nutrients recovery from wastewater streams. [In:] Lema J.M. and Suarez S. (Eds.), Innovative Wastewater treatment and resource Recovery Technologies. Impacts on Energy, Economy and the Environment, IWA Publishing Alliance House, London.

Taragó Abella E. (2017) Assessment of struvite and K-struvite recovery from digested manure. PhD Thesis, University of Girona.

Wang Y., Li X., Zhen L., Zhang H., Zhang Y. and Wang C. (2012) Electro-Fenton treatment of concentrates generated in nanofiltration of biologically pretreated landfill leachate. Journal of Hazardous Materials 229–230, 115–21, DOI: 10.1016/j.jhazmat.2012.05.108.

Zhang T., Jiang R. and Deng Y. (2017) Phosphorus recovery by struvite crystallization from livestock wastewater and reuse as fertilizer: a review. [In:] Physico-chemical wastewater treatment and resource recovery, Farooq R. and Ahmad Z. (Eds.), IntechOpen.
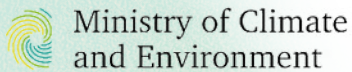
ORGANISER

**Mineral and Energy
Economy Research
Institute**
Polish Academy of Sciences

PARTNERS

Green Back
Innovation for nature

FUNDACJA
OPTIMUS

PROMAN

Trener Nauki
Dr Justyna Małkuch-Świtalska

SCHWANDER
POLSKA

MŁODZI
DLA KLIMATU

HONORARY PATRONAGE

Ministry of Climate
and Environment

Minister
Edukacji i Nauki

Izba Gospodarcza
WODOCIĄGI POLSKIE

PATRONAGE

State Water
Holding
Polish Waters

The National Centre
for Research and Development

AMU
Polish Young Academy
POLISH ACADEMY OF SCIENCES

Publication co-financed by NAWA as part of the project "Monitoring of water and sewage management in the context of the implementation of the circular economy assumptions (MonGOS)"

MonGOS NAWA POLISH NATIONAL AGENCY
FOR ACADEMIC EXCHANGE

MEERI PAS